

**Distribution Agreement:**

In presenting this thesis or dissertation as a partial fulfillment of the requirements for an advanced degree from Emory University, I hereby grant to Emory University and its agents the non-exclusive license to archive, make accessible, and display my thesis or dissertation in whole or in part in all forms of media, now or hereafter known, including display on the world wide web. I understand that I may select some access restrictions as part of the online submissions of this thesis or dissertation. I retain all ownership rights to the copyright of the thesis or dissertation. I also retain the right to use in future works (such as articles or books) all or part of this thesis or dissertation.

Signature

\_\_\_\_\_  
Danny E. Mancheno

\_\_\_\_\_  
Date

Development of a Copper Catalyzed Aminoacetoxylation Reaction of Olefins,  
Development of an Intermolecular and Diastereoselective Iminium Cascade Reaction and  
Studies Towards the Synthesis of a Malagasy Alkaloid.

By

Danny E. Mancheno  
Doctor of Philosophy

Chemistry

---

Simon B. Blakey, Ph.D.  
Advisor

---

Dennis C. Liotta, Ph.D.  
Committee Member

---

Huw M. L. Davies, Ph.D.  
Committee Member

Accepted:

---

Lisa A. Tedesco, Ph.D.  
Dean of the James T. Laney School of Graduate Studies

---

Date

Development of a Copper Catalyzed Aminoacetoxylation Reaction of Olefins,  
Development of an Intermolecular and Diastereoselective Iminium Cascade Reaction and  
Studies Towards the Synthesis of a Malagasy Alkaloid

By

Danny E. Mancheno  
B.A., Queens College (CUNY), 2002

Advisor: Simon B. Blakey, Ph.D.

An abstract of  
A dissertation submitted to the Faculty of the  
James T. Laney School of Graduate Studies of Emory University  
in partial fulfillment of the requirements for the degree of  
Doctor of Philosophy  
in Chemistry  
2013

## Abstract

Development of a Copper Catalyzed Aminoacetoxylation Reaction of Olefins,  
Development of an Intermolecular and Diastereoselective Iminium Cascade Reaction and  
Studies Towards the Synthesis of a Malagasy Alkaloid

By

Danny E. Mancheno

Nitrogen heterocycles are important intermediates in the synthesis of medicinal compounds, agricultural chemicals, polymers and analytical reagents. Although, there are several approaches to the synthesis of nitrogen heterocycles, a lot of challenges still remain. Moreover, the recent demand by society to develop more environmentally and economically friendly synthetic methods has given rebirth to the need for new methodologies across organic chemistry. Thus, a lot emphasis has been directed towards the development of new and mild conditions for the formation of nitrogen heterocycles. Since its inception, the Blakey lab has been working on developing new methods for synthesis of nitrogen heterocycles. With that aim, we have developed new methodology that involves metallonitrenes intermediates for the formation of carbon-nitrogen bonds. Additionally, our lab has also developed an iminium based cascade annulation reaction for the synthesis of the structural cores of some unusual strychnos alkaloids. Three main projects that have branched out of this initial work will be discussed in this thesis: the development of a copper catalyzed aminoacetoxylation reaction of olefins (part 1); development of a diastereoselective intermolecular cascade annulation reaction (part 2) and application of the intramolecular cascade cyclization reaction towards the total synthesis of a Malagasy alkaloid (part 3).



Development of a Copper Catalyzed Aminoacetoxylation Reaction of Olefins,  
Development of an Intermolecular and Diastereoselective Iminium Cascade Reaction and  
Studies Towards the Synthesis of a Malagasy Alkaloid

By

Danny E. Mancheno  
B.A., Queens College (CUNY), 2002

Advisor: Simon B. Blakey, Ph.D.

A dissertation submitted to the Faculty of the  
James T. Laney School of Graduate Studies of Emory University  
in partial fulfillment of the requirements for the degree of  
Doctor of Philosophy  
in Chemistry  
2013

*To my brother Francisco, who first introduced me  
to the wonderful world of science.*

## Acknowledgements

The journey to obtain a doctoral degree is not an easy journey. I know that in my case, this journey could not have been possible without a number of people. First and foremost, I am forever grateful to Dr. Blakey not only because he took a lot of his time to teach and mentor me during these doctoral studies, but also because he was very kind to me and allowed me to spend some quality time with my daughter Sofie during her first year.

I thank my committee members, Dr. Davies, Dr. Liotta and Dr. Liebeskind for their guidance and helpful advice over the past five years. I would also like to thank a Dr. Wu and Dr. Wang at the NMR Center. Not only did they teach me a lot about NMR spectroscopy, but were kind enough to trust me with their NMR instrumentation time after time. I believe that life as a chemistry graduate student would be a hundred times more complicated if it wasn't for Ann Dasher. Ann, you are an incredible and efficient graduate program coordinator, thank you.

This past five years could also not been possible without the kindness, support and teaching of my fellow lab mates. Ricardo, you are paranoid, but you are a great person and a superb chemist, I learned a lot from you, thanks *bo*. Aaron, it was great sharing the lab with you, your drive and focus is admirable. Vèronique, thank you for keeping the lab running for the time that you were here. Jen, thanks for keeping the lab running after Vèronique left. Aidi, you are a great chemist and even a better person. Clay, you and I have shared most of this journey together, from orientation week to my last days at Emory. I have witnessed your grow from a first year chemistry student into a very

good scientist. I hope that you have learned as much from me as I have from you. More importantly, is the fact that you have become one of my closest friends. Thank you guys for all your help during my time in Atlanta, I really appreciate it.

I obviously would not have been able to complete this journey without the love and support of my family. Mom and dad, thank you for installing good and positive values in me. A big thank thank you to my brother and sister for their continuous love over the past five years.

Last but not least Juliya. You did not hesitate and moved to Atlanta with me so that I could pursue this doctoral degree. You have also taken care of all our responsibilities in NYC while we here in Atlanta. I cannot say thank you enough for that. Above all, however, is your everyday love to me, which has kept me sane and focused through out this time. I love you.

# Table of Contents

<b>1 Chapter One: Introduction to Vicinal Amino Alcohols and Aminohydroxylation Reactions.....</b>	<b>2</b>
1.1 Vicinal Amino Alcohols.....	2
1.2 Aminohydroxylation Reactions.....	3
1.2.1 Osmium Catalyzed Aminohydroxylation Reactions.....	4
1.2.2 Palladium Catalyzed Aminohydroxylation Reactions.....	5
1.2.3 Copper Catalyzed Amino-oxygenation Reactions.....	7
1.2.4 Gold Catalyzed Amino-oxygenation Reactions.....	8
1.2.5 Metal Free Amino-oxygenation Reactions.....	9
1.2.6 Blakey's Group Entry into Amino-oxygenation Reactions.....	10
<b>2 Chapter Two: Copper Catalyzed Aminoacetoxylation of Olefins.....</b>	<b>12</b>
2.1 Synthesis of Sulfonamide <b>3</b> .....	12
2.1.1 Initial Synthesis of Sulfonamide <b>3</b> .....	12
2.1.2 New Synthesis of Sulfonamide <b>3</b> .....	13
2.2 Initial Investigations.....	14
2.3 Optimization Studies.....	16
2.3.1 NMR Assay.....	16
2.3.2 Oxidant Optimization and Activating Group Optimization.....	16
2.3.3 Base and Catalyst Optimization.....	17
2.3.4 Solvent Optimization.....	18
2.4 Intermolecular aminoacetoxylation of $\gamma$ -aminoolefins.....	19

2.4.1	Terminal Olefins .....	19
2.4.2	Mechanism.....	25
2.4.3	Aminoacetoxylation of 1,2 disubstituted olefins.....	26
2.5	Conclusions and Future Work .....	32
<b>3</b>	<b>Chapter Three: Introduction to the Banyaside Alkaloids .....</b>	<b>35</b>
3.1	Banyaside A and B: Isolation, Structure and Stereochemistry .....	35
3.2	Biological Activity.....	37
3.3	Carreira's Synthesis of Banyaside B.....	38
3.4	Our Approach to the Core of the Banyaside Alkaloids.....	40
<b>4</b>	<b>Chapter Four: Development of an Intermolecular Iminium Cascade Reaction for the Synthesis of the Banyaside Core .....</b>	<b>43</b>
4.1	Early Attempts with <i>N</i> -Tosyl- <i>O</i> -TMS Aminol <b>77</b> .....	43
4.1.1	Synthesis of $\alpha,\beta$ unsaturated acid <b>86</b> .....	43
4.1.2	Synthesis of <i>N</i> -Tosyl- <i>O</i> -TMS aminol <b>77</b> .....	48
4.1.3	Cascade Annulation with <i>N</i> -Tosyl- <i>O</i> -TMS aminol <b>77</b> .....	49
4.2	Intermolecular Iminium Cascade with <i>N</i> -Cbz- <i>O</i> -TMS Aminol <b>99</b> .....	49
4.2.1	Synthesis of <i>N</i> -Cbz- <i>O</i> -TMS aminol <b>37</b> .....	49
4.2.2	Cascade Annulation of <i>N</i> -Cbz- <i>O</i> -TMS aminol <b>99</b> .....	50
4.2.3	Synthesis of <i>N</i> -benzyl-cyclohexanol <b>103</b> .....	53
4.2.4	Synthesis of <i>N</i> -methyl-cyclohexanol <b>104</b> .....	54
4.2.5	Synthesis of <i>N</i> -benzyl- <i>O</i> -TBDMS-cyclohexanol <b>106</b> .....	54
4.2.6	Proposed Transition State for the Cyclization of <b>99</b> .....	56

## 5 Chapter Five: Studies Towards an Enantioselective Intermolecular Cascade

### Reaction..... 58

5.1	Introduction.....	58
5.2	Thiourea Based Catalysts (Hydrogen-Bonding Catalysts).....	59
5.3	Investigations into thioureas as catalysts for our methodology.....	63
5.3.1	Synthesis of chiral thiourea <b>58</b> .....	63
5.3.2	Iminium Cascade Reaction with Sulfonic Acids.....	65
5.3.3	Cyclization with chiral thiourea catalyst <b>58</b> .....	66
5.4	Ti(IV) based catalyst.....	67
5.4.1	Braun's dynamic kinetic asymmetric allylations.....	67
5.4.2	Synthesis of Ti(IV) Catalyst <b>130</b> .....	68
5.4.3	Synthesis and Allylation of <b>65</b> .....	71
5.5	Conclusions.....	72

## 6 Chapter Six: Introduction to the Malagasy Alkaloids and Initial Efforts

### Towards the Synthesis of Malagashanine ..... 77

6.1	The Malagasy Alkaloids.....	77
6.2	Malagashanine: Structure.....	78
6.3	Myrtoidine and Demethoxymyrtoidine.....	79
6.3.1	Myrtoidine.....	79
6.3.2	11-Dimethoxymyrtoidine.....	80
6.4	Biological Activity.....	80
6.5	Blakey's Lab Approach to the Malagasy Alkaloids.....	83
6.5.1	Early Cascade Annulation Work.....	83

6.5.2	Extending the Scope of Methodology to Incorporate the C(16) Stereocenter.....	84
6.5.3	Synthesis of Advanced Pyran <b>166</b> .....	85
<b>7</b>	<b>Chapter Seven: Total Synthesis of Epi-malagashanine.....</b>	<b>88</b>
7.1	Development of a Scalable Route for the Synthesis of Key Dihydropyran <b>169</b> .	88
7.1.1	Synthesis of <i>N</i> -Tosyl-amide <b>161</b> .....	88
7.1.2	Optimization Studies for the Synthesis of <i>N</i> -Tosyl- <i>O</i> -TMS aminol <b>161</b> , Imidazole as a Mild Lewis Acid. ....	90
7.1.3	Key intramolecular cascade reaction. ....	93
7.1.4	Synthesis of dihydropyran <b>175</b> . ....	93
7.2	Synthesis of Ester 182: Original Approach and New Approach Circumventing the Problematic Oxidation Step. ....	95
7.2.1	Original Approach to Methyl-Ester <b>184</b> . ....	95
7.2.2	Second Generation Approach to Methyl-ester <b>184</b> .....	97
7.2.3	Third Generation Approach to Methyl-Ester <b>184</b> . Trifluoroacetic anhydride as a Carbonyl Source. ....	99
7.2.4	Fourth Generation Approach to Methyl Ester <b>184</b> . ....	102
7.3	Reduction of the C(19)-C(20) Tetrasubstituted Olefin of Methyl Ester <b>184</b> .....	104
7.3.1	Hydrogenation on Model System. ....	104
7.3.2	Hydrogenation of the C(19)-C(20) Tetrasubstituted Olefin of Acid <b>183</b> and Ester <b>184</b> . ....	105
7.4	Ionic Reduction of the C(19)-C(20) Tetrasubstituted Olefin.....	107



7.5	Synthesis of Epi-Malagashanine; Removal of the N <sub>b</sub> Tosyl Auxiliary and Reductive Methylation.....	109
<b>8</b>	<b>Chapter Eight: Efforts Towards the Synthesis of 11-Demethoxymyrtoidine and a New Strategy Towards Malagashanine .....</b>	<b>111</b>
8.1	First Generation Strategy Towards the Synthesis of 11-demethoxymyrtoidine ( <b>154</b> ) and New Strategy Towards Malagashanine ( <b>151</b> ). .....	111
8.1.1	First Generation Strategy Towards Demethoxymyrtoidine by Direct C-H functionalization .....	111
8.1.2	New Approach to Malagashanine from Intermediate <b>210</b> .....	112
8.1.3	Allylic Halogenation of Methyl-ester <b>182</b> . .....	113
8.1.4	Allyl Oxidation <i>via</i> an Extended Enolate. ....	114
8.1.5	Oxidation via C-H activation. ....	118
8.2	Second Generation Approach: Introduction of the Oxygen Atom <i>via</i> Hydroacylation with Acetoxyacetyl Chloride .....	119
8.2.1	Retrosynthetic Analysis .....	119
8.2.2	Initial Synthesis of dihydropyran <b>234</b> .....	120
8.2.3	Acylation of Dihydropyran <b>242</b> . .....	122
8.2.4	Vilsmeier-Haack Formylation .....	124
8.3	Third-generation Approach: Synthesis of Tetric Acid.....	127
8.3.1	Retrosynthetic Analysis. ....	127
8.3.2	Hydrolysis of $\alpha$ -Acetoxy Ketone <b>239</b> . ....	128
8.3.3	Attempts to Synthesize Tetric Acid <b>259</b> .....	129
8.4	Conclusions.....	132

<b>9</b>	<b>Experimentals.....</b>	<b>134</b>
9.1	Materials and Methods: General Information.....	134
9.2	Part 1: Copper Catalyzed Aminoacetoxylation of Olefins.....	135
9.3	NMR Spectra-Part 1.....	153
9.4	Part 2: Efforts Towards the Development of an Enantioselective Intermolecular Cascade Reaction to Access the Core of the Banyaside Peptides. ....	160
9.5	NMR Spectra Part 2.....	173
9.6	Part 3. Studies Towards the Total Synthesis of a Malagasy Alkaloid.....	176
9.7	X-ray Structures-Part 3.....	203
<b>10</b>	<b>References.....</b>	<b>252</b>

## Table of Schemes

<b>Scheme 1.1</b> Sharpless asymmetric aminohydroxylation used in Taxol synthesis.....	4
<b>Scheme 1.2</b> Intramolecular variant to the AA reaction .....	5
<b>Scheme 1.3</b> Palladium catalyzed amino-oxygenation reactions.....	6
<b>Scheme 1.4.</b> Copper mediated amino-oxygenation reactions. ....	8
<b>Scheme 1.5</b> Gold catalyzed amino-oxygenation of olefins.....	8
<b>Scheme 1.6</b> Metal-free amino-oxygenation reactions.....	10
<b>Scheme 1.7</b> Discovery of the copper-catalyzed aminooxygenation reaction.....	11
<b>Scheme 2.1</b> Initial synthesis of sulfonamide <b>3</b> . ....	13
<b>Scheme 2.2</b> Convergent synthesis for sulfonamide <b>3</b> .....	14
<b>Scheme 2.3.</b> Aminoacetoxylation of amino-olefin <b>3</b> .....	19
<b>Scheme 2.4</b> Synthesis of $\beta$ -geminal dimethyl sulfonamide <b>11</b> . ....	20
<b>Scheme 2.5</b> Cyclization of $\beta$ -gem-dimethyl sulfonamide <b>11</b> . ....	21
<b>Scheme 2.6</b> Cyclization of $\gamma$ -gem-dimethyl sulfonamide <b>16</b> . ....	21
<b>Scheme 2.7</b> Synthesis of <i>N</i> -Nosyl allyl aniline <b>23</b> . ....	22
<b>Scheme 2.8</b> Aminoacetoxylation of <i>N</i> -Nosyl allyl aniline <b>23</b> .....	23
<b>Scheme 2.9.</b> Synthesis of benzyl amine <b>29</b> and aminoacetoxylation. ....	24
<b>Scheme 2.10</b> Cyclization of sulfmate ester <b>32</b> . ....	24
<b>Scheme 2.11</b> Synthesis of 1,2-disubstituted $\gamma$ -aminoolefins <b>34</b> and <b>35</b> . ....	26

<b>Scheme 2.12.</b> Cyclization of 1,2-disubstituted $\gamma$ -amino-olefins <b>34</b> and <b>35</b> .....	27
<b>Scheme 2.13</b> Synthesis of <i>Cis</i> -phenyl $\gamma$ -aminoolefins <b>42</b> . ....	28
<b>Scheme 2.14</b> Synthesis of <i>trans</i> -phenyl $\gamma$ -aminoolefin <b>47</b> .....	29
<b>Scheme 2.15</b> Cyclization of <i>cis</i> - and <i>trans</i> -phenyl $\gamma$ -aminoolefins <b>42</b> and <b>47</b> .....	29
<b>Scheme 2.16</b> Synthesis of <i>trans</i> -isopropyl $\gamma$ -aminoolefin <b>54</b> .....	30
<b>Scheme 2.17</b> Aminoacetoxylation of <i>trans</i> -isopropyl $\gamma$ -aminoolefin <b>54</b> . ....	31
<b>Scheme 2.18.</b> Aminoacetoxylation of OBn substituted olefin <b>59</b> . ....	32
<b>Scheme 3.1</b> Carreira's Approach to abn core <b>65</b> .....	39
<b>Scheme 3.2</b> Intermolecular cascade annulation reaction.....	40
<b>Scheme 3.3.</b> Extension of our methodology to banyasides.....	41
<b>Scheme 3.4</b> Our retrosynthetic approach to banyaside core <b>65</b> .....	42
<b>Scheme 4.1</b> Previous synthesis of key unsaturated acid <b>86</b> .....	43
<b>Scheme 4.2</b> Second-generation synthesis of acid <b>86</b> .....	44
<b>Scheme 4.3.</b> Retrosynthetic analysis for acid <b>86</b> .....	45
<b>Scheme 4.4</b> Optimized synthetic route to acid <b>86</b> . ....	47
<b>Scheme 4.5</b> Synthesis of <i>N</i> -Tosyl- <i>O</i> -TMS aminol <b>77</b> .....	48
<b>Scheme 4.6</b> Attempt at cyclization of <b>77</b> .....	49
<b>Scheme 4.7</b> Synthesis of <i>N</i> -Cbz- <i>O</i> -TMS aminol <b>99</b> . ....	50
<b>Scheme 4.8</b> Cyclization of <i>N</i> -Cbz- <i>O</i> -TMS aminol <b>99</b> . ....	51

<b>Scheme 4.9</b> Synthesis of amine <b>103</b> and key nOe correlations.....	53
<b>Scheme 4.10</b> Reduction of carbamate <b>102</b> with LiAlH <sub>4</sub> . .....	54
<b>Scheme 4.11</b> Synthesis of <i>N</i> -benzyl- <i>O</i> -TBDMS-cyclohexanol <b>106</b> . .....	55
<b>Scheme 4.12</b> Proposed mechanism for the cyclization of <b>99</b> . .....	56
<b>Scheme 5.1</b> General strategy for an asymmetric cascade reaction.....	58
<b>Scheme 5.2</b> Thiourea Catalyzed Pictet-Spengler Reaction. ....	60
<b>Scheme 5.3</b> Urea catalyzed Povarov Reaction. ....	61
<b>Scheme 5.4</b> Thiourea catalyzed cation polycyclization. ....	62
<b>Scheme 5.5</b> Proposed mechanistic strategy with a thiourea catalyst.....	63
<b>Scheme 5.6</b> Synthesis of chiral thiourea <b>124</b> . .....	64
<b>Scheme 5.7</b> Attempts to cyclized with achiral Brønsted acids.....	65
<b>Scheme 5.8</b> Cyclization with methane sulfonic acid.....	66
<b>Scheme 5.9</b> Braun's dynamic kinetic asymmetric allylation using catalyst <b>130</b> . ....	67
<b>Scheme 5.10</b> Postulated mechanism for DKAA with <b>130</b> . ....	68
<b>Scheme 5.11</b> Synthesis of difluorotitanate <b>130</b> . .....	69
<b>Scheme 5.12</b> Synthesis of model substrate <b>131</b> . .....	72
<b>Scheme 5.13</b> Proposed extension of methodology with <i>Z</i> and <i>E</i> -trisubstituted olefins. ..	73
<b>Scheme 5.14</b> Cyclization with disubstituted enol ethers <b>148</b> and <b>149</b> . ....	74
<b>Scheme 6.1</b> Cascade annulation for the synthesis of the Malagasy core. ....	83

<b>Scheme 6.2</b> Cyclization of <i>E</i> -isomer leading to correct stereochemistry at C(16). .....	85
<b>Scheme 6.3</b> Formal hydroacylation of <b>162</b> .....	86
<b>Scheme 6.4</b> Synthesis and structural assignment of pyran <b>169</b> .....	87
<b>Scheme 7.1</b> Synthesis of iodo-alcohol <b>173</b> .....	88
<b>Scheme 7.2</b> Synthesis of $\beta,\gamma$ -unsaturated acid <b>175</b> . .....	89
<b>Scheme 7.3</b> Coupling of acid <b>175</b> and tosylamide <b>176</b> . .....	89
<b>Scheme 7.4</b> Initial conditions for the synthesis of <i>N</i> -Tosyl- <i>O</i> -TMS aminol <b>161</b> .....	90
<b>Scheme 7.5</b> Hypothesized role of imidazole in reaction sequence. ....	91
<b>Scheme 7.6</b> Optimized synthesis of <i>N</i> -Tosyl- <i>O</i> -TMS aminol <b>161</b> .....	93
<b>Scheme 7.7</b> Key cyclization of <i>N</i> -Tosyl- <i>O</i> -TMS aminol <b>161</b> .....	93
<b>Scheme 7.8</b> Conversion of tetracyclic <b>162</b> into dihydropyran <b>169</b> . .....	94
<b>Scheme 7.9</b> Synthesis of aldehyde <b>182</b> . .....	95
<b>Scheme 7.10</b> Synthesis of ester <b>184</b> . .....	97
<b>Scheme 7.11</b> Trost's group use of trichloroacetyl chloride for the synthesis of esters. ....	98
<b>Scheme 7.12</b> Second generation approach to ester <b>184</b> . .....	98
<b>Scheme 7.13</b> Possible formation of chloride <b>190</b> and previously reported elimination in simpler systems. ....	99
<b>Scheme 7.14</b> Synthesis of methyl trifluoroketone <b>195</b> and X-ray structure.....	100
<b>Scheme 7.15</b> Alcoholysis attempt on trifluoroketone <b>195</b> . .....	101
<b>Scheme 7.16</b> Hydrolysis of methyl trifluoroketone <b>195</b> . .....	101

<b>Scheme 7.17</b> Synthesis of methyltrifluoro ketone <b>199</b> .....	102
<b>Scheme 7.18.</b> Decarboxylation of methyl trifluoroketone <b>199</b> . ....	103
<b>Scheme 7.19</b> Synthesis of ester <b>184</b> via hydrolysis of <b>199</b> . ....	103
<b>Scheme 7.20</b> Synthesis of model dihydropyran <b>200</b> . ....	104
<b>Scheme 7.21</b> Ionic reduction of methyl-ester <b>184</b> with Et <sub>3</sub> SiH-TFA reagent.....	107
<b>Scheme 7.22</b> Rationalization for the lack of enolate formation for compound <b>205</b> .....	109
<b>Scheme 7.23</b> Synthesis of epi-malagashanine ( <b>206</b> ). ....	110
<b>Scheme 8.1</b> First generation strategy to 11-demethoxymyrtoidine ( <b>154</b> ). ....	112
<b>Scheme 8.2</b> Proposed synthesis of malagashanine ( <b>151</b> ) from butyrolactone <b>210</b> . ....	112
<b>Scheme 8.3</b> Korte's Synthesis of butyrolactone <b>217</b> . ....	113
<b>Scheme 8.4</b> Free radical halogenation of methyl-ester <b>184</b> . ....	114
<b>Scheme 8.5</b> Oxidation of 2-methylpyridine ( <b>220</b> ) via anion formation. ....	115
<b>Scheme 8.6</b> Sarpong's oxidative C-N bond formation.....	115
<b>Scheme 8.7</b> Synthesis of butyrolactone <b>217</b> via extended enolate.....	116
<b>Scheme 8.8</b> Attempts at functionalization <i>via</i> enolate formation.....	117
<b>Scheme 8.9</b> Attempted oxidation <i>via</i> enolate formation of acid <b>183</b> . ....	117
<b>Scheme 8.10</b> Benzolactone formation by palladium catalyzed C-H activation. ....	118
<b>Scheme 8.11</b> Palladium-catalyzed C-H functionalization attempt.....	119
<b>Scheme 8.12</b> Retrosynthetic analysis for the second-generation approach to 11-demethoxymyrtoidine ( <b>154</b> ). ....	120

<b>Scheme 8.13</b> Synthesis of $\alpha$ -acetoxy hemiacetal <b>240</b> .....	121
<b>Scheme 8.14</b> Initial-access to dihydropyran <b>242</b> .....	122
<b>Scheme 8.15</b> Acylation attempts for compound <b>242</b> .....	122
<b>Scheme 8.16</b> Synthesis of dihydropyran <b>245</b> . ....	123
<b>Scheme 8.17</b> Acylations of model system <b>245</b> .....	124
<b>Scheme 8.18</b> Synthesis of model butyrolactone <b>217</b> from trifluoroketone <b>248</b> . ....	124
<b>Scheme 8.19</b> Synthesis of trifluoroacetamide <b>252</b> . ....	125
<b>Scheme 8.20</b> Vilsmeier-Haack reaction of trifluoroacetamide <b>252</b> . ....	125
<b>Scheme 8.21</b> Mechanistic rationale for the formation of chloride <b>254</b> . ....	126
<b>Scheme 8.22</b> Retrosynthetic analysis of the third-generation approach to demethoxymyrtoidine .....	128
<b>Scheme 8.23</b> Hydrolysis of acetate <b>239</b> . ....	129
<b>Scheme 8.24</b> Smith and coworkers methodology for the synthesis of tetronic acids. ...	130
<b>Scheme 8.25</b> Attempt to form tetronic acid via dianion formation.....	130
<b>Scheme 8.26</b> Mechanistic-rationale for the formation of dioxolenone <b>264</b> . ....	131



## Table of Figures

<b>Figure 1.1.</b> Vicinal amino alcohol motif in biologically active molecules.....	2
<b>Figure 1.2.</b> Synthetic approaches to vicinal amino alcohols.....	3
<b>Figure 2.1</b> Proposed mechanism for Cu(I)-catalyzed aminoacetoxylation.....	25
<b>Figure 3.1</b> Banyaside A ( <b>63</b> ) and banyaside B ( <b>64</b> ).....	35
<b>Figure 3.2</b> Important nOes correlations for banyaside A.....	36
<b>Figure 4.1</b> Stacked VT-NMR experiments on cyclohexene <b>102</b> , top (CDCl <sub>3</sub> at 300 K), bottom (DMSO at 343 K). .....	52
<b>Figure 5.1</b> Comparison of strategies for an asymmetric cascade reaction.....	59
<b>Figure 5.2</b> HRMS (left) and <sup>19</sup> F NMR (right) of difluorotitanate <b>130</b> . .....	71
<b>Figure 6.1</b> The malagashanine alkaloids and related compounds.....	77
<b>Figure 6.2</b> nOe studies on the malagashanine alkaloids. ....	79
<b>Figure 6.3</b> X-ray structure for methoxy-analog <b>160</b> . .....	84
<b>Figure 7.1</b> TLCs taken after incremental additions of imidazole. ....	92
<b>Figure 7.2</b> Compound <b>182</b> is a vinylogous formate ester. ....	96
<b>Figure 7.3</b> X-ray structure for compound <b>205</b> . ....	108
<b>Figure 8.1</b> Rational for the difference in reactivity.....	127

## Table of Tables

<b>Table 2.1</b> Initial investigations .....	15
<b>Table 2.2</b> Oxidant and activating group optimization.....	17
<b>Table 2.3</b> Base and catalyst optimization.....	18
<b>Table 2.4</b> Solvent optimization .....	19
<b>Table 2.5</b> Summary of results for the copper catalyzed aminoacetoxylation of olefins ..	33
<b>Table 4.1</b> Oxidation of homo-propargyl alcohol <b>93</b> .....	46
<b>Table 5.1</b> Cyclization with thiourea catalyst <b>124</b> .....	66
<b>Table 5.2</b> NMR data ( <sup>1</sup> H: 600; <sup>13</sup> C 151; <sup>19</sup> F 565 MHz) for <b>130</b> (CD <sub>3</sub> CN) and ( <sup>1</sup> H: 500; <sup>13</sup> C 125; <sup>19</sup> F 470 MHz) for <b>140</b> (CD <sub>3</sub> CN).....	70
<b>Table 6.1</b> Chloroquine potentiating activity of malagashanine on CQR strain of <i>Plasmodium falciparum</i> FCM 29/Cameroon.....	81
<b>Table 7.1</b> Hydrogenation results on model dihydropyran <b>200</b> .....	105
<b>Table 7.2</b> Results from the hydrogenation of acid <b>183</b> . .....	106

## Abbreviations

Ac	acetyl
AcOH	acetic acid
9-BBN	9-borabicyclo[3.3.1]nonene
Boc	<i>tert</i> -butoxycarbonyl
Bn	benzyl
br	broad
<i>n</i> -BuLi	<i>n</i> -butyllithium
<i>t</i> -BuOOH	<i>tert</i> -butylhydroperoxide
Cbz	benzyloxycarbonyl
d	doublet
dba	dibenzylideneacetone
DCE	1, 2-dichloroethane
DCM	dichloromethane
DIBAL-H	diisobutylaluminum hydride
DMAP	<i>N, N</i> -dimethylaminopyridine
DME	1, 2-dimethoxyethane
DMF	<i>N, N</i> -dimethylformamide
DMP	Dess-Martin periodinane
DMPU	<i>N, N'</i> -dimethyl- <i>N, N'</i> -propylene urea
DMS	dimethylsulfide
DMSO	dimethylsulfoxide
EDCI	1-ethyl-3-(3-dimethylaminopropylcarbodiimide)

equiv.	equivalent
ESI	electrospray ionization
EtOAc	ethyl acetate
HMPA	hexamethylphosphoric triamide
HOBt	1-hydroxybenzotriazole
HRMS	high resolution mass spectroscopy
IBX	2-iodoxybenzoic acid
KHMDS	potassium <i>bis</i> (trimethylsilyl)amide
LA	Lewis acid
LAH	lithium aluminum hydride
LDA	lithium diisopropylamide
LiHMDS	lithium <i>bis</i> (trimethylsilyl)amide
LiTMP	lithium 2,2,6,6-tetramethylpiperidide
m	multiplet
mmol	millimole
NaHMDS	sodium <i>bis</i> (trimethylsilyl)amide
Naph	naphtyl
NIS	<i>N</i> -iodosuccinimide
NMO	<i>N</i> -methylmorpholine <i>N</i> -oxide
NMR	nuclear magnetic resonance
Ns	4-nitrobenzenesulfonyl
PIDA	phenyliododiacetate
Ph	phenyl

PMP	<i>para</i> -methoxyphenyl
ppm	parts per million
PTSA	<i>para</i> -toluenesulfonic acid
q	quartet
quint	quintet
rt	room temperature
s	singlet
t	triplet
TBAHS	tetrabutylammonium hydrogen sulfate
TBME	<i>tert</i> -butyl methyl ether
TBDMS	<i>tert</i> -butyldimethylsilyl
TBDPS	<i>tert</i> -butyldiphenylsilyl
TCBoc	2,2,2-trichloro- <i>tert</i> -butyloxycarbonyl
Tf	trifluoromethanesulfonyl
TFA	trifluoroacetic acid
TFAA	trifluoroacetic anhydride
TFP	tris(2-furyl)phosphine
THF	tetrahydrofuran
THP	tetrahydropyran
TMS	trimethylsilyl
TPAP	tetrapropylammonium perruthenate
Ts	<i>para</i> -toluenesulfonyl
w	weak

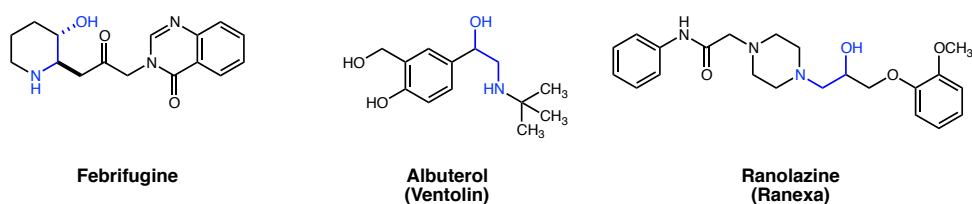
**Part 1**  
**Copper Catalyzed Aminoacetoxylation of Olefins**

# 1 Chapter 1

## *Introduction to Vicinal Amino Alcohols and Aminohydroxylation Reactions.*

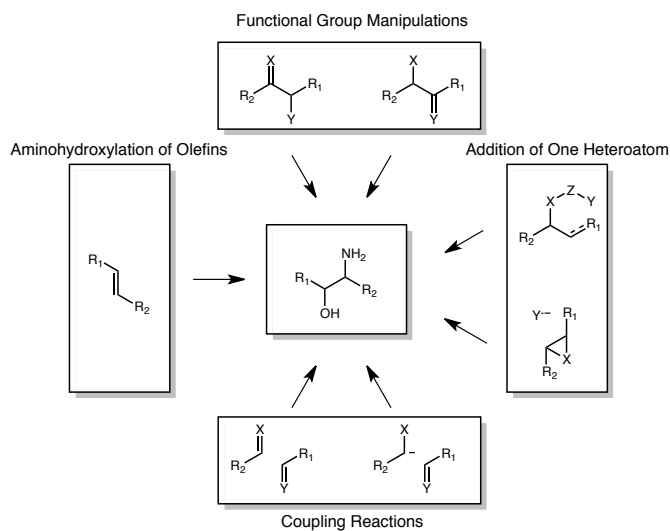
### 1.1 Vicinal Amino Alcohols.

Vicinal amino alcohols are an important structural component commonly found in a variety of naturally occurring molecules, organic based catalysts and active pharmaceutical ingredients.<sup>1</sup> In addition, 1,2 amino alcohols or  $\beta$ -amino alcohols, as they are also known, are commonly used as pharmacophores by computational chemists in drug discovery processes.<sup>2</sup> Three examples of important molecules containing a vicinal amino alcohol motif are: febrifugine, salbutamol and ranolazine (Figure 1.1). Febrifugine has recently been shown to exhibit potent anti-malaria activity.<sup>3</sup> Salbutamol or albuterol has been used for almost 50 years as a  $\beta_2$ -adrenergic receptor agonist for the relief of bronchospasms.<sup>4</sup> Lastly, ranolazine is an antianginal medication with sales of over 250 million a year.<sup>5</sup>



**Figure 1.1.** Vicinal amino alcohol motif in biologically active molecules.

A vicinal amino alcohol can have either the amine or the oxygen acylated, alkylated or contained within rings. Moreover, the relative (as well as absolute) stereochemistry plays a critical role in the biological activity of molecules containing a vicinal amino alcohol. Therefore, a number of approaches for the stereoselective synthesis of vicinal amino alcohols have been developed. These approaches can be divided into four major classes: (1) functional group manipulation of a molecule containing both heteroatoms; (2) coupling of two molecules each containing one heteroatom (3) addition of one heteroatom to a molecule already containing another heteroatom; (4) addition of both heteroatoms to a molecule that contains neither or what is better known as olefin aminooxygenation reaction (Figure 1.2).



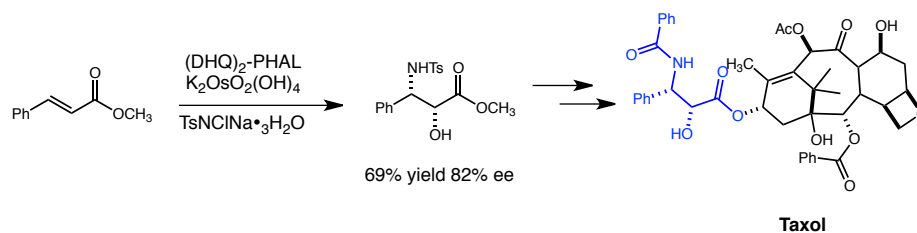
**Figure 1.2.** Synthetic approaches to vicinal amino alcohols.

## 1.2 Aminohydroxylation Reactions.



### 1.2.1 Osmium Catalyzed Aminohydroxylation Reactions

One of the most powerful methods for the synthesis of vicinal amino alcohols is the difunctionalization of alkenes. Considering that alkenes are easily accessible and robust synthetic intermediates, a difunctionalization reaction is an attractive and easy route for the synthesis of vicinal amino alcohols. Moreover, this method is attractive because it introduces both nitrogen and oxygen in one chemical step.<sup>6</sup> Pioneered by elegant work of Sharpless and co-workers, the enantioselective *intermolecular* osmium-catalyzed *cis*-amino-oxygenation of alkenes is still one of the best examples of this type of transformation.<sup>7</sup> Its practicality has been showcased in the synthesis of various complex molecules, such as Taxol®.<sup>8</sup>

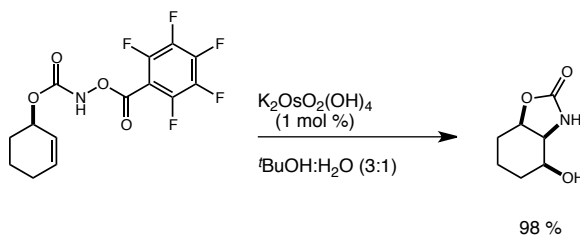


**Scheme 1.1** Sharpless asymmetric aminohydroxylation used in Taxol synthesis.

While the Sharpless asymmetric aminohydroxylation (AA) reaction is a powerful reaction for the difunctionalization of olefins due to its high stereospecificity, this reaction suffers from issues of regioselectivity as well as issues with the use of substoichiometric amounts of potassium osmate, which could become an environmental and economic burden in large-scale processes. Furthermore, for a transformation to be attractive in organic synthesis, it needs to tolerate other functional groups as well as

reduce the number of manipulations necessary to convert that product into the desired synthetic target. Thus, an *intramolecular* amino-oxygenation reaction, in which either the nitrogen or the oxygen atom is tethered to part of a molecule, would be an excellent variant of the AA reaction.

The Donohoe group has been able to develop an *intramolecular* variant of the AA reaction.<sup>9</sup> Tethering a carbamate group containing an *O*-pentafluorobenzoyl group, (osmium oxidant) to an allylic alcohol, the Donohoe group has been able to prepare various oxazolidines with good diastereoselectivities. Although this methodology does provide an intramolecular variant to the (AA) reaction, it in itself has some limitations. The *O*-pentafluorobenzoyl group, which is not only a coordinating group, but the oxidant as well, is not a very common reagent and its price and availability can be a problem.

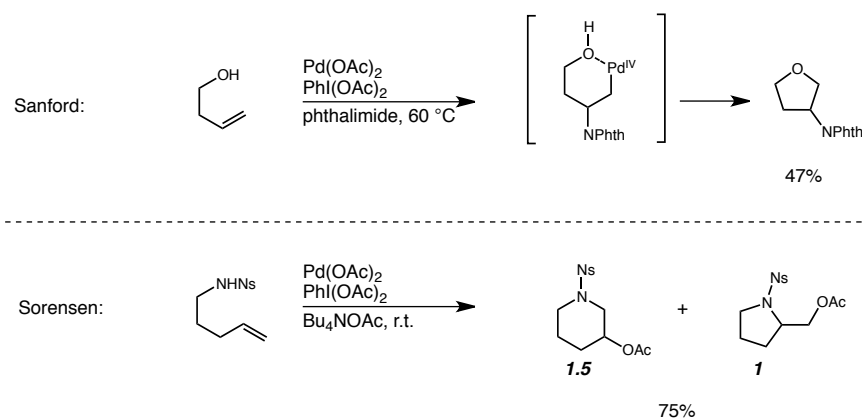


**Scheme 1.2** Intramolecular variant to the AA reaction

## 1.2.2 Palladium Catalyzed Aminohydroxylation Reactions

The past ten years have seen the development of methodologies for the amino-oxygenation of olefins using palladium as the transition metal catalyst. In general, these reactions take place in the presence of a strong and readily available oxidant.<sup>10</sup> For

example, the Sanford group has developed an intermolecular amino-oxygenation reaction that generates substituted furans as products. Mechanistic studies have shown that presence of a strong oxidant is crucial in order to rapidly oxidize the alkyl Pd<sup>II</sup> intermediate to an alkyl Pd<sup>IV</sup> intermediate, thereby suppressing the common  $\beta$ -hydride elimination or aza-Wacker type products.<sup>6</sup> Sorensen and co-workers have developed a similar process for the amino-oxygenation of unsaturated sulfonamides to construct pyrrolidine and piperidine adducts.<sup>11</sup> In this case, a nitrogen atom instead of an oxygen atom is tethered to the olefinic chain. Phenyl iododiacetate [PhI(OAc)<sub>2</sub>] is used as an oxidant with stoichiometric quantities of Bu<sub>4</sub>NOAc which serves as a base.



**Scheme 1.3** Palladium catalyzed amino-oxygenation reactions.

While these two methodologies made good progress towards a catalytic intramolecular amino-oxygenation reaction, they still possess some limitations. For example, in Sanford's methodology, the nucleophile, phthalimide, is the limiting reagent and a large excess of olefin is necessary. In addition, often times cyclization must be induced by using substrates that take advantage of the Thorpe-Ingold effect, thereby

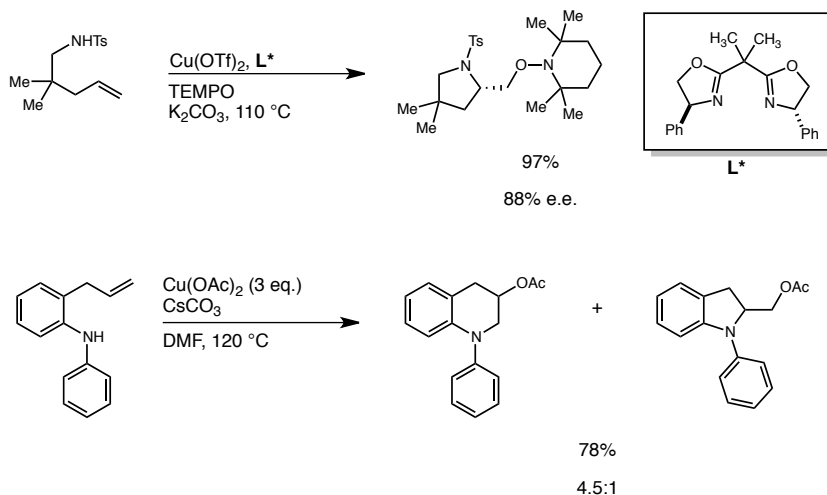
limiting the generality of this methodology. The Sorensen methodology is accompanied by its own limitations as well. There is often no control of regioselectivity, *endo* (piperidine) vs *exo* (pyrrolidine). Although the regioselectivity can be improved with a set of different conditions (AcOH/H<sub>2</sub>O), these set of new conditions are not mild and might not be suitable for substrates containing acid sensitive functionalities. It is important to realize that lack of regioselectivity can become a problem when the separation of regioisomers by traditional chromatographic techniques is not possible.<sup>11</sup>

### 1.2.3 Copper Catalyzed Amino-oxygenation Reactions.

The Chemler group at SUNY Buffalo has developed a methodology for the diastereoselective amino-oxygenation of olefins based on a copper (II) catalyst system.<sup>12a</sup>  
<sup>12b</sup> This methodology has been extended to the use of chiral ligands to effect the enantioselective formation of vicinal amino alcohols. Interestingly, treatment of aniline based olefins with stoichiometric copper (II) acetate yields a mixture of regioisomeric products.<sup>13</sup>

While this methodology has advanced the field of olefin amino-oxygenation reactions, first by using a readily available and cheap metal (copper) and, second by providing pyrrolidine adducts in moderate to good enantioselectivities, it still has some limitations. High temperatures in basic medium are required, which again are not mild conditions. More importantly this chemistry is applicable to the synthesis of the *exo* regioisomer, (i.e. the pyrrolidine adduct), unless *stoichiometric* copper is used. Lastly,

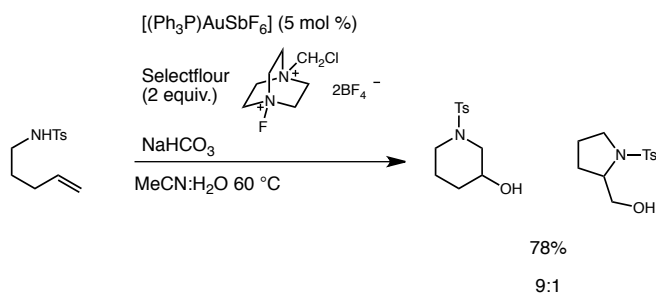
like the Pd catalyzed reactions developed previously, this methodology does not tolerate 1,2 disubstituted olefin, which show a lack of reactivity under these conditions.



**Scheme 1.4.** Copper mediated amino-oxygenation reactions.

### 1.2.4 Gold Catalyzed Amino-oxygenation Reactions.

Concurrent with our studies, the Nevado group, has developed a gold-based intramolecular amino-oxygenation reaction with Selectfluor as the oxidant.<sup>14</sup> This methodology yields amino alcohols in good yields and with good control of regioselectivity, favoring the 6-*exo*-cyclization products.



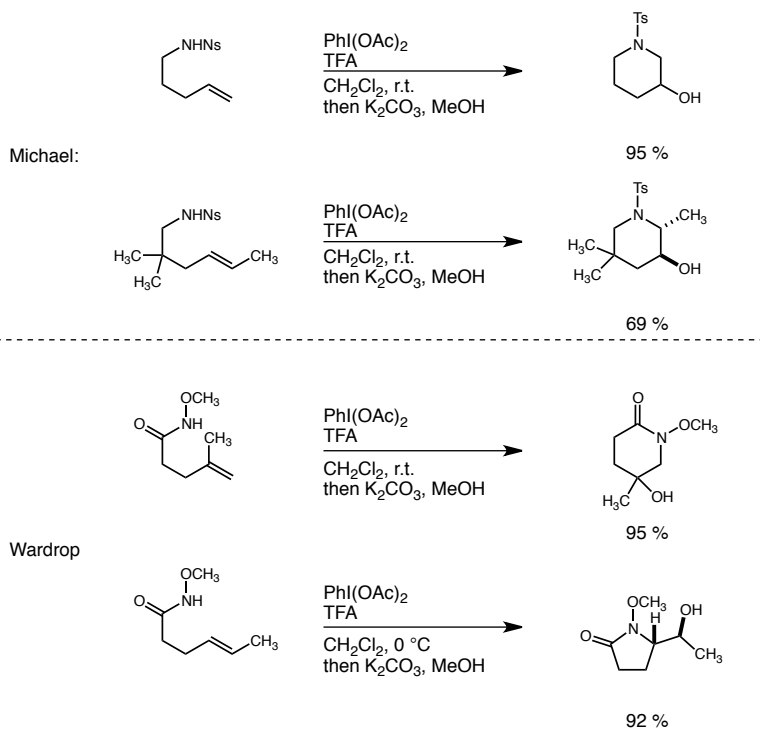
**Scheme 1.5** Gold catalyzed amino-oxygenation of olefins.

Although this reaction is highly regioselective, problems still exist with reactivity of 1,2 disubstituted olefins. The authors of this publication state that “*a 1,2 substitution pattern on the olefin seemed to be an intrinsic limitation for these gold-catalyzed aminooxygenation reaction.*” In general, 1,2 disubstituted olefins have been a problem for metal catalyzed amino-oxygenation reactions. In fact, Liu and Stahl have stated that: “*in general, internal olefins appear to be a ineffective substrates.*”<sup>15</sup>

### 1.2.5 Metal Free Amino-oxygenation Reactions.

Recent reports from both the Michael and Wardrop showed that the intramolecular amino-oxygenation reactions could be performed in a metal-free fashion.<sup>16a, 16b</sup> Unlike the metal catalyzed amino-oxygenation reactions, these two methodologies show reactivity towards 1,2 disubstituted olefins.

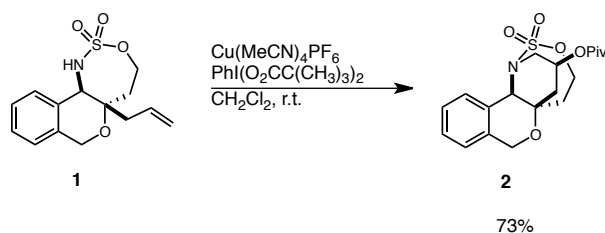
Although both methodologies show complimentary reactivity towards 1,2 disubstituted olefins, in both cases strong acidic media (typically TFA) is necessary to accelerate these reactions, provide useful levels of conversion and be the oxygen source. Therefore, these conditions may not be applicable to complex substrates bearing acid sensitive functionalities.



**Scheme 1.6** Metal-free amino-oxygenation reactions.

### 1.2.6 Blakey's Group Entry into Amino-oxygenation Reactions

During the course of expanding the scope of our metallonitrine chemistry, Dr. Armin Stoll made an intriguing observation. Oxathiazopene **1**, which is a product of our metallonitrine cascade reaction methodology, could be converted to tetracyclic oxygenated piperidine **2** when treated with 20%  $\text{Cu}(\text{MeCN})_4\text{PF}_6$  and  $\text{PhI}(\text{O}_2\text{CC}(\text{CH}_3)_3)_2$  in  $\text{CH}_2\text{Cl}_2$  at room temperature (Scheme 1.7).<sup>17</sup>



**Scheme 1.7** Discovery of the copper-catalyzed amino-oxygenation reaction.

This amino-oxygenation reaction resulted in diastereoselective and regioselective formation of tetracycle **2**, a result of a 6-*endo*-cyclization. This result stood in stark contrast to previously developed metal catalyzed amino-oxygenations of olefins, which often resulted in the formation of the 5-*exo*-cyclized or pyrrolidine products. In addition, we realized that the mild conditions could offer a useful complement to the metal-free amino-oxygenation protocols. However, at the time, we needed to determine if these unique features were a property of the newly discovered set of conditions or simply due to the rigid and unique architecture of **1**. The following chapter will detail our efforts to optimize these early conditions as well as the application to a variety of substrates including the challenging 1,2 disubstituted olefins.



## 2 Chapter 2

### *Copper Catalyzed Aminoacetoxylation of Olefins.*

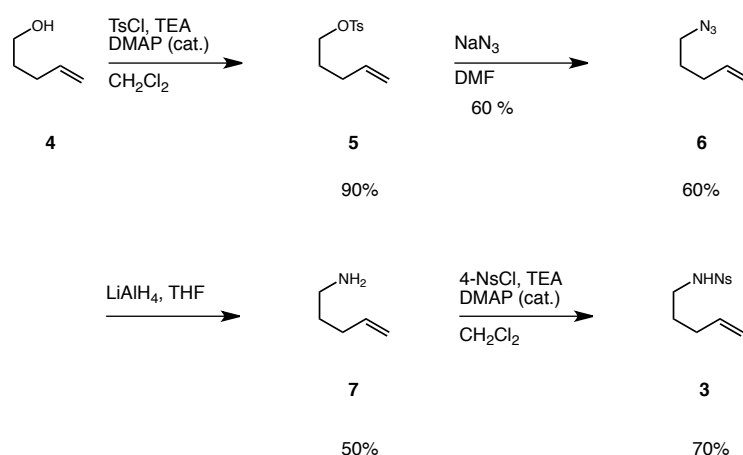
#### 2.1 Synthesis of Sulfonamide **3**.

##### 2.1.1 Initial Synthesis of Sulfonamide **3**

Our studies into the copper catalyzed amino-oxygenation of olefins started by stripping off the complexity of oxathiazopane **1**, while at the same time, keeping the functional groups of **1** that were involved in the amino-oxygenation reaction. In addition, we realized that our conditions resembled the ones developed by the Sorensen's group in their palladium-catalyzed amino-oxygenation of olefins. Therefore, we decided to start investigating the generality of our conditions using sulfonamide **3**, which was also used by the Sorensen's group for the development of their Pd catalyzed methodology (*vide supra*).

The synthesis of **3** began with tosylation of commercially available unsaturated alcohol **4** with 3 equivalents of tosyl chloride and catalytic DMAP as described in the literature (Scheme 2.1).<sup>18</sup> Unfortunately, our initial attempts to separate the excess tosyl chloride from the product via flash chromatography were unsuccessful. Fortunately, we found that excess tosyl chloride was unnecessary for the reaction to reach completion. Thus, tosylation of **3** with 1.05 equivalents of tosyl chloride and catalytic DMAP

followed by simple purification via silica gel plug yielded the desired O-Tosyl intermediate **5** in excellent yield (90%). Nucleophilic displacement of the tosyl group yielded unsaturated azide **6**, which proved to be a highly volatile material.<sup>19</sup> Nevertheless, this compound was reduced to the desired 4-pentene-1-amine (**7**) in 60% yield. Treatment of **7** with triethylamine and 4-nitrobenzenesulfonyl chloride yielded sulfonamide **3** in good yield (70%).

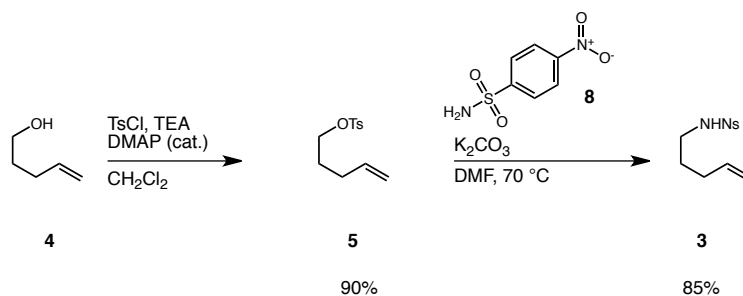


**Scheme 2.1** Initial synthesis of sulfonamide **3**.

### 2.1.2 New Synthesis of Sulfonamide **3**

Although we were able to obtain small quantities of sulfonamide **3** via this initial route, it was far from robust and not scalable due to the low molecular weight and volatility of azide **6** and amine **7**. Therefore, we decided to come up with a new route for the synthesis of **3**. Since the synthesis of tosylate **4** was relatively simple and high yielding, we decided to start by looking at a new route that would involved sulfonate

esters as intermediates. We adapted a procedure found in the literature for the synthesis of tosylamines from mesylates.<sup>20</sup> Thus, reaction of the tosylate **4** with 4-nitrobenzene sulfonamide (**8**) in DMF at 70 °C gave the desired nitrobenzenesulfonamide **3** in 85% yield (Scheme 2.2). This new route has provided up to 5 grams of sulfonamide **3**.

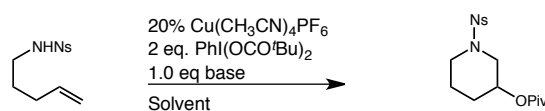


**Scheme 2.2** Convergent synthesis for sulfonamide **3**.

## 2.2 Initial Investigations.

With sulfonamide **3** in hand, we began to investigate whether the amino-oxygenation conditions found for oxathiazopane **1** could be also be applied to simple systems. Unfortunately, the initial discovery conditions, 20% Cu(MeCN)<sub>4</sub>PF<sub>6</sub> and PhI(O<sub>2</sub>CC(CH<sub>3</sub>)<sub>3</sub>)<sub>2</sub> in CH<sub>2</sub>Cl<sub>2</sub> at room temperature, did not give any amino-oxygenated product **9** and just returned starting material (Table 2.1). Next we decided to introduce Bu<sub>4</sub>NOAc (TBAA) into our reaction conditions. TBAA was previously shown by the Sorensen's group to improve the rate and yield of their amino-oxygenation reactions by acting as a mild base.<sup>11</sup> However, with TBAA we were not able to isolate the amino-oxygenation product **9** and again just returned starting material (entry 2). At this point we

hypothesized that  $\text{Bu}_4\text{NOAc}$  was not a strong enough base to affect cyclization of the amine, therefore we turned to  $\text{KO}^t\text{Bu}$  instead.  $\text{KO}^t\text{Bu}$  proved too strong of a base and only decomposition was observed for this reaction (entry 3). Finally, we decided to use  $\text{K}_2\text{CO}_3$ , which had some precedence in diamination reactions of similar substrates.<sup>21</sup> Reaction of sulfonamide **3** with  $\text{K}_2\text{CO}_3$ , in  $\text{CH}_2\text{Cl}_2$  gave exclusively the *endo* cyclized amino-oxygenated product **9**, although in a modest 50% isolated yield (entry 4). Although we had established proof of concept for the amino-oxygenation reaction of olefins using our conditions, we were unsatisfied with the low yield generated under our conditions. Therefore, we decided to initiate some optimization studies.



Entry	Base	Solvent	Temperature	Results
1	-----	$\text{CH}_2\text{Cl}_2$	r.t.	no reaction
2	$\text{Bu}_4\text{NOAc}$	$\text{CH}_2\text{Cl}_2$	r.t.	no reaction
3	$\text{K}^t\text{OBu}$	$\text{CH}_2\text{Cl}_2$	r.t.	decomposition
4	$\text{K}_2\text{CO}_3$	$\text{CH}_2\text{Cl}_2$	r.t.	50% yield

**Table 2.1** Initial investigations

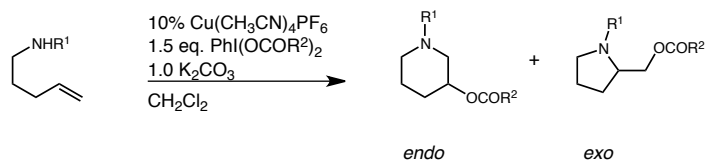
## 2.3 Optimization Studies

### 2.3.1 NMR Assay

To expedite the optimization process, we needed to develop a quick and easy assay for the determination of yields of crude reaction mixtures. Unfortunately neither GC nor HPLC provided satisfactory assays for the optimization. In the case of HPLC, we found it difficult to resolve starting sulfonamide **3** from product(s). We next turned to NMR spectroscopy for a crude assay. NMR is increasingly being used as a tool for quantitative analysis. NMR is a powerful quantitative tool as the integrated intensity of a signal is proportional to the number of nuclei represented by the signal.<sup>22</sup> Thus a quantitative <sup>1</sup>H NMR spectroscopy assay (qNMR) was developed with trimethoxybenzene as an internal standard.

### 2.3.2 Oxidant Optimization and Activating Group Optimization.

We began our optimization studies by examining how the nature of the carboxyl group on the oxidant impacted yield (Table 2.2). The pivaloate carboxylate, which had been so far as the oxidant gave a 73% assay yield with an excellent regioselectivity (entry 1). Similar assay yields and regioselectivity were obtained when the more soluble dimethylphenyl acetate carboxylate was used (entry 2). Lastly, PIDA gave the highest assay yield (88%) of all three oxidants screened (entry 3).



Entry	R <sub>1</sub>	R <sub>2</sub>	% yield <sup>a</sup>	endo:exo
1	Ns	<sup>t</sup> Bu	73	9:1
2	Ns	C(Me <sub>2</sub> Ph)	70	9:1
<b>3</b>	<b>Ns</b>	<b>CH<sub>3</sub></b>	<b>88</b>	<b>9:1</b>
4	Ts	CH <sub>3</sub>	47	4:1
5	Ac	CH <sub>3</sub>	---	---
6	Boc	CH <sub>3</sub>	---	---

*a*= assay yield determined by <sup>1</sup>H NMR with 1,3,5 trimethoxybenzene as internal standard

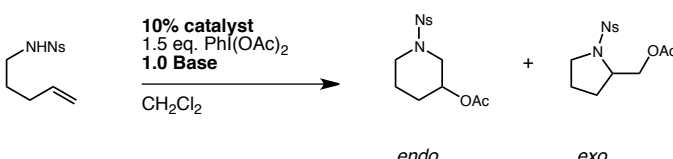
**Table 2.2** Oxidant and activating group optimization.

Next, we examined the nature of the activating group on the nitrogen atom. Reactivity was not observed when carbamoyl and acyl groups were used on the nitrogen (entries 5-6). In fact, reactivity was only observed when sulfonyl based activating groups were present (entries 3-4). Additionally, qNMR revealed that the nosyl activating group (entry 3) had an assay yield that was almost two times greater than the tosyl group (entry 4).

### 2.3.3 Base and Catalyst Optimization.

Having established PIDA as the best oxidant and 4-nosyl group as the best activating group, we decided to revisit the effect of bases on yields (Table 2.3). Carbonate bases (entries 1-2) were shown to be more effective than the more soluble tetrabutylammonium acetate or stronger KO<sup>t</sup>Bu (entries 3-4). Again, we were pleased to

find that all bases were selective for *piperidine* formation. In addition, a screen of catalysts, showed that  $\text{Cu}(\text{MeCN})_4\text{PF}_6$  was the best catalyst when compared to other copper (I) sources (entries 2, 5-7).



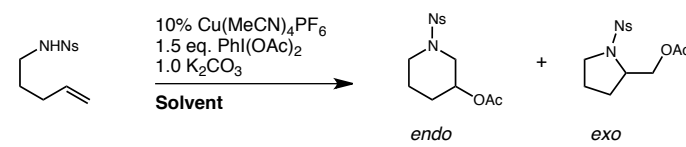
Entry	Base	Catalyst	% yield <sup>a</sup>	endo:exo
1	$\text{CsCO}_3$	$\text{Cu}(\text{MeCN})_4\text{PF}_6$	72	9:1
<b>2</b>	<b><math>\text{K}_2\text{CO}_3</math></b>	<b><math>\text{Cu}(\text{MeCN})_4\text{PF}_6</math></b>	<b>88</b>	<b>9:1</b>
3	$\text{Bu}_4\text{NOAc}$	$\text{Cu}(\text{MeCN})_4\text{PF}_6$	34	9:1
4	$\text{KO}^t\text{Bu}$	$\text{Cu}(\text{MeCN})_4\text{PF}_6$	43	4:1
5	$\text{K}_2\text{CO}_3$	$\text{Cu}(\text{MeCN})_4\text{ClO}_4$	10	9:1
6	$\text{K}_2\text{CO}_3$	$\text{CuI}$	----	----
7	$\text{K}_2\text{CO}_3$	$\text{CuOTf}$	37	9:1

<sup>a</sup> = assay yield determined by <sup>1</sup>H NMR with 1,3,5 trimethoxybenzene as internal standard

**Table 2.3** Base and catalyst optimization

### 2.3.4 Solvent Optimization.

The nature of the solvent had a profound effect on both the reaction yield and regioselectivity (Table 2.4). Dichloromethane and trifluorotoluene gave similar yields and regioselectivities (entries 1-2). On the other hand, we observed a loss of yield with benzene and toluene (entries 3-4). Interestingly, we observed a considerable improvement in regioselectivity with benzene (entry 4). Finally, THF did not yield any product(s) and showed just starting material by qNMR.



Entry	Solvent	% yield <sup>a</sup>	endo:exo
<b>1</b>	<b>CH<sub>2</sub>Cl<sub>2</sub></b>	<b>88</b>	<b>9:1</b>
2	CF <sub>3</sub> C <sub>6</sub> H <sub>6</sub>	72	11:1
3	CH <sub>3</sub> C <sub>6</sub> H <sub>6</sub>	18	7:3
4	C <sub>6</sub> H <sub>6</sub>	29	19:1

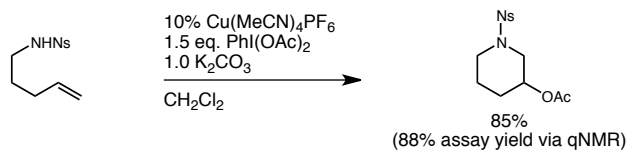
<sup>a</sup>= assay yield determined by <sup>1</sup>H NMR with 1,3,5 trimethoxybenzene as internal standard

**Table 2.4** Solvent optimization

## 2.4 Intermolecular aminoacetoxylation of $\gamma$ -aminoolefins.

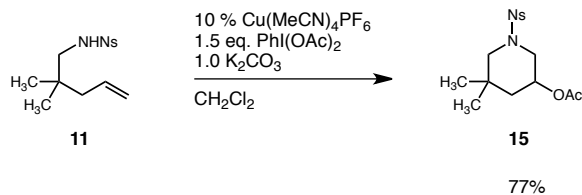
### 2.4.1 Terminal Olefins.

Under the optimized reaction conditions (Table 2.4, entry 1) a variety of  $\gamma$ -aminoolefins were investigated. Aminoacetoxylation of pentenyl nitrobenzenesulfonamide **3** gave exclusively the *endo* (piperidine) product **10**, which was isolated as single compound in very good purity and good yield. Additionally we were pleased to find out that the isolated yield obtained (85%) closely match the assay yield (88%) of our optimization studies *vide supra*.

**Scheme 2.3.** Aminoacetoxylation of amino-olefin **3**.

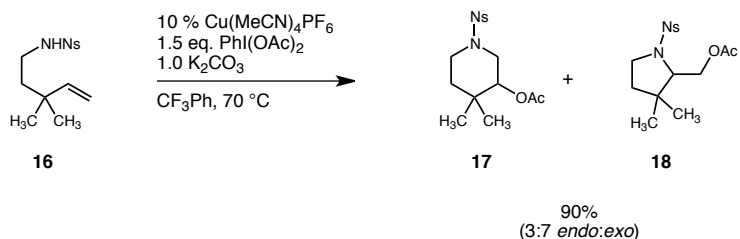






**Scheme 2.5** Cyclization of  $\beta$ -gem-dimethyl sulfonamide **11**.

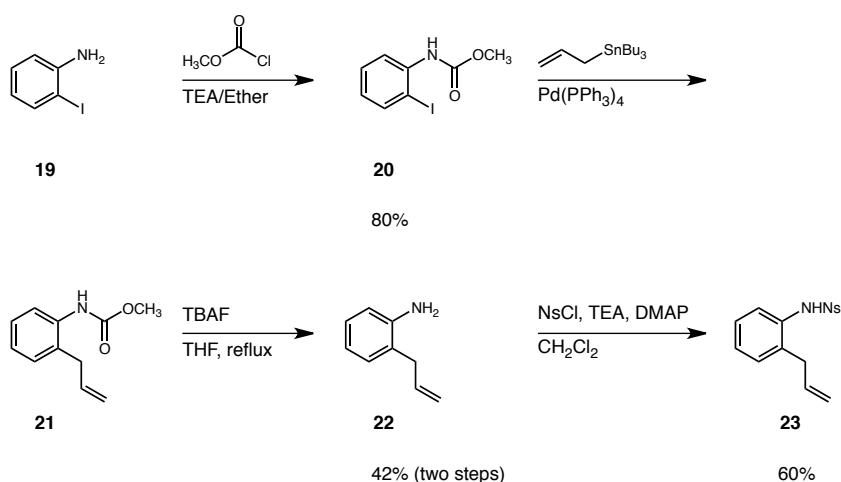
Continuing to study the effect(s) of the steric environment around the olefin, we decided to construct  $\gamma$ -gem-dimethyl sulfonamide **16**. At this point, Dr. Armin Stoll rejoined the project and was responsible for constructing and cyclizing compound **16**. Stoll found that the aminoacetoxylation of  $\gamma$ -gem-sulfonamide **16** was slow compared to **11**. In fact, it was necessary to heat to 70 °C for efficient cyclization. Additionally, a *loss and reversal of regioselectivity* was observed and a mixture of *endo* (**17**) and *exo* (**18**) regioisomer (3:7) was obtained after aminoacetoxylation (Scheme 2.6). These results indicate that the steric environment around the olefin can have a detrimental impact on the rate of reaction and product distribution.



**Scheme 2.6** Cyclization of  $\gamma$ -gem-dimethyl sulfonamide **16**.

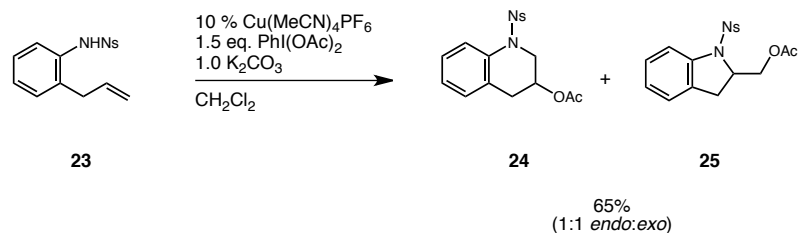
We also wanted to examine our cyclization conditions on aromatic substrates such as *N*-nosyl-2-allylaniline **23**, which was shown in previous methodology to give

exclusively the *exo* (pyrrolidine) adduct (Scheme 2.7).<sup>12b</sup> Substrate **23** was obtained from the corresponding allylaniline **22** by nosylation under standard conditions. Allylaniline **22** was prepared from *o*-iodoaniline **19** in three steps. Thus, iodoaniline **19** was converted to the corresponding carbamate **20**, which underwent Stille coupling with the allyl stannane as reported previously.<sup>25</sup> Unfortunately the carbamate group was not cleaved during aqueous work up with NaF as reported in this procedure to give allyl-phenyl amine **22** in one step.<sup>26</sup> Fortunately, however, refluxing allyl carbamate **21** with TBAF for 2 hours resulted in cleavage and the desired allyl-phenyl amine **22** was obtained in 42% yield (2 steps).<sup>26</sup> Finally nosylation gave the desired allyl-phenylsulfonamide **23** in 60% yield.



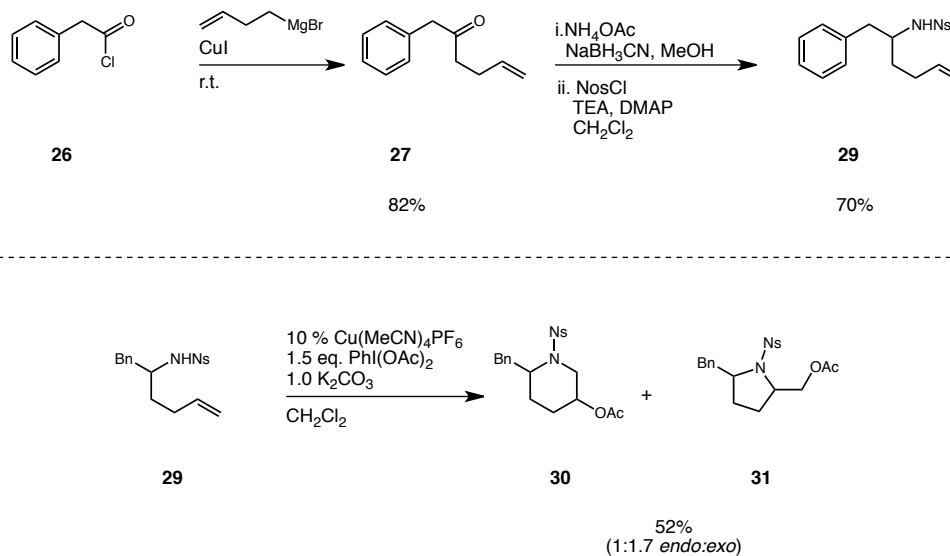
**Scheme 2.7** Synthesis of *N*-Nosyl allyl aniline **23**.

Aminoacetoxylation of substrate **23** under our conditions generated a (1:1) mixture of *endo* and *exo* regioisomers **24** and **25** (Scheme 2.8). This ratio is similar to the previously reported (1:1.9) ratio of *endo* and *exo* regioisomers.<sup>11</sup>



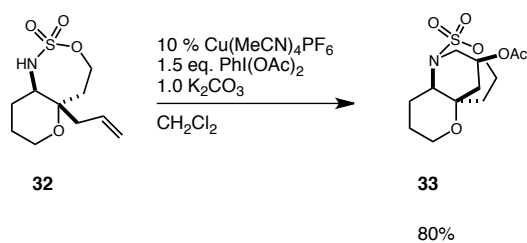
**Scheme 2.8** Aminoacetoxylation of *N*-Nosyl allyl aniline **23**.

Next we wanted to investigate the effect of a benzyl substituent on cyclization. Thus, we proceeded to construct benzyl sulfonamide **29**. Substrate **29** was obtained *via* nosylation from its respective benzyl amine (Scheme 2.9). Benzyl amine was synthesized from a previously reported process, starting from commercially available phenylacetyl chloride **26**.<sup>28</sup> Thus, alkyl-cuprate addition to the acyl chloride **26** afforded ketone **27** in 82% yield. Reductive amination gave the desired benzyl amine, which was then nosylated to generate the desired benzylpentenyl benzyl sulfonamide **29** in 70% yield. Aminoacetoxylation of substrate **29** afforded a (1:1.7) of *endo* and *exo* regioisomers **30** and **31**. The explanation for the partial reversal in regioselectivity for the cyclization of **29** is not apparent at this point.



**Scheme 2.9.** Synthesis of benzyl amine **29** and aminoacetoxylation.

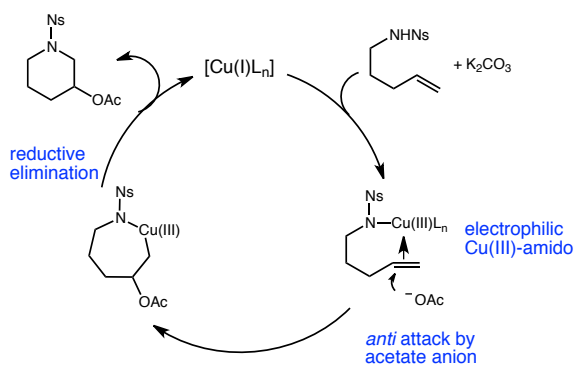
We were pleased to find that sulfamate ester **32** underwent successful conversion to the desired piperidine adduct **33** in good yield and excellent diastereoselectivity. The relative stereochemistry of compound **33** was determined by analogy to **2** (Scheme 2.10).<sup>17</sup>



**Scheme 2.10** Cyclization of sulfamate ester **32**.

## 2.4.2 Mechanism.

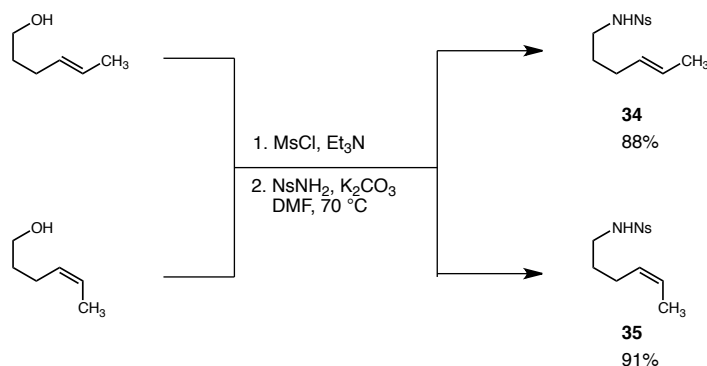
We believe that the difference in regioselectivity observed for our reaction conditions as compared to other Cu or Pd amino-oxygenation reactions, may be explained by an alternate mechanism, consistent with our results from the ensuing study (*vide infra*). Thus, we propose a mechanism in which the Cu-catalyst and the *N*-Ns amine combine under the oxidative reaction conditions to form an electrophilic Cu(III) amido species (Figure 2.1).<sup>29a, 29b, 29c, 29d, 29e</sup> Coordination of the tethered olefin to the Cu(III) center activates the double bond for *anti* attack by an acetate nucleophile at the position best able to stabilize the build-up of a positive charge.<sup>30a, 30b</sup> The resulting cyclic Cu(III) species may then undergo reductive elimination to yield the observed aminoacetoxylation product, in turn regenerating a Cu(I) species. Thus, in the case of mono substituted olefins, acetate attack occurs at the internal position, leading to the observed *endo* cyclization.<sup>31a, 31b, 31c, 31d</sup> If the internal position is significantly hindered (Schemes 2.6 & 2.8), then these steric factors may override the electronic bias leading the nucleophile to preferentially attack the 1° carbon.



**Figure 2.1** Proposed mechanism for Cu(I)-catalyzed aminoacetoxylation.

### 2.4.3 Aminoacetoxylation of 1,2 disubstituted olefins.

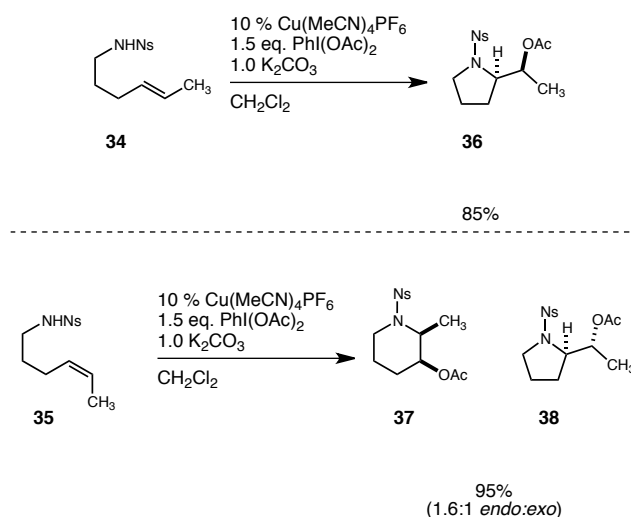
Following these studies, we next examined the possibility of utilizing 1,2-disubstituted olefins for this aminoacetoxylation reaction. We felt that this feature could potentially distinguish this methodology from previously developed aminoxygenation methods, and in turn provide a distinct advantage. At this time, Dr. Aaron Thornton joined the project in order to expedite the synthesis and cyclization of some 1,2 disubstituted olefins. Thus, *cis*- and *trans*-*N*-Ns substituted  $\gamma$ -aminoolefins (**34**) and (**35**) were constructed from their corresponding commercially available alcohols through a one-pot, two-step procedure (Scheme 2.11).<sup>32</sup>



**Scheme 2.11** Synthesis of 1,2-disubstituted  $\gamma$ -aminoolefins **34** and **35**.

When *trans*- $\gamma$ -aminoolefin **34** was exposed to our general aminoacetoxylation reaction conditions we observed complete consumption of starting material within 30 minutes, leading to the formation of pyrrolidine **36** in 77% yield as a single diastereomer, the structure of which was determined by X-ray crystallography (Scheme 2.12). However, when *cis*-  $\gamma$ -aminoolefin **35** was exposed to the same reaction conditions we

isolated a mixture of piperidine **37** and pyrrolidine **38** in 95% overall yield and a 1.6:1 ratio as determined by  $^1\text{H}$  NMR. The relative stereochemistry of piperidine **37** was determined by nOe NMR experiments, while the relative stereochemistry of pyrrolidine **38** was determined by comparison of spectral data obtained from its diastereomer: pyrrolidine **36**.



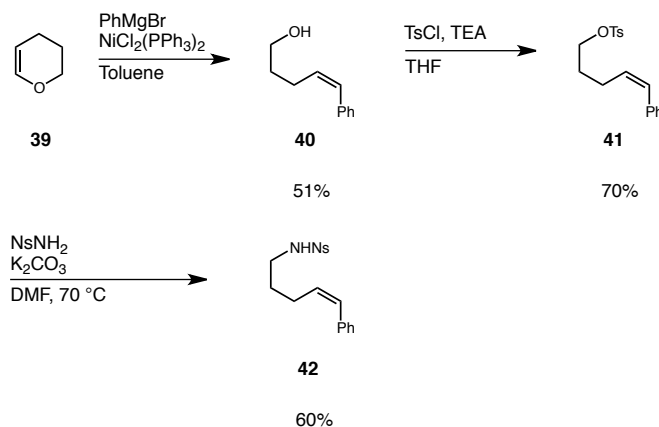
**Scheme 2.12.** Cyclization of 1,2-disubstituted  $\gamma$ -amino-olefins **34** and **35**.

The ability of this methodology to cyclize traditionally less reactive 1,2-disubstituted olefins provides a distinct advantage, and stands in contrast to, previously developed methods. Additionally, these reactions are consistent with our proposed mechanism. For example, the cyclizations of both **34** and **35** are diastereoselective and result from the overall *anti* addition of the amine and acetate nucleophile. This is consistent with the proposed bimolecular addition of acetate anion to the Cu(III)-olefin complex (Figure 2.1). The explanation for the complete reversal in regioselectivity for the cyclization of *trans*-olefin **34**, versus the formation of a mixture of regioisomers with



*cis*-olefin **35**, is not apparent at this point. However, because there is no obvious electronic bias (positive charge stabilization) within these dialkyl-substituted systems, the most likely explanation is due to subtle geometric factors that cannot be predicted at this time. To determine if these features are general for the cyclization of 1,2-disubstituted olefins, we next investigated the cyclization of electronically biased systems. The cyclization of *cis*- and *trans*-phenyl  $\gamma$ -aminoolefins **42** and **48** was thus pursued.

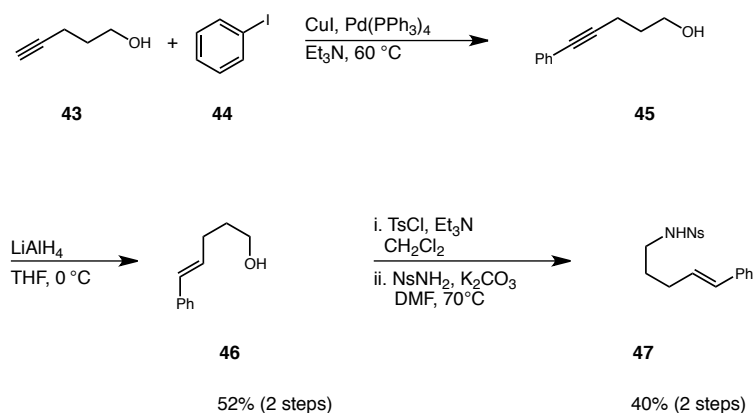
*Cis*-phenyl  $\gamma$ -aminoolefin **42** was obtained from tosylate **41** by  $S_N2$  displacement with  $NsNH_2$  in the presence of  $K_2CO_3$ . *Cis*-phenyl tosylate **41** was synthesized from a previously reported process.<sup>33</sup> Thus, Ni(II) mediated ring opening of dihydropyran **39** gave *cis*-phenyl alcohol **40**, which was tosylated under standard conditions to give *cis*-tosylate **41** in 36% over two steps (Scheme 2.13).



**Scheme 2.13** Synthesis of *Cis*-phenyl  $\gamma$ -aminoolefins **42**.

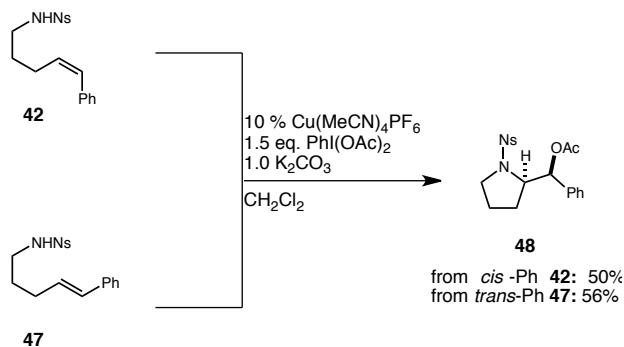
*Trans*-phenyl  $\gamma$ -aminoolefin **48** was obtained in five steps from previously reported intermediates.<sup>20</sup> Sonogashira coupling of commercial pent-4-yn-1-ol (**43**) and iodobenzene (**44**) followed by hydroxyl directed reduction to give the *trans*-phenyl

alcohol **46** exclusively in 52% yield over two steps (Scheme 2.14). Tosylation under standard conditions gave the desired tosylate. Nucleophilic displacement of the corresponding *trans*-phenyl tosylate **47** with NsNH<sub>2</sub> in the presence of K<sub>2</sub>CO<sub>3</sub> gave *trans*-phenyl  $\gamma$ -aminoolefin **48** in 40% over 2 steps.



**Scheme 2.14** Synthesis of *trans*-phenyl  $\gamma$ -aminoolefin **47**.

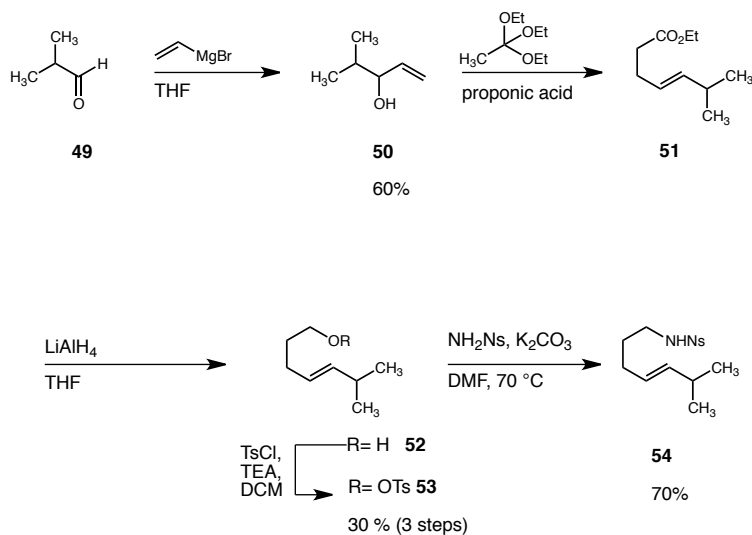
We observed that both olefins **42** and **47** converge upon a single pyrrolidine product **48** when exposed to our general reaction conditions (Scheme 2.15). The relative stereochemistry of **48** was confirmed by X-ray crystallography.



**Scheme 2.15** Cyclization of *cis*- and *trans*-phenyl  $\gamma$ -aminoolefins **42** and **47**.

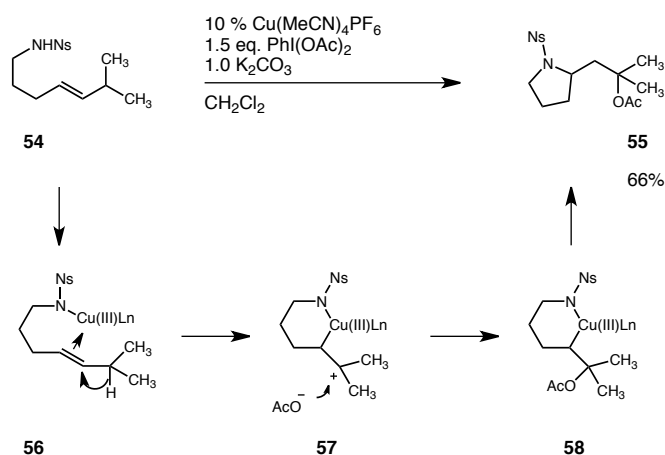
With these electronically biased systems we now see that the addition of the acetate nucleophile occurs at the position that is most able to stabilize the ensuing positive charge (benzylic). The fact that both geometric isomers converge to a single product may be explained by the formation of discrete carbocation intermediate, thereby leading to a loss in stereochemical bias from the starting olefin.

Lastly, to display the versatility of this new methodology, we looked at 1,2-disubstituted olefins with more complex functionalities. Thus, we chose to pursue *trans*-isopropyl  $\gamma$ -aminoolefin **54** and *trans*-benzyl  $\gamma$ -amino-olefin **59**. Isopropyl  $\gamma$ -aminoolefin **54** was synthesized starting from commercially available isopropyl aldehyde **49**. Thus, allyl Grignard addition to isopropyl aldehyde **49** gave allylic alcohol **50**, which underwent Johnson-Claisen rearrangement to give exclusively *trans*-isopropyl ester **51**. Reduction followed by tosylation under standard conditions gave *trans*-isopropyl tosylate **53** (Scheme 2.16).<sup>34</sup> S<sub>N</sub>2 displacement with N<sub>3</sub>NH<sub>2</sub> in the presence of K<sub>2</sub>CO<sub>3</sub> gave the desired *trans*-isopropyl  $\gamma$ -aminoolefin **54** in 15% overall yield.



**Scheme 2.16** Synthesis of *trans*-isopropyl  $\gamma$ -aminoolefin **54**.

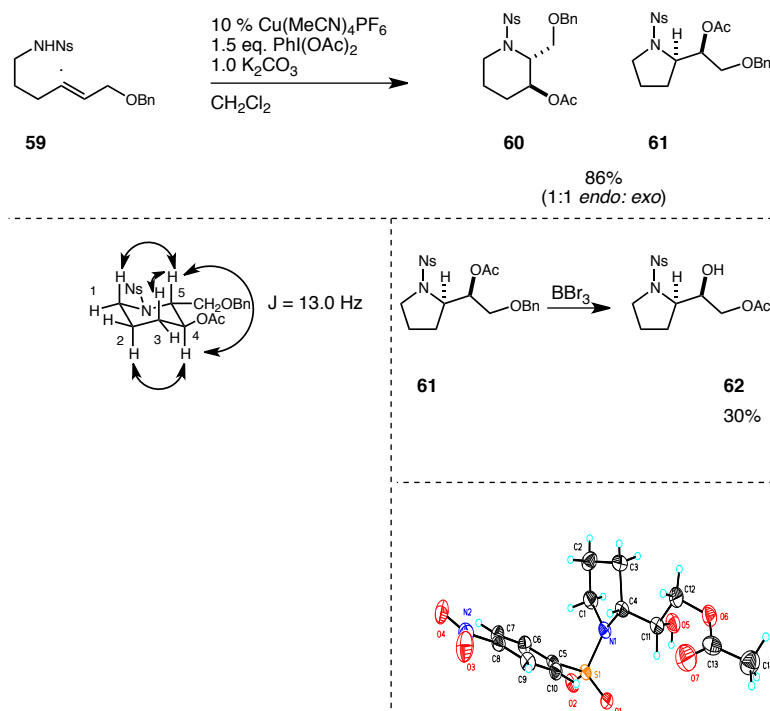
Cyclization of *trans*-isopropyl  $\gamma$ -aminoolefin **54** unexpectedly gave rise to a 1,3-aminoacetoxylation pyrrolidine **55** (Scheme 2.17). In this case, we believe that a 1,2-hydride shift in the activated olefin complex **56** would provide stable 3° cation **57** prior to external acetate attack. Finally, reductive elimination of **58** produces the observed product **55**.



**Scheme 2.17** Aminoacetoxylation of *trans*-isopropyl  $\gamma$ -aminoolefin **54**.

Finally, aminoacetoxylation of the OBn substituted olefin **59**, which was obtained from 1,4-butanediol,<sup>32</sup> gave a mixture of *syn-endo* piperidine adduct **60** and *syn-exo* pyrrolidine adduct **61** in a 1:1 ratio (Scheme 2.18). The relative stereochemistry of piperidine **60** was determined by 1D, 2D and nOe NMR experiments. <sup>1</sup>H NMR showed a coupling constant of 13.1 Hz between C(5)-C(4) protons, which indicated a *trans*-axial relationship between these two protons. In addition, nOe experiments indicated a spatial relationship between axial hydrogens C(1)-C(5), C(2)-C(4), C(3)-C(5). On the other hand, relative stereochemistry of pyrrolidine **61** was determined by X-ray crystallography

of **62**, which was obtained by benzyl deprotection with  $\text{BBr}_3$  followed by in-situ transesterification.



**Scheme 2.18.** Aminoacetoxylation of OBn substituted olefin **59**.

## 2.5 Conclusions and Future Work

In conclusion, we have developed a new aminoacetoxylation protocol that provides complimentary regioselectivity to previously reported palladium and copper catalyzed reactions. The new reaction proceeds under complimentary pH conditions to recently reported metal free reactions, allowing for the selective formation of 3-acetoxy piperidine products from  $\gamma$ -aminoolefins (see summary Table 2.5). Future work will focus on screening chiral ligands in order to induce asymmetry for this methodology.

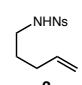
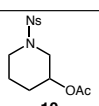
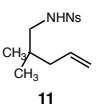
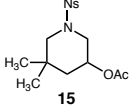
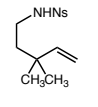
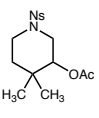
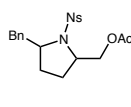
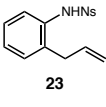
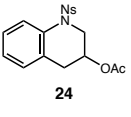
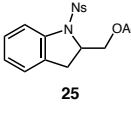
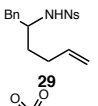
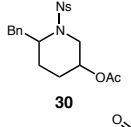
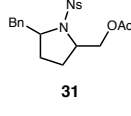
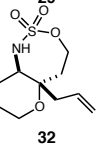
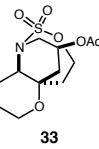
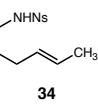
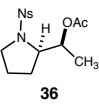
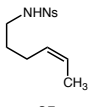
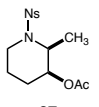

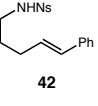
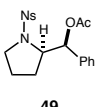
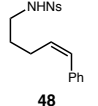
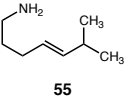
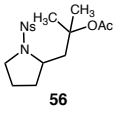
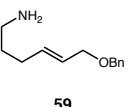
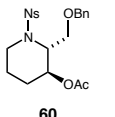
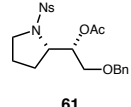
Entry	Substrate	Product(s)	% yield
1	 <b>3</b>	 <b>10</b>	85
2	 <b>11</b>	 <b>15</b>	77
3	 <b>16</b>	 <b>17</b>	90 (3:7)
	 <b>18</b>		
4	 <b>23</b>	 <b>24</b>	70 (1:1)
	 <b>25</b>		
5	 <b>29</b>	 <b>30</b>	52 (1:1.5)
	 <b>31</b>		
6	 <b>32</b>	 <b>33</b>	80
7	 <b>34</b>	 <b>36</b>	85
8	 <b>35</b>	 <b>37</b>	95 (1.6:1)
	 <b>38</b>		
9	 <b>42</b>	 <b>49</b>	50
10	 <b>48</b>		56
11	 <b>55</b>	 <b>56</b>	66
12	 <b>59</b>	 <b>60</b>	86 (1:1)
	 <b>61</b>		

Table 2.5 Summary of results for the copper catalyzed aminoacetoxylation of olefins

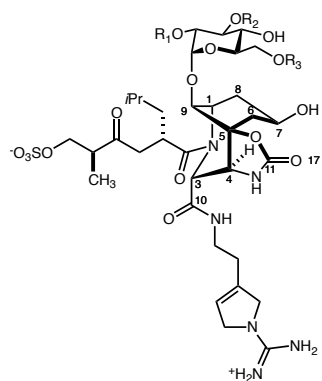
**Part 2**  
**Efforts Towards the Development of an**  
**Enantioselective Intermolecular Cascade Reaction to**  
**Access the Core of the Banyaside Alkaloids**

### 3 Chapter 3

#### Introduction to the Banyasides Alkaloids.

### 3.1 Banyaside A and B: Isolation, Structure and Stereochemistry

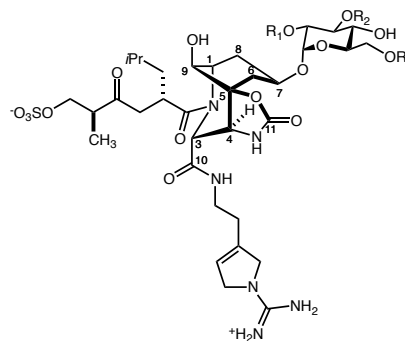
In 2005 Carmeli and coworkers reported the isolation of two new novel alkaloids from the hydrophilic extract of a natural bloom of a cyanobacterium *Nostoc* sp: banyaside A (**63**) and banyaside B (**64**) (Figure 3.1).<sup>35</sup> Banyaside A and B were isolated through a serine protease inhibition guided separation using size exclusion and high performance liquid chromatography.



**Banyaside A:**  $R_1 = C(O)C_5H_{11}$ ,  $R_2 = C(O)NH_2$ ,  $R_3 = H$  (**63**)

**Banyaside B:**  $R_1 = H$ ,  $R_2 = H$ ,  $R_3 = C(O)C_5H_{11}$  (**64**)

ORIGINAL STRUCTURE



**Banyaside A:**  $R_1 = C(O)C_5H_{11}$ ,  $R_2 = C(O)NH_2$ ,  $R_3 = H$  (**63**)

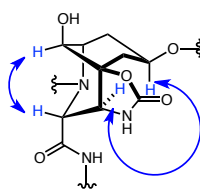
**Banyaside B:**  $R_1 = H$ ,  $R_2 = H$ ,  $R_3 = C(O)C_5H_{11}$  (**64**)

REVISED STRUCTURE

**Figure 3.1** Banyaside A (**63**) and banyaside B (**64**).



The molecular formula of banyaside A was established to be  $C_{40}H_{64}N_8O_{19}S$  by HRFABMS. The structure of **63** was assigned based on 1D and 2D NMR experiments. In  $DMSO-d_6$  **63** appeared as a 1:7 mixture of *cis* and *trans*-rotamers of the azabicyclononane-leucine peptidic bond. Nonetheless, proton and carbon NMR spectra indicated that banyaside A was glycopeptidic in nature. Initially the glucose unit was assigned to the C-7 oxygen in the azabicyclononane (abn). This assignment was based on an HMBC correlation, which indicated correlation of H-1 in the glucose unit to the C-7 in the abn unit. However, recently Carrera and co-workers have reassigned the glucose unit to the axial oxygen at C-9 via synthetic studies.<sup>36</sup> The structure of the  $\alpha$ -glucose unit, D-leucine and the amidino aminoethyl pyrroline unit were assigned via COSY, TOCSY, HMQC and HMBC experiments. The azabicyclononane (abn) core unit was assigned by COSY, TOCSY and HMBC. The relative stereochemistry of the abn moiety was made via nOes from a ROESY experiment (Figure 3.2). The major correlations observed from the ROESY experiment were those of H-3 to H-9 and H-4 to H-7 (Figure 3.2).



**Figure 3.2** Important nOes correlations for banyaside A.

The molecular formulation of banyaside B (**64**) was established to be  $C_{39}H_{63}N_7O_{18}S$  by HRFABMS. NMR data of banyaside B showed it to be structurally similar to banyaside A (**1**). In fact, NMR data suggested that **63** and **64** differ only on the

substitution pattern of the glycoside unit. In banyaside B (**64**), the carbomyl moiety is missing and the hexanoic acid chain is now attached to one of the oxygens in the glucose unit (C-6).

### 3.2 Biological Activity.

Banyaside A and B belong to a larger group of compounds known as the aeruginosin family.<sup>37</sup> Some aeruginosins have shown in-vitro inhibitory activity against serine proteases, which are enzymes that are involved in a number of important biological processes.<sup>37</sup> In addition, high inhibitory activity has been found against serine proteases such as trypsin. Trypsin is a digestive enzyme and inhibition of trypsin may also be of interest for the treatment of pancreatic disorders, such as pancreatitis.<sup>38</sup> Finally the importance of serine proteases in the complex coagulation process has been recently been established.<sup>39</sup>

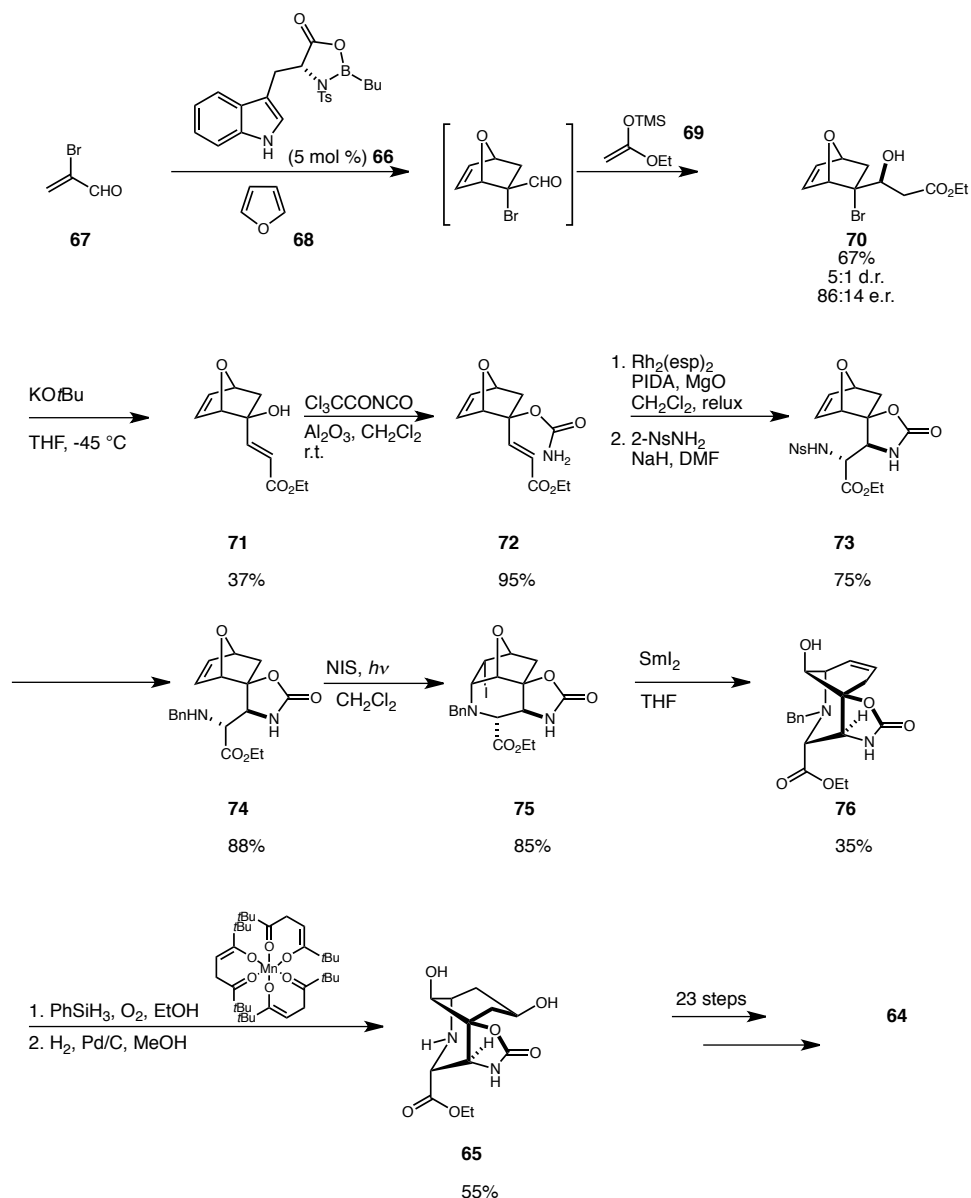
Banyasides A and B are known to be serine protease inhibitors. In fact, banyasides A and B inhibited the proteolytic activity of trypsin at a concentration of 45  $\mu\text{g}/\text{mL}$ . Moreover, the  $\text{IC}_{50}$  values of banyaside A were determined for inhibition of serine proteases: trypsin and thrombin. Banyaside A inhibited trypsin with an  $\text{IC}_{50}$  value of 1.48  $\mu\text{g}/\text{mL}$  and thrombin with an  $\text{IC}_{50}$  value of 0.39  $\mu\text{g}/\text{mL}$ . This important biological activity along with the challenging and complex chemical structure is what makes both banyaside A and B attractive targets for synthesis.

### 3.3 Carreira's Synthesis of Banyaside B.

In 2008 the Carreira group reported an enantioselective synthesis of the abn core **65** of the banyaside alkaloids (Scheme 3.1).<sup>40</sup> Carreira's approach to the abn core **65** started with a tandem Diels-Alder and a Mukiyama Aldol reaction catalyzed by Corey's oxazaborolidine **66**. Thus, 2-bromoacrolin (**67**) and furan (**68**) were allowed to react in the presence of **66** (5 mol %). The cycloadduct obtained was then allowed to react in situ with silyl ketene acetal (**69**) to afford **70** in 67% with good diastereoselectivity and enantioselectivities (d.r. 5:1, e.r. 86:14).

Treatment of both diastereoisomers of **70** with KO $t$ Bu in THF led to the formation of an intermediate epoxide that under the reaction conditions eliminated to give allylic alcohol **71** in 37% yield. Reaction of allylic alcohol **71** with trichloroacetyl isocyanate produced carbamate **72** (95%). Aziridination reaction with Du Bois' Rh<sub>2</sub>(esp)<sub>2</sub> catalyst afforded an intermediate aziridine, which was opened with *o*-nitrobenzenesulfonamide to produce carbamate **73** in 75% yield. Nosyl deprotection under standard conditions (K<sub>2</sub>CO<sub>3</sub>, PhSH) yielded the desired amine, which was benzylated under standard conditions to yield benzylamine **74**. Photo-haloamination of **74** with NIS gave exclusive formation of the *endo*-iodide **75** in 89% yield. Treatment of **75** with excess SmI<sub>2</sub> in THF achieved cleavage of the C7-O bond to yield olefin **76**. Finally, Mn-catalyzed hydration of the olefin of **76** afforded a diol, which was deprotected under standard conditions to give abn core **65** in (55%). Subsequent publication by the Carreira's group completed the synthesis of banyaside B in an

additional 23 steps. In addition through their synthesis the Carreira group was able to revise the structure of banyaside B (*vide supra*).<sup>36</sup>



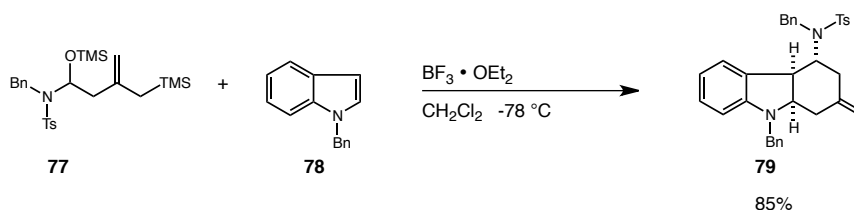
**Scheme 3.1** Carreira's Approach to abn core **65**.

To date this has been the only total synthesis reported for either **63** or **64**. Although, Carreira's synthesis of the abn core is elegant, it is highly linear. In addition, the initial Diels-Alder reaction has only a modest enantiomeric ratio (86:14) and the

conversion from **70** to **71** is low yielding leaving significant room for improvement. Thus, we believe that our iminium cascade methodology can potentially give access the abn core of the Banyaside peptides in a more convergent and efficient manner.

### 3.4 Our Approach to the Core of the Banyaside Alkaloids.

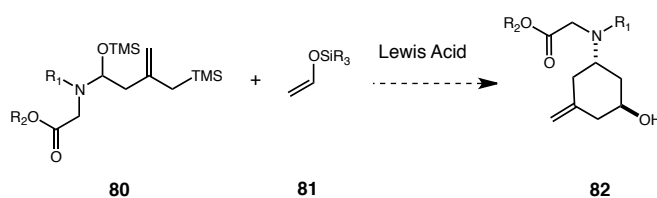
Our lab has recently developed new methodology based on an *intramolecular* iminium cascade annulation reaction of tryptamine derivatives for the construction of complex tetracyclic compounds.<sup>41</sup> This reaction yields a complex tetracyclic compound, which is the core of an important class of compounds known as the Malagasy alkaloids (Part 3) *vide infra*. We have also developed an *intermolecular* variant of this methodology for the construction of complex tricyclic compounds (Scheme 3.2).<sup>42</sup> For example, treatment of *N*-tosyl-*O*-TMS-aminol **77** and *N*-benzyl indole (**78**) with  $\text{BF}_3 \cdot \text{OEt}_2$  at  $-78^\circ\text{C}$  afforded the tricyclic compound **79** in 85% yield as a single diastereoisomer.



**Scheme 3.2** Intermolecular cascade annulation reaction.

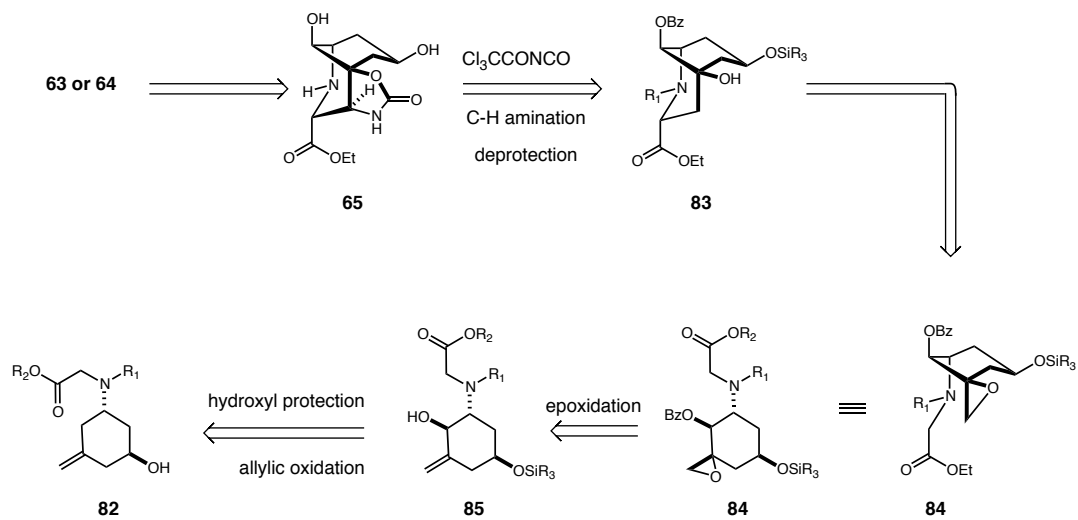
We recognized that the latter case was relevant to the development of a general strategy for the construction of the abn core **65** of the banyaside alkaloids. We believed that the key would be to extend the scope of this reaction to include silyl enol ethers as

traps instead of indoles. Thus, reaction of aminol **80** with silyl enol ether **81** under Lewis acid conditions would yield functionalized cyclohexane **82** containing two new stereogenic centers and an olefin (Scheme 3.3). Moreover, we were hopeful that the relative stereochemistry and high diastereoselectivity observed in the case of indole **78** as nucleophile would be translated into this new extension of the methodology as well.



**Scheme 3.3.** Extension of our methodology to banyasides.

With cyclohexane **82** in hand, we believed that the synthesis of abn core **65** could be achieved in a fast and efficient manner (Scheme 3.4). Our retrosynthetic approach is outlined on Scheme 3.4. We believe that core abn core **65** could come from the C-H amination of **83** (oxazolidinone ring formation) followed by global deprotection.<sup>43</sup> Bicyclononane **83** would come from a base mediated epoxide opening of **84** followed by cyclization. Hydroxyl-directed epoxidation of **85** would in turn afford epoxide **84**. Finally, compound **85** could come from a protection of the secondary alcohol of **82**, followed by allylic oxidation.<sup>44a, 44b</sup>



**Scheme 3.4** Our retrosynthetic approach to banyaside core **65**.

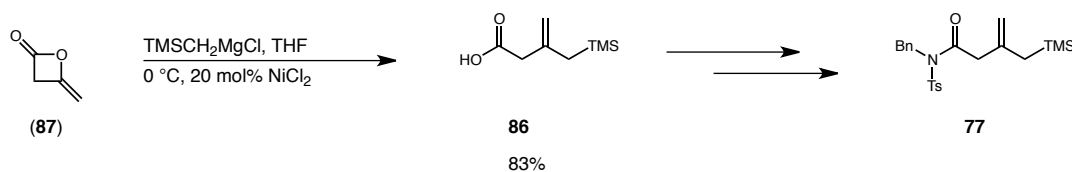
## 4 Chapter 4

*Development of an Intermolecular Iminium Cascade Reaction for the Synthesis of the Banyaside Core.*

### 4.1 Early Attempts with *N*-Tosyl-*O*-TMS Aminol **77**.

#### 4.1.1 Synthesis of $\alpha,\beta$ unsaturated acid **86**.

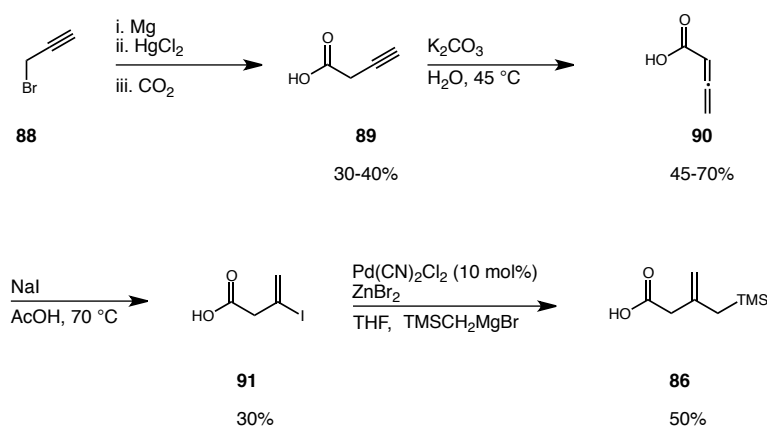
We decided to begin our investigations into a new cascade reaction for the synthesis of the banyaside cores by examining *N*-tosyl-*O*-TMS-aminol **77** as the iminium ion precursor. Our reasoning behind this decision was based on the fact that compound **77** had worked well in our previous intermolecular cascade reaction (*vide supra*). Compound **77** was previously synthesized in our lab from unsaturated acid **86**. In turn, acid **86** was synthesized from commercially available diketene (**87**) and (trimethylsilyl)methylmagnesium chloride in the presence of catalytic amount of NiCl<sub>2</sub>, using conditions developed by Itoh and coworkers (Scheme 4.1).<sup>45</sup>



**Scheme 4.1** Previous synthesis of key unsaturated acid **86**.



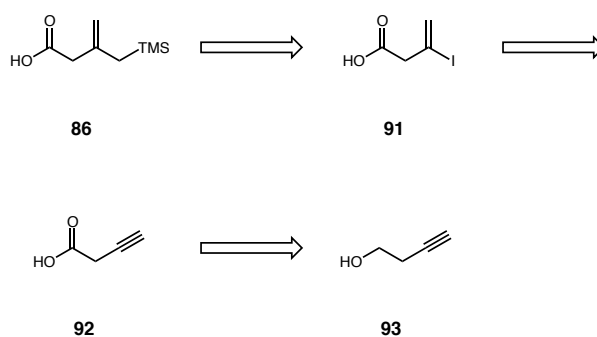
Unfortunately by the start of this project, diketene (**87**) was discontinued from Sigma-Aldrich and we were not able to find another supplier for this important starting material. In addition, the production of diketene from ketene is a complex process due to the fact that diketene polymerization is fast, even at low temperatures.<sup>46</sup> Therefore, we needed to come up with a completely new synthetic route for acid **86**. The first route for the synthesis of acid **86** commenced with commercially available propargyl bromide (**88**) (Scheme 4.2). Formation of the Grignard reagent from propargyl bromide (**88**) with magnesium metal in the presence of stoichiometric amounts of HgCl<sub>2</sub>, followed by subsequential treatment with carbon dioxide afforded homo-propargyl acid **89** in low yields (30-40%).<sup>47</sup> Homopropargyl acid **89** was treated with aqueous K<sub>2</sub>CO<sub>3</sub> to afford allene **90**, which was then treated with NaI in acetic acid to yield iodoacid **91**.<sup>48a, 48b</sup> Finally, Negishi coupling of **91** and (trimethylsilyl)-methylmagnesium chloride afforded the desired acid **86** in 65% yield.<sup>49</sup>



**Scheme 4.2** Second-generation synthesis of acid **86**.

Unfortunately, this first generation route to acid **86** was far from practical. Carbonylation reaction of bromide **88** used large amounts of  $\text{HgCl}_2$  and was run very dilute, thus it was not scalable. The alkyne isomerization step to give allene **28** was accompanied by variable yields (45 – 70%). Hydroiodination of **90** proceeded with low yields (30%). Additionally, due to the high water solubility of **91**, extraction required large amounts of organic solvents. With all these challenges we were only able to make milligram quantities of acid **86**. Therefore, we decided to find a better process for the synthesis of acid **86** before continuing on with the project.

We felt that the Negishi coupling was a robust reaction, therefore we decided to start from iodo acid **91**, which we envisioned could be accessible from homo-propargyl alcohol **93** (Scheme 4.3). This new route would be one step shorter than the early route to acid **86** and would avoid the challenging carbonylation step as well as the non-robust allene formation step.



**Scheme 4.3.** Retrosynthetic analysis for acid **86**.

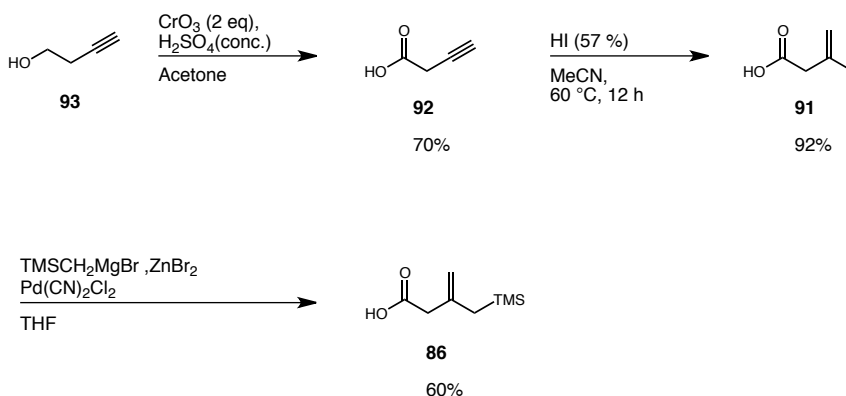
The oxidation of homo-propargylic alcohol **93** proved to a more challenging reaction than anticipated. Our efforts are summarized in Table 4.1. Our first attempt was a sequential Dess-Martin and Pinnick oxidation protocol (entry 1).<sup>50</sup> Although this reaction showed some presence of an aldehyde in the <sup>1</sup>H NMR of the crude DMP reaction, oxidation to the desired acid **92** was not possible. The next set of conditions that were attempted relied on catalytic chromium with NaIO<sub>4</sub> as the stoichiometric oxidant (entry 2).<sup>51</sup> We were excited to find out that this reaction gave acid **92** in 41% yield. However, subsequent attempts to repeat this result were futile. Typical Jones oxidation conditions yielded the desired acid **92** in 40 % yield (entry 3).<sup>52</sup> Running this reaction with more concentrated H<sub>2</sub>SO<sub>4</sub> and additional chromium improved this yield to 70%, thus making the Jones oxidation the ideal protocol to access acid **92** (entry 4).

Entry	Conditions	% yield
1	1. DMP, CH <sub>2</sub> Cl <sub>2</sub> 2. NaClO <sub>4</sub> , NaHPO <sub>4</sub>	n.a.
2	NaIO <sub>4</sub> 1 mol% Na <sub>2</sub> Cr <sub>2</sub> O <sub>7</sub> 5 mol % HNO <sub>3</sub>	41
3	CrO <sub>3</sub> (1.5 eq.) 10 N H <sub>2</sub> SO <sub>4</sub>	40
4	CrO <sub>3</sub> (2.0 eq.) conc. H <sub>2</sub> SO <sub>4</sub>	70

**Table 4.1** Oxidation of homo-propargyl alcohol **93**.

The hydroiodination of acid **92** with HI (57 % aq.) to give iodoacid **91** was previously reported in the literature to give a maximum yield of 69%.<sup>49</sup> Indeed under the

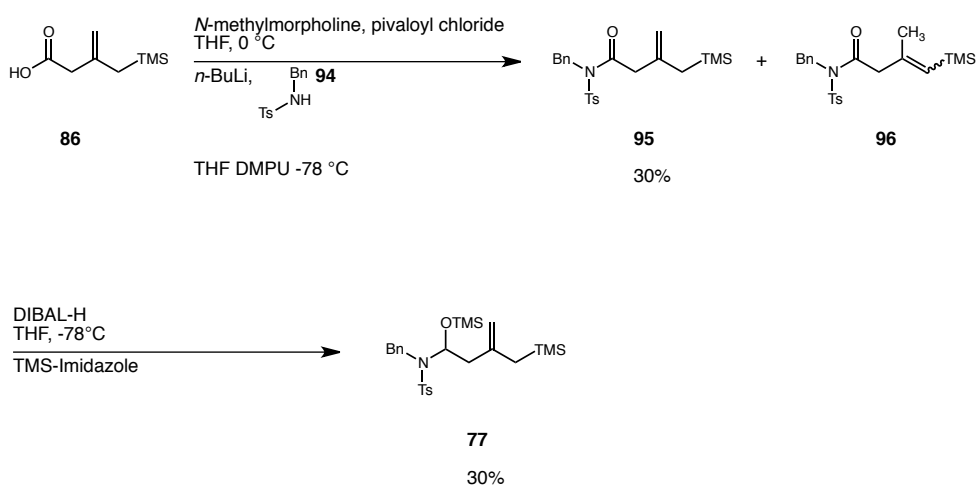
original conditions (HI 57%, 70 °C, 6h) a consistent yield of 65% was obtained in our experience. However, we felt that there was room for optimization of these conditions. A GC assay was developed to monitor the progress of this reaction, which enable us to rapidly optimize the reaction conditions. The first thing we tried was to add acetonitrile as an organic solvent. GC assay showed this change gave a much cleaner GC trace as compared to the original conditions. Finally, we realized that lowering the temperature of the reaction to 60 °C had no impact on the rate of the reaction, but gave an even cleaner GC trace than at 70 °C. With our new and optimized conditions, hydroiodination of homo-propargylic acid **92** produced iodoacid **91** with >99 % conversion and 92% isolated yield after purification *via* flash chromatography (Scheme 4.4). Finally, Negishi coupling of **91** and (trimethylsilyl)-methylmagnesium chloride afforded the desired acid **86** in overall 40% yield.



**Scheme 4.4** Optimized synthetic route to acid **86**.

### 4.1.2 Synthesis of *N*-Tosyl-*O*-TMS aminol **77**.

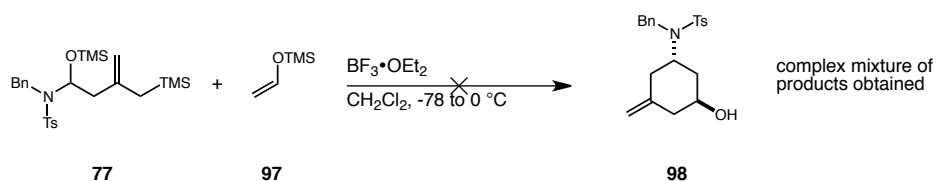
Having established a robust synthetic route towards the synthesis of **86**, we proceeded to complete the synthesis of *N*-Tosyl-*O*-TMS aminol **77**. Thus, treatment of acid **86** with pivaloyl chloride and *N*-methylmorpholine to generate the corresponding mixed anhydride, followed by treatment with the lithium anion of *N*-benzyl sulfonamide **94** at  $-78\text{ }^{\circ}\text{C}$ , generated *N*-tosyl amide **95** in 30% yield (Scheme 4.5).<sup>42</sup> Among the side products detected by crude  $^1\text{H}$  NMR was olefin isomer **96**, which probably arises from olefin isomerization under the strong basic conditions used in this reaction. Nonetheless, compound **95** was reduced by DIBAL-H at  $-78\text{ }^{\circ}\text{C}$  to the aluminum hemiacetal, which was trapped in-situ with trimethylsilyl-imidazole to yield *N*-Tosyl-*O*-TMS aminol **77** in 30% yield.<sup>53a, 53b, 53c</sup>



**Scheme 4.5** Synthesis of *N*-Tosyl-*O*-TMS aminol **77**.

### 4.1.3 Cascade Annulation with *N*-Tosyl-*O*-TMS aminol **77**.

With *N*-Tosyl-*O*-TMS aminol **77** in hand, an investigation into the intermolecular cascade reaction with silyl enol ethers was undertaken. Vinyloxy-trimethylsilane (**97**) was chosen as the external trap due to its commercial availability. Unfortunately, treatment of *N*-tosyl-*O*-TMS-aminol **77** and vinyloxy-trimethylsilane (**97**) with  $\text{BF}_3 \cdot \text{OEt}_2$  at  $-78^\circ\text{C}$  did not afford any of the desired cyclohexene **98** and instead yielded a complex mixture of unidentified products (Scheme 4.6). At this point, we decided to change the electronics of the aminol substrate, since we had previously observed that electronics play an important role in iminium ion cyclizations.<sup>41, 42</sup>



**Scheme 4.6** Attempt at cyclization of **77**.

## 4.2 Intermolecular Iminium Cascade with *N*-Cbz-*O*-TMS Aminol **99**.

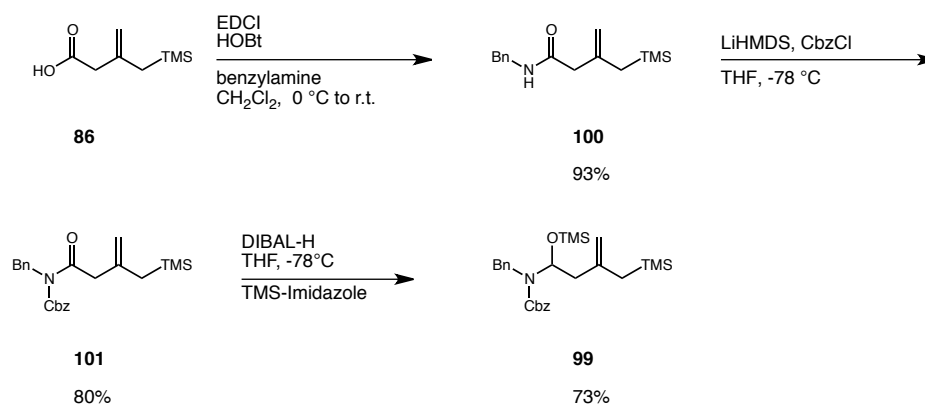
### 4.2.1 Synthesis of *N*-Cbz-*O*-TMS aminol **37**.

We decided that *N*-Cbz-*O*-TMS aminol **99** would be a good iminium ion precursor, since similar Cbz aminols had worked well in our previously developed intramolecular methodology.<sup>42</sup> The synthesis of *N*-Cbz-*O*-TMS amino **99** was achieved in three high yielding steps from acid **86**. Treatment of acid **86** and benzylamine in the

presence of EDCI and HOBT afforded *N*-Cbz amide **100** in 75% yield (Scheme 4.7).<sup>54a, 54b</sup>

Amide **100** was acylated with LiHMDS and CbzCl in 80% and converted to the corresponding *N*-Cbz-*O*-TMS aminol **99** under now standard conditions in 73% yield.

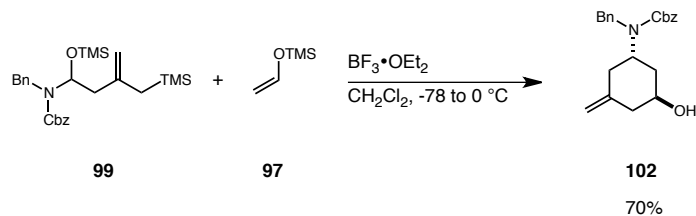
We were pleased that the synthesis of compound **99** was superior to that of **77** since it avoided the problematic mix-anhydride coupling step. This allowed us to produce ample quantities of **99** for our investigations.



**Scheme 4.7** Synthesis of *N*-Cbz-*O*-TMS aminol **99**.

#### 4.2.2 Cascade Annulation of *N*-Cbz-*O*-TMS aminol **99**.

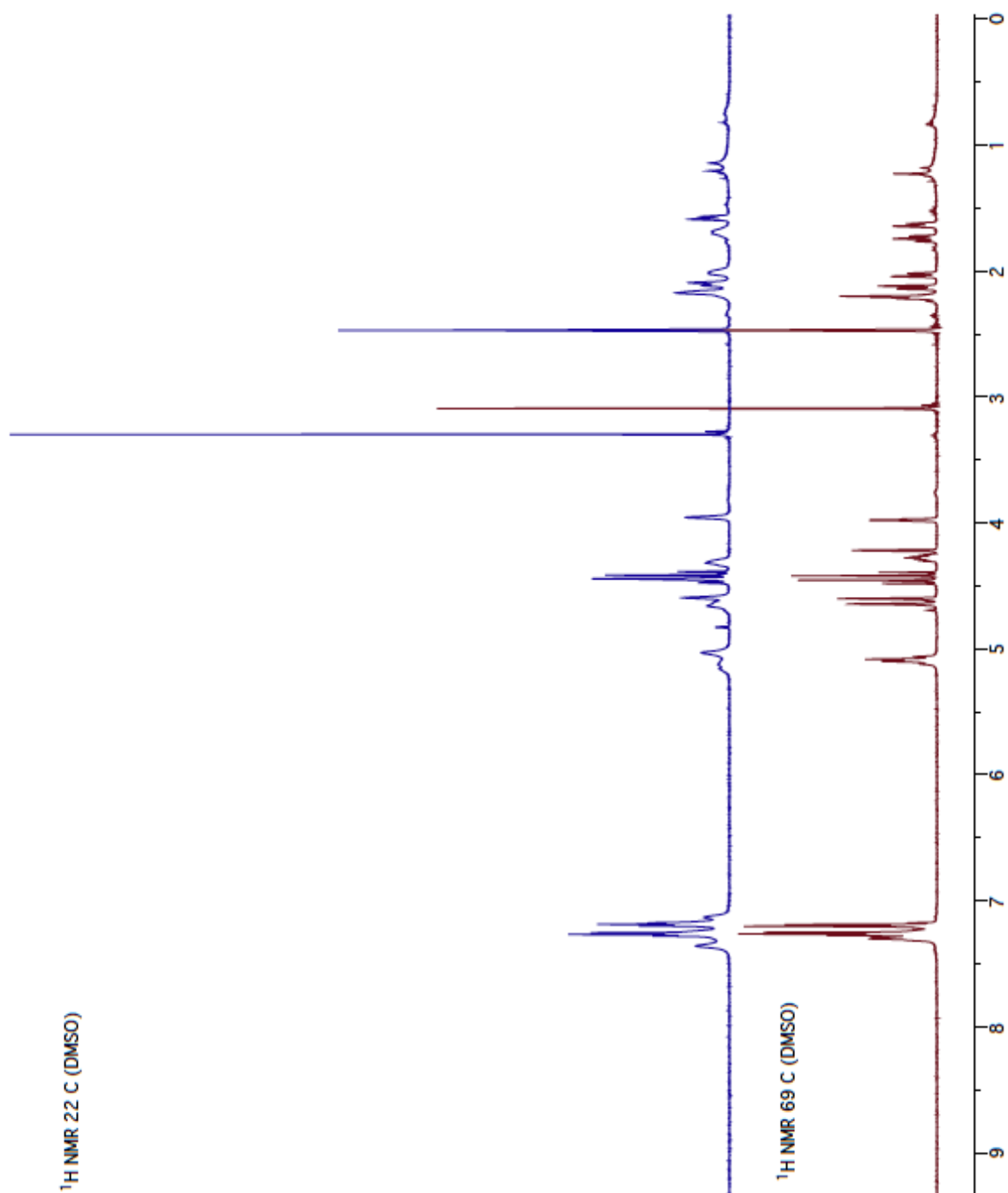
With *N*-Cbz-*O*-TMS aminol **99** in hand, we turned to the key cascade annulation reaction for this compound. To our delight, treatment of compound **99** and vinyloxy-trimethylsilane (**97**) with  $\text{BF}_3 \cdot \text{OEt}_2$  at  $-78\text{ }^\circ\text{C}$  and slowly warming the reaction mixture to  $0\text{ }^\circ\text{C}$  cleanly afforded cyclohexane **102** in 70% as a single diastereoisomer (Scheme 4.8).



**Scheme 4.8** Cyclization of *N*-Cbz-*O*-TMS aminol **99**.

Characterization via NMR spectroscopy of cyclohexene **102** was initially complicated by the presence of a mixture of rotamers at 300 K due to the benzyl carbamate group (Figure 4.1). Conducting variable-temperature (VT) NMR experiments and switching the NMR solvent to DMSO, allowed us to obtain clean  $^1\text{H}$  NMR spectra for cyclohexane **102** (Figure 4.1). Although we were able to obtain clean 1D NMR spectra of cyclohexane **102**, we were not able to obtain clean and reliable 2D NMR data for **102** due to the high temperature of the experiments (69 °C). Thus, we realized that we needed to remove the carboxybenzyl (cbz) group if we wanted to determine the relative stereochemistry of **102** via NMR experiments.

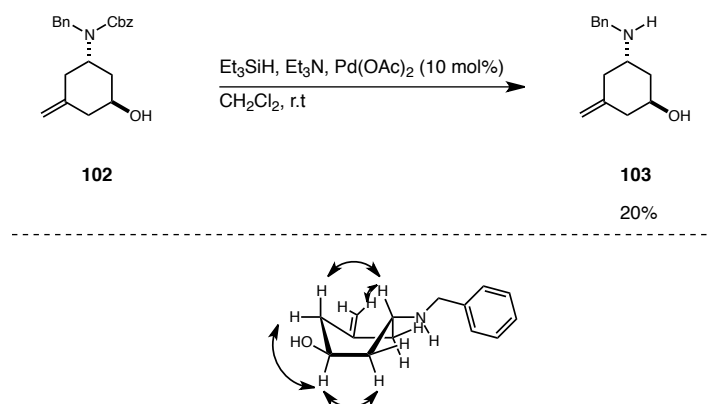




**Figure 4.1** Stacked VT-NMR experiments on cyclohexene **102**, top ( $\text{CDCl}_3$  at 300 K), bottom (DMSO at 343 K).

### 4.2.3 Synthesis of *N*-benzyl-cyclohexanol **103**.

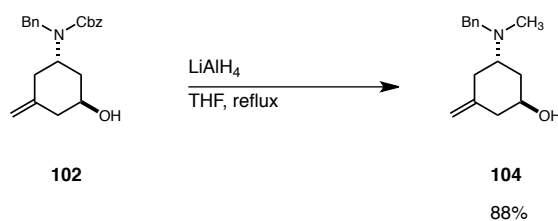
The mildest and most common way for the removal of the *N*-carboxybenzyl (Cbz) group is via hydrogenolysis with Pd/C and a hydrogen source.<sup>55</sup> In the case of compound **102** the presence of a benzyl group and an olefin makes hydrogenolysis impractical. Therefore, we sought an alternative way of removing the Cbz group. Our first attempt involved strong alkaline conditions, which have been used in systems containing olefins.<sup>56</sup> Unfortunately, treatment of compound **102** with KOH (40% aq) in MeOH at 100 °C did not give any of the desired amine **103** and just returned starting material. Fortunately, reaction of carbamate **102** with triethylsilane, triethylamine and catalytic amounts of Pd(OAc)<sub>2</sub> in CH<sub>2</sub>Cl<sub>2</sub> yielded the desired amine **103**, albeit in low yield (20%) (Scheme 4.9).<sup>57</sup> The relative stereochemistry of compound **103** was determined to be *trans* based on 1D, 2D and nOe experiments. Unfortunately, attempts to make a crystalline salt for X-ray crystallography of **103** in order to confirm these assignments were futile.



**Scheme 4.9** Synthesis of amine **103** and key nOe correlations.

#### 4.2.4 Synthesis of *N*-methyl-cyclohexanol **104**.

In an effort to obtain a crystalline salt that could be used for X-ray crystallography experiments, we decided to reduce the carbamate moiety down to the methyl moiety. Thus, reaction of **102** with LiAlH<sub>4</sub> under refluxing THF yielded *N*-methyl-cyclohexanol **104** in 88% yield (Scheme 4.10).<sup>58</sup> Unfortunately, our efforts to obtain a crystalline salt of **104** by screening different conditions (acids, temperatures and solvents) failed.



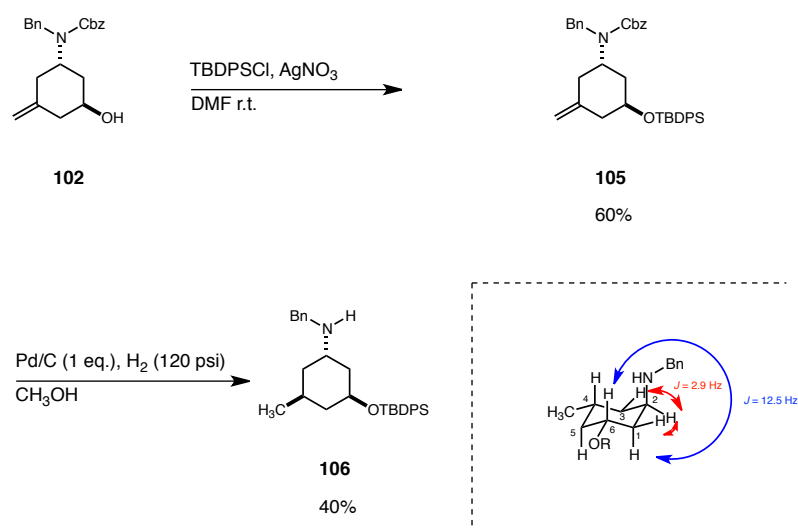
**Scheme 4.10** Reduction of carbamate **102** with LiAlH<sub>4</sub>.

At this point we decided to run conformational analysis in a cyclohexane ring system in order to confirm the stereochemical assignments from **103**. Thus, we decided to derive derivative **102** in order to begin new stereochemical studies.

#### 4.2.5 Synthesis of *N*-benzyl-*O*-TBDMS-cyclohexanol **106**.

We expected that direct hydrogenation of **102** would not only reduce the olefin, but also cleave both the benzyl and cbz group at the same time. Although, this process would give us a theoretically ideal cyclohexane ring system for stereochemical studies,

we did not want to lose the UV-activity of **102**. To this end, we decided to begin the derivatization of **102** with silylation of the alcohol unit with *tert*-butylchlorodiphenylsilane. Thus, treatment of cyclohexanol **102** with *tert*-butylchlorodiphenylsilane and AgNO<sub>3</sub> in DMF at room temperature yielded *O*-TBDMS ether **105** in 75% yield (Scheme 4.11).<sup>59</sup> Unexpectedly, treatment of **105** with Pd/C under 120 psi of H<sub>2</sub> gas generated a single diastereoisomer containing a benzyl group. Based on 1D and 2D (COSY, HMBC) NMR experiments the structure of this compound was assigned as *N*-benzyl-*O*-TBDMS-cyclohexanol **106**.



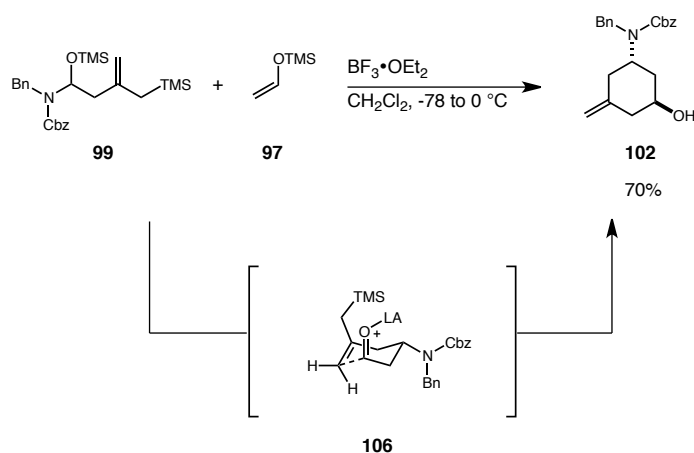
**Scheme 4.11** Synthesis of *N*-benzyl-*O*-TBDMS-cyclohexanol **106**.

Unfortunately, nOe experiments on **106** were inconclusive due to the presence of a strong signal for the *tert*-butyl group, which overlapped with signals of key hydrogens at C-4 and C-5. In addition, TBAF deprotection of **106** did not yield the desired cyclohexanol and a complex mixture of products was obtained. However, based on

coupling constants of **106** obtained and COSY correlations, as well nOe experiments on **103**, we believe compound **102** we believe that a *trans* stereochemical exists between C-2 and C-6. However, we also believe this assignment needs further confirmation by additional NMR experiment or X-ray data.

#### 4.2.6 Proposed Transition State for the Cyclization of **99**.

Based on the exclusive formation of *trans*-cyclohexane **102**, we believe that cyclization of **99** proceeds through a chair like transition state **106** (Scheme 4.12). This transition state makes the bulky carbamate group attain an equatorial conformation. Moreover, Denmark and coworkers have shown that intramolecular allylsilane terminated cyclizations proceed through a synclinal transition state which places that carbonyl group in a pseudo-axial position.<sup>60</sup>



**Scheme 4.12** Proposed mechanism for the cyclization of **99**.

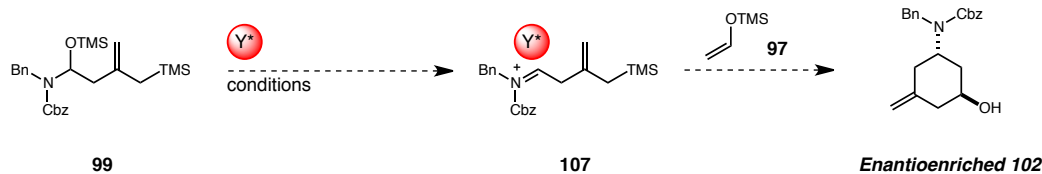


## 5 Chapter 5

### *Studies Towards an Enantioselective Intermolecular Cascade Reaction.*

#### 5.1 Introduction.

Having developed new methodology to access substituted cyclohexanolamines, we quickly turned our attention into the development of an asymmetric version of this new methodology. Since our key reaction intermediate is achiral iminium cation **107**, we focused our attention on organocatalysts and transition-metal catalysts that could provide a chiral-anionic counterion to control the stereoselectivity of a reaction (Scheme 5.1). In this case, the interaction between the catalyst ( $Y^*$ ) and the substrate is *noncovalent* and the chiral ion pair ( $Y^*$ -**107**) is the real activated species.

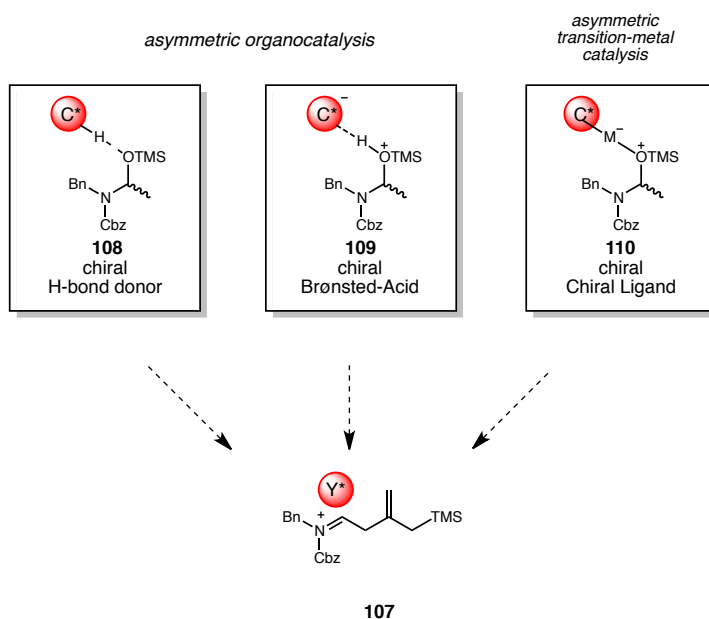


**Scheme 5.1** General strategy for an asymmetric cascade reaction.

Catalysts that provide a chiral-anionic counterion can be divided into two major categories: organic based catalysts and transition metal based catalysts. In addition, organocatalysts can be further subdivided into two classes based on the mechanism of activation of the prochiral species: chiral hydrogen-bonding catalysts and chiral Brønsted

acids.<sup>61a, 61b</sup> Chiral hydrogen-bonding catalysts rely on hydrogen bonding between the catalyst and substrate for the activation of an achiral species, while activation by a chiral Brønsted acid is generally by protonation of the achiral substrate.

We believe that our *N*-Cbz-*O*-TMS aminol **99** can in principle take advantage of this noncovalent chiral ion pair to induce asymmetry in our methodology (Figure 5.1). Thus, in the case of the hydrogen-bonding catalysts, hydrogen-bonding activation of **99** should resemble reactive intermediate **108**. On the other hand, protonation by a chiral Brønsted acid should give a reactive intermediate such as **109**. Finally, we believe that a transition metal catalyst can also activate substrate **99** to produce activated species **110**.



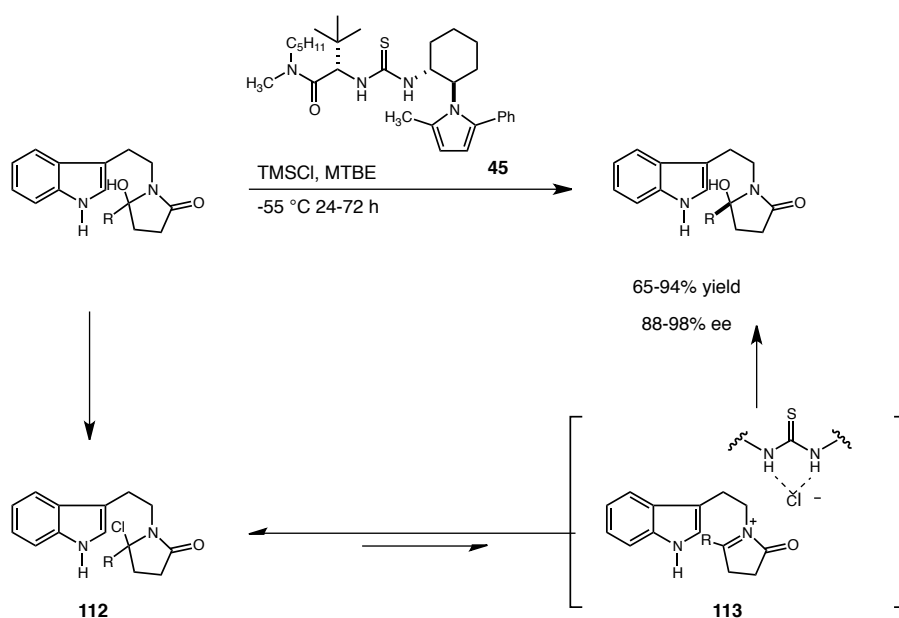
**Figure 5.1** Comparison of strategies for an asymmetric cascade reaction

## 5.2 Thiourea Based Catalysts (Hydrogen-Bonding Catalysts).

We began by investigating chiral thioureas as potential catalyst for our methodology. Chiral thioureas are effective directional double hydrogen-bonding



catalysts that are capable of electrophilically activating substrates such as imines while at the same time provide a highly stereodefined environment.<sup>62</sup> As such, they have been popular organocatalysts in recent years. The Jacobsen group has been the leader in the development of chiral ureas and thioureas for enantioselective transformations. For example, the Jacobsen group has used chiral thiourea catalyst **111** for an enantioselective Pictet-Spengler reaction of  $\beta$ -indolyl hydroxylactams (Scheme 5.2).<sup>63</sup>

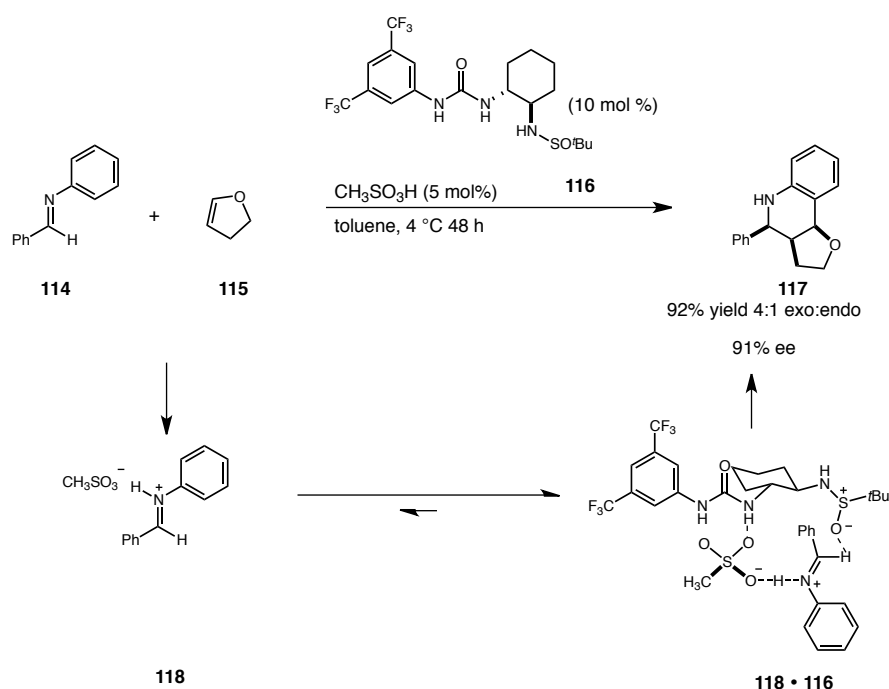


**Scheme 5.2** Thiourea Catalyzed Pictet-Spengler Reaction.

The proposed mechanism for this transformation involves activation of the hydroxyl lactam with TMSCl to give chloro lactam **112** followed by thiourea **111**-assisted chloride disassociation. The diastereomeric *N*-acyliminium ion pair obtained **113** gives rise to the observed enantiopure Pictet-Spengler products after cyclization.

The Jacobsen group has also reported a urea catalyzed cycloaddition (Povarov reaction) of imine **114** and furan **115** in the presence of **116** to generate cycloadduct **117**

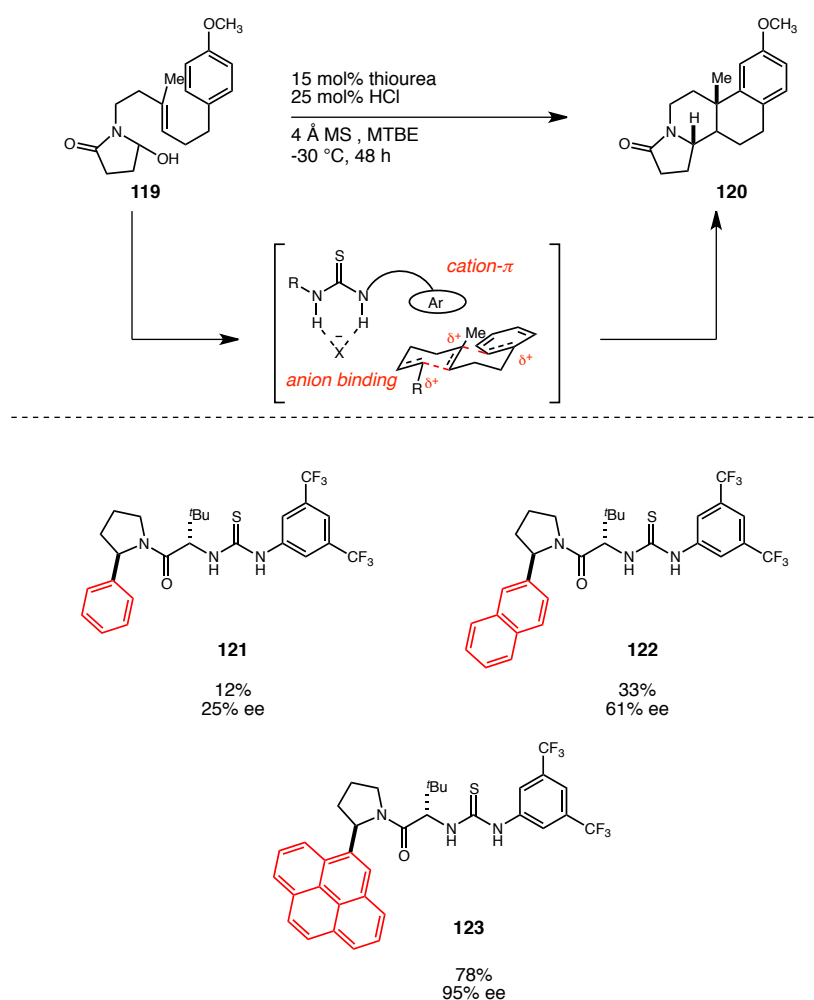
in good yield and ee (Scheme 5.3).<sup>64</sup> This reaction proceeds through iminium ion **118**, which is in equilibrium with complex **118 • 116** with the equilibrium strongly favoring complex **118 • 116**. In addition, the total concentration of iminium ion **118** never exceeds that of the catalyst **116** since a catalytic amount of the Brønsted acid is used. Thus the racemic cycloaddition of **114** with furan **115** is suppressed and the reaction proceeds with high enantiospecificity.



**Scheme 5.3** Urea catalyzed Povarov Reaction.

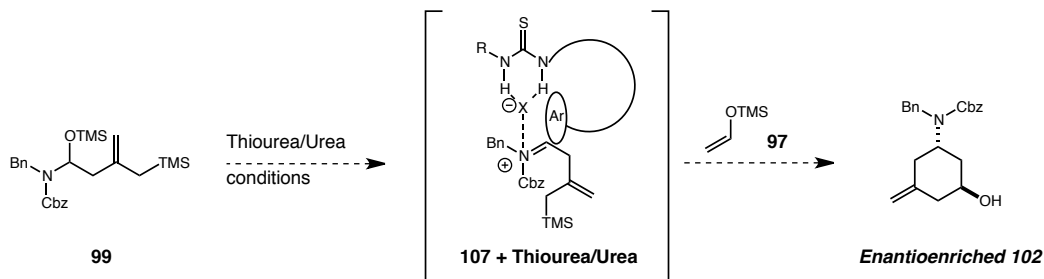
Shortly after we began our investigations into an enantioselective variant to the intermolecular iminium cascade reaction, the Jacobsen group showed that arene substituents on thiourea catalysts can have a significant effect on enantioselectivities.<sup>65</sup> For example, cationic polycyclization of **119** in the presence of **121** yields adduct **120** in 12% yield and 20% ee (Scheme 5.4). On the other hand, polycyclization in the presence

of naphthyl substituted thiourea **122** yields **120** in 33% yield and 61% ee. Pyrenyl substituted thiourea **123** gives the best yield (90%) and excellent ee (95%). These studies indicate that the arene substituents appear to stabilize the transient cations via cation- $\pi$  interactions. This cation- $\pi$  interaction as well as the anionic binding interaction of the thiourea motif makes this catalysis a two point binding and are responsible for the enantioselectivities observed.



**Scheme 5.4** Thiourea catalyzed cation polycyclization.

Based on these reports by the Jacobsen lab, we believe that an arene thiourea or urea catalyst in conjunction with an achiral Brønsted acid could yield a stabilized chiral cation **107** + **thiourea/urea** complex (Scheme 5.5). We believe this arene stabilized cation intermediate will determine the stereoselectivity of the cascade reaction.



**Scheme 5.5** Proposed mechanistic strategy with a thiourea catalyst.

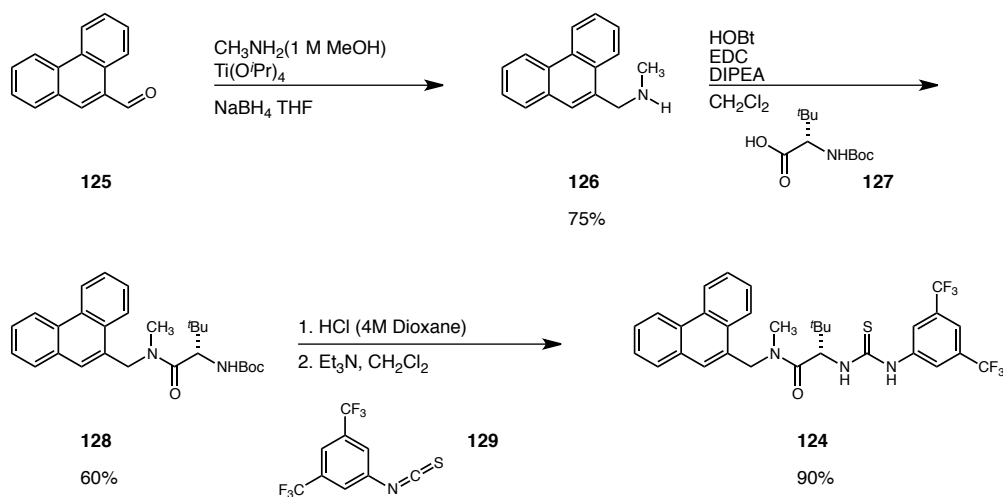
## 5.3 Investigations into thioureas as catalysts for our methodology.

### 5.3.1 Synthesis of chiral thiourea **58**.

As mentioned earlier, our investigations into thioureas as chiral catalysts for the asymmetric intermolecular cascade reaction started shortly before the Jacobsen group published their results with catalysts (**121-123**) on the importance of arene groups as cation stabilizers. However, we were aware of some unpublished results that arenes played an important role on cation stabilization from a seminar presented at Emory University. Based on this unpublished data, we chose chiral thiourea **124** as our starting catalyst. Catalyst **124** had the required arene motif as well as the thiourea unit, which is

critical for hydrogen bonding catalysis. In addition, catalyst **124** could be accessed in a quick manner from cheap and commercially available materials.

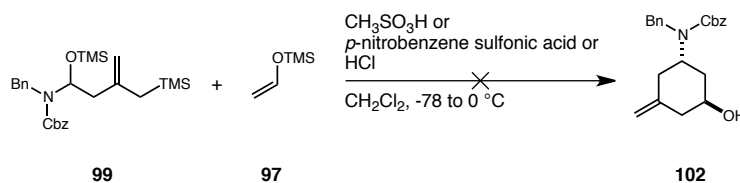
The synthesis of catalyst **124** commenced with the synthesis of amine **126** via reductive amination. Thus treatment of 9-phenanthrene-carboxaldehyde (**125**) and methylamine in the presence of  $\text{Ti}(\text{O}^i\text{Pr})_4$  and  $\text{NaBH}_4$  produced amine **126** in 75% yield (Scheme 5.6).<sup>66</sup> Peptide coupling of amine **126** and commercially available *N*-Boc-*L*-tert-leucine (**127**) mediated by  $\text{HOBT}\cdot\text{H}_2\text{O}$  and EDC yielded carbamate **128** in 60% yield. Boc deprotection of **128** with HCl in dioxane, followed by treatment of the crude amine obtained with isothiocyanate **129** produced the desired thiourea catalyst **124** in excellent yield.<sup>65</sup>



**Scheme 5.6** Synthesis of chiral thiourea **124**.

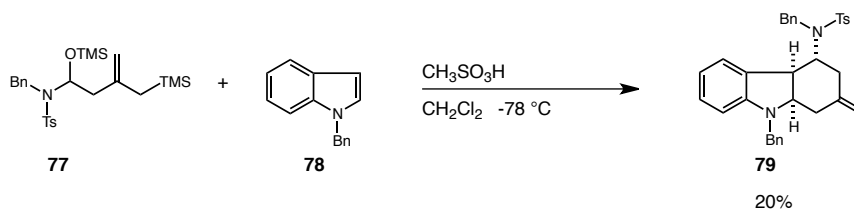
### 5.3.2 Iminium Cascade Reaction with Sulfonic Acids.

With chiral thiourea **124** in hand, we were excited by the prospect of running our intermolecular reaction with this catalyst. However, we needed to determine whether our intermolecular cascade reaction could be run with achiral Brønsted acids, in particular sulfonic acids beforehand. Unfortunately, reaction of *N*-Cbz-*O*-TMS aminol **99** and vinyloxy-trimethylsilane (**97**) with a variety of achiral Brønsted acids (MeSO<sub>3</sub>H, *p*-nitrobenzenesulfonic acid and HCl) did not yield any of the desired cyclohexanol **102** (Scheme 5.7).



**Scheme 5.7** Attempts to cyclized with achiral Brønsted acids

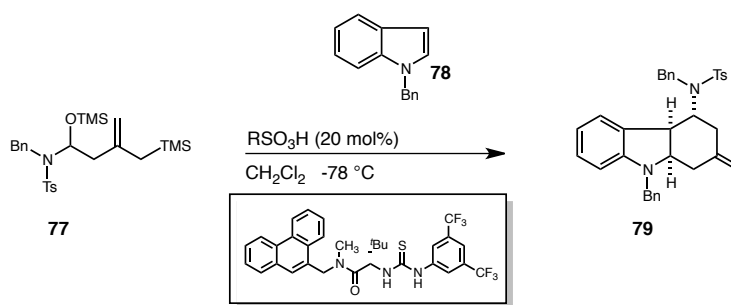
Under the strong protic conditions, we believed that vinyloxy-trimethylsilane (**97**) was decomposing faster than it could react with iminium ion **107**. Therefore, we decided to revisit the cyclization with the protic acids, but using *N*-benzyl indole (**78**) as the nucleophile instead. Cyclization of *N*-tosyl-*O*-TMS-aminol **99** and *N*-benzyl indole (**78**) with MeSO<sub>3</sub>H at -78 °C afforded the tricyclic compound **79**, albeit in low yield (20%) (Scheme 5.8). Nonetheless, we believed that this reaction was a good candidate to attempt cyclization using chiral thiourea catalyst **124**.



**Scheme 5.8** Cyclization with methane sulfonic acid.

### 5.3.3 Cyclization with chiral thiourea catalyst **58**.

Having established that the cyclization of **77** and **78** does occur under protic acid conditions, we were now ready to attempt the cyclization using catalyst **124**. Unfortunately, under a variety of conditions we did not observe any significant enantioselectivity (Table 5.1). A small enantioselectivity was observed when the cyclization was run at low temperatures (entries 2 and 4). However, the enantioselectivities observed were lower than 5%.



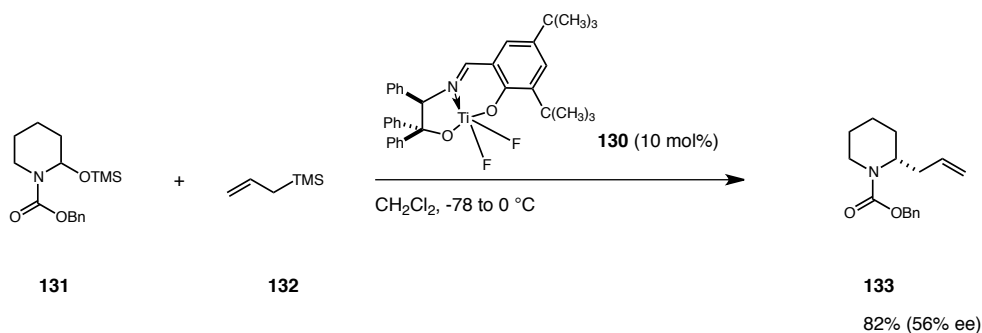
Entry	Acid	Temperature $^\circ\text{C}$	% yield	% ee
1	$\text{CH}_3\text{SO}_3\text{H}$	-20	10	----
2	$\text{CH}_3\text{SO}_3\text{H}$	-78	15	<5
3	$\text{CF}_3\text{SO}_3\text{H}$	-20	10	----
4	$\text{CF}_3\text{SO}_3\text{H}$	-78	5	<5

**Table 5.1** Cyclization with thiourea catalyst **124**.

## 5.4 Ti(IV) based catalyst.

### 5.4.1 Braun's dynamic kinetic asymmetric allylations.

The negative results obtained with chiral thiourea catalyst **124** prompted us to revisit the literature. We were drawn to a recent report by Braun and coworkers on the dynamic kinetic asymmetric allylations (DKAA) of tertiary alcohols, hemiacetals and aminols, using Ti(IV) catalyst **130**.<sup>67</sup> For example, allylation of *N*-Cbz-*O*-TMS aminol **131** with allylsilane **132** in the presence of **130** (10 mol%) yielded carbon-allylation product **133** in 82% and 56% ee (Scheme 5.9).

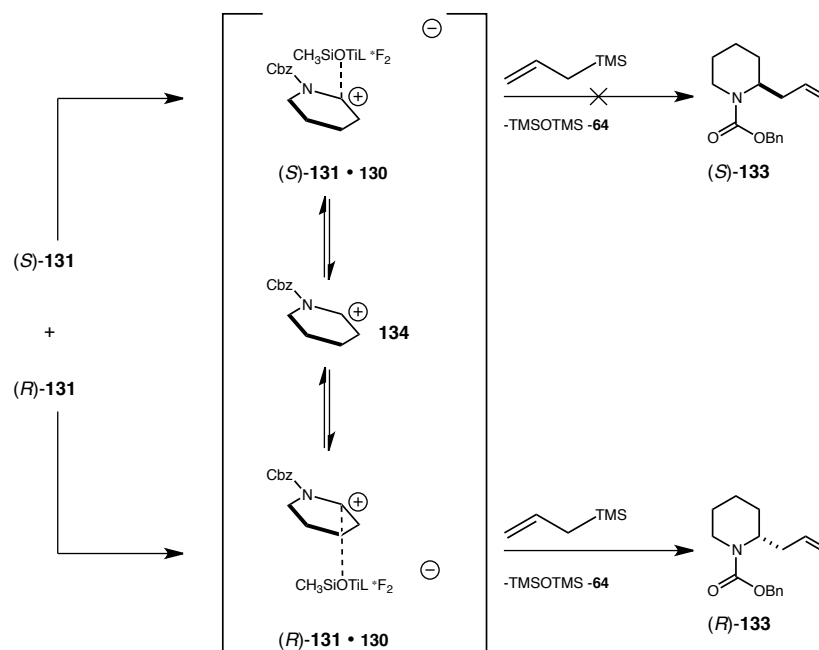


**Scheme 5.9** Braun's dynamic kinetic asymmetric allylation using catalyst **130**.

The high conversion as well as the moderate to high enantiomeric excesses observed in these allylation reactions with **130**, was rationalized by means of a dynamic kinetic asymmetric mechanism (Scheme 5.10).<sup>67</sup> Thus, in the case of racemic **131**, both enantiomers are believed to engage the Lewis acid catalyst **130** giving rise to two diastereomeric ion pairs: (*R*)-**131** • **130** and (*S*)-**131** • **130**. These two diastereomeric salts are proposed to rapidly equilibrate via planar achiral iminium ion **134**. Finally, one of the



ion pairs, (*R*)-**131** • **130**, was postulated to react faster with the allylsilane, which is assumed to attack from the opposite face of the bulky titanium catalyst.



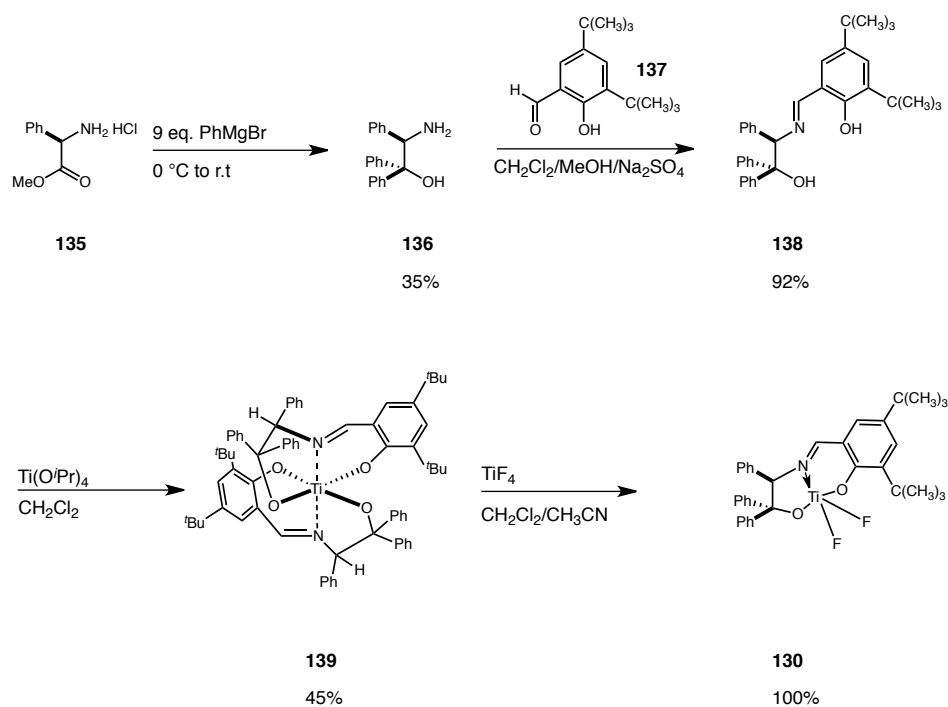
**Scheme 5.10** Postulated mechanism for DKAA with **130**.

We were excited about this work, based on the similarity of the functional groups of **131** with our own aminol **99** and the proposed mechanism for this dynamic kinetic asymmetric allylation reaction, which involved a chiral-ion pair. Thus, we began efforts for the synthesis of **130**.

#### 5.4.2 Synthesis of Ti(IV) Catalyst **130**.

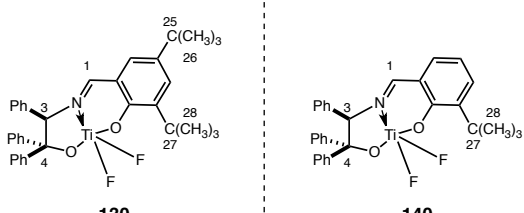
Although our research in the literature revealed that the synthesis and characterization of catalyst **130** was never reported, we began the synthesis of **130** based on an earlier report by the Braun group on the synthesis similar catalysts.<sup>48a</sup> The synthesis

of **130** commenced with commercially available (*R*)-phenylglycine methyl ester HCl (**135**). Thus treatment of **135** with excess phenylmagnesium bromide yielded amino alcohol **136** in 35% yield (Scheme 5.11). Condensation of amine **136** with di-*tert*-butyl hydroxyaldehyde **137** under dehydrative conditions produced the half-salen ligand **138** in 92% yield. Treatment of 2 equivalents of Schiff base **138** with 1 equivalent of titanium tetrakisopropoxide yielded the air and moisture stable bis-chelated complex **139** as a single isomer in 45% yield. Lastly, catalyst **130** was made by treatment of bis-chelated complex **139** with titanium tetrafluoride under inert atmosphere to give difluorotitanate **130** in quantitative yield.



Scheme 5.11 Synthesis of difluorotitanate **130**.

Although we were unable to find any published reports detailing the full characterization of difluorotitanate **130**, we able to find published data for **140**.<sup>48a</sup> Table 5.2 tabulates some important chemical shifts ( $^1\text{H}$  and  $^{13}\text{C}$ ) for both **130** and **140**.

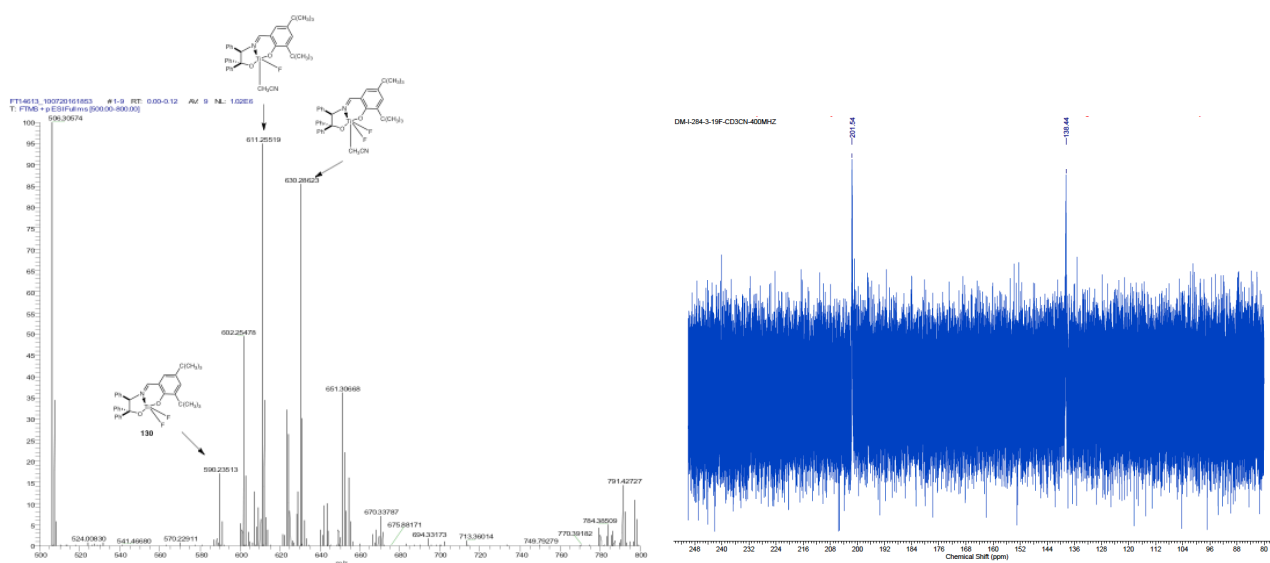


Position	$\delta_{\text{H}}$	$\delta_{\text{H}}$
C1	8.86 s	8.82 s
C3	6.57 s	6.54 s
C4	---	---
C26	1.28	---
C28	1.33	1.34 s
Position	$\delta_{\text{C}}$	$\delta_{\text{C}}$
C1	168.8	167.8
C3	86.2	85.8
C4	94.6	94.0
C26	31.9	---
C28	30.1	29.6
$\delta_{\text{F}}$		$\delta_{\text{F}}$
138.4 s		140.0 s
201.5 s		201.2 s

**Table 5.2** NMR data ( $^1\text{H}$ : 600;  $^{13}\text{C}$  151;  $^{19}\text{F}$  565 MHz) for **130** ( $\text{CD}_3\text{CN}$ ) and ( $^1\text{H}$ : 500;  $^{13}\text{C}$  125;  $^{19}\text{F}$  470 MHz) for **140** ( $\text{CD}_3\text{CN}$ ).

As shown on Table 5.2, NMR data for obtained for difluorotitanate **130** matches closely the data reported for titanium complex **140**. Interestingly, the signal to noise ratio

of complex **130** in the  $^{19}\text{F}$  NMR was low. We ruled out the possibility that most of the complex was in the dimeric form **139** since the  $^1\text{H}$  NMR spectra for both **139** and **130** are distinct. Further confirmation of the synthesis of difluorotitanate **130** was provided by HRMS, which showed a base peak corresponding to  $[\text{M-F}+\text{CH}_3\text{CN}]$  at 611.2522 (calculated 611.2553) (Figure 5.2).

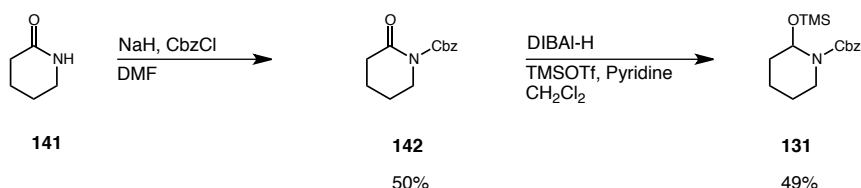


**Figure 5.2** HRMS (left) and  $^{19}\text{F}$  NMR (right) of difluorotitanate **130**.

### 5.4.3 Synthesis and Allylation of **65**.

Having successfully synthesized titanium catalyst **130** we were excited at the prospect of using this catalyst in our system. However, before investing amounts of now precious aminol **99**, we decided to bench test this catalyst on substrate **131**. Substrate **131** was quickly obtained in two steps from  $\gamma$ -valerolactam (**141**) (Scheme 5.12). Thus,

acylation of **141** with NaH and CbzCl produced **142** in 50% yield. DIBAL-H reduction and treatment of the aluminum hemiacetal with trimethylsilyl-imidazole to yield aminol **131** in 45% yield.



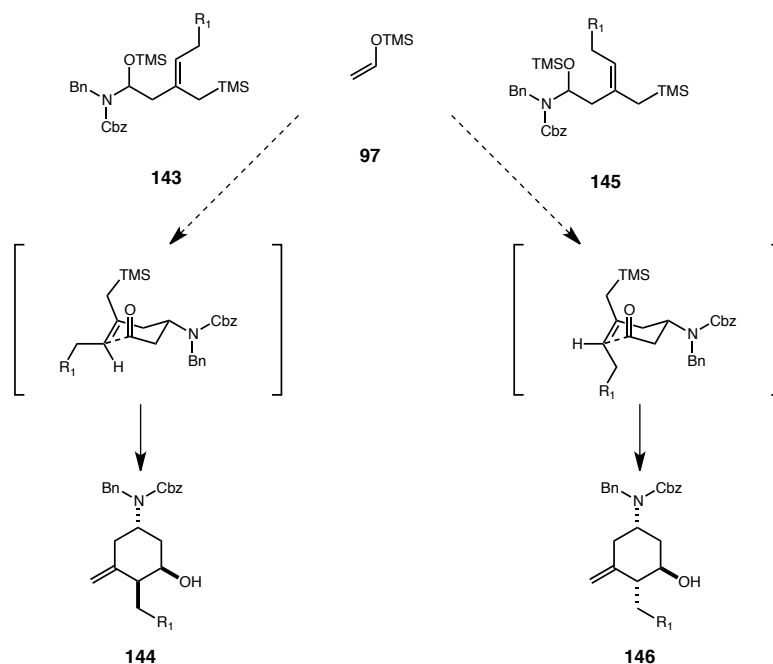
**Scheme 5.12** Synthesis of model substrate **131**.

With aminol **131** in hand, we were ready to bench test catalyst **130**. Unfortunately, we were never able to reproduce the results reported by Braun and coworkers. In fact, several attempts were made at trying to reproduce this reaction. Different batches of catalysts and aminol were used as well as varying the temperature of the reaction and rate of addition of the allylsilane. In all cases, the reaction of *N*-Cbz-*O*-TMS aminol **131** with allylsilane **132** in the presence of **130** (10-40 mol%) did not yield any of the desired allylation product **133**. With these negative results we decided not move forward with catalyst **130** and decided to put an indefinite hold on our studies towards the development of an enantioselective intermolecular cascade reactions.

## 5.5 Conclusions.

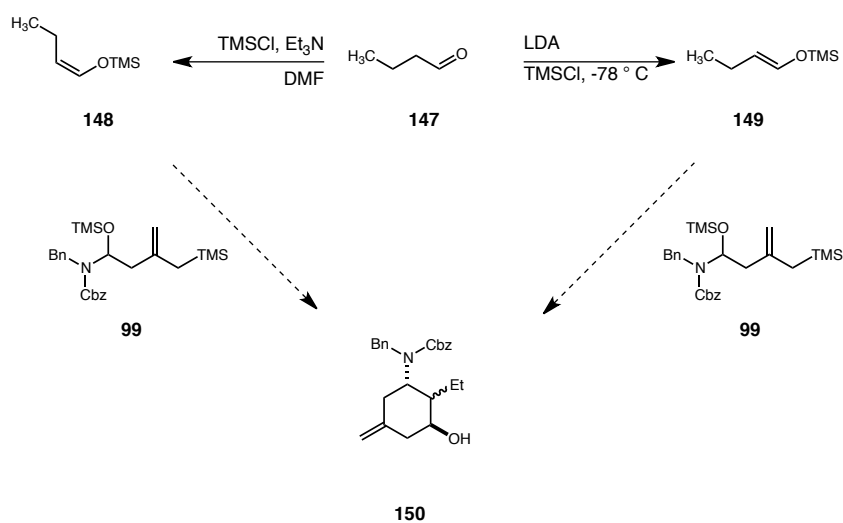
We have successfully adapted our intermolecular iminium ion cascade cyclization reaction to include silyl enol ethers as external traps. This methodology yields highly

substituted *trans*-cyclohexanol rings in good yield and high diastereoselectivity. Since this project is still in its infancy, a lot of exciting new possibilities exist that will enable the construction of highly substituted amino- cyclohexanol rings. For example, we have shown can extend our *intramolecular* cascade annulation reaction to include trisubstituted olefins (*vide infra*). In addition, we have demonstrated that *E* and *Z* -trisubstituted olefins, give access to *two diastereoisomers* stereospecifically. If this fact holds true for this methodology, we could access two new diastereoisomers of the cyclohexanol ring by simply changing the geometry of the olefin (Scheme 5.13). Thus *Z*-trisubstituted olefin **143** is expected to cyclize through a chair-like transition state, such as the one proposed for **99**, and is expected to produce trisubstituted cyclohexanol **144**. *E*-trisubstituted olefin **145** is also expected to cyclize through a similar chair-like transition state and is expected to produce cyclohexanol **146**.



**Scheme 5.13** Proposed extension of methodology with *Z* and *E*-trisubstituted olefins.

Future work could also include the use of more substituted enol ethers as traps. Thus, *Z* and *E* olefins could be accessed in stereoselective manner from the corresponding aldehydes (Scheme 5.14). Thus, the *Z*-silyl enol ether **148** could be accessed from aldehyde **147** by thermodynamic conditions.<sup>68</sup> On the other hand, *E*-silyl enol ether **149** could be accessed through kinetic conditions from aldehyde **147**.<sup>69</sup> Cyclization of both *Z*-silyl enol ether **148** and *E*-silyl enol ether **149** with **99** is expected to yield a diastomeric mixture of new tetrasubstituted cyclohexamines **150**.



**Scheme 5.14** Cyclization with disubstituted enol ethers **148** and **149**.

These proposed studies will not only expand the scope of this methodology, but will also showcase its utility for the construction of complex cyclohexamine which otherwise could be difficult to access by current methods, such as the Diels-Alder reaction.





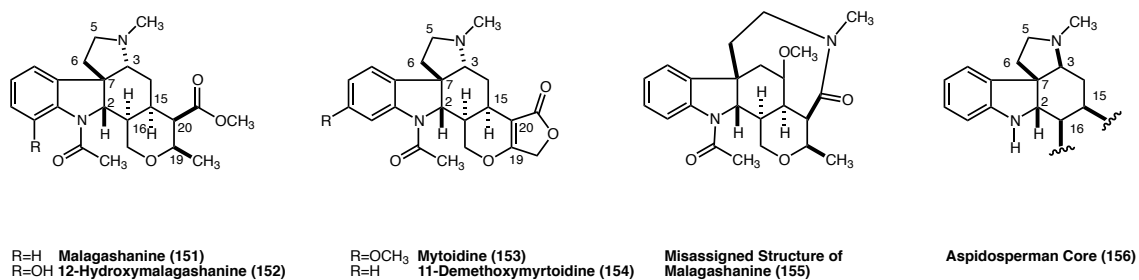
**Part 3**  
**Studies Towards the Total Synthesis of a Malagasy**  
**Alkaloid**

## 6 Chapter 6

*Introduction to the Malagasy Alkaloids and Initial Efforts Towards the Synthesis of Malagashanine.*

### 6.1 The Malagasy Alkaloids.

Scientific surveys conducted in Madagascar have shown that populations living in areas where chloroquine (CQ) was ineffective against malaria could be treated by using CQ in combination with tea made from a local shrub: *Strychnos myrtoides*.<sup>70</sup> Subsequent research by Rasoanaivo and coworkers led to the isolation of Malagashanine (**151**) as the active component (Figure 6.1).<sup>71</sup> Malagashanine was isolated using countercurrent distribution (CCD) that afforded  $8.0 \times 10^{-4}$  % yield based on dry weight. Other related compounds isolated from the same plant extract include 12-hydroxymalagashanine (**152**), myrtoidine (**153**) and 11-demethoxymyrtoidine (**154**).<sup>72</sup> Additionally, minor C(3) epimers of myrtoidine have also been isolated.<sup>73</sup>

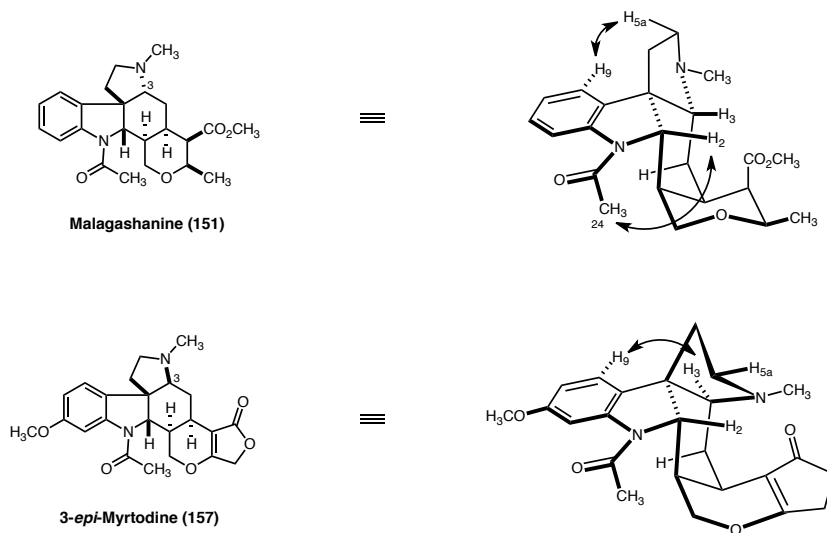


**Figure 6.1** The malagashanine alkaloids and related compounds.

## 6.2 Malagashanine: Structure.

The molecular formula of malagashanine was established to be  $C_{23}H_{30}N_2O_4$  by EI-MS.<sup>74</sup> The structure was originally assigned as  $N_b,C(3)$  secocuran alkaloid **155** having a  $N_b$ -methyl, 14-methoxy and C(21) carbonyl substituents. The assignment was based on  $^1H$ - $^1H$  selective decoupling and  $^1H$ - $^1H$  COSY experiments, as well as comparisons to other secocuran alkaloids. However shortly after this original disclosure, the authors subsequently revised their assignment using X-ray crystallographic data and unequivocally assigned the structure as **151**.<sup>75</sup> Malagashanine presents an interesting pentacyclic structure with seven contiguous stereocenters in a stereochemically unique arrangement. Unlike all other known strychnos and aspidosperma alkaloids, which display the C(2)-H, C(7)-C(6), and C(3)- $N_b$  bonds all in *syn* relationship to each other as shown in Figure 6.1 (aspidosperma core **156**), malagashanine possesses an inverted relative stereochemistry at C(3). NOESY studies also support the revised structure and show cross peaks between H-5a and H-9 that are only explainable if the C(3) stereocenter is inverted (Figure 6.1). Additionally, 3-*epi*-myrtoidine (**157**), which possesses the usual aspidosperma stereochemistry, shows cross peaks between H-3 and H-9 that are not observed in malagashanine.

Only one conformer of malagashanine is detectable by NMR at 300 K despite the presence of an *N*-methylacetamide moiety (Figure 6.2). This is in contrast to the usual mixture of rotamers observed with most members of the malagashanine family. NOE between H-2 and  $CH_3(24)$  indicate that the *Z*-isomer is the predominant conformer in malagashanine.



**Figure 6.2** nOe studies on the malagashanine alkaloids.

### 6.3 Myrtoidine and Demethoxymyrtoidine.

#### 6.3.1 Myrtoidine

The molecular formula of myrtoidine (**153**) was established to be  $C_{23}H_{26}N_2O_5$  by HREIMS.<sup>76</sup> The structure of **153** was assigned by comparison of UV and NMR spectra to malagashanine. For example, NMR studies suggested the presence of a 11-methoxy group in the indole ring. The UV spectrum ( $\lambda_{max}$  220, 242,sh, 289 nm) of myrtoidine was different than the classical  $N_a$ -acylindolinic alkaloids and showed an intermediate absorption as a shoulder of the first maximum instead of a separate maximum. This suggested the presence of a new chromophore in the molecule. In addition,  $^1H$  and  $^{13}C$  NMR showed the disappearance of Me(18), H-19 and H-20 signals as compared to malagashanine. HMBC showed correlations between two new downfield signals; H-18a

and H-18b and C(19), C(20) and C(21). Furthermore, a drastic shielding was observed for C(20) and strong deshielding was observed for C(19) suggesting a mesomeric effect of an  $\alpha$ ,  $\beta$ -unsaturated  $\gamma$ -lactone ring system.

### 6.3.2 11-Dimethoxymyrtoidine.

The molecular formula of 11-demethoxymyrtoidine (**154**) was established to be  $C_{22}H_{24}N_2O_4$  by HREIMS.<sup>76</sup> The structural assignment was based on UV,  $^1H$  and  $^{13}C$  NMR spectra, which suggested that it was closely related to myrtoidine. In fact, comparison of the NMR data showed that the only difference was the disappearance of the methoxy group in **154** and the presence of only four aromatic protons.

Unlike malagashanine, both myrtoidine (**153**) and 11-demethoxymyrtoidine (**154**) show the presence of more than one conformer by NMR at 300 K due to the presence of the *N*-methylacetamide moiety.

## 6.4 Biological Activity

The World Health Organization (WHO) estimates that malaria is responsible for about 1 million deaths per year, mainly women and young in tropical and subtropical regions of the world. Although artemisinin combination-based therapies (ACTs) are the currently drug therapy for the treatment of malaria, chloroquine (CQ) (discovered in 1934) is still being used as the first line of treatment in several countries.<sup>77</sup> The emergence and spread of drug resistant strains of malaria to even modern drugs such as ACTs has led to the rise of infections and deaths. For example, CQ resistant *Plasmodium falciparum*, is alone responsible for 80% of infections and 90% of deaths.<sup>78</sup> Although

considerable effort has been directed towards the development of new anti-malarial drugs with novel mechanisms of action, the understanding of the mechanism by which the malaria parasite develops resistance to current drugs, such as CQ, is of paramount importance.

Scientific surveys conducted in Madagascar showed that populations living in areas where CQ was ineffective against malaria could be cured by using CQ in combination with tea made from the local shrubs: *Strychnos myrtoides* and *Strychnos mostueoides*.<sup>71</sup> This herbal decoction is claimed to work as an adjuvant to treat malaria, and is used with seeming success even with low doses of CQ (100-200 mg). A series of studies conducted by Rasoanaivo and coworkers beginning in 1991 identified malagashanine **154** as one of the main components of the extract of *Strychnos myrtoides* and *Strychnos mostueoides*. *In vitro* studies using a chloroquine resistant (CQR) strain of *Plasmodium falciparum* FCM 29/Cameroon revealed that malagashanine exhibited marked CQ enhancement activity (Table 6.1).<sup>79</sup> Subsequent *in vitro* biological testing showed that malagashanine acted by preventing CQ efflux in drug resistant *Plasmodium falciparum* strains.<sup>70</sup> There is evidence suggesting that it stimulates CQ influx as well.

Malagashanine Dose (µg/ml)	Chloroquine Activity (nM)		
	IC <sub>50</sub>	IC <sub>90</sub>	AEI <sup>a</sup>
0 <sup>b</sup>	226.0 +/- 4.7	522.7 +/- 9.4	
5	90.6 +/- 5.5	207.0 +/- 6.7	2.5
10	52.9 +/- 4.6	142.8 +/- 6.3	3.7
15	38.5 +/- 3.6	116.9 +/- 5.1	4.5
20	33.2 +/- 3.2	95.6 +/- 5.4	5.5
25	25.5 +/- 2.7	76.6 +/- 5.2	6.3

<sup>a</sup> AEI or activity enhancement index is calculated by dividing the IC<sub>90</sub> of CQ by the IC<sub>90</sub> of CQ combined with malagashanine.

<sup>b</sup> Control plate with CQ alone.

**Table 6.1** Chloroquine potentiating activity of malagashanine on CQR strain of

*Plasmodium falciparum* FCM 29/Cameroon.

*In vivo* studies using the crude alkaloid extracts from *S. myrtooides* were carried out on Swiss mice infected with a line of *Plasmodium yoelii* subsp. *nigeriensis* N67 resistant to CQ and susceptible to pyrimethamine and mepacrine. These studies revealed an 81.1% suppression of parasitaemia by the fifth day of the experiment in mice receiving 0.75 mg/Kg dosages of CQ and 100 mg/Kg of crude alkaloid extract. No toxicity was detected against the extract at oral dosages of 100 mg/Kg.<sup>70</sup>

The mechanism through which chloroquine resistance operates still is a topic of debate.<sup>80</sup> There is some evidence suggesting that it is caused by Pgh-1, an ortholog of one of the P-glycoproteins expressed in multi-drug resistant human cancer cells (ABC transporter).<sup>81</sup> Additionally, some research suggests that a *Pf*CRT protein might be responsible for the increased resistance either by changing the vacuolar pH (which would result in reduced CQ uptake or lower binding affinity for ferriprotoporphyrin IX) or by facilitating the efflux of CQ itself.<sup>82</sup> The ability of malagashanine to negate drug resistance in CQR *Pf* strains provides an excellent opportunity to probe the biological mechanisms controlling these processes. Moreover, such studies could well impact the field of cancer research provided that the parallels of chloroquine resistance and multi-drug resistance in human cancer cells proved accurate. Consequently, useful quantities of malagashanine and synthetic analogs are required. The following chapter describes our continuing efforts to develop a reliable and efficient synthesis of malagashanine and 12-demethoxymyrtoidine, which will allow us to generate a useful amount of these materials for further biological evaluations.

## 6.5 Blakey's Lab Approach to the Malagasy Alkaloids

### 6.5.1 Early Cascade Annulation Work.

At the outset of this project, research in the literature revealed that all methods available for the synthesis of strychnos or aspidosperma alkaloids were not suitable for the synthesis of the Malagasy alkaloids. The main deficiency with all these methods is that they yield the common *syn* relationship between C(2)-H, C(7)-C(6), and C(3)-N<sub>b</sub>.<sup>83a, 83b, 83c, 83d, 83e, 83f</sup> The unique *trans* relationship between C(7) and C(3)-N<sub>b</sub> of the Malagasy alkaloids makes the development of new methodology to synthetically access these important alkaloids a necessity.

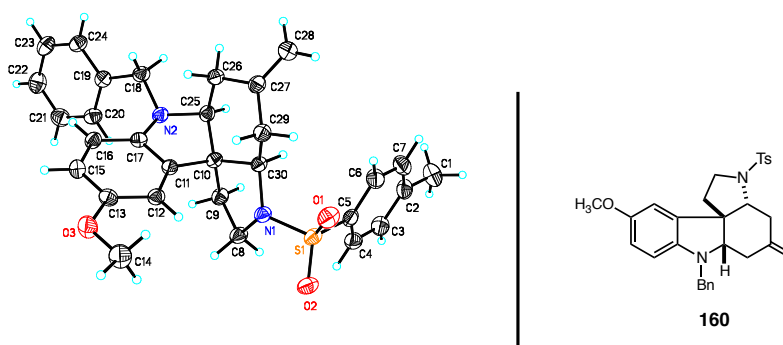
Our lab recognized this necessity and embarked on synthetic studies to develop new methodology to access the Malagasy alkaloids. In fact, Dr. Ricardo Delgado recently developed methodology in our lab to access the core of the Malagasy alkaloids.<sup>41, 42</sup> Based on an intramolecular cascade annulation reaction, the core of the Malagasy alkaloids can be accessed in one step in a highly diastereoselective manner. Thus, treatment of *N*-Tosyl-*O*-TMS aminol **158** with BF<sub>3</sub>•OEt<sub>2</sub> at 0°C generates tetracyclic compound **159** in 82% as a single diastereoisomer (Scheme 6.1). Compound **159** contains the desired *trans* relationship between C(7) and C(3)-N<sub>b</sub>, that is observed in the Malagasy alkaloids.



**Scheme 6.1** Cascade annulation for the synthesis of the Malagasy core.



The structure of compound **159** was established through 1D and 2D NMR experiments. In addition, the structure of **159** was further supported by comparison to the methoxy-substituted analog **160**, the structure of which was established by X-ray crystallography and displayed similar nOes to those of **159** (Figure 6.3).

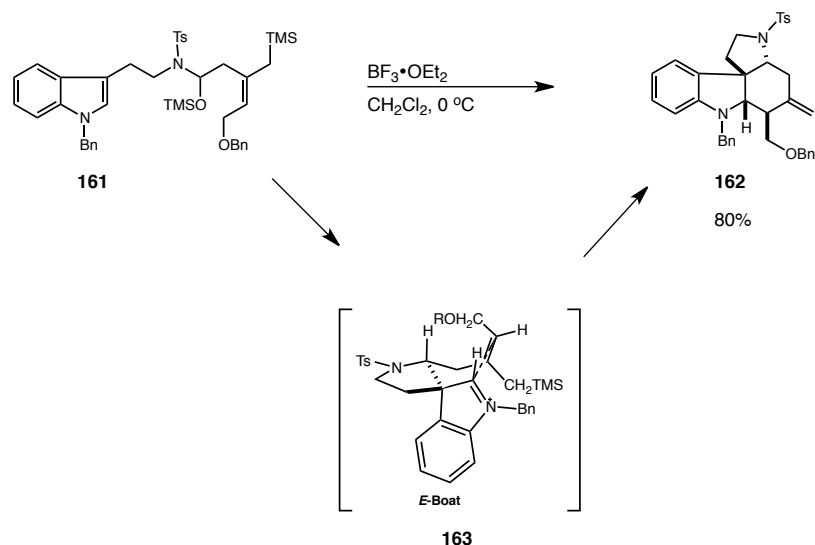


**Figure 6.3** X-ray structure for methoxy-analog **160**.

### 6.5.2 Extending the Scope of Methodology to Incorporate the C(16) Stereocenter.

Having demonstrated the utility of the intramolecular cascade annulation reaction for the synthesis of the core of the Malagasy alkaloids, efforts were undertaken to extend this methodology to include an extra degree of olefin substitution in order to install a fourth stereocenter at C(16). Dr. Ricardo Delgado in cooperation with Dr. Nadège Boudet demonstrated that this was indeed possible. Thus, reaction of the *E*-olefin *N*-tosyl-*O*-TMS aminol **161** with 5 equivalents of  $\text{BF}_3 \cdot \text{OEt}_2$  at  $0^\circ\text{C}$ , generated the desired tetracyclic compound core **162** in 80% yield as a single diastereoisomer (Scheme 6.2).

The exclusive formation of one diastereomer at C(16) suggested that the intermediate iminium ion underwent cyclization exclusively through a boat transition state **163**. More importantly, this reaction yields from an achiral starting material, a heterocycle **162** that now contains four out of the seven contiguous stereocenters required for malagashanine. In addition, compound **162** comprises ~70% of the carbon, nitrogen and oxygen framework of malagashanine.

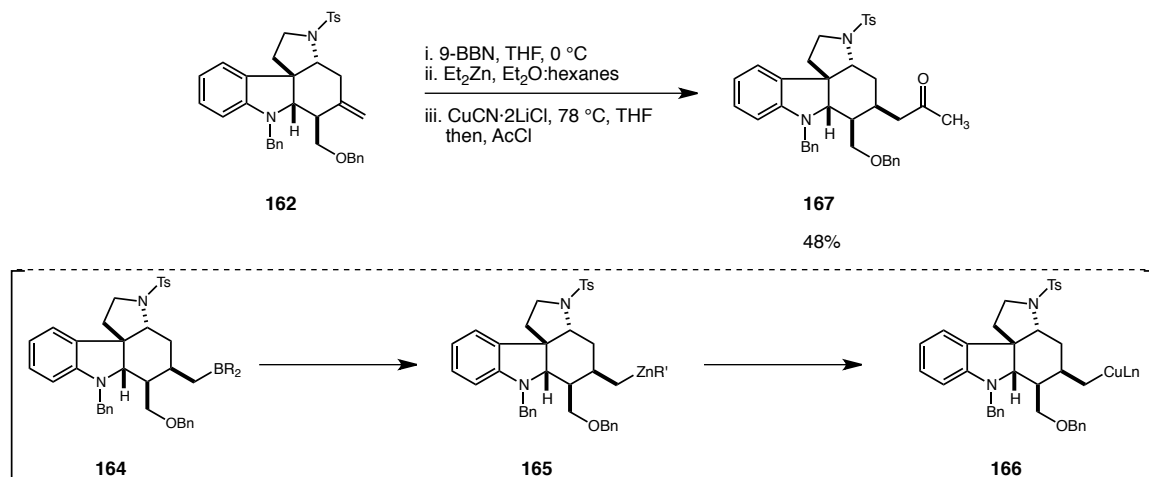


**Scheme 6.2** Cyclization of *E*-isomer leading to correct stereochemistry at C(16).

### 6.5.3 Synthesis of Advanced Pyran **166**

With heterocycle **162** in hand, Delgado and Boudet devoted considerable efforts to advance this material to malagashanine. After many setbacks, the synthesis of the E ring began with the formal hydroacylation of the olefin using a method developed by

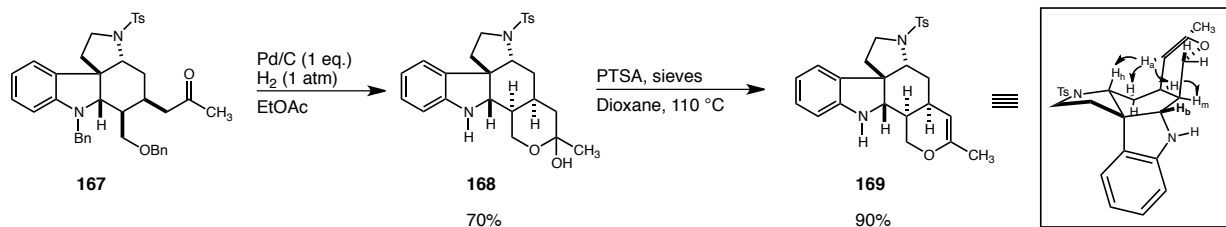
Knochel and co-workers.<sup>84a, 84b</sup> Hydroboration of **162** with 9-BBN set the stereocenter at C(15) and produced the corresponding alkyl-borane species **164** (Scheme 6.3). In order to functionalize C(20) by reaction with acetyl chloride, it was first necessary to transmetalate the alkyl-boron species to a more suitable metal like copper. This was accomplished by first exchanging the alkyl boron species with zinc, which then facilitated the subsequent exchange with copper to form the desired intermediate **166**. Treatment with acetyl chloride at -78 °C afforded ketone **167** in 48% yield and 10:1 diastereoselectivity.



**Scheme 6.3** Formal hydroacylation of **162**.

With ketone **167** in hand, hydrogenolysis of the benzyl group over stoichiometric amounts of palladium on carbon, yielded hemiacetal **168** in 70%. Hemiacetal **168** could be converted into the desired pyran **169** *via* dehydration in a Dean-Stark trap, or by heating in anhydrous dioxane at 110 °C in the presence of PTSA and activated molecular sieves (Scheme 6.4). Both methods could generate **169** in over 90% yield, but the latter

method was preferred because it required shorter reaction times. The structure of **169** was assigned based on COSY, HMQC and NOESY experiments.



**Scheme 6.4** Synthesis and structural assignment of pyran **169**.

Delgado was able to carry additional exploratory work for the introduction of the acyl group in dihydropyran **169** (*vide infra*). However, neither Delgado nor Boudet were able to complete this project, before leaving Emory University. Thus, I was given the task to continue where they left off. The following chapters detail my studies on the synthesis of malagashanine as well as the investigation towards the synthesis of 12-demethoxymyrtoidine.

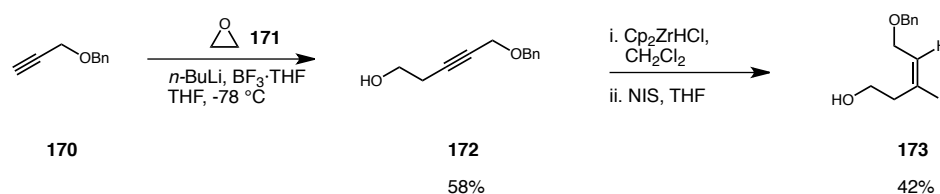
## 7 Chapter 7

*Total Synthesis of Epi-malagashanine.*

### 7.1 Development of a Scalable Route for the Synthesis of Key Dihydropyran 169.

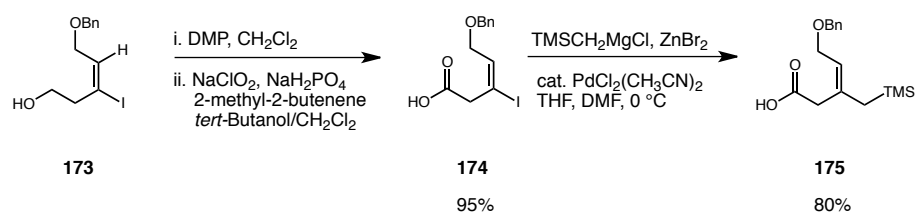
#### 7.1.1 Synthesis of *N*-Tosyl-amide 161.

My initial efforts on this project focused on the scale up for the synthesis of *N*-tosyl-*O*-TMS amide **161**. Previously designed in our group, this convergent synthesis involved seven steps from commercially available propargyl ether **170**.<sup>42</sup> Thus, addition of the lithium salt of alkyne **170** to oxirane (**172**) produced homopropargylic alcohol **173** in 58% yield (Scheme 7.1).<sup>85</sup> This was followed by alkoxy-directed hydrozirconation of **173**, and NIS quench of the intermediate vinylzirconocene to afford iodo-alcohol **174** in 42% yield.<sup>86a, 86b</sup>



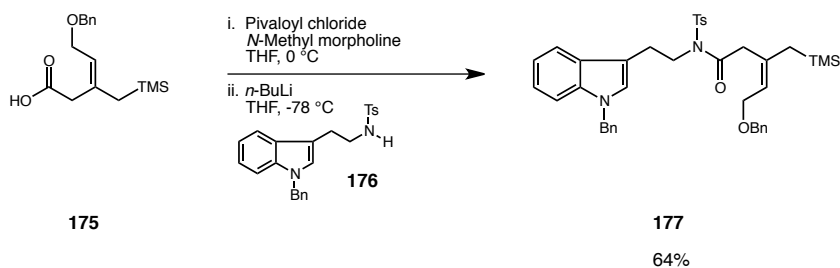
**Scheme 7.1** Synthesis of iodo-alcohol **173**.

With iodo-alcohol **173** in hand, we carried out a Dess-Martin oxidation to produce the corresponding  $\beta,\gamma$ -unsaturated aldehyde, which was used directly in the subsequent Pinnick oxidation to generate acid **174** in nearly quantitative yield over two steps (Scheme 7.2). Negishi cross-coupling with the allylzinc reagent generated *in situ* from (trimethylsilyl)-methyl magnesium chloride at 0 °C afforded the required tri-substituted acid **175** in good yield (80%).



**Scheme 7.2** Synthesis of  $\beta,\gamma$ -unsaturated acid **175**.

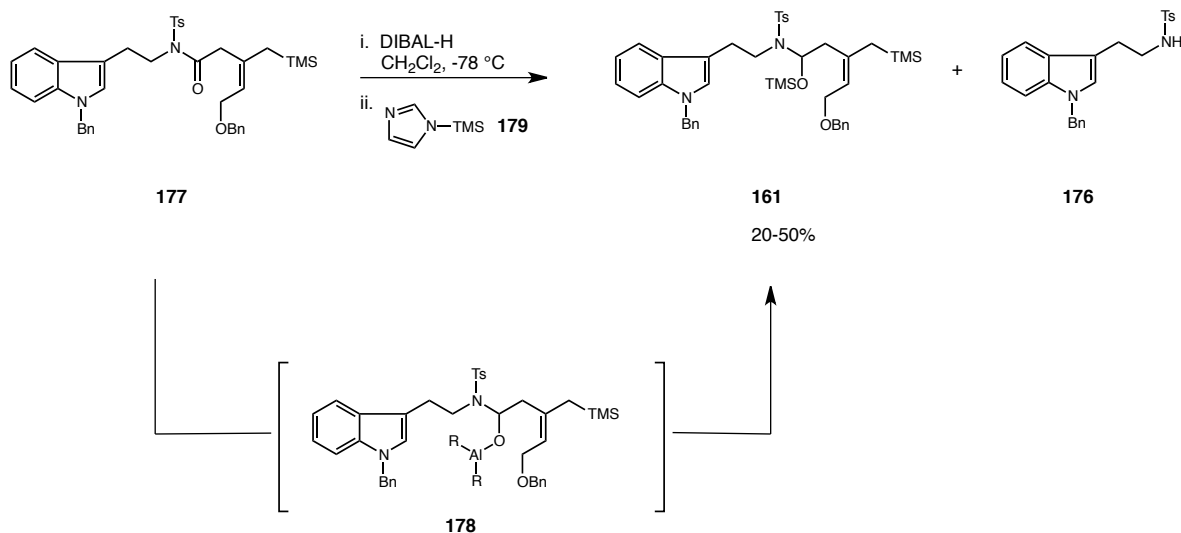
Treatment of acid **175** with pivaloyl chloride generated the corresponding mix anhydride, which was subsequently reacted with the lithium anion of **176** at -78 °C.<sup>87</sup> This mild coupling conditions generated the desired *N*-tosylamide **177** in 64% yield (Scheme 7.3). Although this route is not optimal, it is highly robust. In fact, we have been able to scale this route to yield up to 10 mmols of amide **177**.



**Scheme 7.3** Coupling of acid **175** and tosylamide **176**.

### 7.1.2 Optimization Studies for the Synthesis of *N*-Tosyl-*O*-TMS aminol **161**, Imidazole as a Mild Lewis Acid.

With tosylamide **177** in hand the synthesis of *N*-Tosyl-*O*-TMS aminol **161** was explored in large scale.<sup>42</sup> Reduction of amide **177** with DIBAL-H followed by trapping of the aluminoxy acetal **178** initially generated with TMS-imidazole yielded (**179**) aminol **161** in variable and low yields (20 -50%) along with variable amounts of **176** (Scheme 7.4).

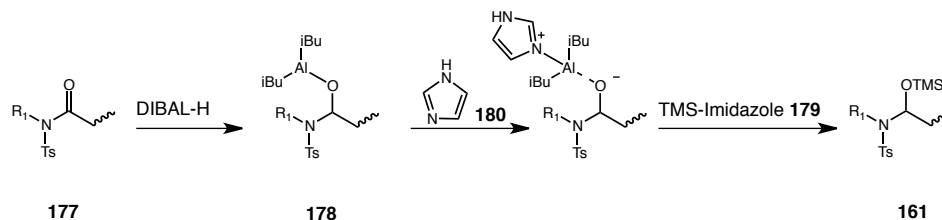


**Scheme 7.4** Initial conditions for the synthesis of *N*-Tosyl-*O*-TMS aminol **161**.

In all runs of this reaction sequence, the starting amide **177** was never recovered from the reaction mixture. In addition, TLC showed the complete disappearance of amide **177**. These results indicated that the complete reduction of the amide carbonyl had taken place. TLC also showed that the subsequent trapping of the aluminoxy acetal by TMS-imidazole was sometimes incomplete, even after additional TMS-imidazole was added

into the reaction mixture. These observations explain the formation compound **176**, which arises from hydrolysis of any left over aluminoxy acetal **158** under the aqueous quench.

We began to troubleshoot this reaction sequence by careful fractional distillation of commercial available TMS-imidazole. Upon distillation of various batches of TMS-imidazole, we observed a solid precipitating on the walls of the receiving flask.  $^1\text{H}$  NMR spectra of this unknown solid, revealed it to be mostly free imidazole (**180**). This observation led us to hypothesize that free imidazole was necessary for an efficient trap of the aluminoxy acetal **178**. In fact, we hypothesized that the free imidazole was complexing with the highly Lewis-acidic aluminoxy acetal, thus weakening the Al-O bond and facilitating the formation of the O-Si bond (Scheme 7.5).<sup>53b, 88</sup>

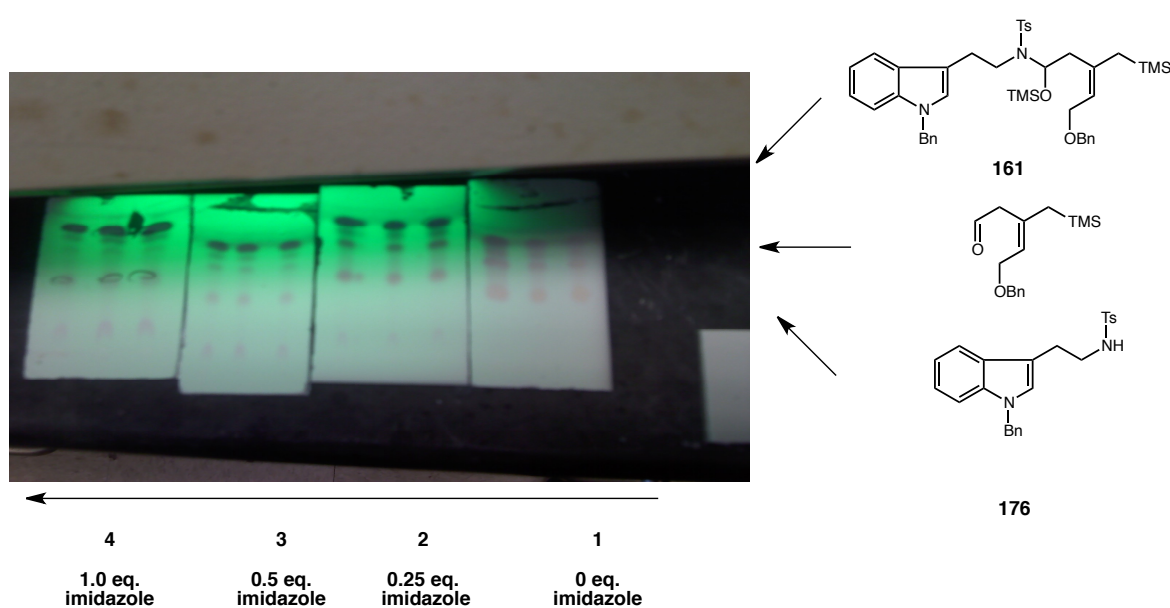


**Scheme 7.5** Hypothesized role of imidazole in reaction sequence.

At this stage, we decided to test this hypothesis by adding incremental amounts of imidazole as a solution in  $\text{CH}_2\text{Cl}_2$  to observe the effects of this compound on the formation aminol **161**. Figure 7.1 shows TLCs taken after each addition of imidazole. From left to right, TLC #1 shows the reaction mixture with no additional imidazole added. As shown on TLC #1, roughly equal amounts of triptamine **176** (bottom spot) aldehyde (middle spot) and TMS-aminol **161** (top) were seen at this stage. TLC #2 shows

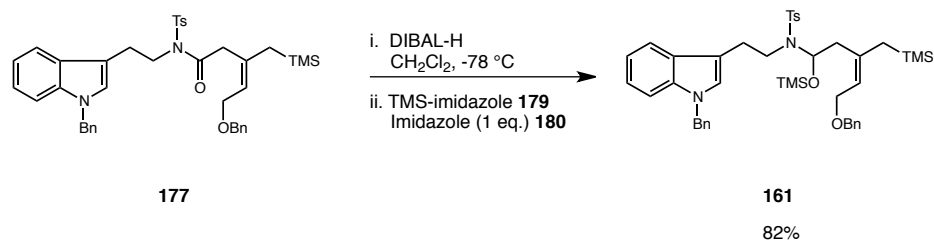


the reaction mixture after 0.25 equivalents of imidazole had been added. Real improvement was seen in TLC #3, which showed the reaction mixture after 0.5 eq. were added. Finally, after 1 eq. of imidazole, TLC #4 showed the presence of mostly the desired TMS-aminol **161**.



**Figure 7.1** TLCs taken after incremental additions of imidazole.

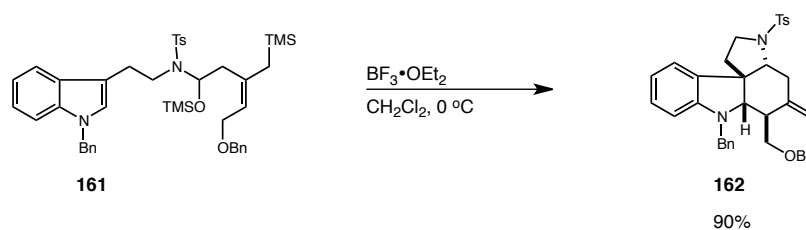
This experiment led us to an optimized sequence for synthesis of *N*-Tosyl-*O*-TMS aminol **161** (Scheme 7.6). Thus, reduction of amide **177** with DIBAL-H followed by trapping of the aluminoxy acetal **178** generated with TMS-imidazole (**179**) with 1 eq. of imidazole (**180**) as an additive yielded aminol **161** in 82% yield and completely suppressed the formation of tosylamide **176**. This new protocol has proven to be highly robust.



**Scheme 7.6** Optimized synthesis of *N*-Tosyl-*O*-TMS aminol **161**.

### 7.1.3 Key intramolecular cascade reaction.

With a robust synthesis of *N*-Tosyl-*O*-TMS aminol **161** in hand, the key cyclization was carried out. We were delighted to find that treatment of **161** with  $\text{BF}_3 \cdot \text{OEt}_2$  at 0 °C afforded tetracyclic amine **162** 90% yield as single diastereoisomer (Scheme 7.7). This yield is 10% higher than the highest yield observed previously on small scale.



**Scheme 7.7** Key cyclization of *N*-Tosyl-*O*-TMS aminol **161**.

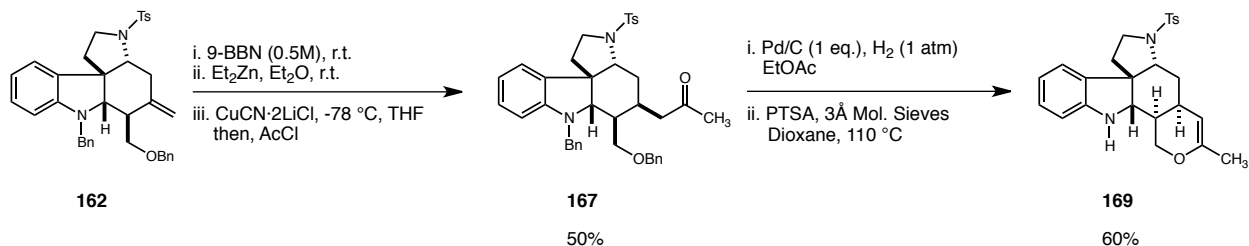
### 7.1.4 Synthesis of dihydropyran 175.

We next attempted to scale up of the hydroacylation sequence of **162**. Thus, as previously described hydroboration of **162** produces the corresponding alkyl-borane

species, which is then transmetallated to the high order cuprate species (via an alkyl-zinc) and treated with acetyl chloride at  $-78\text{ }^{\circ}\text{C}$  to afford ketone **167**.<sup>84a, 84b</sup>

The original conditions for the hydroboration of **162**, involved addition of 1.1 equivalents of a 0.5M solution of 9-BBN in THF to a 0.2M solution of **162** in THF at  $0\text{ }^{\circ}\text{C}$ , followed by stirring at this temperature for 42h. In our hands, these exact set of conditions for the hydroboration of **162** were not robust. Fortunately, we found that the addition of 1.5 equivalents of 0.5M solution of 9-BBN to neat heterocycle **162** at room temperature followed by stirring at this temperature for 12 h consistently provided the alkyl-borane species **164** (Scheme 6.3). The subsequent transmetalation sequences and acylation did not give any problems during scale up and we were able to obtain ketone **167** in 50% yield (up from 45% original, Scheme 7.8).

With ketone **167** in hand, hydrogenolysis of the benzyl group over stoichiometric amounts of palladium on carbon yielded hemiacetal **168** (Scheme 7.8). Unlike the original conditions, we decided not to isolate **168** and instead submit crude **168** to the dehydration conditions (dioxane at  $110\text{ }^{\circ}\text{C}$  in the presence of PTSA and activated molecular sieves). This new through process produced dihydropyran **169** in similar yields (60%) than the original two-step sequence, but avoided the unnecessary purification step for **168**, thus decreasing solvent waste and time needed for the synthesis of **169**.

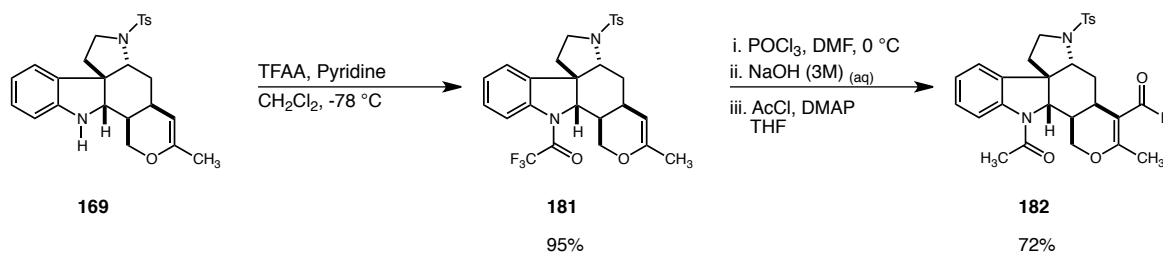


**Scheme 7.8** Conversion of tetracyclic **162** into dihydropyran **169**.

## 7.2 Synthesis of Ester 182: Original Approach and New Approach Circumventing the Problematic Oxidation Step.

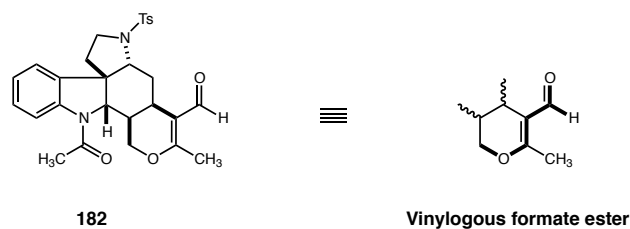
### 7.2.1 Original Approach to Methyl-Ester 184.

The next step in the sequence for the synthesis of malagashanine required the installation of a methyl-ester group at C(20). Exploratory work by Delgado and Boudet revealed that this moiety could be installed via a Vilsmeier-Haack formylation, oxidation and esterification sequence (Scheme 7.9). Thus, protection of indole nitrogen of dihydropyran **169** with trifluoroacetic anhydride in the presence of pyridine at  $-78\text{ }^{\circ}\text{C}$  afforded the corresponding trifluoroacetamide **181** in 95% yield.<sup>89</sup> Compound **181** was subjected to standard Vilsmeier formylation conditions to afford the desired aldehyde, which was treated *in situ* with base to remove the trifluoroacetyl moiety.<sup>90</sup> Treatment of the intermediate indoline aldehyde with acetyl chloride and DMAP generated acetamide **182** in 72% yield.



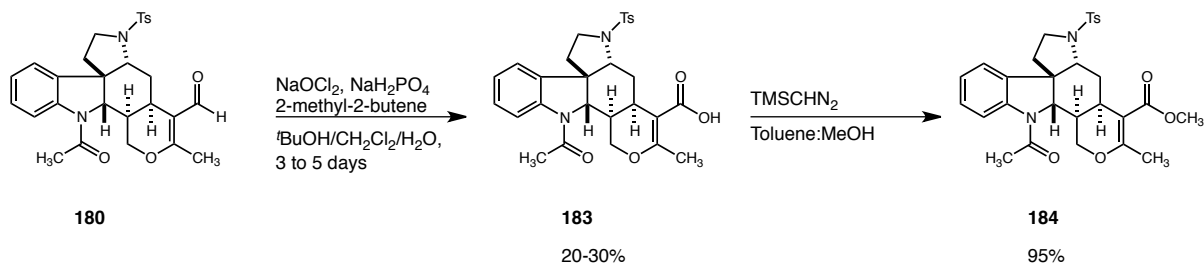
Scheme 7.9 Synthesis of aldehyde **182**.

With aldehyde **182** in hand, Delgado and Boudet explored the conversion of this compound into methyl ester **184**. A variety of standard oxidative conditions were screened to attempt the oxidation of aldehyde **182** to acid **183**, but they mostly returned starting material. The overall lack of reactivity of aldehyde **182** towards standard oxidation protocols was not entirely surprising given that compound **182** could also be thought of as an vinylogous formate ester by virtue of its  $\beta$ -alkoxy substituent (Figure 7.2).



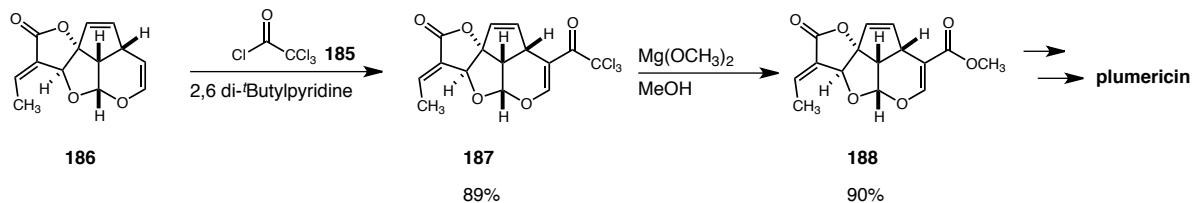
**Figure 7.2** Compound **182** is a vinylogous formate ester.

Ultimately, prolonged exposure (>3 days) of aldehyde **182** to a Pinnick oxidation protocol generated some acid **183** in 20-30% yield.<sup>91</sup> Compound **183** was then converted to the corresponding ester **184** using trimethylsilyl diazomethane (Scheme 7.10). Although this exploratory route provided initial amounts of methyl-ester **184**, attempts to scale up the oxidation protocol were unsuccessful. In most cases aldehyde **182** was recovered from the reaction mixture. Therefore, my research focused on a different route for the installation of the ester moiety.

Scheme 7.10 Synthesis of ester **184**.

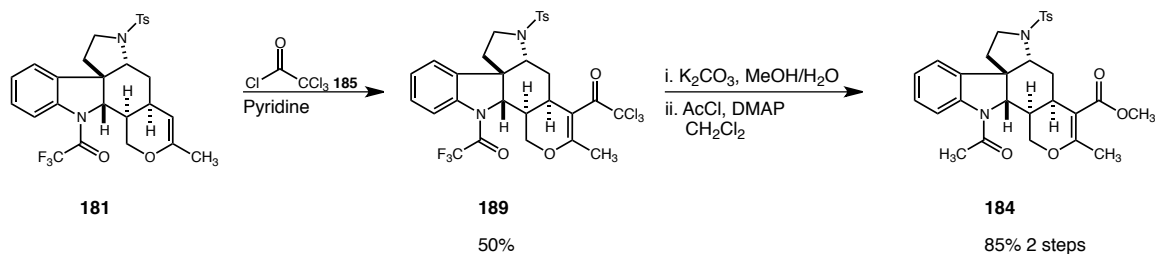
### 7.2.2 Second Generation Approach to Methyl-ester **184**.

In order to circumvent the problematic oxidation of aldehyde **182**, a new route for the synthesis methyl-ester **184** required the introduction of a carbonyl unit with the same oxidation state as the final methyl-ester moiety. We were quickly drawn to trichloroacetyl chloride (**185**), which has been shown to add to heterocycles in a Friedel-Crafts fashion.<sup>92</sup> In addition, the trichloromethyl ketones obtained can undergo haloform type reactions to generate aryl acids, esters and amides.<sup>93a, 93b</sup> For example, Trost and co-workers have used trichloroacetyl chloride for the introduction of an ester moiety into a dihydropyran **186** in their synthesis of plumericin (Scheme 7.11).<sup>94</sup> Thus, reaction of compound **186** and trichloroacetyl chloride in the presence of 2,6-di-*tert*-butylpyridine produced trichloroketone **187**. Treatment of **187** with magnesium methoxide in methanol then gave ester **188** in 90% yield.



**Scheme 7.11** Trost's group use of trichloroacetyl chloride for the synthesis of esters.

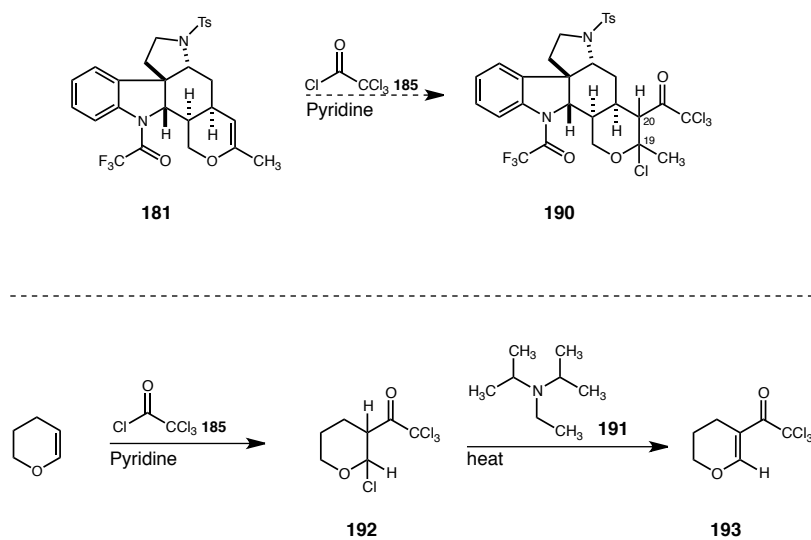
We decided that this was a perfect start point to a new route for the synthesis of ester **184**. Treatment of TFA protected dihydropyran **181** with trichloroacetyl chloride (**185**) and pyridine generated the desired trichloromethyl ketone **189**, albeit in 50% yield (Scheme 7.12). Initial attempts to displace the trichloromethyl group with magnesium methoxide were unsuccessful. Fortunately, displacement of the trichloromethyl group and simultaneous cleavage of the TFA group were achieved by treatment of **189** with  $K_2CO_3$  in methanol-water solution. The intermediate ester obtained was then acylated *in situ* to give the desired methyl ester **184**.



**Scheme 7.12** Second generation approach to ester **184**.

Unfortunately, as we attempted to scale up the Friedel-Crafts reaction using this protocol, we were faced with great difficulty in obtaining reproducible yields. In most cases, TLC indicated the consumption of starting material. We believe that a potential

complication for the effective trichloacylation of **181** may be the formation of chloride **190** (Scheme 7.13). Elimination of HCl in similar adducts has been reported to be facile in the presence of heat and Hünigs base (**191**).<sup>94</sup> For example, treatment of simple chloride **192** with Hünigs base (**191**) produced the elimination of HCl to yield compound **193**. Unfortunately in our case, these exact set of conditions did not improve the yields of **189**.



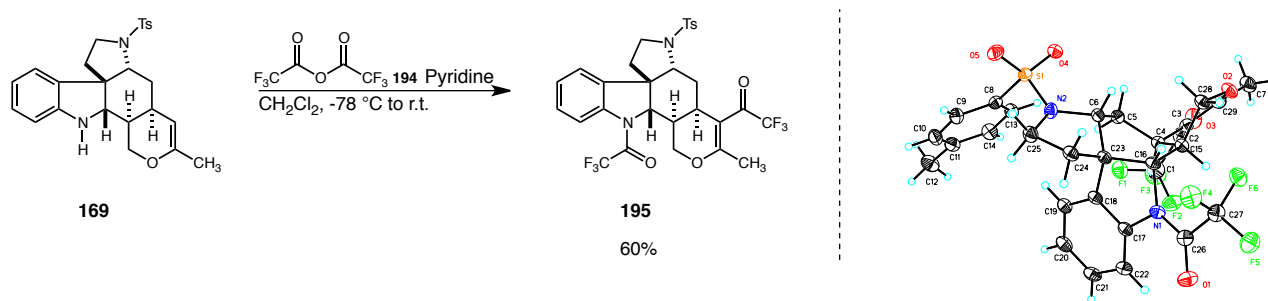
**Scheme 7.13** Possible formation of chloride **190** and previously reported elimination in simpler systems.

### 7.2.3 Third Generation Approach to Methyl-Ester **184**. Trifluoroacetic anhydride as a Carbonyl Source.

Although the trichloacylation of **181** was not robust process, the sequence above did suggest that the problematic oxidation step could be circumvented with the right acylating agent. Thus, we decided to seek an alternative to trichloroacetyl chloride. Our

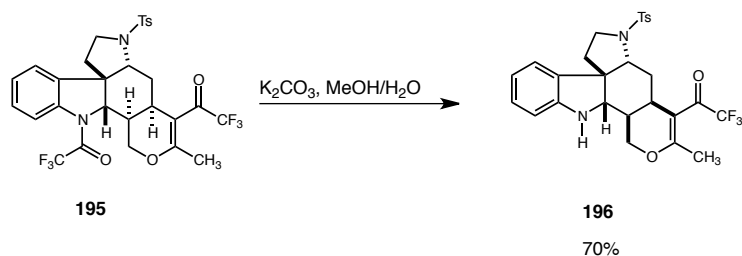


attention was quickly drawn to trifluoroacetic anhydride (**194**), which has also found utility in the facile Friedel-Crafts acylations of heterocycles.<sup>95</sup> At this point, rather than attempt the acylation of **181** with TFAA, we sought a one-pot procedure for the protection of the indole nitrogen and the acylation of the dihydropyran **169**. Thus, treatment of **169** with excess trifluoroacetic anhydride (**194**) in the presence of pyridine at  $-78\text{ }^{\circ}\text{C}$  followed by warming of the reaction mixture to room temperature, produced methyl trifluoroketone **195** in 60% yield (Scheme 7.14). Furthermore, we were pleased to find that the trifluoroacylation of **169** was a robust reaction consistently giving yields in the 60% range. We were also pleased to find that compound **195** was a crystalline solid, which allowed us for the first time since the start of this project, to obtain an X-ray structure of an advanced intermediate. Thus, compound **195** allowed us to unequivocally confirm the relative stereochemical assignment of all five stereocenters for the first time.



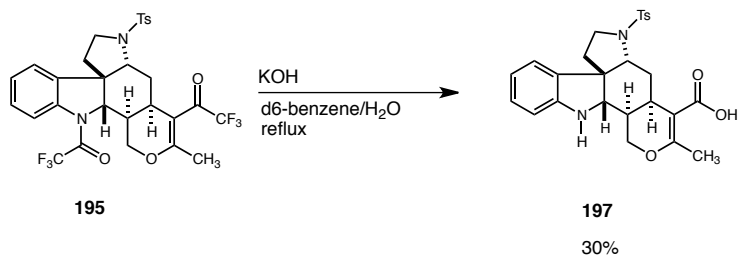
**Scheme 7.14** Synthesis of methyl trifluoroketone **195** and X-ray structure.

Unfortunately treatment of compound **195** with  $\text{K}_2\text{CO}_3$  in methanol-water solution only achieved the cleavage of the trifluoroacetamide group and produced compound **196** in 70% yield (Scheme 7.15).



**Scheme 7.15** Alcoholysis attempt on trifluoroketone **195**.

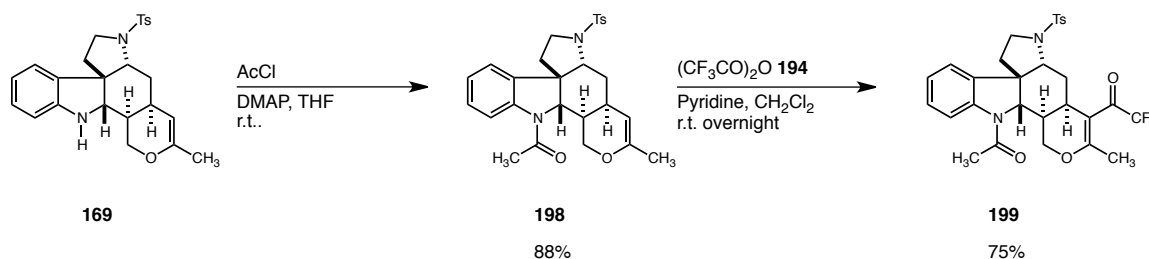
Subsequent literature research indicated that the hydrolysis or alcoholysis of the trifluoromethyl ketone group was indeed not an easy process, when compared to the analogous trichloroketone.<sup>95</sup> Interestingly, the hydrolysis proceeded well when compound **195** was refluxed in wet d6-benzene (1% v/v H<sub>2</sub>O) in the presence of powdered potassium hydroxide for 4 h, giving the corresponding amino acid **197** in 30% isolated yield (Scheme 7.16). Deuterated benzene was chosen as solvent in order to monitor directly the progress of the hydrolysis *via* <sup>19</sup>F NMR experiments. Attempts to improve this low yield were unsuccessful, possibly due to the high solubility of amino acid **197** in aqueous solutions.



**Scheme 7.16** Hydrolysis of methyl trifluoroketone **195**.

### 7.2.4 Fourth Generation Approach to Methyl Ester 184.

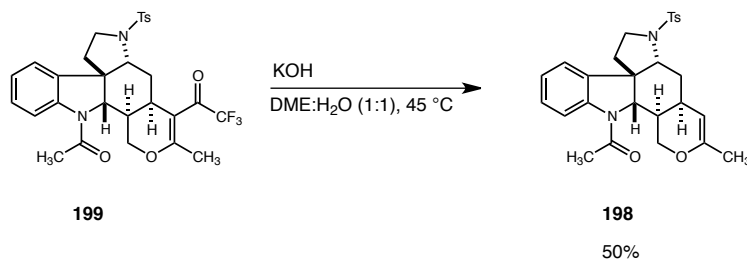
In order to circumvent the solubility problem encountered with amino acid **197**, we decided to attempt the acylation with **194** on acetamide **198** (Scheme 7.17). Originally the trifluoroacetamide group was used as a protecting group in the Vilsmeier formylation sequence due to side reactions encountered with the more reactive acetamide **198**.<sup>42</sup> We were confident that in this case the trifluoroacetic anhydride was not going to react with acetamide **198**, since it is not as strong of an electrophile as the Vilsmeier reagent. Thus, reaction of free indoline **169** with excess acetyl chloride in the presence of DMAP in THF afforded the desired acetamide **198** in excellent yield (88%, Scheme 7.17). We were pleased to find that acylation with trifluoroacetic anhydride (**194**) in pyridine at room temperature afforded the desired methyltrifluoro ketone **199** in 75% yield.



**Scheme 7.17** Synthesis of methyltrifluoro ketone **199**.

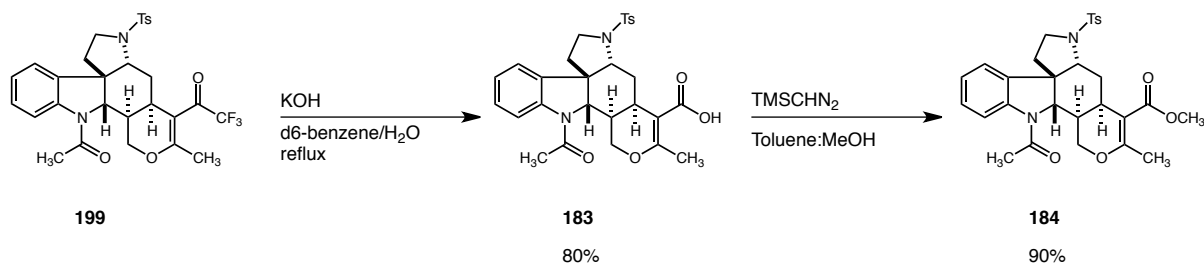
With methyltrifluoroketone **199** in hand, we proceeded to attempt the hydrolysis of this compound. However, before attempting the conditions developed for the hydrolysis of **195**, we decided to try milder conditions. Therefore, treatment of compound **199** with KOH in DME:H<sub>2</sub>O solution (1:1 v/v) at 45 °C did not yield the any desired acid **183**, but instead we observed clean conversion to acetamide **198** (Scheme 7.18).

Decarboxylation of the carboxylate salts derived from trifluoroketones is a well-known complication observed in the hydrolysis of trifluoroketones.<sup>96</sup> Our attempts to stop the reaction at the carboxylate stage by closely monitoring the reaction conditions and carefully controlling the temperature of the reaction mixture were futile.



**Scheme 7.18.** Decarboxylation of methyl trifluoroketone **199**.

At this point, we decided to go back to the original conditions developed for the hydrolysis of **195**. Thus, refluxing **199** in wet d<sub>6</sub>-benzene (1% v/v H<sub>2</sub>O) with powdered potassium hydroxide for 4 h, gave the corresponding acid **183**. Acid **181** could be isolated after flash chromatography (80% yield) or could be converted directly into to ester **184** by treatment of the crude mixture with trimethylsilyl diazomethane in 90% yield (Scheme 7.19).

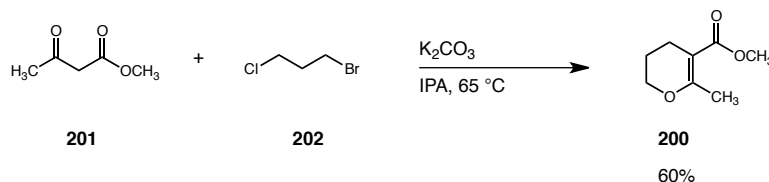


**Scheme 7.19** Synthesis of ester **184** via hydrolysis of **199**.

### 7.3 Reduction of the C(19)-C(20) Tetrasubstituted Olefin of Methyl Ester 184

#### 7.3.1 Hydrogenation on Model System.

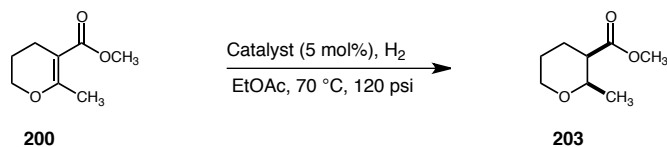
Having developed a robust route for the synthesis of acid **183** and ester **184**, attention turned to the reduction of the tetrasubstituted olefin, which was the next step in the synthesis of malagashanine. Early studies, had shown that reduction of the C(19)-C(20) tetrasubstituted olefin was going to be a challenge. Therefore, we decided to perform some exploratory studies on dihydropyran model **200** before committing any advanced intermediates. Dihydropyran **200** was available in one step from readily available materials. Thus, reaction of methylaceto acetate (**201**) and 1-bromo-3-chloropropane (**202**) in the presence of  $K_2CO_3$  gave the desired dihydropyran **200** in 60% yield after Kugelrohr distillation (Scheme 7.20).



**Scheme 7.20** Synthesis of model dihydropyran **200**.

At this stage we proceeded to explore the hydrogenation of model system **200** under a variety of conditions, which are summarized in Table 7.1. Reduction of dihydropyran **200** was accomplished with a variety of heterogeneous catalysts at 120 psi and 70 °C (entries 2-4).<sup>97a, 97b, 97c, 97d, 97e</sup> Moreover, we found that Rh/Al (5 mol %) was

the best heterogeneous catalyst giving complete conversion to saturated dihydropyran **203** (entry 3).



Entry	Catalyst	% conversion <sup>a</sup>
1	PtO <sub>2</sub>	0
2	Pd(OH) <sub>2</sub> /C	50
3	Rh/Al	100
4	Pd/C	62

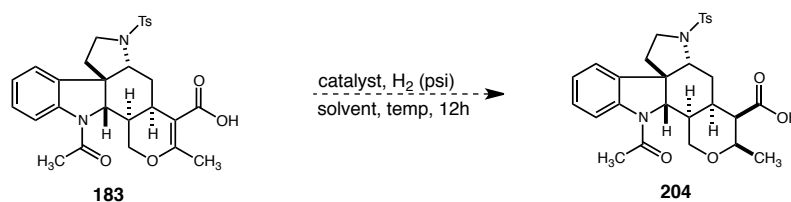
<sup>a</sup> = conversion relative to starting material as determined by GC

**Table 7.1** Hydrogenation results on model dihydropyran **200**.

### 7.3.2 Hydrogenation of the C(19)-C(20) Tetrasubstituted Olefin of Acid **183** and Ester **184**.

Encouraged by the hydrogenation results on model compound **200**, we were very excited to begin the reduction of the tetrasubstituted olefin in the in ester **184**. Unfortunately, the positive results found for compound **200** could not be translated into ester **184**. In all cases, the unreacted unsaturated ester **184** was recovered from the hydrogenation mixture. At this point, we decided to attempt the hydrogenation of unsaturated acid **183**, since carboxylates have been shown to be directing groups in the hydrogenation of olefins with heterogeneous and homogenous catalysts.<sup>98</sup> Results from our studies on the hydrogenation of unsaturated acid **183** are summarized in Table 7.2.

Our studies showed that hydrogenation with palladium-based catalysts only returned unreacted starting **183**, regardless of the solvent, temperature or pressure (entries 3-9). Interestingly, decarboxylation of **183** was observed when Crabtree's catalyst (homogenous) in CH<sub>2</sub>Cl<sub>2</sub> was used under high pressure and temperatures giving **198** (entry 10). Hydrogenation with Rh in alumina at 70 psi did not reduce the tetrasubstituted olefin, but instead reduced the indoline ring (entries 1-2).<sup>99a, 99b, 99c, 99d, 99e, 99f</sup> These results are not surprising since the reduction of anilines with Rh/Al<sub>2</sub>O<sub>3</sub> has been documented in the literature.<sup>100</sup>



entry	catalyst	solvent	pressure (psi)	temp (°C)	results
1	5 % Rh/Al <sub>2</sub> O <sub>3</sub>	EtOAc	70	23	indoline ring reduction
2	5 % Rh/Al <sub>2</sub> O <sub>3</sub>	MeOH/H <sub>2</sub> O (3:1)	70	23	indoline ring reduction
3	5% Pd/C (wet)	THF	70	23	SM recovered
4	5% Pd/C (wet)	THF	150	23	SM recovered
5	10% Pd(OH) <sub>2</sub> /C	THF	150	23	SM recovered
6	5% Pd/C (wet)	EtOAc	250	23	SM recovered
7	10% Pd(OH) <sub>2</sub> /C	EtOAc	250	23	SM recovered
8	5% Pd/C (wet) <sup>a</sup>	EtOAc	250	80	SM recovered
9	10% Pd(OH) <sub>2</sub> /C <sup>a</sup>	EtOAc	250	80	SM recovered
10	Crabtree's	CH <sub>2</sub> Cl <sub>2</sub>	250	80	SM recovered + 30% <b>198</b>

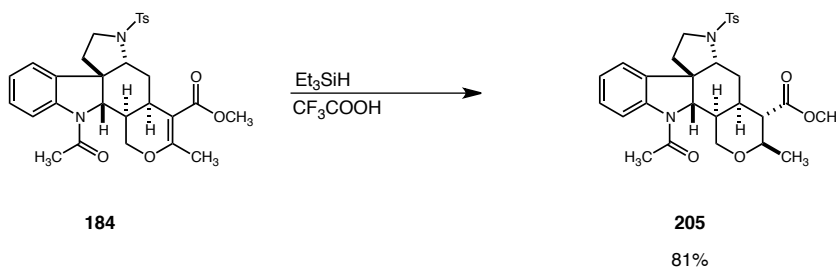
a. Reaction aged for 48 hours.

**Table 7.2** Results from the hydrogenation of acid **183**.

## 7.4 Ionic Reduction of the C(19)-C(20) Tetrasubstituted Olefin.

Having determined that the hydrogenation of the tetrasubstituted olefin was complicated by the competitive reduction of the indoline ring, we decided to pursue a different reductive strategy. Literature studies revealed that the triethylsilane-trifluoroacetic acid combination is an effective reagent for the reduction of tetrasubstituted and electron-rich olefins.<sup>101a, 101b</sup> In addition, the literature suggested that the ionic reduction with triethylsilane is stereoselective, giving mostly products having the *cis*-conformation.<sup>102</sup>

We were pleased to find that treatment of tetrasubstituted olefin **184** with 10 equivalents of triethylsilane in trifluoroacetic acid as solvent cleanly reduced the tetrasubstituted olefin to yield saturated ester **205** in 81% yield (Scheme 7.21).



**Scheme 7.21** Ionic reduction of methyl-ester **184** with Et<sub>3</sub>SiH-TFA reagent.

Given that **205** existed as a 1:0.7 mixture of rotamers by <sup>1</sup>H NMR, it was not possible to carry out 2D experiments to assess its structure. However, the <sup>1</sup>H NMR data at 25 °C indicated that the rotameric allylic methyl signals (2.4 – 2.0 ppm) had been replaced by two rotameric methyl doublet signals (1.50 ppm), which was a good



indication that the C(19)-C(20) double bond had undergone reduction. Further confirmation that the reduction had taken place was obtained from HRMS. Compound **205** was obtained as a single diastereomer, and initially we assumed that the hydrogenation had taken place from the most accessible convex face of the E ring in a *syn* fashion.

Unfortunately, X-ray structure for compound **205** indicated that the ionic reduction had occurred in a *trans*-fashion rather than the assumed *syn* fashion. Thus, protonation at C(20) had occurred from the undesired concave face of the molecule leading to the undesired stereoisomer **205**. We believe that **205** is the thermodynamically favored diastereoisomer for this reduction, since it places both the methyl group at C(19) and the ester group at C(20) equatorial.

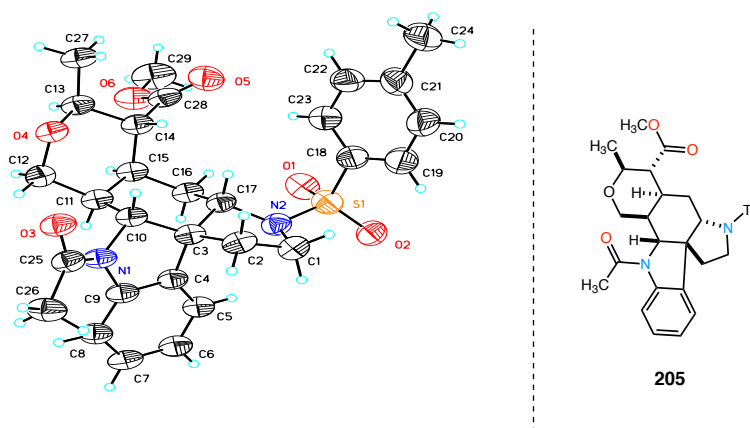
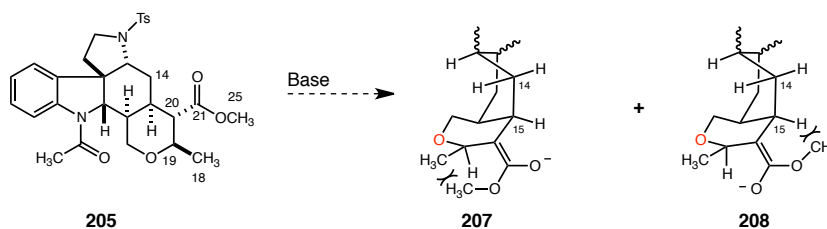


Figure 7.3 X-ray structure for compound **205**.

Attempts to correct the C(20) stereocenter of **205** via enolate formation with a strong base (*t*-BuLi, *n*-BuLi and LDA) followed by kinetic protonation with bulky H<sup>+</sup> donors (pyridinium salts) were unsuccessful. In addition, attempts to incorporate a

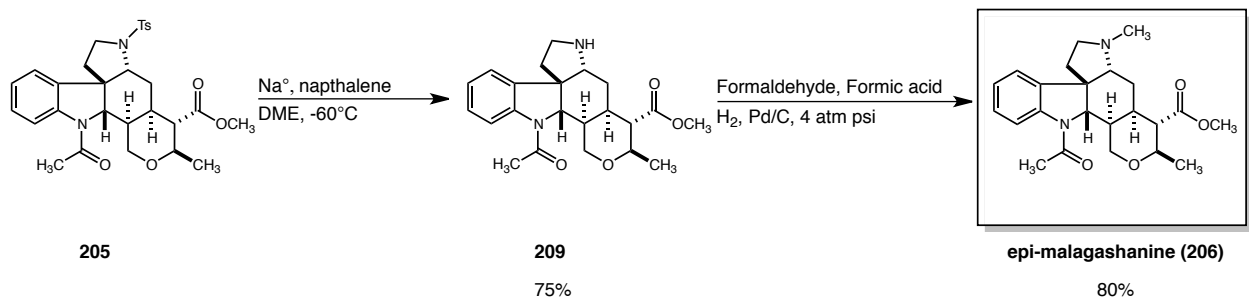
deuterium atom at C(20) by quenching the reaction with deuterium donors (D<sub>2</sub>O and acetic acid-d<sub>4</sub>) were also unsuccessful. These results suggest that enolate formation at C(20) was not taking place. We rationalized that as enolate formation is taking place and the C(20)-C(21) bond starts to become sp<sup>2</sup> hybridized, C(25) starts to suffer severe steric repulsions from both; C(18) **207** and C(14) **208** (Scheme 7.22). Thus, in this particular case, enolate formation is high in energy.



**Scheme 7.22** Rationalization for the lack of enolate formation for compound **205**.

## 7.5 Synthesis of Epi-Malagashanine; Removal of the N<sub>b</sub> Tosyl Auxiliary and Reductive Methylation.

With compound **205** in hand, we began our efforts towards the endgame for the synthesis of epi-malagashanine. The endgame towards the synthesis of epi-malagashanine, began with the removal of the N<sub>b</sub> tosyl auxiliary. Thus, treatment of **205** with sodium naphthalide in 1,2-dimethoxyethane at -60 °C yielded free amine **209** in 78% yield (Scheme 7.23).<sup>103a, 103b, 103c</sup> Finally, treatment of secondary amine **209** with excess formaldehyde solution (37% in H<sub>2</sub>O) in the presence of palladium on carbon under 4 atmospheres of H<sub>2</sub> gas, produced epi-malagashanine (**206**) in 60% yield.<sup>104</sup>



Scheme 7.23 Synthesis of epi-malagashanine (206).

## **8 Chapter 8**

*Efforts Towards the Synthesis of 11-Demethoxymyrtoidine and a New Strategy Towards Malagashanine.*

### **8.1 First Generation Strategy Towards the Synthesis of 11-demethoxymyrtoidine (154) and New Strategy Towards Malagashanine (151).**

#### **8.1.1 First Generation Strategy Towards Demethoxymyrtoidine by Direct C-H functionalization**

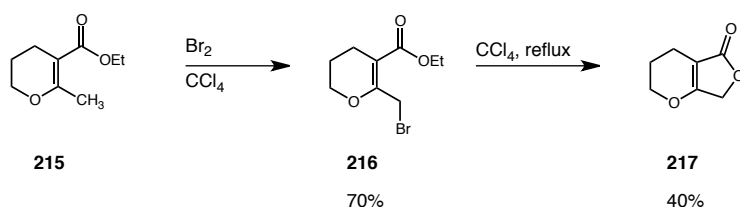
Concurrent with our synthesis of epi-malagashanine (**206**), we engaged in efforts to access other members of the malagashanine family utilizing advanced intermediates **183** or **184** (Scheme 8.1). Specifically, we focused our attention to the minor Malagasy alkaloid: 11-demethoxymyrtoidine (**154**).

Our retrosynthetic analysis to 11-demethoxymyrtoidine (**154**) is outlined in Scheme 8.1. We believed that 11-demethoxymyrtoidine could be accessed from late stage intermediate **210**, which we envisioned would arise from functionalized acid **211** or methyl ester **212**. The key to our approach would involve a late stage allylic functionalization of carboxylic acid **183** or methyl ester **184**.



### 8.1.3 Allylic Halogenation of Methyl-ester **182**.

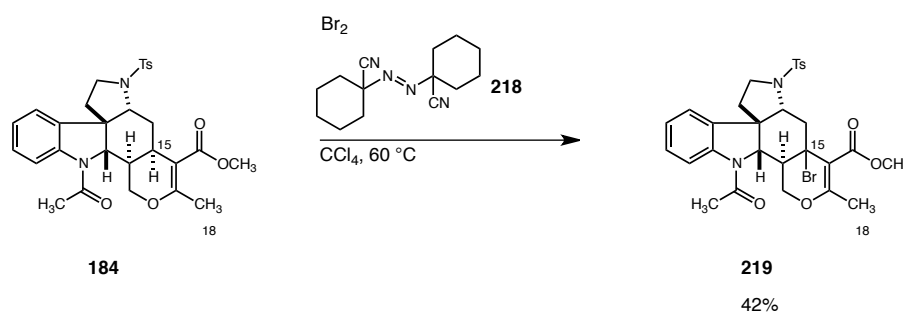
The first general approach to the functionalization of the allylic methyl group involved an allylic halogenation. Literature studies showed that this approach had an excellent precedent in the literature for systems with a dihydropyran moiety (Scheme 8.3).<sup>105</sup> A classical approach by Korte and colleagues demonstrated that treatment of dihydropyran **215** with Br<sub>2</sub> in carbon tetrachloride at room temperature produced allylic bromide **216** in 70% yield (Scheme 8.3). Furthermore, they showed that heating bromide **216** in carbon tetrachloride at 170 °C yielded butyrolactone **217** in 40% yield. Interestingly, Korte's work is the only published example for the synthesis of fused dihydropyran-butylolactone system.



**Scheme 8.3** Korte's Synthesis of butyrolactone **217**.

Unfortunately Korte's exact reaction conditions did not work on methyl ester **184** and only starting material was recovered from the reaction mixture. At this point, we decided to introduce a free radical initiator to facilitate the allylic halogenation.<sup>106</sup> Treatment of methyl ester **184** with Br<sub>2</sub> and 1,1'-azobis(cyclohexanecarbonitrile) (**218**) in CCl<sub>4</sub> at 60 °C yielded a single compound that showed HRMS with a mass equal to the calculated mass for the brominated methyl group as well as peak patterns characteristic of

a compound containing bromine atom. Unfortunately,  $^1\text{H}$  NMR spectra showed the presence of the singlet for the C(18) methyl group at 2.2 ppm and the disappearance of a single proton at around 2.4 ppm. On the basis of these data, we tentatively hypothesized that the structure of this compound corresponds to **219**, which arises from allylic halogenation of the C(15) hydrogen (Scheme 8.4).

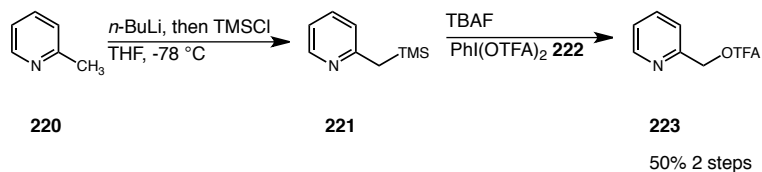


**Scheme 8.4** Free radical halogenation of methyl-ester **184**.

#### 8.1.4 Allyl Oxidation *via* an Extended Enolate.

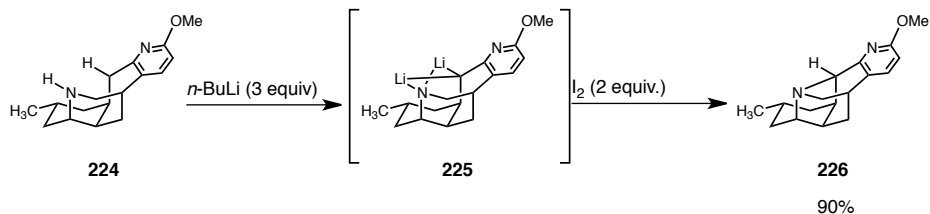
Having established that the allylic halogenation of methyl-ester **184** does not yield the desired product, we decided to take a bolder approach to the functionalization of C(18). This second approach involved the direct oxidation of the allylic hydrogens at C(18). Unfortunately, direct oxidations by classical methods (i.e. Railley's oxidation) did not work on methyl-ester **184**. Work by Andrew's and coworkers showed that treatment of 2-methylpyridine (**220**) could be oxidized at the methyl position *via* a two-step process.<sup>107</sup> Thus, treatment of **220** with *n*-BuLi followed by quenching of the anion produced with TMSCl yielded silane **221**. Treatment of silane **221** with TBAF in the

presence of hypervalent iodo oxidant **222** yielded trifluoroacetate **223** in 50% yield over two steps (Scheme 8.5).



**Scheme 8.5** Oxidation of 2-methylpyridine (**220**) via anion formation.

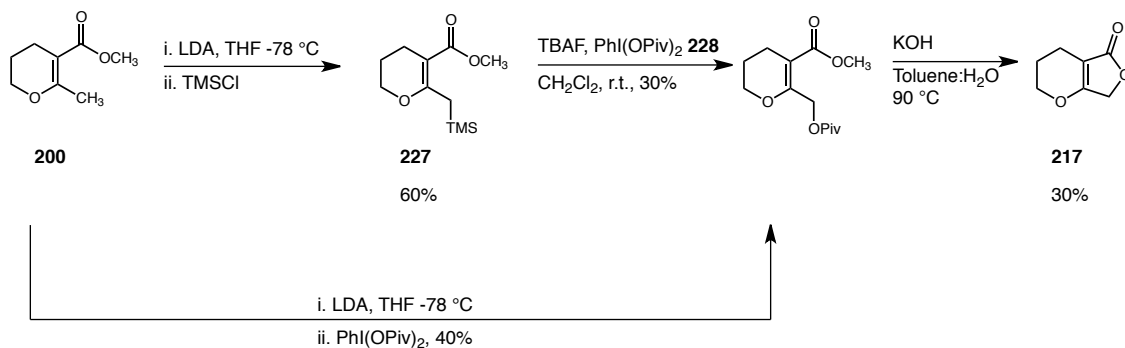
Similar methodology has been more recently been used by Sarpong and co-workers in their synthesis of (+) lyconadin.<sup>108</sup> Thus, treatment of secondary amine **224** with excess *n*-BuLi gave a proposed lithium amide anion serves as an intramolecular base to effect lateral deprotonation of the pyridine moiety to ultimately yield dianion **225**. Dianion **225** was then quenched with I<sub>2</sub> to produce the alkyl-iodide, which cyclized spontaneously under the reaction conditions to give piperidine **226** (Scheme 8.6). It is worth noting that the Sarpong's group stresses the vitality of the deprotonation of the secondary amine for this process to work, since experimental observations showed that the protection of this nitrogen shut down this process completely.



**Scheme 8.6** Sarpong's oxidative C-N bond formation.

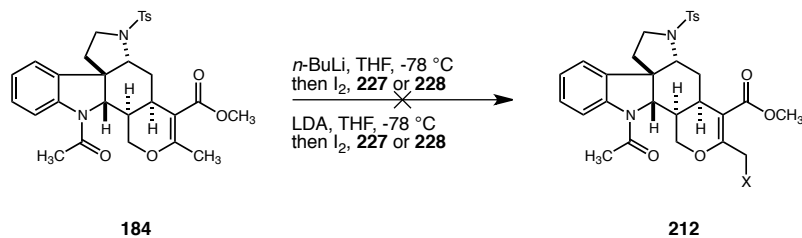


Although the examples above are a good precedent for the oxidation of pyridinyl methyl groups via deprotonation with strong base, methyl-ester **184** is not a pyridine but a dihydropyran moiety instead. Therefore, before submitting methyl-ester **184** to these reaction conditions, we decided to rely again on model dihydropyran **193** for some exploratory studies. Treatment of compound **200** with a milder base (i.e. LDA) gave an extended enolate (bright yellow color), which was initially trapped with TMSCl to yield silane **227** in 60% yield (Scheme 8.7). Treatment of compound **227** with TBAF and hypervalent oxidant **228** then gave the desired pivaloylate **229** in 30% yield. We were also able to demonstrate that we can access pivaloylate **229** directly from **200** in 40% yield. In addition, we demonstrated that reaction of **229** with KOH in toluene:water (3:1) mixture at 90 °C yields butyrolactone **217** in 30% yield.



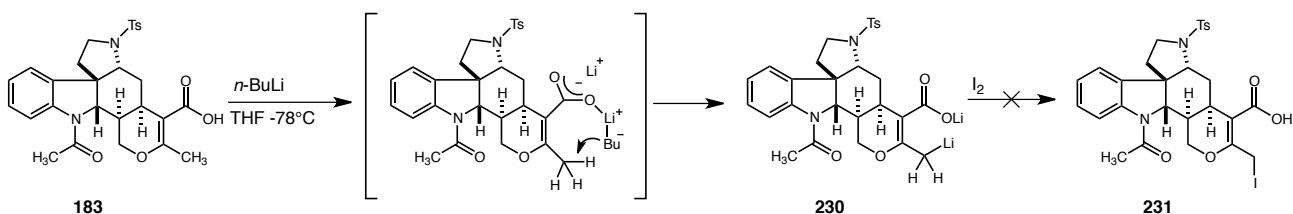
**Scheme 8.7** Synthesis of butyrolactone **217** via extended enolate.

Unfortunately, treatment of methyl-ester **184** with LDA or *n*-BuLi followed by quenching of the extended enolate with either TMSCl, oxidants **222**, **228** or I<sub>2</sub> did not yield any of the desired C-H functionalized C(18) methyl group. In all cases, starting material was recovered from the reaction mixture almost quantitatively (Scheme 8.8).



**Scheme 8.8** Attempts at functionalization *via* enolate formation.

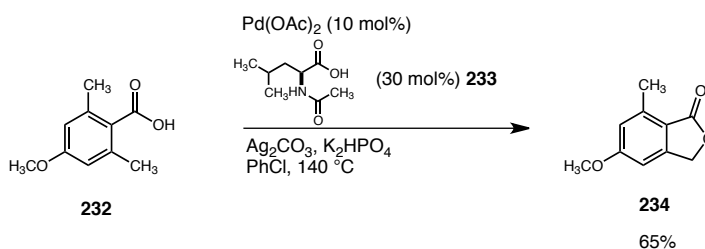
At this point, we were wondering whether the carboxylate moiety in acid **183** could serve as a directing group to facilitate deprotonation of at C(18) by a lithium based base to give the bis lithium salt **230** (Scheme 8.9). This hypothesis was based on the fact that carboxylic acids are known to serve as directing groups for the ortholithiation of aromatic systems.<sup>109</sup> Thus, treatment of acid **183** with *n*-BuLi (2 equiv.) generated a yellow solution, which was subsequently quenched with I<sub>2</sub>. Unfortunately, as previously observed, this reaction did not yield the desired functionalized acid **231**, but only returned unreacted starting material.



**Scheme 8.9** Attempted oxidation *via* enolate formation of acid **183**.

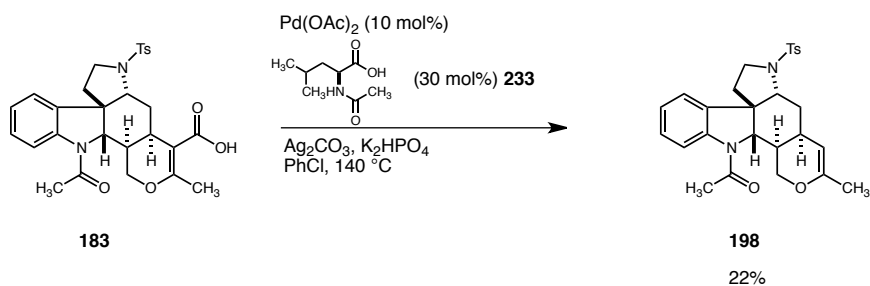
### 8.1.5 Oxidation via C-H activation.

A final tactic attempted by this investigator for the functionalization of the C(18) methyl group was based on recent methodology developed by the Martin group for the synthesis of benzolactones.<sup>110</sup> This new methodology relies on the C-H activation of sp<sup>3</sup> carbons by palladium acetate. For example, reaction of mesitoic acid (**232**) with catalytic amounts of Pd(OAc)<sub>2</sub>, amino acid ligand **233**, Ag<sub>2</sub>CO<sub>3</sub> and KH<sub>2</sub>PO<sub>4</sub> in chlorobenzene at 140 °C, yields benzolactone **234** in 95% yield (65% in our hands) (Scheme 8.10).



**Scheme 8.10** Benzolactone formation by palladium catalyzed C-H activation.

Treatment of acid **183** under the conditions outlined above for the formation of benzolactones did not yield the desired butyrolactone (Scheme 8.11). Only starting material **183** and decarboxylated dihydropyran **198** were recovered from the reaction mixture. Decarboxylation was also observed by Martin and coworkers in the development of their methodology.<sup>110</sup>



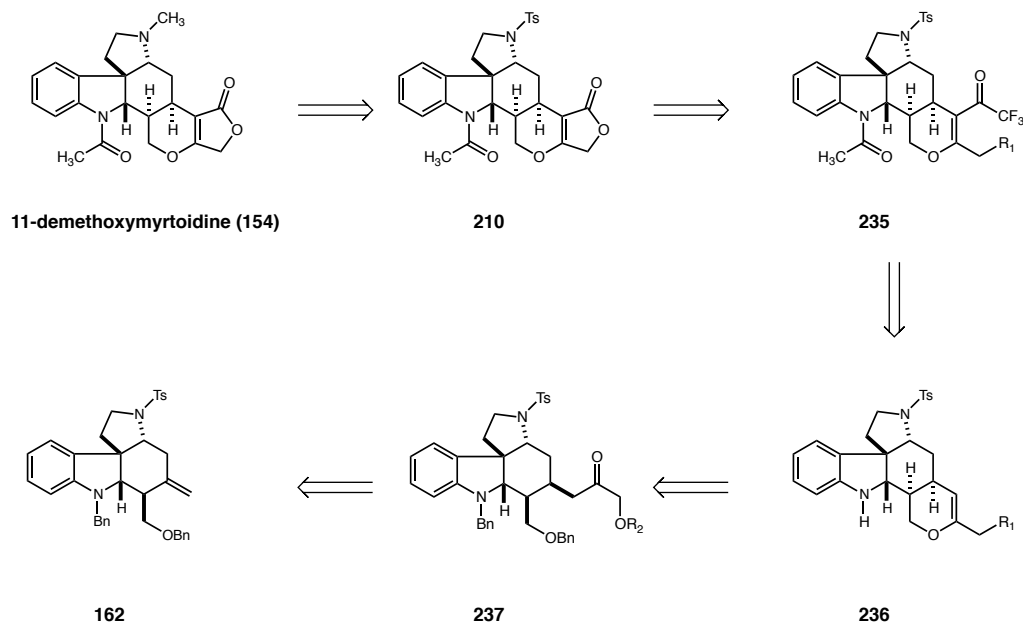
**Scheme 8.11** Palladium-catalyzed C-H functionalization attempt.

## 8.2 Second Generation Approach: Introduction of the Oxygen Atom *via* Hydroacylation with Acetoxyacetyl Chloride

### 8.2.1 Retrosynthetic Analysis

Since we were unable to synthesize the butyrolactone moiety for 11-demethoxymyrtoidine (**154**) by direct functionalization of the allylic position, we revised our initial strategy and decided to introduce the oxygen atom necessary for the lactone moiety earlier in the synthesis. We also decided that the most appropriate place to introduce this atom was during the hydroacylation of core structure **162** (Scheme 8.12). Thus, advance intermediate **210** would come from cyclization of **235** under basic conditions. Trifluoroketone **235** could be accessed from acylation of the dihydropyran ring of compound **236**. In turn, compound **236** would be available from ketone **237** after benzyl deprotection ketone and dehydration of the hemiacetal produced. Key to our strategy was the synthesis of ketone **237**, which we believed would be generated from

core **162** by choosing the right electrophile during the adaption of the Knochel chemistry.

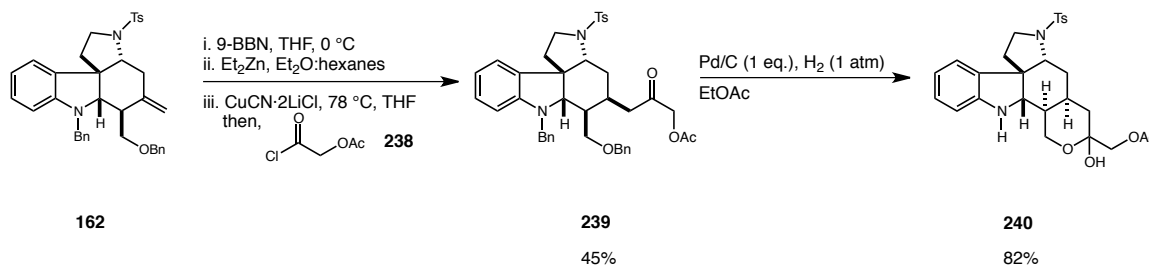


**Scheme 8.12** Retrosynthetic analysis for the second-generation approach to 11-demethoxymyrtoidine (**154**).

### 8.2.2 Initial Synthesis of dihydropyran **234**.

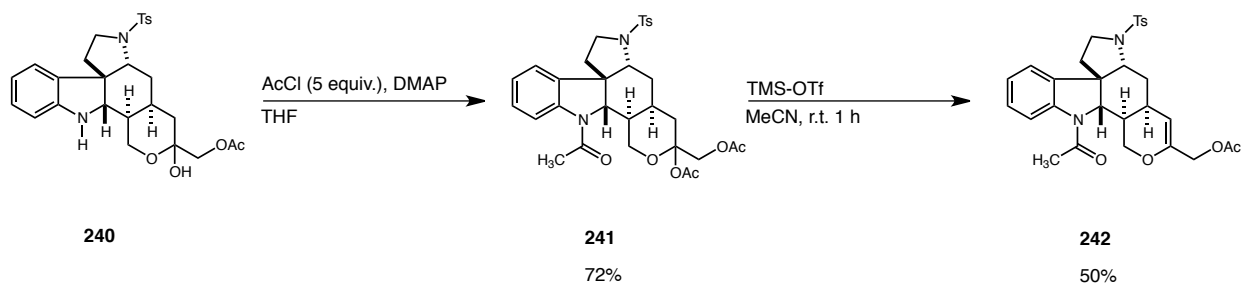
Acetoxyacetyl chloride (**238**) was chosen as the electrophile for the Knochel chemistry sequence due to its similarities with acetyl chloride and availability from commercial sources. We were very pleased to find that reagent **238** was compatible with the Knochel chemistry (Scheme 8.13). Thus, hydroboration of **162** produced the corresponding alkyl-borane species, which was then transmetallated to the high-order cuprate species (via an alkyl-zinc) and treated with acetoxyacetyl chloride (**238**) at  $-78\text{ }^{\circ}\text{C}$  to afford  $\alpha$ -acetoxy ketone **239** in 45% yield as a single diastereoisomer. With acetoxy ketone **239** in hand, hydrogenolysis of the benzyl group over stoichiometric amounts of

palladium on carbon, yielded hemiacetal **240** in 62% yield.



**Scheme 8.13** Synthesis of  $\alpha$ -acetoxy hemiacetal **240**.

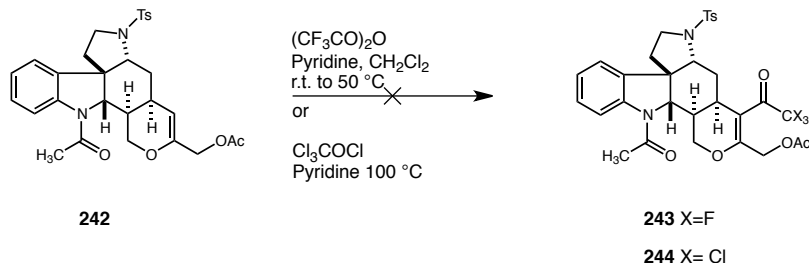
Unfortunately, submitting hemiacetal **240** to the dehydration conditions (dioxane at 110 °C in the presence of PTSA and activated molecular sieves) that worked in the epimalagashanine series did not give the desired dihydropyran, but instead gave back starting material. The use of more forcing dehydrative conditions (HCl, dioxane, 80 °C) led to the complete decomposition of hemiacetal **240**. At this point, we thought that hemiacetal **240** needed to be activated in order to promote elimination (Scheme 8.14). Thus, treatment of **240** with excess acetyl chloride and DMAP in THF led to the formation of bis acetoxy acetamide **233** in 72% yield. Reaction of acetamide **241** with a Lewis acid (trimethylsilyl-triflate) in acetonitrile at room temperature for 1 hour led to the formation of the desired dihydropyran **242** in 50% yield.<sup>111</sup>



**Scheme 8.14** Initial-access to dihydropyran **242**.

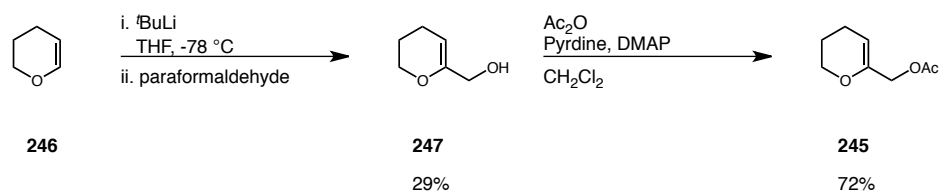
### 8.2.3 Acylation of Dihydropyran **242**.

With dihydropyran **242** in hand, we were very excited at the prospect of finishing the synthesis of a Malagasy alkaloid, since we had a lot of previous experience acylating the C(19) position (*vide supra*). Unfortunately treatment of compound **242** with the previously developed conditions (TFAA, Pyridine, 0 °C) did not produce the desired trifluoroketone **243** and instead just returned unreacted **242** (Scheme 8.15). Trying to force the acylation by raising the temperature to 50 °C (TFAA's b.p.) did not change the previously observed outcome. Switching the electrophiles to trichloroacetyl chloride and heating the reaction to 100 °C did not give any of the desired acylated compound **244**.



**Scheme 8.15** Acylation attempts for compound **242**.

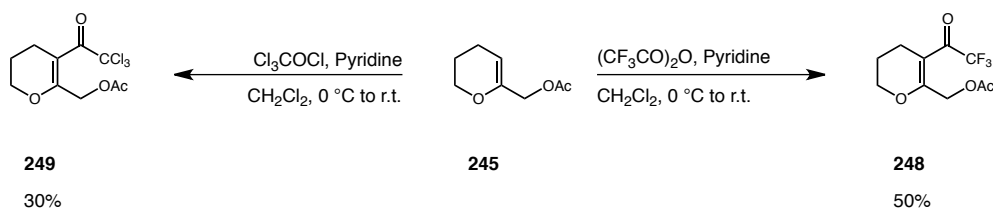
The observed lack of reactivity of dihydropyran **242** and difference in reactivity as compared to dihydropyran **198** led us to initially believe that the electron withdrawing nature of the acetoxy group was deactivating the dihydropyran **242**. In order to test this hypothesis, simple dihydropyran acetate **245** was synthesized in two steps from 3,4-dihydro-2H-pyran (**246**) (Scheme 8.16). Thus, abstraction of C(6) hydrogen of **246** with *t*-BuLi followed by reaction with formaldehyde gave the allylic alcohol **247** in 29% yield.<sup>112</sup> Treatment of **247** with acetic anhydride, pyridine and catalytic amounts (10%) of DMAP produced the desired acetate **245** in 72% yield.<sup>113</sup>



**Scheme 8.16** Synthesis of dihydropyran **245**.

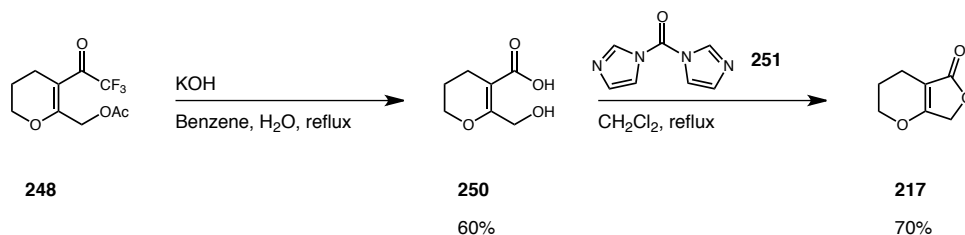
With model substrate **245** in hand, we were ready to explore the acylation in this simpler system. Reaction of **245** with trifluoroacetic anhydride and pyridine cleanly produced the desired trifluoromethyl ketone **248** in moderate yield (50%, Scheme 8.17). We were also able to show that acylation of **245** also proceeds with trichloroacetyl chloride in pyridine to yield trichloro ketone **249** in 30% yield.





**Scheme 8.17** Acylations of model system **245**.

In addition, hydrolysis of **248** was accomplished with KOH in wet benzene (10 % v/v) at reflux to produce carboxylic acid **250** (Scheme 8.18). These results suggest our initial hypothesis that the acetoxy group deactivated the dihydropyran ring for nucleophilic attack was incorrect and that we needed a new hypothesis (*vide infra*). Finally, butyrolactone formation was accomplished by treatment of **250** with 1,1'-carbonyldiimidazole (**251**) in dichloromethane to give compound **217** in 60% yield.

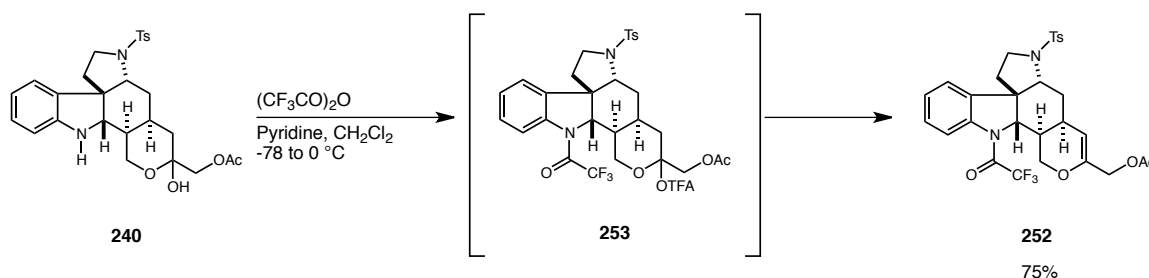


**Scheme 8.18** Synthesis of model butyrolactone **217** from trifluoroketone **248**.

### 8.2.4 Vilsmeier-Haack Formylation

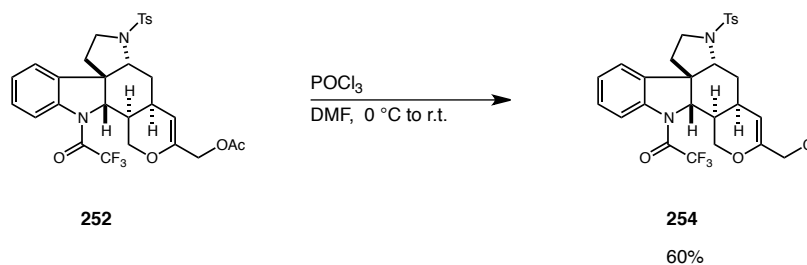
Our next attempt was a Vilsmeier formylation for the functionalization of the dihydropyran **242** at C(19). We postulated that the high electrophilicity of the Vilsmeier reagent could override the lack of reactivity the dihydropyran. However, from our past

experience with the Vilsmeier reagent (*vide supra*), we knew that acetamide **242** was not an ideal starting material to study this methodology.<sup>89</sup> Therefore, trifluoroacetamide **252** was chosen as the ideal dihydropyran for this new approach. Fortunately, we realized that trifluoroacetamide **252** could be synthesized from hemiacetal **240** in *one* chemical step. Thus, treatment of **240** with excess trifluoroacetic anhydride (5 equiv.) protected the indoline nitrogen and produced the mixed acetal **253**, which under the reaction conditions eliminated to yield trifluoroacetamide **252** in 75% yield (Scheme 8.19).



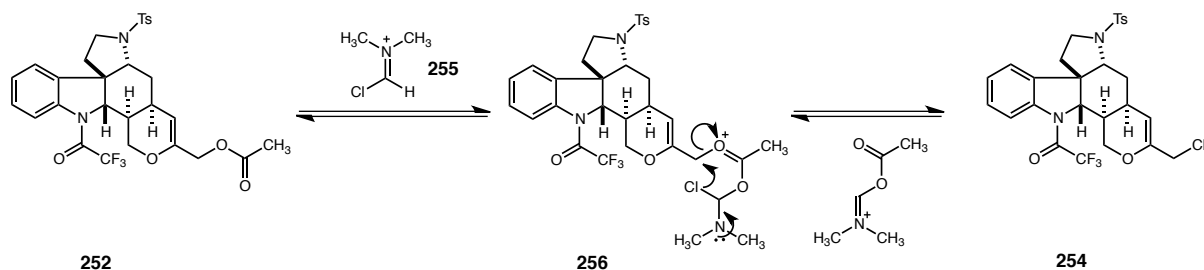
**Scheme 8.19** Synthesis of trifluoroacetamide **252**.

Unfortunately, formylation of trifluoroacetamide **252** under standard Vilsmeier-Haack conditions (DMF, POCl<sub>3</sub>, 0 °C to r.t.) did not produce the desired aldehyde, but instead produced chloride **254** in 60% yield (Scheme 8.20).



**Scheme 8.20** Vilsmeier-Haack reaction of trifluoroacetamide **252**.

Compound **254** is probably formed *via* nucleophilic attack of the Vilsmeier reagent (**255**) by acetoxy group of **252** to generate intermediate **256** (Scheme 8.21). Intramolecular attack by the pendant chloride atom of **256** generates the observed chloride **254**.



**Scheme 8.21** Mechanistic rationale for the formation of chloride **254**.

We also attempted the reaction of chloride **254** with POCl<sub>3</sub> in DMF at 60 °C, but only starting material was detected but <sup>1</sup>H NMR. Raising the temperature to 90 °C finally led to the decomposition of **254**.

We believe that steric effects are responsible for the observed lack of reactivity of dihydropyrans **242** and **252** (Figure 8.1). Although in the case of dihydropyrans **181** and **198** (epi-malagashanine series) the top face of C(19)-C(20) sp<sup>2</sup> bond is sterically not accessible due to mostly the C(14) hydrogens **257**, the bottom face is accessible for reaction with a suitable electrophile. Thus, in the case of both **179** and **191** we observed reactivity with a variety of electrophiles. On the other hand, we believe that in the case of dihydropyrans **242** and **252**, both faces of the sp<sup>2</sup> bond are sterically not accessible. The top face was blocked by the C(14) hydrogens and the bottom face in the case is now blocked by the acetate moiety.

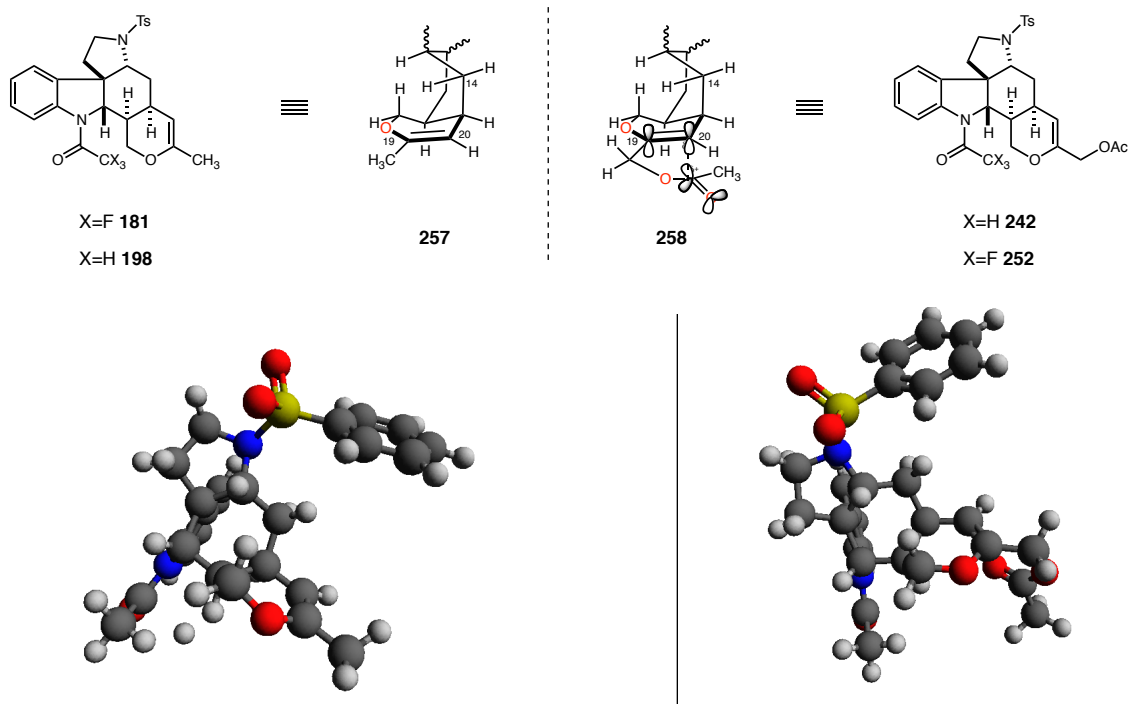


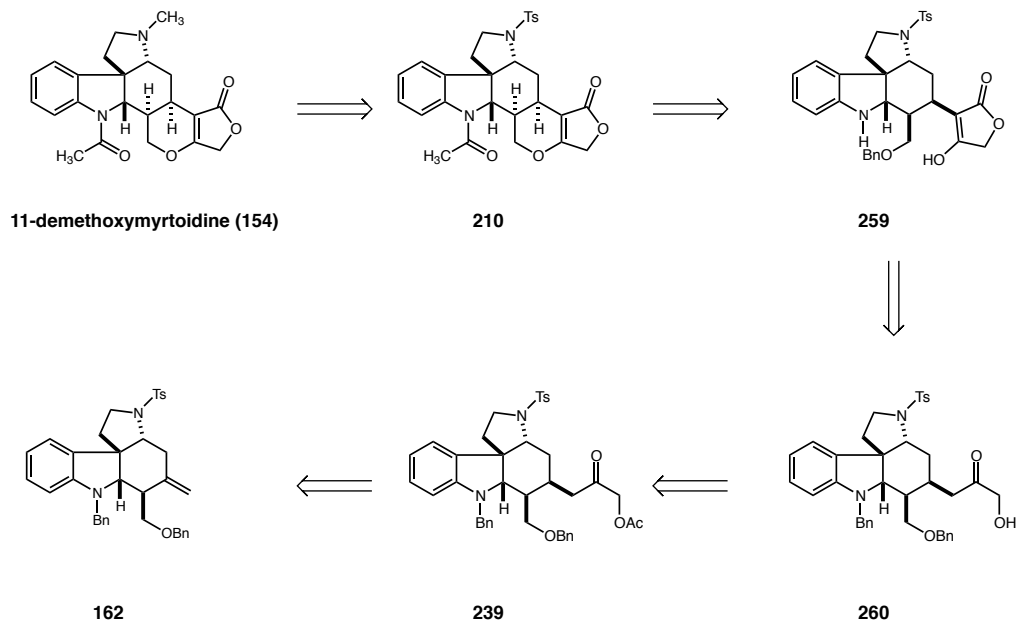
Figure 8.1 Rational for the difference in reactivity.

### 8.3 Third-generation Approach: Synthesis of Tetric Acid.

#### 8.3.1 Retrosynthetic Analysis.

Although our second approach to 11-demethoxymyrtoidine was not successful, we believed that  $\alpha$ -acetoxy ketone **239** could be a key intermediate in a new approach towards 11-demethoxymyrtoidine (Scheme 8.22). Thus, key butyrolactone intermediate **210** could arise from cyclization of tetric acid **259**. Key to this new approach would be synthesis of tetric acid **259**, which potentially could be accessed from  $\alpha$ -hydroxy

ketone **260**.

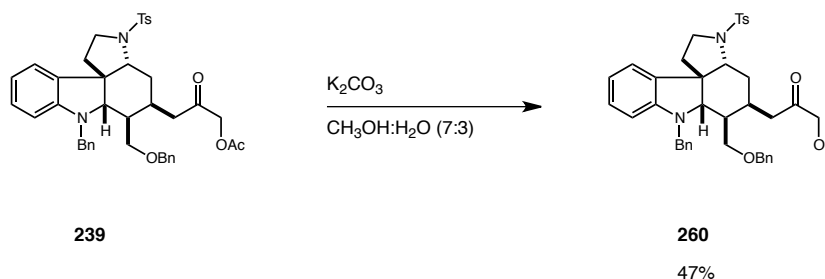


**Scheme 8.22** Retrosynthetic analysis of the third-generation approach to demethoxymyrtoidine

### 8.3.2 Hydrolysis of $\alpha$ -Acetoxy Ketone **239**.

The third generation approach to 11-demethoxymyrtoidine began by attempting the hydrolysis of the  $\alpha$ -acetoxy ketone **239**. Our first attempt was to use potassium cyanide in ethanol to mediate the hydrolysis of the acetate group, which had been previously shown to be useful for acid and base sensitive compounds.<sup>114</sup> Unfortunately, this protocol did not work well in the case of compound **239** and a mixture of unidentified products was obtained. Fortunately when  $\alpha$ -acetoxy ketone **239** was treated with  $K_2CO_3$  in methanol:water mixture (7:3 v/v) the clean hydrolysis of the acetate group was observed

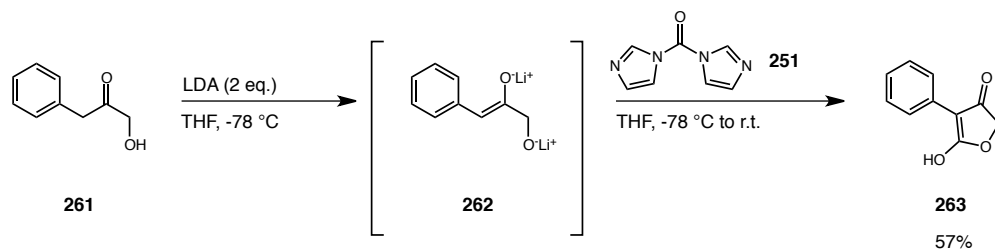
(Scheme 8.23). Thus, acyloin **260** was obtained after an aqueous work-up, albeit in low yield (45%). Subsequently we realized that acyloin **260** was a highly sensitive compound, decomposing during solvent removal, upon standing at room temperature and prolonged storage at low temperatures.



Scheme 8.23 Hydrolysis of acetate **239**.

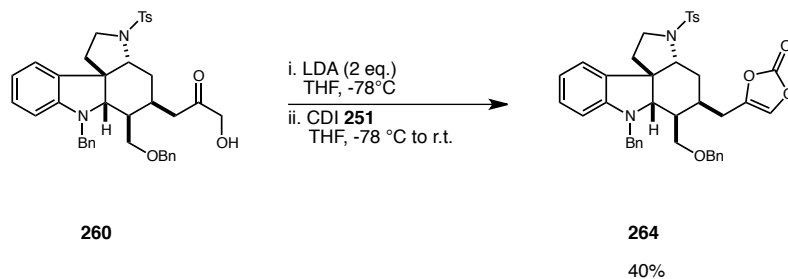
### 8.3.3 Attempts to Synthesize Tetronic Acid **259**

With acyloin **260** in hand, we began to explore the synthesis of key tetronic acid **259**. Previous work by Smith and coworkers showed that tetronic acids could be easily accessed from the corresponding  $\alpha$ -hydroxyketone (Scheme 8.24).<sup>115</sup> For example, treatment of phenyl  $\alpha$ -hydroxyketone **261** with 2.5 equivalents of freshly prepared LDA produced dianion intermediate **262**. *In situ* condensation of dianion **262** with 2.0 equivalents of 1,1'-carbonyldiimidazole (**251**) yielded the desired tetronic acid **263** in 57% yield.



**Scheme 8.24** Smith and coworkers methodology for the synthesis of tetronic acids.

Although the yields reported for this methodology are moderate (31 – 57%), we were attracted and excited by the directness of this methodology. Treatment of  $\alpha$ -hydroxyketone **260** with 2.5 equivalents of LDA followed by 2.0 equivalents of previously dried 1,1'-carbonyldiimidazole (**251**) only produced cyclic carbonate **264** (40% yield) (Scheme 8.25). The use of other carbonyl sources such as triphosgene and phosgene resulted in the recovery of starting material.



**Scheme 8.25** Attempt to form tetronic acid via dianion formation.

It is known that *O*-alkylation is prevalent when the enolate is disassociated, while *C*-alkylation is favored when ion clustering occurs.<sup>116</sup> Since lithium enolates in THF solution are known to form ion clusters,<sup>117</sup> the exclusive formation of **264** cannot be explained based on disassociation and clustering effects of enolate ions. Thus, we believe





## 8.4 Conclusions.

During this phase of studies towards the total synthesis of malagashanine (**151**) we showed that through careful optimization studies a robust and scalable route for the synthesis of key methyl-ester **184** could be developed. Early on we were able to fix the problematic synthesis of *N*-Tosyl-*O*-TMS aminol **161** by realizing the importance of free imidazole over the course of the reaction. We were also able to circumvent the problematic oxidation of aldehyde **182** by using trifluoroacetic anhydride as the carbonyl source to make trifluoroketone **199**, which bears the right oxidation state.

We performed an extensive screening of hydrogenation conditions that revealed that reduction of the C(19)-C(20) tetrasubstituted olefin of acid **182** was complicated by the competitive reduction of the indoline ring. However, we showed that we could complete the synthesis of epimalagashanine (**206**) *via* ionic reduction with Et<sub>3</sub>SiH and TFA.

We have proposed a new strategy for the synthesis of malagashanine (**151**) that involves the synthesis of the minor Malagasy alkaloid 11-demethoxymyrtoidine (**154**). Our first generation strategy for the synthesis of 11-demethoxymyrtoidine which centered around direct functionalization of the C(18) allylic methyl group of either acid **182** or methyl-ester **184** was characterized by the lack of reactivity of either advance intermediate or the functionalization of the wrong allylic position at C(15). These results highlighted the need for further development of a directed palladium catalyzed C-H functionalization. This challenge is currently being investigated by our collaborators (Yu and co-workers) in the Center for C-H Functionalization.

In light of these negative results we took a step back and decided to include the oxygen functionality during the hydroacylation of core **162**. Although the modified hydroacylation of **162** was a success, this strategy failed when we attempted the acylation of dihydropyrans **242** or **252**.

Our third generation approach to 11-demethoxymyrtoidine involved the synthesis of tetronic acid **259**, which if successful would directly produce the butyrolactone unit. However, our attempt to make tetronic acid **259** from  $\alpha$ -hydroxyketone **260** was not successful and instead produced cyclic carbonate **264**. Our lab is currently studying different approaches to the synthesis of tetronic acid **259** from  $\alpha$ -hydroxyketone **260**. We anticipate that a route to tetronic acid **259** and will facilitate the synthesis of 11-demethoxymyrtoidine (**154**), myrtoidine (**153**) and malagashanine (**151**).

## 9 Experimentals

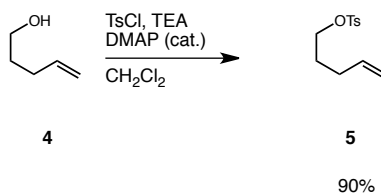
### 9.1 Materials and Methods: General Information.

$^1\text{H}$  and  $^{13}\text{C}$  NMR spectra were recorded on a Varian Inova 600 spectrometer (600 MHz  $^1\text{H}$ , 150 MHz  $^{13}\text{C}$ ), a Varian Unity plus 600 (600 MHz  $^1\text{H}$ , 150 MHz  $^{13}\text{C}$ ) or a Varian Inova 400 spectrometer (400 MHz  $^1\text{H}$ , 100 MHz  $^{13}\text{C}$ ) at room temperature (unless otherwise stated) in  $\text{CDCl}_3$  with internal  $\text{CHCl}_3$  as the reference (7.26 ppm for  $^1\text{H}$  and 77.23 ppm for  $^{13}\text{C}$ ),  $(\text{CD}_3)_2\text{SO}$  with internal  $(\text{CH}_3)_2\text{SO}$  as reference (2.50 ppm for  $^1\text{H}$  and 39.51 ppm for  $^{13}\text{C}$ ) or  $\text{C}_6\text{D}_6$  (7.16 ppm for  $^1\text{H}$  and 128.39 ppm for  $^{13}\text{C}$ ). Chemical shifts ( $\delta$  values) were reported in parts per million (ppm) and coupling constants ( $J$  values) in Hz. Multiplicity is indicated using the following abbreviations: s = singlet, d = doublet, t = triplet, q = quartet, qn = quintet, hep = heptet, m = multiplet, b = broad signal). Infrared (IR) spectra were recorded using Thermo Electron Corporation Nicolet 380 FT-IR spectrometer. High-resolution mass spectra were obtained using a Thermo Electron Corporation Finigan LTQFTMS (at the Mass Spectrometry Facility, Emory University). We acknowledge the use of shared instrumentation provided by grants from the NIH and the NSF. Melting points (mp) were taken using a Fisher-Johns melting point apparatus and are not corrected. Analytical thin layer chromatography (TLC) was performed on precoated glass backed EMD 0.25 mm silica gel 60 plates. Visualization was accomplished with UV light, ethanolic anisaldehyde, phosphomolybdic acid or CAM stain (Verghn's), followed by heating. Flash column chromatography was carried out using EMD Geduran® silica gel 60 (40-63  $\mu\text{m}$ ) or Fluka® aluminum oxide (0.05-0.15 mm); pH 7.0. All reactions were conducted with anhydrous solvents in oven dried or

flame-dried and argon-charged glassware. Anhydrous solvents were purified by passage through activated alumina using a *Glass Contours* solvent purification system unless otherwise noted. Solvents used in workup, extraction and column chromatography were used as received from commercial suppliers without prior purification. All reagents were purchased from Sigma-Aldrich and used as received unless otherwise noted.

## 9.2 Part 1: Copper Catalyzed Aminoacetoxylation of Olefins.

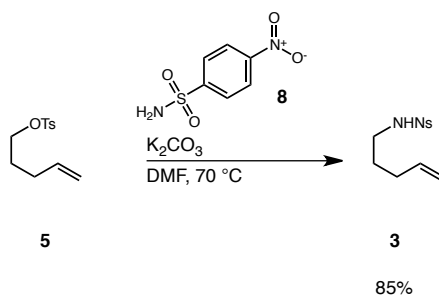
### Pent-4-enyl 4-methylbenzenesulfonate (**5**):



To a solution of pent-4-en-1-ol (8.6 g, 0.1 mol) (**4**) in dichloromethane (0.2 M) was added p-toluenesulfonyl chloride (27.4 g, 0.11 mol) and 4-dimethylaminopyridine (2.44 g, 0.02 mol) at room temperature. The mixture was then cooled with an ice bath to 0 °C. and triethylamine (16.7 mL, 0.12 mol) was slowly added over the course of 5 minutes. The solution obtained was removed from the ice bath and allowed to reach room temperature. Once the reaction was judged to be complete by TLC (slurry may develop), it was quenched with H<sub>2</sub>O (20 mL). The biphasic mixture was then extracted twice with diethyl ether (100 mL). The collected organic phases were then washed with 2N HCl (10 mL) and brine (10 mL) and dried over solid NaSO<sub>4</sub>. Removal of the solvent yielded a crude product, which was purified via silica gel plug (4:1 hexanes/EtOAc, R<sub>f</sub> = 0.70) to yield pent-4-enyl 4-methylbenzenesulfonate (**5**) (20.35 g, 86 %) as a clear oil. **IR** (thin film, cm<sup>-1</sup>) 3076, 2977, 2923, 1355, 1187, 1371, 1172, 1097, 966, 914, 812, 739, 661; **<sup>1</sup>H**

**NMR** (CDCl<sub>3</sub>, 400 MHz)  $\delta$  7.77 (dt, 2H,  $J$  = 8.5, 1.8 Hz), 7.33 (d,  $J$  = 8.5 Hz), 5.73-5.62 (m, 1H), 4.97-4.94 (m, 1H), 4.93-4.91 (m, 1H), 4.02 (t, 2H,  $J$  = 6.5 Hz), 2.44 (s, 3H), 2.10-2.03 (m, 2H), 1.77-1.68 (m, 2H).; **<sup>13</sup>C NMR** (CDCl<sub>3</sub>, 100 MHz)  $\delta$  144.9, 136.8, 133.2, 130.0, 128.0, 116.0, 70.0, 29.5, 28.1, 21.8, 21.8; **HRMS** (+ APCI) calculated for C<sub>12</sub>H<sub>17</sub>O<sub>3</sub>S 283.0893, found 263.0893 [M+H]<sup>+</sup>.

**4-Nitro-N-(pent-4-enyl)benzenesulfonamide (3):**



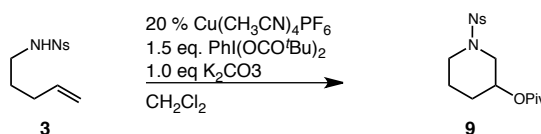
To a solution of tosyl olefinic alcohol **5** (2 g, 8.3 mmol) in DMF (0.3 M) was added K<sub>2</sub>CO<sub>3</sub> (3.45g, 24.97 mmol) and 4-nitrobenzenesulfonamide (5.05g, 24.97 mmol) at room temperature. The yellow slurry obtained was heated to 70 °C until it was judged to be complete by TLC. After this time, it was cooled to room temperature and quenched with H<sub>2</sub>O (50 mL). The biphasic mixture was then extracted twice with ethyl acetate (200 mL). The collected organic phases were then washed with 2N HCl (20 mL), water (3 x30 mL), brine (10 mL) and dried over solid NaSO<sub>4</sub>. Removal of solvents yielded a crude product which was purified by column chromatography on silica gel (20 % EtOAc in Hexanes, R<sub>f</sub> = 0.55) to afford 4-nitro-N-(pent-4-enyl)benzenesulfonamide (**3**) (2.24 g, 85 %) as a yellow solid. **Mp** 34.9 – 35.5 °C; **IR** (thin film, cm<sup>-1</sup>) 3275, 2976, 2937, 2900, 2869, 1606, 1558, 1529, 1473, 1463, 1456, 1425, 1402, 1348, 1309, 1161, 1092, 1059, 997, 908, 854, 827, 729, 684, 648, 608.; **<sup>1</sup>H NMR** (CDCl<sub>3</sub>, 600 MHz)  $\delta$  8.37-8.34 (m, 2H), 8.08-8.04 (m, 2H), 5.72-5.64 (m, 1H), 5.15 (t, 1H,  $J$  =5.5 Hz), 4.98-4.92 (m, 2H),

3.03-2.98(m, 2H), 2.04 (q, 2H,  $J = 6.9$  Hz), 1.55-1.62 (m, 2H);  $^{13}\text{C}$  NMR ( $\text{CDCl}_3$ , 150 MHz)  $\delta$  150.2, 146.0, 137.0, 128.5, 124.6, 116.0, 42.9, 30.6, 28.6.; HRMS (- APCI) calculated for  $\text{C}_{11}\text{H}_{13}\text{N}_2\text{O}_4\text{S}$  269.0602, found 269.0600  $[\text{M}-\text{H}]^+$ .

### General Procedure A (Copper Catalyzed Aminoacetoxylation of Olefins).

Nosylamide **X** (1.0 eq.) was mixed with  $\text{PhI}(\text{O}_2\text{CR})_2$  (1.5 eq.),  $\text{K}_2\text{CO}_3$  (1.0 eq.) and  $\text{Cu}(\text{CH}_3\text{CN})_4\text{PF}_6$  (10 mol%) in a round bottom flask equipped with a septum or a 2 dram reaction vial and capped with a teflon lined septum. After evaporation and flushing with argon,  $\text{CH}_2\text{Cl}_2$  (0.2M) was added and the reaction was stirred at room temperature. After the reaction was judge to be complete by TLC, it was quenched with saturated  $\text{NH}_4\text{Cl}$  (10 mL) solution. The biphasic mixture was then extracted with ethyl acetate (2 x 50 mL). The combined organic layers were then washed with saturated  $\text{NH}_4\text{Cl}$  solution (10 mL) and dried under  $\text{Na}_2\text{SO}_4$ . Removal of solvents under reduced pressure yielded a crude mixture, which was purified by silica or alumina oxide.

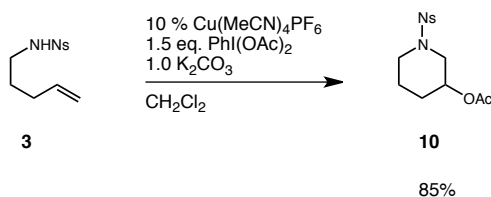
### 1-(4-Nitrophenylsulfonyl)piperidin-3-yl pivalate (**9**):



Prepared according to general procedure **A** using 4-nitro-*N*-(pent-4-enyl)benzenesulfonamide (**3**) (600 mg, 2.1 mmol),  $\text{PhI}(\text{O}_2\text{C}^t\text{Bu})_2$  (1.2 g, 3.16 mmol),  $\text{K}_2\text{CO}_3$  (291 mg, 2.1 mmol) and  $\text{Cu}(\text{CH}_3\text{CN})_4\text{PF}_6$  (106 mg, 0.21 mmol). Purification via flash chromatography with silica gel as the stationary phase (2:2:1 Hexanes:  $\text{CH}_2\text{Cl}_2$ :

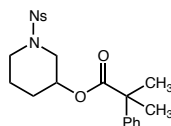
Diethyl Ether) afforded pivalate **9** (529 mg, 68%). **IR** (thin film,  $\text{cm}^{-1}$ ) 3016, 2959, 2869, 1722, 1529, 1348, 1311, 1172, 1156, 1134, 945, 912, 855, 742, 599.;  **$^1\text{H}$  NMR** ( $\text{CDCl}_3$ , 600 MHz)  $\delta$  8.40-8.37 (m, 2H), 7.97-7.95 (m, 2H), 4.86-4.83 (m, 1H), 3.26-3.23 (m, 2H), 3.16 (dd, 1H,  $J = 12.1, 2.9$  Hz), 3.05-3.00 (m, 1H), 1.96-1.89 (m, 1H), 1.76-1.70 (m, 1H), 1.69-1.61 (m, 2H), 1.22 (s, 9H);  **$^{13}\text{C}$  NMR** ( $\text{CDCl}_3$ , 150 MHz)  $\delta$  177.8, 150.3, 143.3, 128.7, 124.6, 66.6, 49.0, 46.2, 39.0, 28.4, 27.3, 21.8.; **HRMS** (+ APCI) calculated for  $\text{C}_{16}\text{H}_{23}\text{N}_2\text{O}_6\text{S}$  371.12714, found 371.12735  $[\text{M}+\text{H}]^+$ .

### 1-(4-Nitrophenylsulfonyl)piperidin-3-yl acetate (**10**):



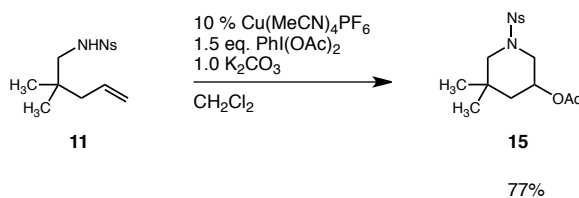
Prepared according to general procedure **A** using 4-nitro-*N*-(pent-4-enyl)benzenesulfonamide (**3**) (542 mg, 1.93 mmol),  $\text{PhI}(\text{OAc})_2$  (933 mg, 2.90 mmol),  $\text{K}_2\text{CO}_3$  (267 mg, 1.93 mmol) and  $\text{Cu}(\text{CH}_3\text{CN})_4\text{PF}_6$  (97 mg, 0.193 mmol) under argon. Purification via flash chromatography with silica gel as the stationary phase afforded piperidine acetate **10** (610 mg, 85%). **IR** (thin film,  $\text{cm}^{-1}$ ) 3015, 2955, 2860, 1734, 1530, 1349, 1240, 1170, 905, 727.;  **$^1\text{H}$  NMR** ( $\text{CDCl}_3$ , 600 MHz)  $\delta$  8.39-8.35 (m, 2H), 7.96-7.93 (m, 2H), 4.92-4.75 (m, 1H), 3.29 (dd, 1H,  $J = 12.1, 3.1$  Hz), 3.15-3.06 (m, 3H), 2.04 (s, 3H), 1.91-1.85 (m, 1H), 1.79-1.73 (m, 1H), 1.66-1.54 (m, 2H);  **$^{13}\text{C}$  NMR** ( $\text{CDCl}_3$ , 150 MHz)  $\delta$  170.3, 150.3, 143.3, 128.8, 124.6, 67.2, 49.1, 46.1, 28.5, 21.8, 21.3.; **HRMS** (+ APCI) calculated for  $\text{C}_{13}\text{H}_{17}\text{N}_2\text{O}_6\text{S}$  329.0818, found 329.0804  $[\text{M}+\text{H}]^+$ .

**1-(4-Nitrophenylsulfonyl)piperidin-3-yl 2-methyl-2-phenylpropanoate (Table 2.2 entry 2):**



Prepared according to general procedure **A** using 4-nitro-*N*-(pent-4-enyl)benzenesulfonamide (**3**) (200 mg, 0.74 mmol),  $\text{PhI}(\text{O}_2\text{CMe}_2\text{Ph})_2$  (589 mg, 1.10 mmol),  $\text{K}_2\text{CO}_3$  (102 mg, 0.74 mmol) and  $\text{Cu}(\text{CH}_3\text{CN})_4\text{PF}_6$  (28 mg, 0.074 mmol). Purification via flash chromatography with silica gel as the stationary phase afforded piperidine (194 mg, 61%). **IR** (thin film,  $\text{cm}^{-1}$ ) 3105, 2924, 2962, 2862, 1724, 1529, 1348, 1211, 1254, 1171, 945, 910, 742.;  **$^1\text{H}$  NMR** ( $\text{CDCl}_3$ , 600 MHz)  $\delta$  8.37-8.33 (m, 2H), 7.93-7.89 (m, 2H), 7.37-7.30 (m, 4H), 7.27-7.22 (m, 1H), 4.88-4.83 (m, 1H), 3.07-3.19 (m, 3H), 3.02-2.96 (m, 1H), 1.76-1.64 (m, 2H), 1.61 (s, 3H) 1.59-1.53 (m, 4H), 1.47-1.53 (m, 1H).;  **$^{13}\text{C}$  NMR** ( $\text{CDCl}_3$ , 150 MHz)  $\delta$  176.0, 150.3, 144.5, 143.2, 128.8, 128.6, 126.9, 125.8, 124.6, 67.2, 48.9, 46.8, 46.1, 28.2, 26.0, 26.4, 21.6.; **HRMS** (+ APCI) calculated for  $\text{C}_{21}\text{H}_{25}\text{N}_2\text{O}_6\text{S}$  433.14279, found 433.14296  $[\text{M}+\text{H}]^+$ .

**5,5-Dimethyl-1-(4-nitrophenylsulfonyl)piperidin-3-yl acetate (15):**

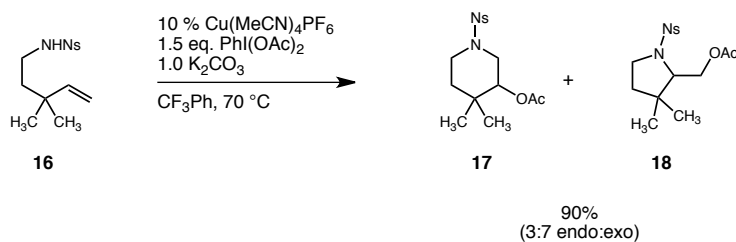


Prepared according to general procedure **A** using 4-nitro-*N*-(pent-4-enyl)benzenesulfonamide (**11**) (1 g, 3.18 mmol),  $\text{PhI}(\text{OAc})_2$  (1.54 mg, 4.78 mmol),



$K_2CO_3$  (440 mg, 3.18 mmol) and  $Cu(CH_3CN)_4PF_6$  (160 mg, 0.318 mmol). Purification via flash chromatography with silica gel as the stationary phase afforded 1-(4-nitrophenylsulfonyl)piperidin-3-yl pivalate (**15**) (920 mg, 77%). **IR** (thin film,  $cm^{-1}$ ) 3105, 2969, 2866, 1735, 1537, 1348, 1242, 1165, 1087, 1060, 907, 728.;  **$^1H$  NMR** ( $CDCl_3$ , 600 MHz)  $\delta$  8.40-8.37 (m, 2H), 7.96-7.93 (m, 2H), 5.02-4.97 (m, 1H), 3.65 (dd, 1H,  $J = 11.4, 4.2$  Hz), 3.09 (d, 1H,  $J = 11.4$  Hz), 2.59-2.53 (m, 1H), 2.44 (d, 1H,  $J = 11.4$  Hz), 2.03 (s, 3H), 1.71 (dd, 1H,  $J = 13.5, 4.3$  Hz), 1.25 (dd, 1H,  $J = 13.5, 4.3$  Hz), 1.06 (s, 3H), 1.02 (s, 3H).;  **$^{13}C$  NMR** ( $CDCl_3$ , 150 MHz)  $\delta$  170.1, 158.3, 148.0, 128.8, 124.6, 66.7, 56.9, 49.1, 41.9, 32.0, 28.0, 25.7, 21.3\.; **HRMS** (+ APCI) calculated for  $C_{15}H_{21}N_2O_6S$  357.1115, found 357.1117  $[M+H]^+$ .

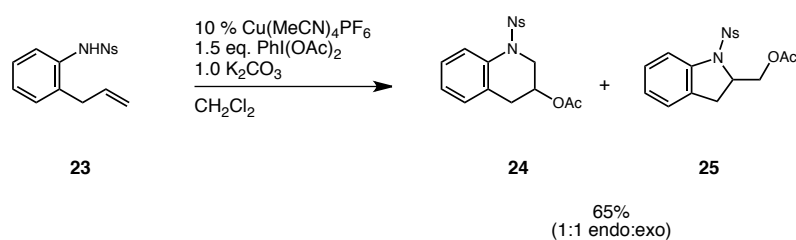
**4,4-Dimethyl-1-(4-nitrophenylsulfonyl)piperidin-3-yl acetate (17) and (3,3-Dimethyl-1-(4-nitrophenylsulfonyl)pyrrolidin-2-yl)methyl acetate (18):**



Prepared according to general procedure **A** using *N*-(3,3-dimethylpent-4-enyl)-4-nitrobenzenesulfonamide (**16**) (51 mg, 0.17 mmol),  $PhI(OAc)_2$  (81 mg, 0.25 mmol),  $K_2CO_3$  (23.2 mg, 0.17 mmol) and  $Cu(CH_3CN)_4PF_6$  (6.3 mg, 0.017 mmol). Purified by flash chromatography on silica gel (1:1 Pentane: Ethyl Acetate) afforded dimethylpiperidine (**17**) (41 mg, 70%); **Mp** 119.7-120.3 °C.; **IR** (thin film,  $cm^{-1}$ ) 3105, 2958, 2871, 1736, 1529, 1350, 1237, 1164, 1092, 1043, 935, 855, 757, 743, 608, 598;  **$^1H$**

**NMR** (CDCl<sub>3</sub>, 400 MHz)  $\delta$  8.40-8.36 (m, 2H), 7.97-7.94 (m, 2H), 4.58 (dd, 1H,  $J = 6.5$ , 3.5 Hz), 3.28-3.08 (m, 4H), 2.08 (s, 3H), 1.74 (ddd, 1H,  $J = 13.5$ , 8.26, 4.13 Hz), 1.42 (ddd, 1H,  $J = 13.5$ , 7.0, 3.8 Hz), 0.98 (s, 3H), 0.88 (s, 3H); **<sup>13</sup>C NMR** (CDCl<sub>3</sub>, 100 MHz)  $\delta$  170.6, 150.3, 143.6, 128.7, 124.6, 73.7, 44.9, 42.1, 35.2, 32.5, 25.5, 22.8, 21.1.; **HRMS** (+ pESI) calculated for C<sub>15</sub>H<sub>20</sub>N<sub>2</sub>O<sub>6</sub>S + <sup>23</sup>Na 379.0934, found 379.0904 [M+ <sup>23</sup>Na]<sup>+</sup> and dimethylpyrrolidine (**18**) (18 mg, 30%); **Mp** 110.2-110.6 °C **IR** (thin film, cm<sup>-1</sup>) 3105, 2963, 1737, 1528, 1398, 1234, 1158, 1094, 856, 738, 688, 617, 576.; **<sup>1</sup>H NMR** (CDCl<sub>3</sub>, 400 MHz)  $\delta$  8.39-8.56 (m, 2H), 8.06-8.03 (m, 2H), 4.30 (dd, 1H,  $J = 11.5$ , 5.9 Hz), 4.12 (dd, 2H,  $J = 11.8$ , 4.13 Hz), 3.54-3.49 (m, 1H), 3.44-3.42 (m, 1H), 3.22-3.15 (m, 1H), 2.04 (s, 3H), 1.92-1.85 (m, 1H), 1.48 (ddd, 1H,  $J = 12.5$ , 7.3, 2.2 Hz), 1.02 (s, 3H), 0.51 (s, 3H).; **<sup>13</sup>C NMR** (CDCl<sub>3</sub>, 100 MHz)  $\delta$  170.6, 150.3, 143.4, 128.8, 124.5, 66.8, 64.9, 46.8, 41.5, 37.7, 27.4, 22.6, 21.1.; **HRMS** (+ pESI) calculated for C<sub>15</sub>H<sub>20</sub>N<sub>2</sub>O<sub>6</sub>S<sup>23</sup>Na 379.0934, found 379.0930 [M+ <sup>23</sup>Na]<sup>+</sup>.

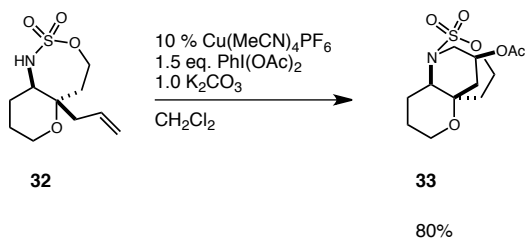
**1-(4-Nitrophenylsulfonyl)-1,2,3,4-tetrahydroquinolin-3-yl acetate (24) and (1-(4-Nitrophenylsulfonyl)indolin-2-yl)methyl acetate (25):**



Prepared according to general procedure **A** using *N*-(2-allylphenyl)-4-nitrobenzenesulfonamide (**23**) (51 mg, 0.16 mmol), PhI(OAc)<sub>2</sub> (77 mg, 0.24 mmol), K<sub>2</sub>CO<sub>3</sub> (22 mg, 0.16 mmol) and Cu(CH<sub>3</sub>CN)<sub>4</sub>PF<sub>6</sub> (8 mg, 0.016 mmol). Purification by

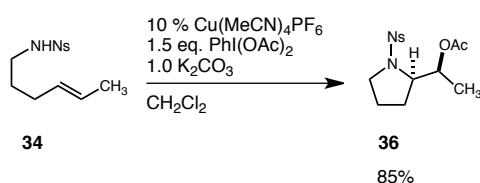
flash chromatography on silica gel (2:2:1 Hexanes: CH<sub>2</sub>Cl<sub>2</sub>: Diethyl Ether) afforded tetrahydroquinoline (**24**) (22 mg, 37% combined); **IR** (thin film, cm<sup>-1</sup>) 3105, 2924, 2825, 1738, 1531, 1350, 1243, 1169, 904, 729.; **<sup>1</sup>H NMR** (CDCl<sub>3</sub>, 600 MHz) δ 8.29-8.26 (m, 2H), 7.90-7.87 (m, 2H), 7.70 (d, 2H, *J* = 8.0 Hz), 7.27-7.23 (m, 1H), 7.16 (dt, 1H, *J* = 7.6, 1.0 Hz), 7.06 (dd, 1H, *J* = 7.6, 1.0 Hz), 4.94-4.90 (m, 1H), 4.15 (dd, 1H, *J* = 13.8, 4.3 Hz), 3.79 (dd, 1H, *J* = 13.8, 6.7 Hz), 2.80 (dd, 1H, *J* = 16.7, 5.7 Hz), 2.57 (dd, 1H, *J* = 16.7, 6.7 Hz), 2.02 (s, 3H).; **<sup>13</sup>C NMR** (CDCl<sub>3</sub>, 150 MHz) δ 170.4, 162.9, 145.6, 142.8, 135.7, 130.0, 128.6, 127.7, 126.5, 124.5, 124.3, 66.4, 49.6, 32.5, 21.2.; **HRMS** (+ APCI) calculated for C<sub>17</sub>H<sub>17</sub>N<sub>2</sub>O<sub>6</sub>S – (C<sub>2</sub>H<sub>3</sub>O<sub>2</sub>) 317.0596, found 317.0592 [M-OAc+H]<sup>+</sup>; and indoline (**25**) (20 mg, 33 %); **IR** (thin film, cm<sup>-1</sup>) 3105, 2923, 2854, 1738, 1530, 1348, 1230, 1170, 1045, 912, 760.; **<sup>1</sup>H NMR** (CDCl<sub>3</sub>, 600 MHz) δ 8.23-8.21 (m, 2H), 7.85-7.82 (m, 2H), 7.68 (d, 2H, *J* = 8.0 Hz), 7.29-7.25 (m, 2H), 7.11-7.06 (m, 2H), 4.57-4.53 (m, 1H), 4.22 (dd, 1H, *J* = 11.0, 6.2 Hz), 4.15 (dd, 1H, *J* = 11.4, 6.7 Hz), 2.79 (dd, 1H, *J* = 16.7, 9.5 Hz), 2.63 (dd, 1H, *J* = 16.7, 2.4 Hz), 2.07 (s, 3H).; **<sup>13</sup>C NMR** (CDCl<sub>3</sub>, 150 MHz) δ 171.2, 150.6, 143.6, 140.4, 131.6, 128.5, 128.4, 126.1, 125.7, 124.5, 117.8, 65.6, 60.6, 31.5, 21.0.; **HRMS** (+ APCI) calculated for C<sub>17</sub>H<sub>17</sub>N<sub>2</sub>O<sub>6</sub>S – [C<sub>2</sub>H<sub>3</sub>O<sub>2</sub>] 317.0596, found 317.0593 [M-OAc+H]<sup>+</sup>.

**2,2-dioxidohexahydro-1,5a-propanopyrano[3,2-*d*][1,2,3]oxathiazepin-11-yl acetate (33):**



Prepared according to general procedure **A** using 5-allyloctahydropyrano[3,2-*d*][1,2,3]oxathiazepine 2,2-dioxide (**32**) (50 mg, 0.2 mmol), PhI(OAc)<sub>2</sub> (98 mg, 0.3 mmol), K<sub>2</sub>CO<sub>3</sub> (28 mg, 0.2 mmol) and Cu(CH<sub>3</sub>CN)<sub>4</sub>PF<sub>6</sub> (7.5 mg, 0.02 mmol). Purification by flash column chromatography (3:1→1:1 Hexanes/EtOAc) afforded 2,2-dioxidohexahydro-1,5a-propanopyrano[3,2-*d*][1,2,3]oxathiazepin-11-yl acetate (**33**) (48 mg, 80 %) as an amorphous solid. **IR** (thin film, cm<sup>-1</sup>) 2947, 1741, 1389, 1362, 1188; **<sup>1</sup>H NMR** (CDCl<sub>3</sub>, 600 MHz) δ 5.21 (sp, 1H, *J* = 5.5 Hz), 4.51 (ddd, 1H, *J* = 13.7, 7.8, 3.2), 4.38 (ddd, 1H, *J* = 13.7, 8.7, 2.8 Hz), 3.98 (dd, 1H, *J* = 14.7, 5.5 Hz), 3.84 (dd, 1H, *J* = 12.4, 4.6 Hz), 3.67 (dd, 1H, *J* = 11.9, 4.6 Hz), 3.55 (dt, 1H, *J* = 11.9, 3.2 Hz), 3.00 (dd, 1H, *J* = 14.7, 11.5), 2.34-2.27 (m, 2H), 2.18-2.13 (m, 1H), 2.07 (s, 3H), 2.01 (dq, 1H, *J* = 12.8, 5.0 Hz), 1.91-1.88 (m, 2H), 1.78-1.70 (m, 2H); **<sup>13</sup>C NMR** (CDCl<sub>3</sub>, 150 MHz) δ 169.9, 73.9, 67.5, 65.9, 60.7, 54.2, 43.7, 43.1, 33.7, 25.6, 23.1, 21.1; **HRMS** (+APCI) calculated for C<sub>12</sub>H<sub>19</sub>NO<sub>6</sub>S 305.0933, found 306.1005 [M+H]<sup>+</sup>.

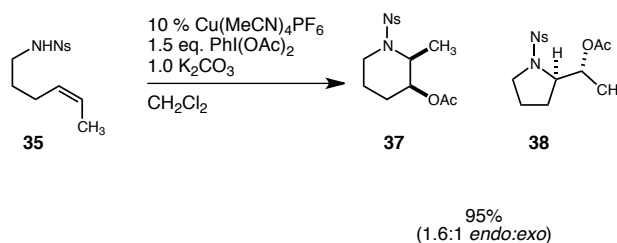
### 1-(4-Nitrophenylsulfonyl)pyrrolidin-2-yl)(phenyl)methyl acetate (**36**):



Prepared according to general procedure **A** using (*E*)-5-phenylpent-4-enyl 4-methylbenzenesulfonate (**34**) (50 mg, 0.14 mmol), PhI(OAc)<sub>2</sub> (70 mg, 0.22 mmol), K<sub>2</sub>CO<sub>3</sub> (19 mg, 0.14 mmol) and Cu(CH<sub>3</sub>CN)<sub>4</sub>PF<sub>6</sub> (5.2 mg, 0.014 mmol). Purification by flash column chromatography (4:1 to 3:1 Hexanes/EtOAc) afforded 1-(4-nitrophenylsulfonyl)pyrrolidin-2-yl)(phenyl)methyl acetate (**35**) (17 mg, 29 %, 10:1 d.r.).

**IR** (thin film,  $\text{cm}^{-1}$ ) 3105, 2980, 1741, 1529, 1350, 1232, 1163;  **$^1\text{H}$  NMR** ( $\text{CDCl}_3$ , 600 MHz)  $\delta$  8.35 (d, 2H,  $J = 8.6$  Hz), 8.0 (d, 2H,  $J = 8.6$ ), 7.38-7.23 (m, 5H), 6.10 (d, 1H,  $J = 2.9$  Hz), 4.21 (dt, 1H,  $J = 8.6, 3.3$  Hz), 3.34-3.25 (m, 2H), 2.15 (s, 3H), 2.01-1.97 (m, 1H), 1.75-1.68 (m, 1H), 1.56-1.51 (m, 2H);  **$^{13}\text{C}$  NMR** ( $\text{CDCl}_3$ , 150 MHz)  $\delta$  170.0, 150.3, 144.2, 137.3, 128.9, 128.8, 128.7, 128.5, 126.6, 124.6, 63.9, 49.8, 26.6, 24.8, 21.4; **HRMS** (+APCI) calculated for  $\text{C}_{19}\text{H}_{20}\text{N}_2\text{O}_6\text{S} - [\text{C}_2\text{H}_3\text{O}_2]$  345.0909, found 345.0898 [ $\text{M-OAc}]^+$ .

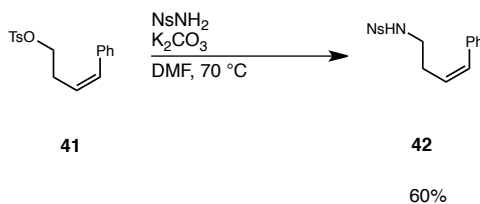
**2-Methyl-1-(4-nitrophenylsulfonyl)piperidin-3-yl acetate (37) and 1-(4-Nitrophenylsulfonyl)pyrrolidin-2-yl)ethyl acetate (38):**



Prepared according to general procedure **A** using (*Z*)-*N*-(hex-4-enyl)-4-nitrobenzenesulfonamide (**35**) (110 mg, 0.4 mmol),  $\text{PhI}(\text{OAc})_2$  (193 mg, 0.6 mmol),  $\text{K}_2\text{CO}_3$  (83 mg, 0.6 mmol) and  $\text{Cu}(\text{CH}_3\text{CN})_4\text{PF}_6$  (15 mg, 0.04 mmol). Purification by flash column chromatography (4:1 to 3:1 Hexanes/EtOAc) afforded 2-methyl-1-(4-nitrophenylsulfonyl)piperidin-3-yl acetate (**37**) (77 mg, 59 %) as an amorphous solid. **IR** (thin film,  $\text{cm}^{-1}$ ) 2954, 1736, 1530, 1350, 1241, 740;  **$^1\text{H}$  NMR** ( $\text{CDCl}_3$ , 600 MHz)  $\delta$  8.36 (d, 2H,  $J = 8.7$  Hz), 8.04 (d, 2H,  $J = 8.7$  Hz), 4.60 (dt, 1H,  $J = 11.9, 5.0$  Hz), 4.45 (qn, 1H,  $J = 6.4$  Hz), 3.76 (dd, 1H,  $J = 13.7, 4.9$  Hz), 3.00 (dt, 1H,  $J = 13.7, 3.2$  Hz), 2.04 (s, 3H), 1.77-1.69 (m, 2H), 1.64-1.57 (m, 2H), 1.42 (qt, 1H,  $J = 13.3, 4.6$  Hz), 1.10 (d, 3H,  $J = 6.8$  Hz);  **$^{13}\text{C}$  NMR** ( $\text{CDCl}_3$ , 150 MHz)  $\delta$  170.1, 150.0, 147.8, 124.9, 70.2, 50.4, 39.8,

24.1, 23.9, 21.1, 10.3; **HRMS** (+APCI) calculated for  $C_{14}H_{18}N_2O_6S$  342.0886, found 344.1033  $[M+H]^+$ , 1-(4-nitrophenylsulfonyl)pyrrolidin-2-yl)ethyl acetate (**38**) (47 mg, 36 %) as a crystalline solid. **IR** (thin film,  $cm^{-1}$ ) 3106, 2981, 1734, 1528, 1350, 1239, 1162;  **$^1H$  NMR** ( $CDCl_3$ , 600 MHz)  $\delta$  8.39 (d, 2H,  $J = 8.6$  Hz), 8.07 (d, 2H,  $J = 9.0$  Hz), 5.21 (qn, 1H,  $J = 6.4$  Hz), 3.80 (dq, 1H,  $J = 4.1, 0.9$  Hz), 3.49 (dt, 1H,  $J = 11.0, 5.9$  Hz), 3.29 (dt, 1H,  $J = 11, 6.4$  Hz), 2.07 (s, 3H), 1.88-1.79 (m, 2H), 1.63-1.50 (m, 4H), 1.28 (d, 3H,  $J = 6.7$  Hz);  **$^{13}C$  NMR** ( $CDCl_3$ , 150 MHz)  $\delta$  170.6, 150.4, 143.4, 129.1, 124.6, 71.4, 61.9, 49.9, 27.1, 24.6, 21.5, 15.3; **HRMS** (+APCI) calculated for  $C_{14}H_{18}N_2O_6S$  342.0886, found 344.1056  $[M+H]^+$ .

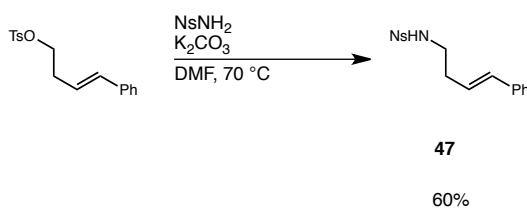
**(Z)-4-nitro-N-(5-phenylpent-4-enyl)benzenesulfonamide (42):**



To a solution of (Z)-5-phenylpent-4-en-1-yl-4-methylbenzenesulfonate (750 mg, 2.4 mmol) (**41**) in DMF (0.3M) was added  $K_2CO_3$  (983 mg, 7.1 mmol) and 4-nitrobenzenesulfonamide (1.4 g, 7.1 mmol) at room temperature at room temperature. The yellow slurry obtained was heated to 70 °C until it was judged to be complete by TLC. After this time, it was cooled to room temperature and quenched with  $H_2O$  (15 mL). The biphasic mixture was then extracted twice with ethyl acetate (2 x 50 mL). The collected organic phases were then washed with 2N HCl (5 mL), water (3 x 5 mL), brine (5 mL) and dried over solid  $NaSO_4$ . Removal of solvents yielded a crude product which was purified by column chromatography on silica gel to afford (Z)-4-nitro-N-(5-phenylpent-4-

enyl)benzenesulfonamide (**42**) as a yellow solid (530 mg, 65 %); **Mp** 67.8-68.5 °C; **IR** (thin film,  $\text{cm}^{-1}$ ) 3249, 3104, 3083, 2949, 1545, 1530, 1433, 1346, 1332, 1306, 1150, 1088, 1071, 854, 735, 680, 614;  **$^1\text{H NMR}$**  ( $\text{CDCl}_3$ , 600 MHz) 8.29-8.28 (m, 2H), 7.96-7.95 (m, 2H), 7.33-7.30 (m, 2H), 7.22-7.21(m, 1H), 7.17-7.18 (m, 2H), 6.43 (d, 1H,  $J = 11.5$  Hz), 5.54-5.50 (m, 1H), 4.67 (t, 1H,  $J = 6.0$  Hz), 3.02 (dt, 2H,  $J = 6.9, 6.4$  Hz), 2.32-2.28 (m, 2H), 1.63-1.59 (m, 2H);  **$^{13}\text{C NMR}$**  ( $\text{CDCl}_3$ , 150 MHz)  $\delta$  150.2, 146.1, 137.2, 130.8, 130.6, 128.8, 128.5, 128.4, 127.1, 124.6, 43.1, 29.9, 25.5; **HRMS** (+APCI) calculated for  $\text{C}_{17}\text{H}_{19}\text{N}_2\text{O}_4\text{S}$  347.1066, found 347.1067  $[\text{M}+\text{H}]^+$ .

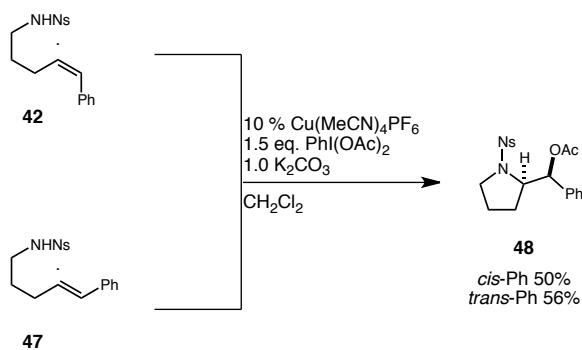
**(E)-4-nitro-N-(5-phenylpent-4-enyl)benzenesulfonamide (47):**



To a solution of (*E*)-6-Methylhept-4-enyl 4-methylbenzenesulfonate (1 g, 3.5 mmol), in DMF (0.3M) was added  $\text{K}_2\text{CO}_3$  (2.15 g, 10.6 mmol) and 4-nitrobenzene-sulfonamide (2.148 g, 10.6 mmol) at room temperature at room temperature. The yellow slurry obtained was heated to 70 °C until it was judged to be complete by TLC. After this time, it was cooled to room temperature and quenched with  $\text{H}_2\text{O}$  (15 mL). The biphasic mixture was then extracted twice with ethyl acetate (2 x 50 mL). The collected organic phases were then washed with 2N HCl (5 mL), water (3 x 5 mL), brine (5 mL) and dried over solid  $\text{NaSO}_4$ . Removal of solvents yielded a crude product, which was purified by column chromatography on silica gel (20 % EtOAc in Hexanes) to produce a yellow solid, which was re-purified by recrystallization from a mixture of  $\text{Et}_2\text{O}$  and Hexanes to

yield a white powder (60 %). **IR** (thin film,  $\text{cm}^{-1}$ ) 3276, 3103, 2958, 2869, 1607, 1531, 1425, 1429, 1346, 1333, 1311, 1159, 1107, 1091, 1073, 972, 852, 737, 682, 611;  **$^1\text{H}$  NMR** ( $\text{CDCl}_3$ , 600 MHz)  $\delta$  8.36 (d, 2H,  $J = 8.7$  Hz), 8.06 (d, 2H,  $J = 8.7$  Hz), 5.33 (dd, 1H,  $J = 15.4, 6.4$  Hz), 5.24-5.18 (m, 1H), 5.05 (t, 1H,  $J = 6.0$  Hz), 2.99 (dt, 2H,  $J = 7.5, 6.9$  Hz), 2.21-2.12 (m, 1H), 1.96 (dt, 2H,  $J = 8.0, 6.9$  Hz), 1.54 (qn, 2H,  $J = 7.3$  Hz), 0.90 (d, 2H,  $J = 6.9$  Hz);  **$^{13}\text{C}$  NMR** ( $\text{CDCl}_3$ , 150 MHz)  $\delta$  150.2, 146.1, 139.5, 128.5, 125.2, 124.6, 43.0, 31.1, 29.5, 22.7; **HRMS** (+ APCI) calculated for  $\text{C}_{14}\text{H}_{21}\text{N}_2\text{O}_4\text{S}$  313.1217, found 313.1218  $[\text{M}+\text{H}]^+$ .

**1-(4-Nitrophenylsulfonyl)pyrrolidin-2-yl)(phenyl)methyl acetate (48):**

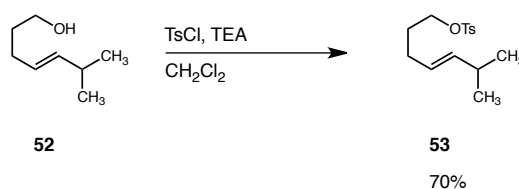


Prepared according to general procedure **A** using (*Z*)-5-phenylpent-4-enyl 4-methylbenzenesulfonate (**42**) or (*E*)-5-phenylpent-4-enyl 4-methylbenzenesulfonate (**47**) (50 mg, 0.14 mmol),  $\text{PhI}(\text{OAc})_2$  (70 mg, 0.22 mmol),  $\text{K}_2\text{CO}_3$  (19 mg, 0.14 mmol) and  $\text{Cu}(\text{CH}_3\text{CN})_4\text{PF}_6$  (5.2 mg, 0.014 mmol). Purification by flash column chromatography on silica get (4:1 to 3:1 Hexanes/EtOAc) afforded 1-(4-nitrophenylsulfonyl)pyrrolidin-2-yl)(phenyl)methyl acetate (**48**) (29 mg, 50 % (from **42**), 10:1 d.r.). **IR** (thin film,  $\text{cm}^{-1}$ ) 3105, 2980, 1741, 1529, 1350, 1232, 1163;  **$^1\text{H}$  NMR** ( $\text{CDCl}_3$ , 600 MHz)  $\delta$  8.35 (d, 2H,  $J$



= 8.6 Hz), 8.0 (d, 2H,  $J = 8.6$ ), 7.38-7.23 (m, 5H), 6.10 (d, 1H,  $J = 2.9$  Hz), 4.21 (dt, 1H,  $J = 8.6, 3.3$  Hz), 3.34-3.25 (m, 2H), 2.15 (s, 3H), 2.01-1.97 (m, 1H), 1.75-1.68 (m, 1H), 1.56-1.51 (m, 2H);  $^{13}\text{C}$  NMR ( $\text{CDCl}_3$ , 150 MHz)  $\delta$  170.0, 150.3, 144.2, 137.3, 128.9, 128.8, 128.7, 128.5, 126.6, 124.6, 63.9, 49.8, 26.6, 24.8, 21.4; HRMS (+APCI) calculated for  $\text{C}_{19}\text{H}_{20}\text{N}_2\text{O}_6\text{S} - [\text{C}_2\text{H}_3\text{O}_2]$  345.0909, found 345.0898  $[\text{M}-\text{OAc}]^+$ .

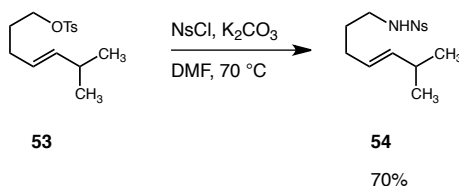
**(E)-6-Methylhept-4-enyl 4-methylbenzenesulfonate (53):**



To a solution of (*E*)-6-methyl-4-hepten-1-ol (1.55 g, 12 mmol) in dichloromethane (0.2 M) was added *p*-toluenesulfonyl chloride (2.54 g, 13 mmol), 4-dimethylaminopyridine (0.3 g, 2.4 mmol) at room temperature. The mixture was then cooled with an ice bath to 0 °C and triethylamine (2.0 mL, 14.5 mmol) was slowly added over the course of 5 minutes. The solution obtained was removed from the ice bath and allowed to reach room temperature. Once the reaction was judged to be complete by TLC (slurry may develop), it was quenched with  $\text{H}_2\text{O}$  (20 mL). The biphasic mixture was then extracted twice with diethyl ether (100 mL). The collected organic phases were then washed with 2N HCl (10 mL) and brine (10 mL) and dried over solid  $\text{NaSO}_4$ . Removal of the solvent yielded a crude product, which via column chromatography on silica gel ((4:1 hexanes/EtOAc,  $R_f = 0.5$ ) to yield (*E*)-6-methyl-4-hept-4-enyl-4-methylbenzenesulfonate (**53**) (2.4 g, 70 %) as a clear oil. IR (thin film,  $\text{cm}^{-1}$ ) 2957, 2869, 1358, 1188, 1174, 968, 946, 921, 813, 662;

$^1\text{H NMR}$  ( $\text{CDCl}_3$ , 400 MHz)  $\delta$  7.78-7.73 (m, 2H), 7.34-7.30 (m, 2H), 5.31-5.25 (m, 1H), 5.20-5.13 (m, 2H), 3.98 (t, 2H,  $J = 6.5$  Hz), 2.41 (s, 1H), 3.74 (t, 2H,  $J = 6.6$  Hz), 2.24 – 2.18 (m, 2H), 1.90 (s, 1H), 1.72 (t, 3H,  $J = 3.2$  Hz);  $^{13}\text{C NMR}$  ( $\text{CDCl}_3$ , 100 MHz)  $\delta$  144.8, 139.3, 133.2, 129.9, 127.9, 124.8, 70.0, 31.0, 28.7, 28.1, 22.6, 21.7; **HRMS** (+APCI)  $\text{C}_{15}\text{H}_{23}\text{O}_3\text{S}$  283.1362, found 283.1363  $[\text{M}+\text{H}]^+$ .

**(*E*)-*N*-(6-methylhept-4-enyl)-4-nitrobenzenesulfonamide (**54**):**

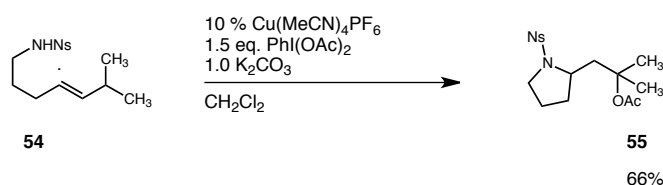


Prepared according to general procedure **A** using (*E*)-6-methyl-4-hept-4-enyl-4-methylbenzenesulfonate (**53**) (1 g, 3.54 mmol),  $\text{K}_2\text{CO}_3$  (2.15 g, 10.62 mmol) and 4-nitrobenzenesulfonamide (2.148 g, 10.62 mmol). Upon concentration of solvents under reduced pressure a crude solid was obtained, which was purified by recrystallization from a mixture of diethyl ether and hexanes to yield (*E*)-*N*-(6-methylhept-4-enyl)-4-nitrobenzenesulfonamide (**54**) (773 mg, 70%) as a white solid. **Mp** 34.9 – 35.5 °C; **IR** (thin film,  $\text{cm}^{-1}$ ) 3276, 3103, 2958, 2869, 1607, 1531, 1425, 1429, 1346, 1333, 1311, 1159, 1107, 1091, 1073, 972, 852, 737, 682, 611.;  $^1\text{H NMR}$  ( $\text{CDCl}_3$ , 600 MHz)  $\delta$  8.36 (d, 2H,  $J = 8.7$  Hz), 8.06 (d, 2H,  $J = 8.7$  Hz), 5.33 (dd, 1H,  $J = 15.4, 6.4$  Hz), 5.24-5.18 (m, 1H), 5.05 (t, 1H,  $J = 6.0$  Hz), 2.99 (dt, 2H,  $J = 7.5, 6.9$  Hz), 2.21-2.12 (m, 1H), 1.96 (dt, 2H,  $J = 8, 6.9$  Hz), 1.54 (qn, 2H,  $J = 7.3$  Hz), 0.90 (d, 2H,  $J = 6.9$  Hz);  $^{13}\text{C NMR}$

(CDCl<sub>3</sub>, 150 MHz)  $\delta$  150.2, 146.1, 139.5, 128.5, 125.2, 124.6, 43.0, 31.1, 29.5, 22.7.;

**HRMS** (+ APCI) calculated for C<sub>14</sub>H<sub>21</sub>N<sub>2</sub>O<sub>4</sub>S 313.1217, found 313.1218 [M-H]<sup>+</sup>.

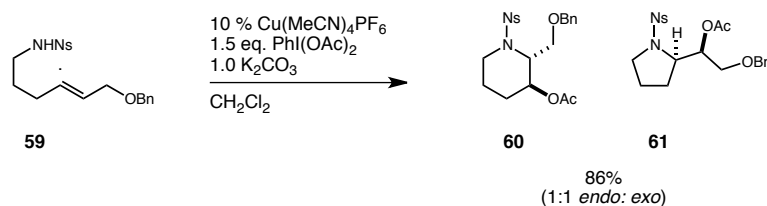
**2-Methyl-1-(1-(4-nitrophenylsulfonyl)pyrrolidin-2-yl)propan-2-yl acetate (55):**



Prepared according to general procedure **A** using (*E*)-*N*-(6-methylhept-4-enyl)-4-nitrobenzenesulfonamide (**54**) (570 mg, 1.8 mmol), PhI(OAc)<sub>2</sub> (882 mg, 2.7 mmol), K<sub>2</sub>CO<sub>3</sub> (252 mg, 1.8 mmol) and Cu(CH<sub>3</sub>CN)<sub>4</sub>PF<sub>6</sub> (92 mg, 0.18 mmol). Purification by flash column chromatography (2:2:1 Hexanes: CH<sub>2</sub>Cl<sub>2</sub>: Diethyl Ether) afforded 2-methyl-1-(1-(4-nitrophenylsulfonyl)pyrrolidin-2-yl)propan-2-yl acetate (**55**) (410 mg, 66%). **IR** (thin film, cm<sup>-1</sup>) 3105, 2980, 2875, 1726, 1531, 1350, 1257, 1163, 1092, 904, 723, 621, 575; **<sup>1</sup>H NMR** (CDCl<sub>3</sub>, 600 MHz)  $\delta$  8.35-8.39 (m, 2H), 8.03-7.99 (m, 2H), 3.81-3.86 (m, 1H), 3.41-3.38 (m, 1H), 3.20-3.15 (m, 1H), 2.25 (dd, 1H, *J* = 14.7, 2.8 Hz), 2.10-2.02 (m, 1H), 1.96 (s, 3H), 1.83-1.80 (m, 1H), 1.76-1.71 (m, 1H), 1.70-1.63 (m, 1H), 1.58-1.52 (m, 4H), 1.51 (s, 3H); **<sup>13</sup>C NMR** (CDCl<sub>3</sub>, 150 MHz)  $\delta$  170.5, 150.2, 143.9, 128.7, 124.6, 81.2, 57.8, 48.7, 47.3, 32.7, 27.3, 25.9, 24.4, 22.7; **HRMS** (+ APCI) calculated for C<sub>16</sub>H<sub>23</sub>N<sub>2</sub>O<sub>6</sub>S 371.1277, found 371.1270 [M+H]<sup>+</sup>.

**2-(Benzyloxymethyl)-1-(4-nitrophenylsulfonyl)piperidin-3-yl acetate (60) and 2-**

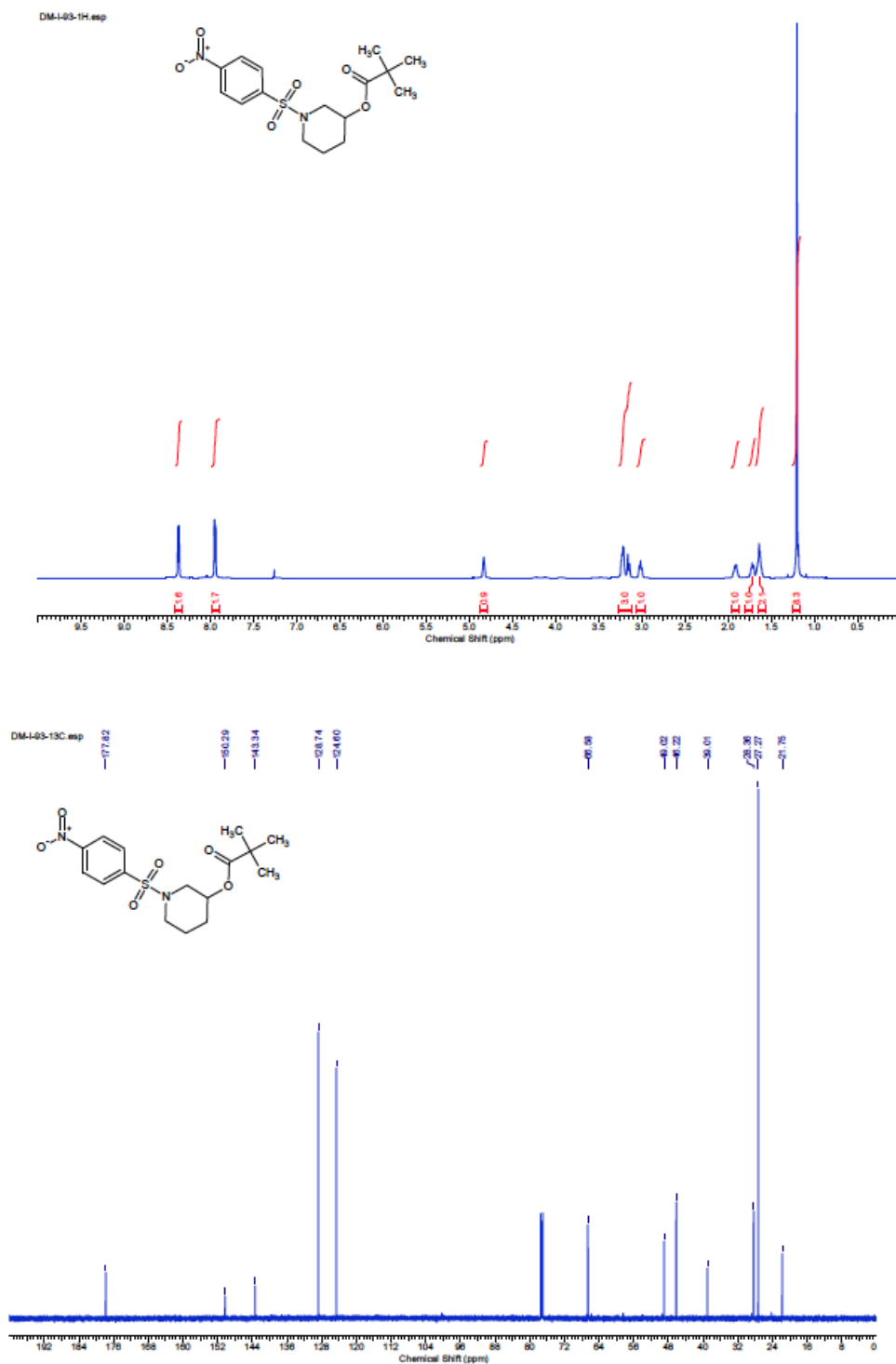
**(Benzyloxy)-1-(1-(4-nitrophenylsulfonyl)pyrrolidin-2-yl)ethyl acetate (61):**

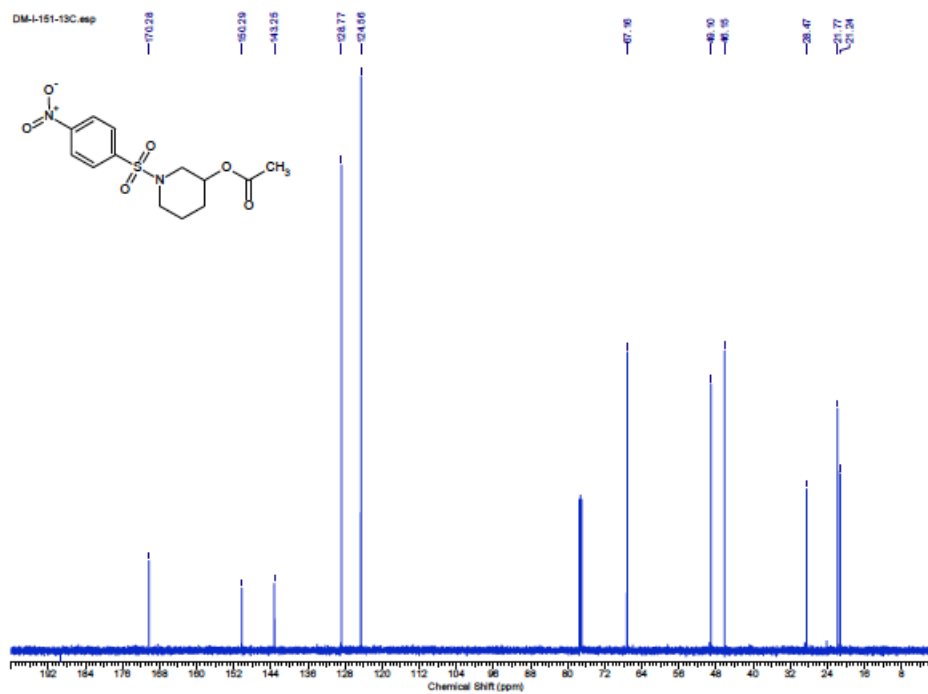
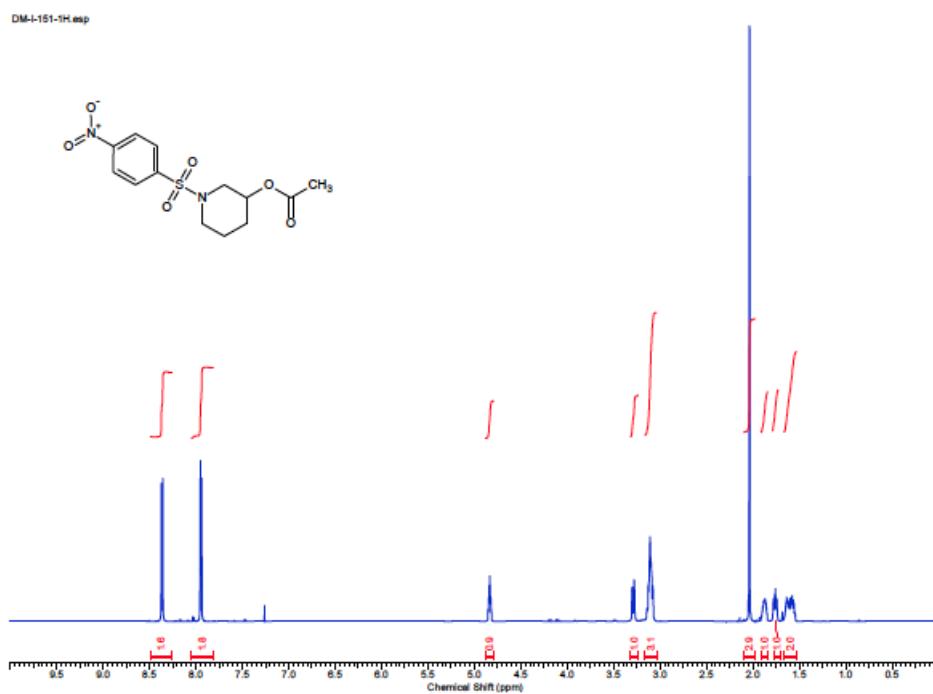


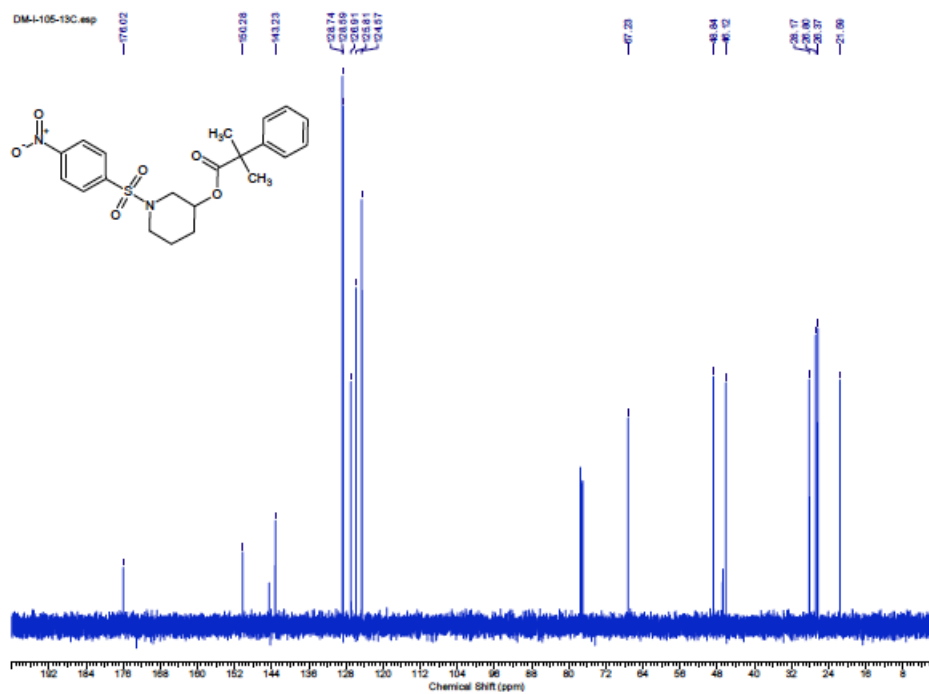
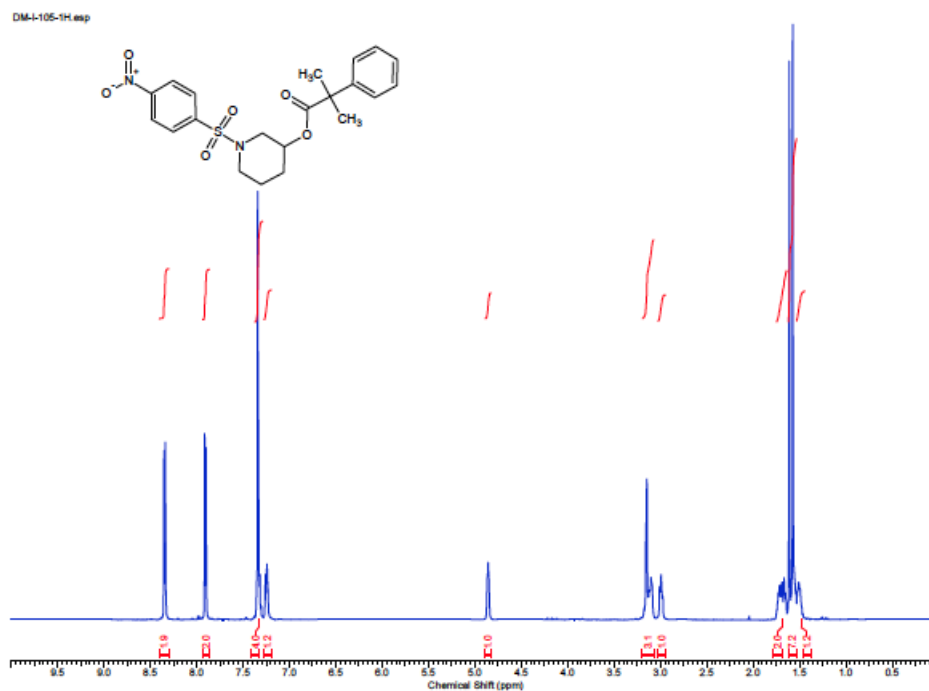
Prepared according to general procedure **A** (*E*)-N-(6-(benzyloxy)hex-4-enyl)-4-nitrobenzenesulfonamide (**59**) (320 mg, 0.82 mmol), PhI(OAc)<sub>2</sub> (396 mg, 1.23 mmol), K<sub>2</sub>CO<sub>3</sub> (113 mg, 0.82 mmol) and Cu(CH<sub>3</sub>CN)<sub>4</sub>PF<sub>6</sub> (41 mg, 0.08 mmol). Flash chromatographic purification (2:2:1 Hexanes: CH<sub>2</sub>Cl<sub>2</sub>: Diethyl Ether eluent) in *aluminum oxide* gel afforded piperidine acetate (**60**) and pyrrolidine acetate (**61**) (310 mg, 86% combined). **IR (piperidine acetate 60)** (thin film, cm<sup>-1</sup>) 3105, 3032, 2955, 2926, 2864, 1734, 1527, 1346, 1309, 1236, 1165, 1055, 1016, 854, 741, 688.; **<sup>1</sup>H NMR (piperidine acetate 60)** (CDCl<sub>3</sub>, 600 MHz) δ 8.12-8.09 (m, 2H), 7.97-7.94 (m, 2H), 7.33-7.29 (m, 3H), 7.17-7.21 (m, 2H), 4.98-4.95 (m, 1H), 4.46-4.36 (m, 3H), 3.78-3.78 (m, 2H), 3.64-3.55 (m, 2H), 3.07 (dt, 1H, *J* = 12.7, 2.9 Hz), 2.01 (s, 3H), 1.88-1.78 (m, 2H), 1.76-1.70 (m, 1H), 1.52-1.46 (m, 1H).; **NMR (piperidine acetate 60)** (C<sub>6</sub>D<sub>6</sub>, 600 MHz) δ 7.55-7.45 (m, 4H), 7.14-7.07 (m, 3H), 7.04-6.99 (m, 2H), 4.85-4.89 (m, 1H), 4.50 (t, 1H, *J* = 6.4 Hz), 4.02 (q, 2H, *J* = 11.4 Hz), 3.54-3.48 (m, 1H), 3.20 (dd, 1H, *J* = 10.0, 7.1 Hz), 3.13 (dd, 1H, *J* = 10.0, 6.2 Hz), 2.56 (dt, 1H, *J* = 13.3, 2.4 Hz), 1.62 (s, 3H), 1.61-1.56 (m, 1H), 1.50-1.43 (mb, 1H), 1.18 (tt, 1H, *J* = 13.8, 3.3 Hz), 0.89-0.75 (m, 1H).; **<sup>13</sup>C NMR (piperidine acetate 60)** (CDCl<sub>3</sub>, 150 MHz) δ 170.5, 149.8, 147.4, 137.4, 128.7, 128.5, 128.3, 128.0, 124.1, 73.5, 67.7, 67.2, 55.8, 41.4, 24.4, 21.4, 19.8.; **HRMS(piperidine acetate 60)** (+ APCI) calculated for C<sub>21</sub>H<sub>25</sub>N<sub>2</sub>O<sub>7</sub>S 449.13770, found 449.13692 [M+H]<sup>+</sup>. **IR (pyrrolidine acetate 61)** (thin film, cm<sup>-1</sup>) 3104, 2870, 1739, 1528, 1456, 1348, 1308, 1231, 1162, 1089, 1028, 855, 734, 699, 687, 610, 678.; **<sup>1</sup>H NMR (pyrrolidine acetate**

**61** (CDCl<sub>3</sub>, 600 MHz)  $\delta$  8.33-8.28 (m, 2H), 8.01-7.96 (m, 2H), 7.40-7.29 (m, 5H), 5.41-5.37 (m, 1H), 4.60 (d, 1H,  $J = 11.7$  Hz), 4.53 (d, 1H,  $J = 11.7$  Hz), 4.04-4.06 (m, 1H), 3.68 (dd, 1H,  $J = 10.5, 5.5$  Hz), 3.58 (dd, 1H,  $J = 10.5, 5.5$  Hz), 3.38-3.33 (m, 1H), 3.29-3.24 (m, 1H), 2.05 (s, 3H), 1.98-1.84 (m, 2H), 1.61-1.53 (m, 2H); <sup>13</sup>C NMR (**pyrrolidine acetate 61**) (CDCl<sub>3</sub>, 150 MHz)  $\delta$  170.2, 150.3, 143.6, 138.0, 129.0, 128.7, 128.0, 127.9, 124.5, 73.4, 73.1, 68.9, 60.1, 49.6, 26.8, 24.8, 21.3.; HRMS(**pyrrolidine acetate 61**) (+ APCI) calculated for C<sub>17</sub>H<sub>17</sub>N<sub>2</sub>O<sub>6</sub>S 449.1377, found 449.1370 [M+H]<sup>+</sup>.

### 9.3 NMR Spectra-Part 1











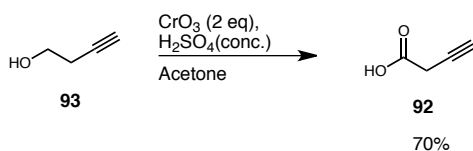






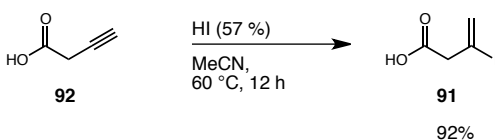
## 9.4 Part 2: Efforts Towards the Development of an Enantioselective Intermolecular Cascade Reaction to Access the Core of the Banyaside Peptides.

### But-3-enoic acid (**92**):



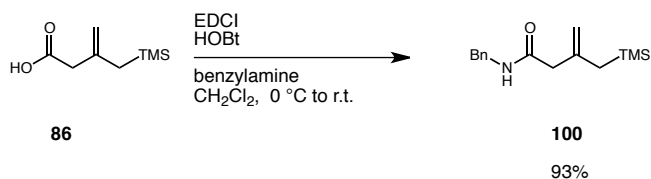
Concentrated H<sub>2</sub>SO<sub>4</sub> (96 mL) was carefully added to 1 L round bottom flask containing (360 mL) of H<sub>2</sub>O at 0 °C. CrO<sub>3</sub> (13.9 g) was then added as a solid in three equal portions to obtain a clear red solution. The ice bath was replaced and a solution of homopropargylic alcohol (5 g 0.071 mol) in acetone (70 mL) was added over a period 1 h via an addition funnel. The reaction mixture was then aged at 0 °C for a period of 4 hours. After this time, the solution was transferred to a 2L separatory funnel and extracted with diethyl ether (3 x 300 mL). The collected organic layers were washed with water (2 x 150 mL) and brine (150 mL). The volatiles were then removed under reduced pressure to yield but-3-enoic acid (**92**) (4.2 g, 52 %) as a white amorphous solid.

### 3-Iodobut-3-enoic acid (**91**):



To solution of but-3ynoic acid (**92**) (2.9 g, 34.5 mmol) in CH<sub>3</sub>CN (5.0 mL) was added HI (5.68 mL, 37.9 mmol). The resulting solution was heated to 60 °C for 10 h. After this time, the reaction was cooled to 0 °C and the pH was slowly adjusted with a sat. solution of NaHCO<sub>3</sub> to 4-5. The biphasic mixture was extracted with ether (2 x 50 mL). The combined organic layers were washed with 10% NaS<sub>2</sub>O<sub>3</sub> (20 mL), brine (20 mL), dried under Na<sub>2</sub>SO<sub>4</sub> and the solvent was then removed under reduced pressure. Flash chromatographic purification (20% EtOAc in Petrol Ether) afforded 3-Iodobut-3-enoic acid (**91**) (6.95 g, 92% yield). NMR data for this compound matched the previously reported NMR data.<sup>11</sup>

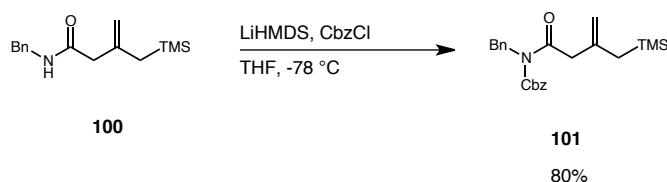
#### Synthesis of *N*-Cbz amide **100**:



To a solution of HOBT·H<sub>2</sub>O (0.424 g, 3.14 mmol) in CH<sub>2</sub>Cl<sub>2</sub> (31 mL) was added benzylamine (0.336 g, 3.14 mmol). The resulting mixture was stirred at r.t. for 5 minutes and then cooled to 0 °C. Carboxylic acid **86** (0.514 g, 2.99 mmol) was added dropwise, followed by dropwise addition of EDCI (0.551 mL, 3.14 mmol) over 10 minutes. The reaction was stirred at 0 °C for 1 h, warmed to r.t. and stirred for 24 h. Et<sub>2</sub>O (70 mL) was added, and the reaction was stirred for 15 minutes. The mixture was washed with 0.1 M aqueous HCl (2 x 20 mL), saturated aqueous NaHCO<sub>3</sub> (2 x 20 mL), and brine (20 mL). The organic layer was dried over anhydrous MgSO<sub>4</sub>, and concentrated *in vacuo*.

Purification by chromatography on silica gel (4:1 → 7:3 hexanes/EtOAc) afforded *N*-Cbz amide **100** as a clear oil (0.725 g, 93%);  $R_f$  0.46 (4:1 hexanes/EtOAc);  $^1\text{H NMR}$  ( $\text{CDCl}_3$ , 600 MHz)  $\delta$  7.34-7.25 (m, 5H), 6.26 (bs, 1H), 4.80 (s, 1H), 4.77 (s, 1H), 4.44 (d,  $J = 5.8$  Hz, 2H), 2.97 (s, 2H), 1.60 (s, 2H), 0.04 (s, 9H);  $^{13}\text{C NMR}$  ( $\text{CDCl}_3$ , 151 MHz)  $\delta$  170.41, 142.45, 138.46, 128.81, 127.74, 127.57, 112.91, 47.04, 43.68, 26.88, -1.34; **IR** (thin film,  $\text{cm}^{-1}$ ); 3290.4, 3065.5, 2952.7, 1645.2, 1543.5 1246.6, 837.0, 727.3, 694.7; **HRMS** (+ESI) calculated for  $\text{C}_{15}\text{H}_{24}\text{N}_1\text{O}_1\text{Si}$  262.1622, found 262.1620  $[\text{M}+\text{H}]^+$ .

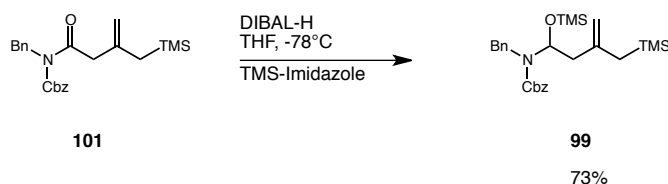
### Synthesis of *N,N*-Bn, Cbz Amide **101**:



A solution of amide **100** (0.200 g, 0.76 mmol) in THF (3.0 mL) was cooled to  $-78$  °C. A freshly prepared LiHMDS solution (0.33 M in THF, 2.3 mL, 0.75 mmol) was cooled to  $-78$  °C and added to the starting material solution *via* cannula. The reaction was stirred for 2 h at  $-78$  °C. Benzyl chloroformate (0.13 mL, 0.92 mmol) was added and the mixture was stirred for 12 h for  $-78$  °C. The reaction was quenched with saturated aqueous  $\text{NH}_4\text{Cl}$  (3.0 mL) and warmed to  $0$  °C.  $\text{H}_2\text{O}$  (3 mL) was added and the mixture was stirred for 5 minutes. The organic layer was separated, and the aqueous layer was extracted with  $\text{Et}_2\text{O}$  (2 x 25 mL). The organic extracts were combined, washed with brine (12 mL), dried over anhydrous  $\text{MgSO}_4$ , and concentrated *in vacuo*. Purification by chromatography on silica gel (9:1 hexanes/EtOAc) afforded *N,N*-Bn, Cbz amide **101** as a colorless oil (0.244 g,

80%);  $R_f$  0.7 (9:1 hexanes/EtOAc);  $^1\text{H NMR}$  ( $\text{CDCl}_3$ , 600 MHz)  $\delta$  7.36-7.31 (m, 4H), 7.26-7.20 (m, 6H), 5.17 (s, 2H), 4.94 (s, 2H), 4.69 (s, 1H), 4.63 (d,  $J = 1.2$  Hz, 1H), 3.62 (s, 2H), 1.57 (s, 2H), 0.01 (s, 6H);  $^{13}\text{C NMR}$  ( $\text{CDCl}_3$ , 151 MHz)  $\delta$  173.88, 154.38, 137.80, 135.01, 128.58, 128.20, 127.99, 127.60, 127.47, 126.98, 116.55, 111.27, 68.88, 47.50, 47.24, 27.43, -1.19; **IR** (thin film,  $\text{cm}^{-1}$ ) 3033.3, 2953.3, 1731.4, 1697.7, 1386.0, 1350.6, 1204.3, 1169.0, 838.2, 694.9; **HRMS** (+pACI) calculated for  $\text{C}_{23}\text{H}_{30}\text{N}_1\text{O}_3\text{Si}$  396.2005, found 396.1997  $[\text{M}+\text{H}]^+$ .

### Synthesis of *N*-Cbz-*O*-TMS-aminol **99**:

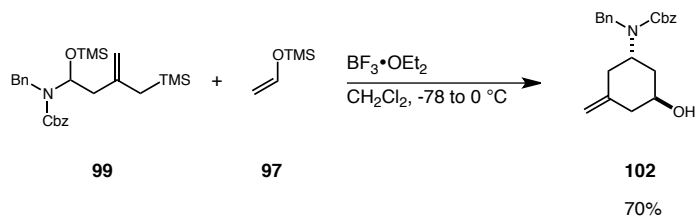


A solution of *N*-Cbz-amide **101** (1.5 g, 3.8 mmol) in  $\text{CH}_2\text{Cl}_2$  (44 mL) was cooled to  $-78$  °C. DIBAL-H (1.0 M in  $\text{CH}_2\text{Cl}_2$ , 7.6 mL, 7.79 mmol) was added dropwise over 15 minutes. The reaction mixture was stirred for 1 h, then trimethylsilyl imidazole (1.7 mL, 11.4 mmol) was added dropwise, followed by a solution of imidazole (0.258 mg, 3.8 mmol) in  $\text{CH}_2\text{Cl}_2$  (44 mL). The mixture was warmed to  $-15$  °C and stirred for 20 hours. The mixture was warmed to  $0$  °C and stirred for 2 hours. The reaction was quenched by slow addition of aqueous 15% Rochelle's salt solution (30 mL). The biphasic mixture was transferred to a 25 mL Erlenmeyer flask, and  $\text{Et}_2\text{O}$  (80 mL) was added. The mixture was stirred vigorously at r.t. until both layers were clear. The organic layer was separated, and the aqueous layer was extracted with  $\text{Et}_2\text{O}$  (2 x 40 mL). The organic extracts were



combined, washed with brine (20 mL), dried over anhydrous MgSO<sub>4</sub>, and concentrated *in vacuo*. Purification by chromatography on silica gel (20:1 → 4:1 Hexanes/EtOAc, silica gel deactivated with 1% Et<sub>3</sub>N) afforded *N*-Cbz-*O*-TMS-aminol **99** as a colorless oil (1.24 g, 73%); *R<sub>f</sub>* 0.40 (4:1 hexanes/EtOAc); <sup>1</sup>H NMR (DMSO<sub>3</sub>, 68 °C, 600 MHz) δ 7.38 – 7.16 (m, 10H), 5.88 (bs, 1H), 5.23 – 5.01 (m, 2H), 4.55 (m, 2H), 4.48 – 4.35 (m, 2H), 2.18 (m, 2H), 1.45 (m, 2H), 0.05 to -0.01 (m, 18H) ; <sup>13</sup>C NMR (DMSO, 68 °C, 151 MHz) δ 154.63, 142.37, 139.11, 136.19, 127.73, 127.46, 126.30, 109.84, 78.93, 66.30, 44.32, 43.99, 26.42, -0.65, -1.74; IR (thin film, cm<sup>-1</sup>) 3032.3, 2954.2, 1700.6, 1412.3, 1248.6, 1069.4, 1028.0, 836.6, 695.0; HRMS (+pESI) calculated for C<sub>26</sub>H<sub>39</sub> N<sub>1</sub>NaO<sub>3</sub>Si<sub>2</sub> 492.2366, found 492.2334 [M+Na]<sup>+</sup>.

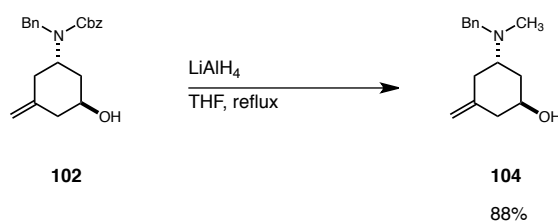
### Synthesis of *N*-Cbz cyclohexanol **102**:



A solution of *N*-Cbz-*O*-TMS-aminol **99** (0.160 g, 0.34 mmol) in CH<sub>2</sub>Cl<sub>2</sub> (10.0 mL) was cooled to -78 °C. Vinoloxysilane **97** (0.05 mL, 0.37 mmol) was added, followed by addition of BF<sub>3</sub>•OEt<sub>2</sub> (0.01 mL, 1.02 mmol) over 5 minutes. The reaction was stirred for 30 minutes at -78 °C. The mixture was warmed up to 0 °C and allowed to stir for 1 hour. The reaction was quenched with saturated aqueous NaHCO<sub>3</sub> (5.0 mL). The organic layer was separated, and the aqueous layer was extracted with CH<sub>2</sub>Cl<sub>2</sub> (2 x 10 mL). The organic extracts were combined, washed with brine (12 mL), dried over anhydrous

MgSO<sub>4</sub>, and concentrated *in vacuo*. Purification by chromatography on silica gel (9:1 hexanes/EtOAc) afforded *N*-Cbz cyclohexanol **102** as a colorless oil (0.084 g, 70%); **R<sub>f</sub>** 0.4 (1:1 hexanes/EtOAc); **<sup>1</sup>H NMR** (DMSO<sub>3</sub>, 68 °C, 600 MHz) 7.38-7.14 (m, 10 H), 5.14 (d, *J* = 13.0 Hz, 1H), 5.10 (d, *J* = 13.0 Hz, 1H), 4.67 (s, 1H), 4.50 (d, *J* = 15.6 Hz, 1H), 4.44 (d, *J* = 15.6 Hz, 1H), 4.35-4.27 (m, 1H), 4.25 (s, 1H), 4.01 (dd, *J* = 6.0, 3.0 Hz, 1H), 2.27-2.20 (m, 2H), 2.16 (d, *J* = 13.7 Hz, 1H), 2.06 (d, *J* = 13.7 Hz, 1H), 1.77 (dt, *J* = 12.5, 3.0 Hz, 1H), 1.70-1.63 (m, 1H); **<sup>13</sup>C NMR** (DMSO<sub>3</sub>, 68 °C, 151 MHz) δ 143.46, 139.37, 127.91, 127.80, 127.29, 127.01, 126.33, 126.21, 110.62, 65.92, 64.69, 51.50, 46.44, 40.26, 38.77, 36.18; **IR** (thin film, cm<sup>-1</sup>) 3446.1, 3065.1, 2924.2, 2853.7, 1685.9, 1452.9, 1416.4, 1242.6, 116.0, 1086.3, 697.3; **HRMS** (+pESI) calculated for C<sub>22</sub>H<sub>25</sub>N<sub>1</sub>Na<sub>1</sub>O<sub>3</sub> 374.1726, found 374.1723 [M+Na]<sup>+</sup>

#### Synthesis *N*-Methylcyclohexanol **104**:



To a solution of *N*-Cbz cyclohexanol **102** (0.042 g, 0.12 mmol) in THF (6.0 mL) was added LiAlH<sub>4</sub> (1M in THF, 0.6 mL, 0.60 mmol) at room temperature. The mixture was heated to reflux, aged for 2 hours and then allowed to cool down to room temperature. The mixture was slowly added to a 15% Rochelle's salt solution (10 mL) at 0 °C. Et<sub>2</sub>O (30 mL) was added and the biphasic mixture was stirred vigorously at r.t. until both layers were clear. The organic layer was separated, and the aqueous layer was extracted

*Experimental-Part 2 Efforts Towards the Development of an Enantioselective Intermolecular 166 Cascade Reaction to Access the Core of the Banyaside Alkaloids.*

with Et<sub>2</sub>O (2 x 20 mL). The organic extracts were combined, washed with brine (20 mL), dried over anhydrous MgSO<sub>4</sub>, and concentrated *in vacuo*. Purification by chromatography on silica gel (3:7 → 1:9 hexanes/EtOAc) afforded *N*-Methylcyclohexanol **104** as a colorless oil (0.024 g, 88%); *R<sub>f</sub>* 0.4 (1:9 hexanes/EtOAc); <sup>1</sup>H NMR (CDCl<sub>3</sub>, 600 MHz) δ 7.37-7.27 (m, 4H), 7.26-7.19 (m, 1H), 4.89 (s, 1H), 4.83 (s, 1H), 4.29-4.21 (m, 1H), 3.61 (d, *J* = 13.4 Hz, 1H), 3.58 (d, *J* = 13.4 Hz, 1H), 2.97 (dt, *J* = 11.7 Hz, 3.9 Hz 1H), 2.53 (d, *J* = 12.5 Hz, 1H), 2.31 (bs, 2H), 2.19 (s, 3H), 2.12 (t, *J* = 12.3 Hz, 1H), 2.08-1.99 (m, 1H), 1.71-1.55 (m, 2H); <sup>13</sup>C NMR (CDCl<sub>3</sub>, 151 MHz) δ 143.98, 128.94, 128.57, 128.47, 127.08, 112.70, 67.27, 58.55, 58.20, 42.38, 37.59, 37.20, 35.37; IR (thin film, cm<sup>-1</sup>) 3355.1, 3050.7, 2925.4, 2849.4, 1455.6, 1045.7; HRMS (+pACI) calculated for C<sub>15</sub>H<sub>22</sub>N<sub>1</sub>O<sub>1</sub> 232.1696, found 232.1695 [M+H]<sup>+</sup>

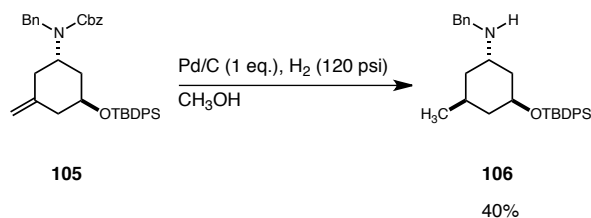
**Synthesis of *N*-Cbz-*O*-TBDPS-cyclohexane **105**:**



To a solution of *N*-Cbz cyclohexenol **102** (0.050 g, 0.14 mmol) in DMF (0.7 mL) was added AgNO<sub>3</sub> (0.072g, 0.43 mmol) followed by TBDPSCl (0.047 mL, 0.18 mmol). The mixture was aged for 2 hours at room temperature. Water (4 mL) and Et<sub>2</sub>O (40 mL) were then added. The organic layer was separated, washed with water (3x 5 mL) and brine (10 mL). The organic layer was dried over anhydrous MgSO<sub>4</sub>, and concentrated *in vacuo*. Purification by chromatography on silica gel (9:1 hexanes/EtOAc) afforded *N*-Cbz-*O*-

TBDPS-cyclohexane **105** as a colorless oil (0.049 g, 60%); **R<sub>f</sub>** 0.35 (9:1 hexanes/EtOAc); **<sup>1</sup>H NMR** (CDCl<sub>3</sub>, 600 MHz) δ 7.63 (d, *J* = 7.7 Hz, 2H), 7.58 (d, *J* = 7.0 Hz, 2H), 7.40 (t, *J* = 7.4 Hz, 2H), 7.36-7.28 (m, 7H), 7.26-7.17 (m, 7H), 5.15 (bs, 2H), 4.78 (s, 1H), 4.66 (s, 1H), 4.53-4.40 (m, 2H), 4.39-4.27 (m, 1H), 4.15 (s, 1H), 2.37 (d, *J* = 9.3 Hz, 1H), 2.10 (d, *J* = 12.7 Hz, 1H), 1.99-1.81 (m, 2H), 1.75 (d, *J* = 10.4 Hz, 1H), 1.48 (s, 1H), 1.02 (s, 9H).; **<sup>13</sup>C NMR** (CDCl<sub>3</sub>, 52 °C, 151 MHz) δ 143.45, 137.18, 136.14, 136.04, 134.52, 129.82, 128.63, 128.10, 128.06, 127.78, 127.73, 127.43, 127.19, 112.04, 68.58, 41.36, 27.25, 19.53, 6.50; **IR** (thin film, cm<sup>-1</sup>) 3069.8, 2931.3, 2891.8, 2856.1, 1698.6, 1453.3, 1240.6, 1111.4, 1089.4, 700.5; **HRMS** (+pACI) calculated for C<sub>38</sub>H<sub>44</sub>N<sub>1</sub>NaO<sub>3</sub>Si 590.3085, found 590.3079 [M+H]<sup>+</sup>

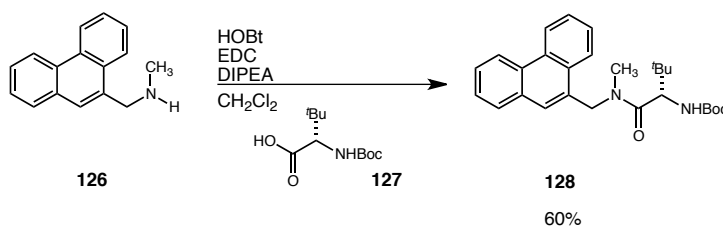
### Synthesis of *O*-TBDPS-cyclohexane **106**:



Palladium on carbon (5 wt%, 0.036g, 0.017 mmole) was added to a solution of *N*-Cbz-*O*-TBDPS-cyclohexane **105** (0.050 g, 0.14 mmol) in EtOH (2 mL). The heterogeneous mixture was aged for 3 hours under hydrogen atmosphere (1 atm). The heterogeneous mixture was filtered through celite and the filter cake was washed with EtOH (6 mL). The clear solution obtained was concentrated *in vacuo*. Purification by chromatography on silica gel (4:1 hexanes/EtOAc) afforded *O*-TBDPS-cyclohexane **106** as a colorless oil (0.026 g, 40%); **R<sub>f</sub>** 0.35 (4:1 hexanes/EtOAc); **<sup>1</sup>H NMR** (CDCl<sub>3</sub>, 600 MHz) δ 7.74-7.64

(m, 4H), 7.42-7.30 (m, 6H), 7.29-7.23 (m, 2H), 7.20 (t,  $J = 7.3$  Hz, 1H), 7.09 (d,  $J = 7.2$  Hz, 2H), 4.05 (dt,  $J = 11.4, 4.5$  Hz, 1H), 3.44-3.29 (m, 2H), 2.92 (t,  $J = 3.6$  Hz, 1H), 1.95 (d,  $J = 12.5$  Hz, 1H), 1.79 (d,  $J = 13.5$  Hz, 1H), 1.76 -1.68 (m, 1H), 1.51 (d,  $J = 13.5$  Hz, 1H), 1.43 (s, 1H), 1.30 (dq,  $J = 11.0, 3.4$  Hz, 2H), 1.26 (s, 2H), 1.06 (s, 9H), 0.86 (d,  $J = 7.0$  Hz, 3H);  $^{13}\text{C}$  NMR (CDCl<sub>3</sub>, 52 °C, 151 MHz)  $\delta$ ; IR (thin film, cm<sup>-1</sup>); HRMS (+pACI) calculated for C<sub>38</sub>H<sub>44</sub>N<sub>1</sub>NaO<sub>3</sub>Si 590.3085, found 590.3079 [M+H]<sup>+</sup>

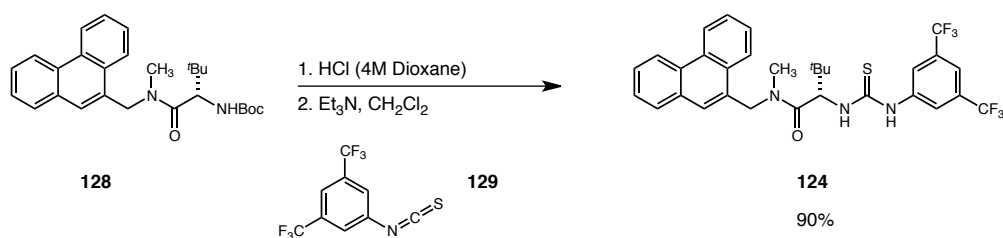
### Synthesis of Carbamate 128:



To a solution of *N*-methyl-anthracene<sup>2</sup> **126** (0.600 g, 2.71 mmol) in CH<sub>2</sub>Cl<sub>2</sub> (27 mL) at 0 °C, was added DIPEA (0.644 mL, 3.69 mmol) followed by HOBT·H<sub>2</sub>O (0.366 g, 2.71 mmol), EDC (0.488 g, 2.17 mmol) and *N*- Boc-*L*-*tert*-leucine **127** (0.570 g, 2.46 mmol). The reaction stirred at room temperature for 18 h. Et<sub>2</sub>O (70 mL) was added, and the reaction was stirred for 15 minutes. The mixture was washed with 0.1 M aqueous HCl (2 x 20 mL), saturated aqueous NaHCO<sub>3</sub> (2 x 20 mL), and brine (20 mL). The organic layer was dried over anhydrous MgSO<sub>4</sub>, and concentrated *in vacuo*. Purification by chromatography on silica gel (9:1 → 4:1 hexanes/EtOAc) afforded carbamate **128** as an amorphous solid (0.700 g, 60%);  $R_f$  0.46 (4:1 hexanes/EtOAc);  $^1\text{H}$  NMR (CDCl<sub>3</sub>, 400 MHz)  $\delta$  8.73 (d,  $J = 7.6$  Hz, 1H), 8.66 (d,  $J = 7.6$  Hz, 1H), 8.13 (d,  $J = 8.1$  Hz, 1H), 7.84 (d,  $J = 7.8$  Hz, 1H), 7.71- 7.52 (m, 5H), 5.52 (d,  $J = 15.0$  Hz, 1H), 5.49-5.42 (m, 1H) ,

4.76 (d,  $J = 15.0$  Hz, 1H), 4.61 (d,  $J = 9.8$  Hz, 1H), 3.02 (s, 3H), 1.47 (s, 9H), 1.01 (s, 9H);  $^{13}\text{C}$  NMR ( $\text{CDCl}_3$ , 101 MHz)  $\delta$  172.25, 156.00, 131.38, 130.91, 130.83, 130.64, 130.52, 128.62, 128.48, 127.20, 127.14, 127.07, 126.96, 124.99, 123.28, 122.71, 79.69, 56.67, 49.64, 35.94, 28.59, 26.67; IR (thin film,  $\text{cm}^{-1}$ ); 2967.4, 1701.4, 1634.6, 1495.6, 1165.9, 1054.9, 906.7, 723.2; HRMS (+APCI) calculated for  $\text{C}_{27}\text{H}_{35}\text{N}_2\text{O}_3$  435.2642, found 435.2641  $[\text{M}+\text{H}]^+$ .

### Synthesis of Thiourea catalyst **124**:

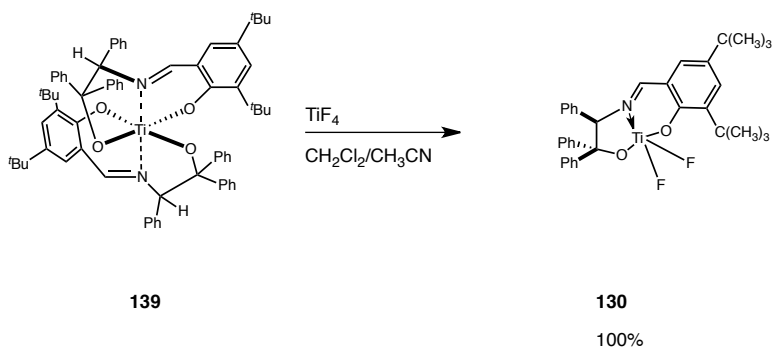


To a flask containing carbamate **128** (0.400 g, 0.92 mmol) was added HCl (4.0M, dioxane, 1.5 mL, 5.98 mmol). The reaction was stirred at room temperature for 2 hours, after which time, the HCl/dioxane mixture was removed *in vacuo*.  $\text{CH}_2\text{Cl}_2$  (20 mL) was then added to the solid residue obtained followed by  $\text{Et}_3\text{N}$  (0.38 mL, 2.76 mmol) and phenyl isothiocyanate **129** (0.24 mL, 1.01 mmol). The new mixture was stirred at room temperature for 4 h, after which time, it was concentrated *in vacuo*. Purification by chromatography on silica gel (9:1  $\rightarrow$  5:1 hexanes/ $\text{EtOAc}$ ) afforded thiourea catalyst **124** as an amorphous solid (0.501 g, 90%);  $R_f$  0.30 (4:1 hexanes/ $\text{EtOAc}$ );  $^1\text{H}$  NMR ( $\text{CDCl}_3$ , 600 MHz)  $\delta$  9.24 (bs, 1H), 8.72 (d,  $J = 8.3$  Hz, 1H), 8.64 (d,  $J = 8.3$  Hz, 1H), 8.11-8.05 (m, 2H), 7.88 (s, 2H), 7.81 (d,  $J = 7.7$  Hz, 1H), 7.61 (dd,  $J = 7.9, 7.2$  Hz, 2H), 7.62 (s, 1H), 7.58 (q,  $J = 7.2$  Hz, 2H), 7.50 (s, 1H), 5.77 (d,  $J = 14.7$  Hz, 1H), 5.72 (d,  $J = 9.2$  Hz,

*Experimental-Part 2 Efforts Towards the Development of an Enantioselective Intermolecular 170 Cascade Reaction to Access the Core of the Banyaside Alkaloids.*

$^1\text{H}$ , 4.50 (d,  $J = 14.7$  Hz, 1H), 3.29 (s, 3H), 1.16 (s, 9H).;  $^{13}\text{C}$  NMR ( $\text{CDCl}_3$ , 151 MHz)  $\delta$ 181.82, 173.85, 140.05, 131.99, 131.77, 131.26, 131.02, 130.57, 130.17, 129.40, 128.76, 128.60, 127.33, 127.17, 127.05, 124.45, 124.12, 123.83, 123.58, 122.70, 122.31, 118.50, 61.88, 50.39, 36.44, 36.17, 27.43; IR (thin film,  $\text{cm}^{-1}$ ) 3322.9, 2969.4, 1606.9, 1581.2, 1535.6, 1473.4, 1385.8, 1274.6, 1178.5, 1131.4, 962.6, 749.7, 730.5; HRMS (+APCI) calculated for  $\text{C}_{31}\text{H}_{30}\text{F}_6\text{N}_3\text{O}_1\text{S}_1$  606.2022, found 606.2035  $[\text{M}+\text{H}]^+$ .

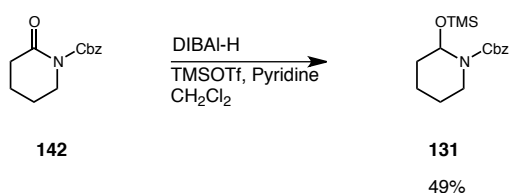
**Synthesis of Imine-alkoxytitanium catalyst **130**:**



An oven dried 10 mL flask, equipped with a stirring bar and connected to an argon/vacuum line was charged with titanium-complex<sup>3</sup> **139** (0.068 mg, 0.06 mmol). The flask was evacuated and subsequently filled with argon. The starting material was then dissolved in  $\text{CH}_2\text{Cl}_2$  (3 mL). In a second flask, titanium tetrafluoride (9 mg, 0.07 mmol) was dissolved in  $\text{CH}_3\text{CN}$  (1 mL) under argon and added via cannula to the flask containing titanium-complex **25**. The mixture was stirred overnight at room temperature. After removal of the solvent *in vacuo* imine-alkoxytitanium catalyst **130** was obtained as a yellow solid. (0.075 g, 100%);  $^1\text{H}$  NMR ( $\text{CD}_3\text{CN}$ , 600 MHz)  $\delta$  8.86 (s, 1H), 7.68 (d,  $J = 7.7$  Hz, 2H), 7.5 (d,  $J = 7.7$  Hz, 2H), 7.56 (d,  $J = 2.7$  Hz, 1H), 7.37 (d,  $J = 2.7$  Hz, 1H),

7.34 (dd,  $J = 8.5, 7.5$  Hz, 2H), 7.23-7.14 (m, 3H), 7.07 (dd,  $J = 7.7, 7.1$  Hz, 2H), 7.04-6.09 (m, 3H), 6.89 (t,  $J = 7.3$  Hz, 1H), 6.57 (s, 1H), 1.33 (s, 9H), 1.28 (s, 9H).;  $^{13}\text{C}$  NMR (CD<sub>3</sub>CN, 151 MHz)  $\delta$  168.8, 161.0, 148.9, 147.8, 143.3, 141.7, 137.7, 132.2, 131.4, 130.0, 129.4, 129.2, 129.1, 128.8, 128.6, 128.4, 128.1, 127.5, 127.1, 123.2, 94.6, 86.2, 36.1, 35.3, 31.9, 30.1; IR (thin film, cm<sup>-1</sup>) 3183.5, 2957.4, 2260.7, 1611.1, 1542.2, 1448.1, 1275.2, 1177.9, 1039.4, 702.8; HRMS (+APCI) calculated for C<sub>35</sub>H<sub>38</sub>F<sub>2</sub>N<sub>1</sub>O<sub>2</sub>Ti<sub>1</sub> 590.2345, found 590.2351 [M+H]<sup>+</sup>.

### Synthesis of *N*-Cbz-*O*-TMS aminol **131**:

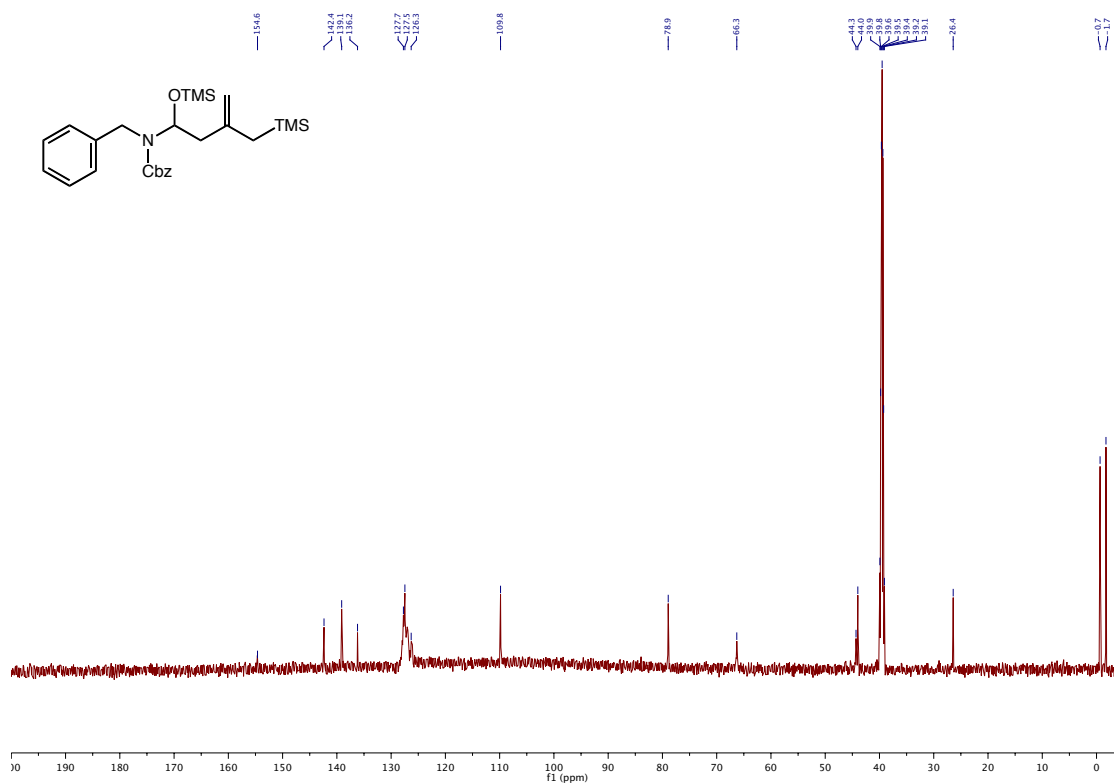
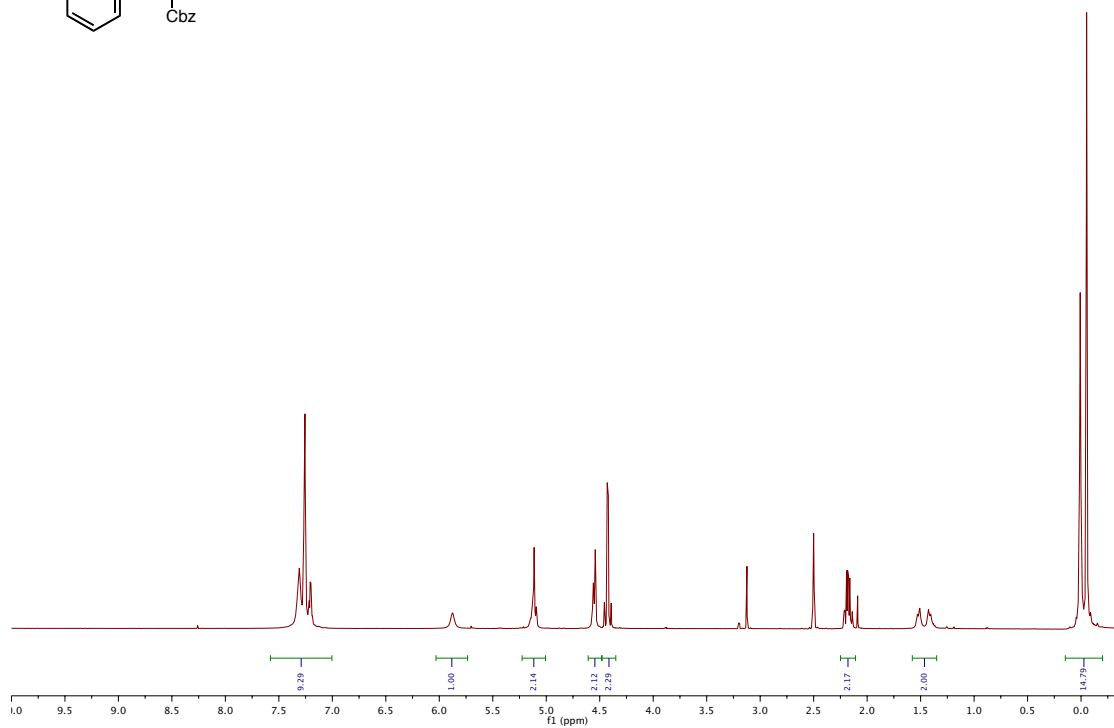
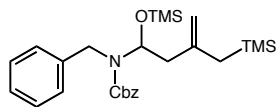


A solution of *N*-CBz-amide<sup>4</sup> **142** (0.5 g, 2.14 mmol) in CH<sub>2</sub>Cl<sub>2</sub> (10 mL) was cooled to -78 °C. DIBAL-H (1.0 M in CH<sub>2</sub>Cl<sub>2</sub>, 2.6 mL, 2.57 mmol) was added dropwise over 15 minutes. The reaction mixture was stirred for 1 h, then pyridine (0.52 mL, 6.43 mmol) and trimethylsilyl triflate (0.97 mL, 5.36 mmol) were added dropwise. The mixture was warmed to -15 °C and stirred for 20 hours. The mixture was warmed to 0 °C and stirred for 2 hours. The reaction was quenched by slow addition of aqueous 15% Rochelle's salt solution (15 mL). The biphasic mixture was transferred to a 25 mL Erlenmeyer flask, and Et<sub>2</sub>O (30 mL) was added. The mixture was stirred vigorously at r.t. until both layers were clear. The organic layer was separated, and the aqueous layer was extracted with Et<sub>2</sub>O (2 x 10 mL). The organic extracts were combined, washed with brine (10 mL), dried over

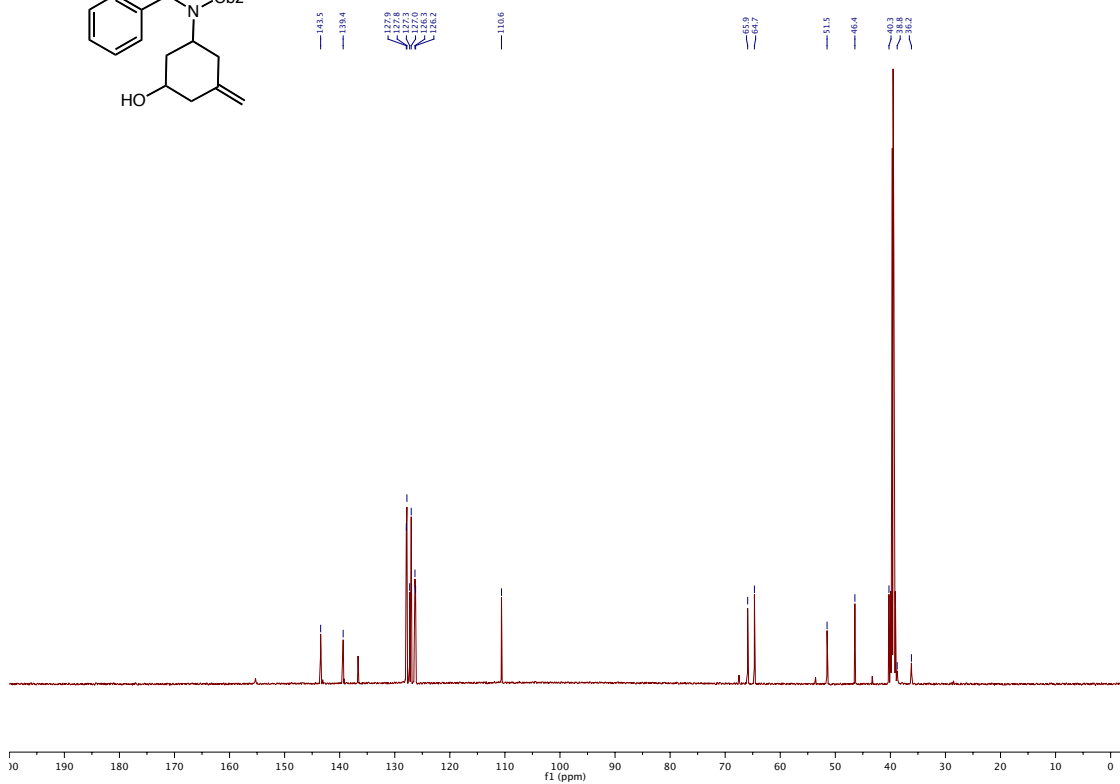
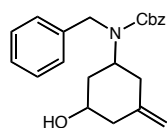
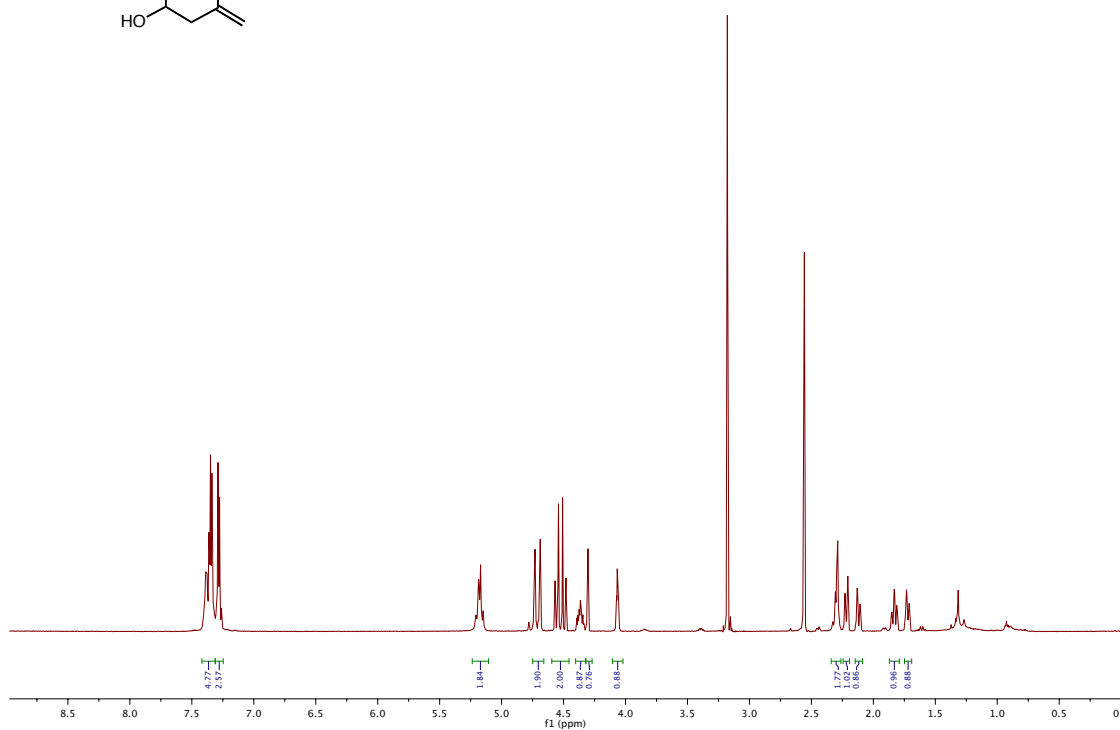
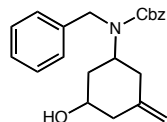


anhydrous MgSO<sub>4</sub>, and concentrated *in vacuo*. Purification by chromatography on silica gel (20:1 → 4:1 Hexanes/EtOAc, silica gel deactivated with 1% Et<sub>3</sub>N) afforded *N*-Cbz-*O*-TMS-aminol **131** as a colorless oil (0.52 g, 49%); **R<sub>f</sub>** 0.40 (4:1 hexanes/EtOAc); **<sup>1</sup>H NMR** (CDCl<sub>3</sub>, 50 °C, 600 MHz) δ 7.43-7.27 (m, 5H), 5.81 (s, 1H), 5.17 (d, *J* = 12.3 Hz, 1H), 5.12 (d, *J* = 12.3 Hz, 1H), 3.89 (d, *J* = 11.5 Hz, 1H), 3.14 (dd, *J* = 13.4, 12.0 Hz, 1H), 1.92-1.79 (m, 1H), 1.69 (d, *J* = 12.4 Hz, 1H), 1.64 (d, *J* = 12.4 Hz, 1H), 1.59-1.49 (m, 2H), 1.49-1.38 (m, 1H), 0.08 (s, 9H); **<sup>13</sup>C NMR** (CDCl<sub>3</sub>, 50 °C, 151 MHz) δ 128.7, 128.2, 75.6, 67.3, 39.2, 33.1, 25.5, 18.1, 0.2; **IR** (thin film, cm<sup>-1</sup>) 2944.5, 1699.3, 1418.7, 1260.1, 1009.0, 838.8, 696.7; **HRMS** (+pESI) calculated for C<sub>16</sub>H<sub>25</sub>N<sub>1</sub>NaO<sub>3</sub>Si<sub>1</sub> 330.1496, found 330.1503 [M+Na]<sup>+</sup>.

## 9.5 NMR Spectra Part 2.



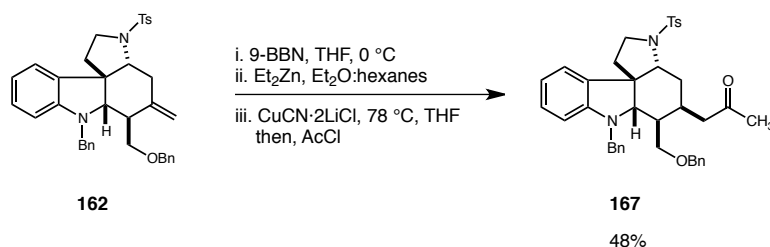
*NMR Spectra-Part 2 Efforts Towards the Development of an Enantioselective Intermolecular Cascade Reaction to Access the Core of the Banyaside Peptides.*





## 9.6 Part 3. Studies Towards the Total Synthesis of a Malagasy Alkaloid.

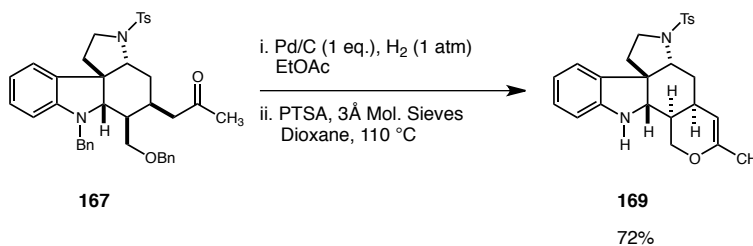
### Synthesis of *N*, *O*-Bn Ketone **167**:



To tetracycle **162** (200 mg, 0.34 mmol) was added 9-BBN (0.5 M in THF, 1.0 mL, 0.51 mmol) and the resulting solution was stirred at room temperature overnight. After removal of the volatiles *in vacuo* (0.1 mmHg, 25 °C, 1 hour), Et<sub>2</sub>O (2.0 mL) and Et<sub>2</sub>Zn (1 M in hexanes, 3.4 mL, 3.4 mmol) were added, and the resulting solution was stirred for 3 hours. The volatiles were removed *in vacuo* (0.1 mmHg, 25 °C, 1 hour), the grey-black residue was diluted with THF (5.0 mL), and the mixture was cooled to -78 °C. A freshly prepared solution of CuCN·2LiCl (1 M in THF, 5.0 mL, 5.07 mmol) was added over 10 minutes, and the mixture was stirred at -78 °C for 30 minutes. Acetyl chloride (1.1 mL, 15.2 mmol) was added slowly over 10 minutes, and the resulting solution was warmed to -20 °C over 12 hours. The reaction was quenched with saturated aqueous NH<sub>4</sub>Cl (50 mL) containing aqueous NH<sub>3</sub> (3.0 mL, 30% in H<sub>2</sub>O), and diluted with EtOAc (100 mL). The resulting biphasic mixture was stirred vigorously for 15 minutes. The organic layer was separated, and the aqueous layer was extracted with EtOAc (2 x 50.0 mL). The organic extracts were combined, washed with brine (150.0 mL), dried over anhydrous MgSO<sub>4</sub>,

and concentrated *in vacuo*. Purification by chromatography on silica gel (8:2 to 1:1 hexanes/EtOAc) afforded ketone **167** as an amorphous white solid (103 mg, 48%);  $R_f$  0.50 (7:3 hexanes/EtOAc);  $^1\text{H NMR}$  ( $\text{CDCl}_3$ , 600 MHz)  $\delta$  7.70 (d,  $J = 8.0$  Hz, 2H), 7.35-7.28 (m, 5H), 7.27-7.23 (m, 5H), 7.17 (d,  $J = 7.8$  Hz, 1H), 7.04 (dt,  $J = 7.7$ , 1.3 Hz, 1H), 6.60 (dt,  $J = 7.4$ , 1.0 Hz, 1H), 6.31 (d,  $J = 7.8$  Hz, 1H), 4.53 (d,  $J = 15.6$  Hz, 1H), 4.38- 4.27 (m, 2H), 4.25 (d,  $J = 15.7$  Hz, 1H), 3.66 (td,  $J = 10.9$ , 7.0 Hz, 1H), 3.45-3.41 (m, 2H), 3.39 (dd,  $J = 11.4$ , 8.0 Hz, 1H), 3.28 (dd,  $J = 9.6$ , 5.5 Hz, 1H), 3.14 (dd,  $J = 10.8$ , 7.4 Hz, 1H), 3.02 (dd,  $J = 9.6$ , 5.4 Hz, 1H), 2.53-2.45 (m, 1H), 2.43 (s, 3H), 2.26-2.18 (m, 3H), 2.06-1.99 (m, 1H), 1.94 (s, 3H), 1.85-1.79 (m, 2H), 1.65-1.60 (m, 1H).  $^{13}\text{C NMR}$  ( $\text{CDCl}_3$ , 101 MHz)  $\delta$  207.5, 150.6, 143.9, 138.5, 138.0, 133.1, 131.3, 129.9, 128.8, 128.7, 128.6, 128.0, 127.8, 127.6, 127.3, 124.4, 117.0, 105.7, 73.1, 70.8, 70.0, 59.5, 53.8, 48.2, 47.8, 47.3, 39.5, 37.4, 30.9, 30.1, 27.7, 21.8. **IR** (thin film,  $\text{cm}^{-1}$ ) 2918.3, 1712.4, 1599.1, 1483.5, 1347.4, 1160.8, 1090.5, 731.6. **HRMS** (+APCI) calculated for  $\text{C}_{39}\text{H}_{43}\text{N}_2\text{O}_4\text{S}$  635.2938, found 635.2943  $[\text{M}+\text{H}]^+$ .

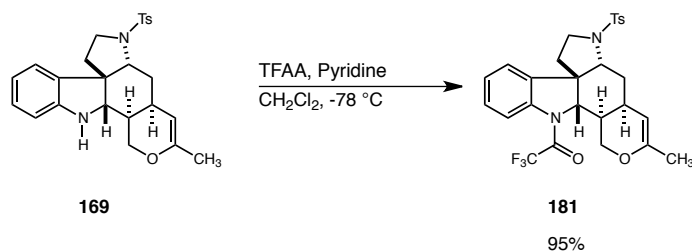
### Synthesis of dihydropyran **169**:



To a solution of ketone **167** (120 mg, 0.189 mmol) in ethyl acetate (15 mL) was added Pd/C (5% by weight, 402 mg, 0.189 mmol). The mixture was subjected to an atmosphere of hydrogen gas (1 atm) for 2 hours. The suspension was filtered through celite, and the

filter cake was washed with EtOAc (4 x 25 mL). The filtrate was concentrated *in vacuo*. The crude mixture of acetals was dissolved in anhydrous dioxane (8.0 mL). PTSA (43 mg, 0.226 mmol) was added, followed by activated powdered 3 Å molecular sieves (0.360 g). The flask was equipped with a reflux condenser and the suspension was heated at 110 °C for 2 hours. The mixture was cooled to reach room temperature and diluted with aqueous saturated NaHCO<sub>3</sub> (12 mL). The organic layer was separated, and the aqueous layer was extracted with EtOAc (3 x 20 mL). The organic extracts were combined, washed with brine (20 mL), dried over anhydrous Na<sub>2</sub>SO<sub>4</sub>, and concentrated *in vacuo*. Purification by chromatography on silica gel (7:3 → 1:1 hexanes/EtOAc) afforded pyran **169** as an amorphous white solid (71 mg, 72%); *R<sub>f</sub>* 0.50 (1:1 hexanes/EtOAc); <sup>1</sup>H NMR (CDCl<sub>3</sub>, 600 MHz) δ 7.76 (d, 2H, *J* = 8.1 Hz), 7.47 (d, 1H, *J* = 7.4 Hz), 7.37 (d, 2H, *J* = 8.1 Hz), 7.09 (t, 1H, *J* = 7.6 Hz), 6.83 (t, 1H, *J* = 7.5 Hz), 6.71 (d, 1H, *J* = 7.8 Hz), 4.26 (s, 1H), 4.05-3.97 (m, 2H), 3.88 (dd, 1H, *J* = 11.2, 1.7 Hz), 3.54 (dt, 1H, *J* = 11.1, 6.9 Hz), 3.40 (t, 1H, *J* = 10.4 Hz), 3.33 (d, 1H, *J* = 8.3 Hz), 3.07 (dd, 1H, *J* = 12.6, 3.0 Hz), 2.67 (br s, 1H), 2.48 (s, 3H), 2.42 (dt, 1H, *J* = 12.9, 2.7 Hz), 1.99 (dt, 1H, *J* = 12.8, 4.5 Hz), 1.70 (s, 3H), 1.67 (dd, 1H, *J* = 11.8, 6.8 Hz), 1.47-1.40 (m, 2H); <sup>13</sup>C NMR (CDCl<sub>3</sub>, 150 MHz) δ 152.0, 149.6, 143.9, 132.6, 131.2, 129.7, 128.2, 128.2, 125.6, 119.9, 111.7, 100.0, 67.3, 63.5, 58.7, 55.4, 47.5, 37.5, 35.8, 31.5, 30.8, 21.8, 20.0; IR (thin film, cm<sup>-1</sup>) 3355.8 (w), 2923.1 (w), 2854.6 (w), 1675.5 (w), 1598.6 (w), 1462.0 (w), 1346.8 (w), 1327.1 (w), 1162.3 (s), 1091.3 (m); HRMS (+APCI) calculated for C<sub>25</sub>H<sub>29</sub>N<sub>2</sub>O<sub>3</sub>S 437.1899, found 437.1895 [M+H]<sup>+</sup>.

### Synthesis of trifluoroacetamide **181**:

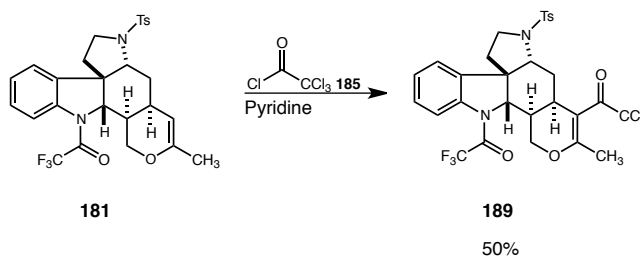


A solution of pyran **169** (0.316 g, 0.724 mmol) in  $\text{CH}_2\text{Cl}_2$  (7.0 mL) was cooled to  $-78\text{ }^\circ\text{C}$ . Pyridine (0.18 mL, 2.17 mmol) was added, followed by dropwise addition of trifluoroacetic anhydride (0.11 mL, 0.80 mmol), and the resulting mixture was stirred at  $-78\text{ }^\circ\text{C}$  for 30 minutes. The reaction was quenched with aqueous phosphate buffer (pH = 7.0, 10 mL). The resulting biphasic mixture was warmed to room temperature and stirred vigorously for 15 minutes. The organic layer was separated, and the aqueous layer was extracted with EtOAc (3 x 10 mL). The organic extracts were combined, washed with brine (20 mL), dried over anhydrous  $\text{Na}_2\text{SO}_4$ , and concentrated *in vacuo*. Purification by chromatography on silica gel (17:3 hexanes/EtOAc) afforded trifluoroacetamide **397** as an amorphous white solid (0.367 g, 95%);  $R_f$  0.50 (7:3 hexanes/EtOAc);  $^1\text{H NMR}$  ( $\text{CDCl}_3$ , 600 MHz) (1:0.3 mixture of rotamers)  $\delta$  7.95 (d, 1H,  $J = 7.9$  Hz), 7.75 (d, 2.6H,  $J = 8.1$  Hz), 7.67 (d, 1.3H,  $J = 7.3$  Hz), 7.41 – 7.25 (m, 5.5H), 4.77 (d, 0.3H,  $J = 8.5$  Hz), 4.37 (d, 1H,  $J = 8.1$  Hz), 4.22 (s, 1.3H), 4.15 (d, 0.3 Hz,  $J = 10.8$  Hz), 4.10 (d, 1H,  $J = 11.4$  Hz), 3.84–3.81 (m, 1.3H), 3.52 (dt, 1.3 H,  $J = 10.8, 7.3$  Hz), 3.47–3.38 (m, 1.3H), 3.13 (dd, 1H,  $J = 12.5, 3.1$  Hz), 3.09 (d, 0.3H,  $J = 12.0$  Hz), 2.77–2.68 (br s, 1.3H), 2.50 (, 3.9H), 2.44–2.42 (m, 1.3 H), 2.01 (dt, 1H,  $J = 12.9, 4.7$  Hz), 1.95–1.88 (m, 0.3H), 1.77–1.70 (m, 3.9H), 1.68–1.48 (m, 3.9H);  $^{13}\text{C NMR}$  ( $\text{CDCl}_3$ , 150 MHz) (1:0.3 mixture of rotamers) 154.7 (q,  $^2J_{\text{C-F}} = 37.3$  Hz, 1C), [153.1], 152.7, 144.4, 140.8, [138.5], [136.5], 135.5, 132.2, [131.8], 130.0, [129.9], 128.6, [128.2], 128.1, 127.0, [126.7], [126.1], 125.6, 121.1, [118.2], 116.2 (q,  $^1J_{\text{C-F}} = 286.2$  Hz, 1C), 99.0,



[67.8], [67.1], 66.0, 66.0, [58.4], 58.2, 55.3, [53.8], [47.0], 46.7, 36.3, [36.1], [35.0], 34.8, 32.0, [31.7], 30.2, [29.9], 21.8, [20.1], 20.0; **IR** (thin film,  $\text{cm}^{-1}$ ) 2922.7 (w), 2882.2 (w), 1690.6 (s), 1598.4 (w), 1475.0 (w), 1462.0 (w), 1428.6 (w), 1350.8 (w), 1331.8 (w), 1275.5 (w), 1207.0 (m), 1154.7 (s), 1091.7 (m); **HRMS** (+APCI) calculated for  $\text{C}_{27}\text{H}_{28}\text{F}_3\text{N}_2\text{O}_4\text{S}$  533.1722, found 533.1722  $[\text{M}+\text{H}]^+$ .

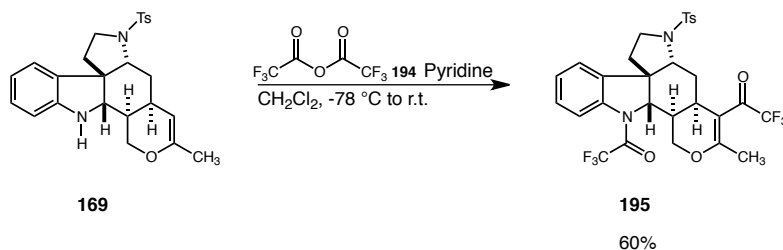
### Synthesis of trichloro ketone **189**:



A solution of trifluoroacetamide **181** (0.041 g, 0.077 mmol) in  $\text{CH}_3\text{Cl}$  (1 mL) was cooled to  $0\text{ }^\circ\text{C}$ . Pyridine (0.13 mL, 1.6 mmol) and imidazole (0.108 g, 1.6 mmol) were added, followed by dropwise addition of trichloro acetylchloride (0.51 mL, 2.3 mmol). The resulting mixture was stirred at room temperature for 15 hours. The reaction was quenched with aqueous phosphate buffer ( $\text{pH} = 7.0$ , 5 mL). The resulting biphasic mixture was warmed to room temperature and stirred vigorously for 15 minutes. The organic layer was separated, and the aqueous layer was extracted with EtOAc (3 x 10 mL). The organic extracts were combined, washed with brine (20 mL), dried over anhydrous  $\text{Na}_2\text{SO}_4$ , and concentrated *in vacuo*. Purification by chromatography on silica gel (95:5  $\rightarrow$  7:3 hexanes/EtOAc) afforded trichloro ketone **189** as an amorphous white solid (0.026 g, 50%);  $R_f$  0.60 (7:3 hexanes/EtOAc);  $^1\text{H NMR}$  ( $\text{CDCl}_3$ , 600 MHz) (1:0.3

mixture of rotamers)  $\delta$  8.07 (d,  $J = 8.0$  Hz, 1H), 7.76 (d,  $J = 8.0$  Hz, 2H), 7.63 (d,  $J = 7.4$  Hz, 1H), 7.44 (d,  $J = 8.0$  Hz, 2H), 7.41 (t,  $J = 7.9$  Hz, 1H), 4.17 (s, 2H), 3.88 (t,  $J = 10.9$  Hz, 1H), 3.62 (td,  $J = 11.0, 7.3$  Hz, 1H), 3.45 (t,  $J = 10.5$  Hz, 1H), 3.38 (dd,  $J = 10.7, 7.3$  Hz, 1H), 2.99 (s, 1H), 2.53 – 2.42 (m, 5H), 2.31- 2.23 (m, 1H), 2.09 (s, 1H), 1.96 (s, 3H), 1.82 (dd,  $J = 12.1, 6.7$  Hz, 1H), 1.64 (dd,  $J = 12.2, 10.4$  Hz, 2H);  $^{13}\text{C}$  NMR ( $\text{CDCl}_3$ , 150 MHz) 147.63, 144.59, 141.86, 140.64, 132.62, 130.29, 129.51, 128.11, 127.36, 124.84, 119.71, 66.59, 65.44, 57.25, 53.88, 53.65, 46.90, 39.17, 35.45, 30.39, 21.89, 20.17; HRMS (+APCI) calculated for  $\text{C}_{29}\text{H}_{27}\text{Cl}_3\text{F}_3\text{N}_2\text{O}_5\text{S}$  677.0653, found 677.0643  $[\text{M}+\text{H}]^+$ .

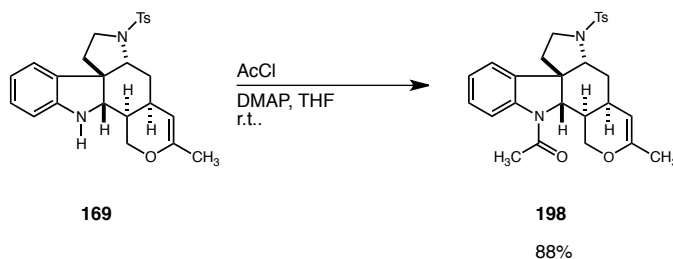
### Synthesis of trifluoroketoamide 195:



A solution of dihydropyran **169** (0.05 g, 0.01 mmol) in  $\text{CH}_2\text{Cl}_2$  (1 mL) was cooled to  $-78^\circ\text{C}$ . Pyridine (0.074 mL, 0.05 mmol) was added followed by the dropwise addition of trifluoroacetic anhydride (0.043 mL, 0.02 mmol). The resulting mixture was stirred at  $0^\circ\text{C}$  for 1 hour followed by stirring at room temperature for 10 hours. The reaction was quenched with aqueous phosphate buffer (pH = 7.0, 5 mL). The resulting biphasic mixture was stirred vigorously for 15 minutes. The organic layer was separated, and the aqueous layer was extracted with EtOAc (3 x 10 mL). The organic extracts were combined, washed with brine (5 mL), dried over anhydrous  $\text{Na}_2\text{SO}_4$ , and concentrated *in*

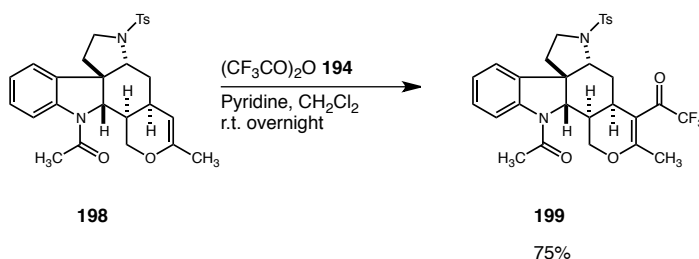
*vacuo*. Purification by chromatography on silica gel (95:5 → 7:3 hexanes/EtOAc) afforded trifluoroketoamide **195** (0.043 g, 60%);  $R_f$  0.40 (7:3 hexanes/EtOAc);  $^1\text{H NMR}$  ( $\text{CDCl}_3$ , 600 MHz) (1:1 mixture of rotamers)  $\delta$  8.07 (d, 1H,  $J = 8.0$  Hz), 7.73 (d, 2.2H,  $J = 8.2$  Hz), 7.63 (d, 1.1H,  $J = 7.4$  Hz), 7.44–7.38 (m, 3.3H), 7.29 (t, 1.1H,  $J = 7.6$  Hz), 4.23 (dd, 1.1H,  $J = 11.0, 2.5$  Hz), 4.15 (s, 1H), 3.84 (at, 1H,  $J = 11.0$  Hz), 3.62 (td, 1H,  $J = 11.0, 6.8$  Hz), 3.51 (dd, 1H,  $J = 11.0, 9.7$  Hz), 3.37 (dd, 1H,  $J = 11.0, 7.7$  Hz), 2.59 (m, 1H), 2.49 (s, 3H), 2.44 (m, 1H), 2.18–2.09 (m, 5H), 1.84 (dd, 1H,  $J = 12.1, 6.8$  Hz), 1.60 (m, 1H).  $^{13}\text{C NMR}$  ( $\text{CDCl}_3$ , 150 MHz)  $\delta$  180.4 (q, 1C,  $^2J_{\text{C-F}} = 32.7$  Hz), 169.6, 153.4 (q, 1C,  $^2J_{\text{C-F}} = 35.1$  Hz), 144.7, 140.5, 134.2, 132.7, 130.3, 130.2, 129.6, 128.1, 127.9, 127.4, 124.7, 119.5, 116.3 (q, 2C,  $^1J_{\text{C-F}} = 296.8$  Hz), 110.4, 67.1, 65.6, 56.8, 53.68, 47.1, 39.8, 35.7, 31.3, 27.2, 21.9, 21.4.; ; **IR** (thin film,  $\text{cm}^{-1}$ ) 2922.9, 1690.1, 1474.2, 1207.0, 1162.4, 1155.1 758.2; **HRMS** (+APCI) calculated for  $\text{C}_{29}\text{H}_{27}\text{F}_6\text{N}_2\text{O}_5\text{S}$  629.1539, found 629.1537  $[\text{M}+\text{H}]^+$ .

### Synthesis of acetamide **198**:



Acetyl chloride (0.083 mL, 1.17 mmol) was added dropwise to a solution of pyran **169** (0.102 g, 0.233 mmol) and DMAP (0.130 g, 1.06 mmol) in THF (2.3 mL), and the resulting mixture was stirred for 1 hour. The reaction was quenched with saturated

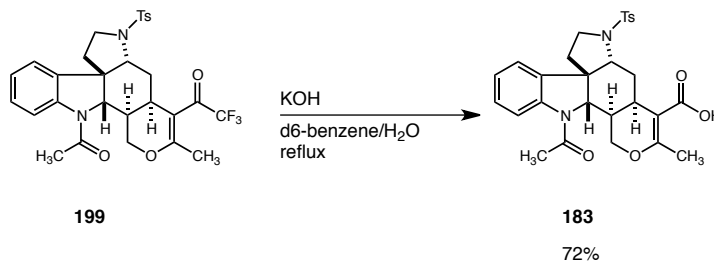
aqueous NaHCO<sub>3</sub> (3 mL). The resulting biphasic mixture was stirred vigorously for 15 minutes. The organic layer was separated, and the aqueous layer was extracted with EtOAc (3 x 3 mL). The organic extracts were combined, washed with brine (10 mL), dried over anhydrous Na<sub>2</sub>SO<sub>4</sub>, and concentrated *in vacuo*. Purification by chromatography on silica gel (3:2 → 1:1 hexanes/EtOAc) afforded acetamide **198** as an amorphous white solid (0.098 g, 88%); *R<sub>f</sub>* 0.32 (3:7 hexanes/EtOAc); <sup>1</sup>H NMR (CDCl<sub>3</sub>, 600 MHz) (1:0.6 mixture of rotamers) δ 8.01 (d, 1H, *J* = 8.0 Hz), 7.78-7.73 (m, 3.2H), 7.63 (d, 0.6H, *J* = 7.4 Hz), 7.56 (d, 1H, *J* = 7.5 Hz), 7.43-7.36 (m, 3.2H), 7.29-7.26 (m, 1.6H), 7.16-7.10 (m, 2.2H), 4.71 (d, 0.6H, *J* = 8.5 Hz), 4.28 (s, 1H), 4.23-4.22 (m, 1.2H), 4.11 (dd, 1H, *J* = 11.5, 1.7 Hz), 4.03 (d, 1H, *J* = 8.6 Hz), 3.88 (d, 1H, *J* = 11.6 Hz), 3.77 (dd, 0.6H, *J* = 10.6, 1.5 Hz), 3.54-3.49 (m, 1.6H), 3.46-3.38 (m, 1.6H), 3.12 (dd, 1H, *J* = 12.7, 3.2 Hz), 3.07 (dd, 0.6H, *J* = 12.6, 2.9 Hz), 2.73 (br s, 1H), 2.66 (br s, 0.6H), 2.49 (s, 4.8H), 2.44 (dt, 1H, *J* = 13.2, 3.0 Hz), 2.41-2.35 (m, 2.4H), 2.29 (s, 3H), 1.99 (dt, 1H, *J* = 12.9, 4.5 Hz), 1.92 (dt, 0.6H, *J* = 12.9, 4.6 Hz), 1.78-1.71 (m, 1.6H), 1.67-1.59 (m, 3.2H), 1.53-1.43 (m, 3H); <sup>13</sup>C NMR (CDCl<sub>3</sub>, 150 MHz) (1:0.6 mixture of rotamers) 168.6, 168.0, 153.1, 152.6, 144.3, 144.2, 141.5, 141.2, 136.7, 134.9, 132.5, 132.0, 129.9, 129.9, 128.5, 128.3, 128.2, 128.2, 126.3, 125.1, 125.0, 124.7, 120.2, 117.7, 99.8, 99.1, 67.4, 66.7, 65.7, 64.5, 58.6, 58.5, 54.9, 54.1, 47.1, 46.9, 37.1, 37.0, 35.8, 35.5, 32.2, 31.6, 30.2, 26.7, 23.4, 23.4, 21.8, 21.8, 20.2, 20.1; IR (thin film, cm<sup>-1</sup>) 2922.2 (w), 1655.8 (s), 1597.6 (w), 1473.4 (m), 1461.7 (m), 1393.9 (m), 1349.9 (m), 1332.8 (w), 1163.1 (s), 1091.6 (m), 730.2 (m); HRMS (+APCI) calculated for C<sub>27</sub>H<sub>31</sub>N<sub>2</sub>O<sub>4</sub>S 479.2005, found 479.1999 [M+H]<sup>+</sup>.

**Synthesis of trifluoroketone 199:**

A solution of acetamide **198** (0.059 g, 0.123 mmol) in  $\text{CH}_2\text{Cl}_2$  (5 mL) was cooled to 0 °C. Pyridine (0.074 mL, 0.5 mmol) was added followed by the dropwise addition of trifluoroacetic anhydride (0.043 mL, 0.54 mmol). The resulting mixture was stirred at 0 °C for 1 hour followed by stirring at room temperature for 10 hours. The reaction was quenched with aqueous phosphate buffer (pH = 7.0, 5 mL). The resulting biphasic mixture was stirred vigorously for 15 minutes. The organic layer was separated, and the aqueous layer was extracted with EtOAc (3 x 15 mL). The organic extracts were combined, washed with brine (5 mL), dried over anhydrous  $\text{Na}_2\text{SO}_4$ , and concentrated *in vacuo*. Purification by chromatography on silica gel (95:5 → 7:3 hexanes/EtOAc) afforded trifluoroketoamide **199** (0.053 g, 75%); (95:5 → 7:3 hexanes/EtOAc);  $^1\text{H}$  NMR ( $\text{CDCl}_3$ , 600 MHz) (1:0.4 mixture of rotamers)  $\delta$  8.06 (d, 0.4H,  $J$  = 8.0 Hz), 7.69 (d, 2.8H,  $J$  = 7.8 Hz), 7.62 (d, 1H,  $J$  = 7.4 Hz), 7.52 (d, 0.4H,  $J$  = 7.4 Hz), 7.41 (d, 6H,  $J$  = 7.8 Hz), 7.33 – 7.27 (m, 1.4H), 7.13 (m, 1.4H), 4.47 (d, 2H,  $J$  = 3.4 Hz), 4.21 (dd, 1H,  $J$  = 10.7, 3.5 Hz), 4.18 – 4.13 (m, 1H), 4.03 – 3.89 (m, 1.8H), 3.62 – 3.53 (m, 1.4H), 3.43 (dd, 1.4H,  $J$  = 11.3, 9.6 Hz), 3.26 (dd, 0.4H,  $J$  = 11.0, 6.7 Hz), 3.21 (dd, 1H,  $J$  = 11.0, 6.7 Hz), 2.89 (m, 0.4H), 2.74 (m, 1H), 2.48 (s, 4.4 H), 2.41 (s, 3H), 2.35 – 2.17 (m, 4.8H), 2.14 – 2.07 (m, 4.8H), 2.03 – 1.91 (m, 1.4H), 1.78 - 1.68 (m, 1.4H), 1.63 – 1.44 (m,

1.8H), 1.41 (d, 0.4 H,  $J = 5.6$  Hz), 1.39 (dd, 0.4H,  $J = 12.5, 5.6$  Hz).  $^{13}\text{C}$  NMR (CDCl<sub>3</sub>, 150 MHz) 169.4, 168.3, 167.6, 144.5, 144.4, 141.5, 140.8, 135.5, 133.5, 132.7, 132.4, 130.2, 129.2, 129.0, 128.0, 125.9, 125.2, 124.78, 124.6, 119.0, 117.6, 115.8, 110.6, 110.3, 99.7, 68.2, 67.7, 65.6, 64.2, 57.5, 57.2, 53.7, 52.1, 47.1, 46.9, 39.0, 38.0, 36.1, 36.0, 30.9, 30.7, 27.7, 23.9, 23.7, 21.8, 21.1, 20.7, 17.6. IR (thin film, cm<sup>-1</sup>) 2971.7, 1652.9, 1596.5, 1544.1, 1393.2, 1162.4, 906.2, 726. HRMS (+APCI) calculated for C<sub>27</sub>H<sub>28</sub>F<sub>3</sub>N<sub>2</sub>O<sub>4</sub>S 533.1722, found 533.1716 [M+H]<sup>+</sup>.

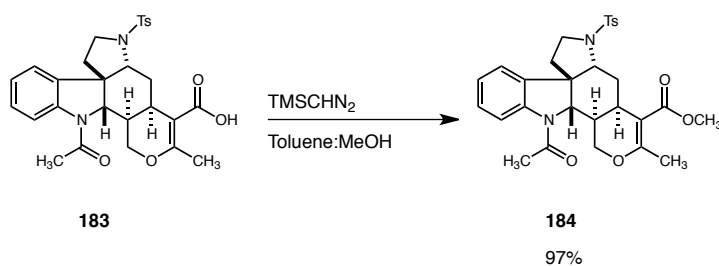
### Synthesis of acid **183**:



To a solution of trifluoroketone **199** (0.044 g, 0.077 mmol) in benzene (5 mL), was added powdered KOH (0.04 mg, 0.71 mmol) and H<sub>2</sub>O (50  $\mu$ L). The reaction mixture was heated at reflux for 6 hours (<sup>19</sup>F shows disappearance of all signals at this time). The solution was cooled to room temperature, EtOAc (20 mL) was added and the pH was adjusted to 7 by the slow addition of 0.5 N HCl solution. After phase separation, the aqueous layer was extracted with EtOAc (3 x 20 mL). The combined organic layers were washed with brine (20 mL), dried over anhydrous Na<sub>2</sub>SO<sub>4</sub>, and concentrated *in vacuo*. Purification by chromatography on silica gel (7:3  $\rightarrow$  1:1 hexanes/EtOAc) afforded acid **183** as an amorphous white solid (29 mg, 72%);  $^1\text{H}$  NMR (CDCl<sub>3</sub>, 600 MHz) (1:1.5 mixture of

rotamers)  $\delta$   $^1\text{H-NMR}$  (600 MHz;  $\text{CDCl}_3$ ):  $\delta$  8.06 (d, 1H,  $J = 8.0$  Hz), 7.72-7.64 (m, 6.5H), 7.66 (d, 1H,  $J = 7.5$  Hz), 7.41 – 7.34 (m, 5H), 7.31-7.28 (m, 2.5H), 7.16 – 7.13 (m, 4H), 4.53 (d, 1.5H,  $J = 4.9$  Hz), 4.01– 3.94 (m, 6H), 3.60-3.53 (m, 2.5H), 3.43 – 3.34 (m, 2.5H), 3.09-3.05 (m, 1H), 3.03 (dd, 1.5H,  $J = 12.3, 4.5$  Hz), 2.83-2.80 (m, 2H), 2.72-2.66 (m, 3H), 2.47 (s, 4.5H), 2.45 (s, 3H), 2.41 (s, 4.5H), 2.27 (s, 3H), 2.25 (s, 4.5H), 2.24 (s, 3H), 2.21– 2.15 (m, 2.5H), 1.95 – 1.90 (m, 1H), 1.90-1.84 (m, 1.5H), 1.71 – 1.62 (m, 2.5H), 1.52 – 1.45 (m, 2.5H);  $^{13}\text{C NMR}$  ( $\text{CDCl}_3$ , 150 MHz) (1:1.5 mixture of rotamers)  $\delta$  172.8, 172.5, 168.5, 168.5, 168.0, 167.5, 144.2, 144.2, 141.5, 140.9, 135.9, 134.1, 132.3, 132.0, 130.1, 130.1, 128.8, 128.7, 128.1, 128.1, 126.3, 125.2, 125.0, 124.8, 119.4, 116.3, 105.5, 105.0, 68.1, 67.5, 66.1, 64.9, 58.5, 58.4, 54.2, 52.8, 47.1, 46.9, 39.4, 38.8, 36.1, 36.0, 30.0, 29.1, 23.9, 23.6, 21.8, 21.8, 21.0, 20.7; **IR** (thin film,  $\text{cm}^{-1}$ ) 2956.8 (s), 2925.1 (s), 1661.4 (s), 1477.1 (m), 1395.4 (m), 1597.2 (m), 1162.9 (s); **HRMS** (+APCI) calculated for  $\text{C}_{28}\text{H}_{31}\text{N}_2\text{O}_4$  523.1903, found 523.1891  $[\text{M}+\text{H}]^+$ .

### Synthesis of *N*-tosyldehydromalagashanine **184**:



Acid **183** (0.01 g, 0.19 mmol) was dissolved in MeOH (0.2 mL) and toluene (0.3 mL). Excess  $\text{TMSCHN}_2$  (2M in  $\text{Et}_2\text{O}$ , 14  $\mu\text{L}$ ) was added. The reaction mixture was stirred at room temperature for 1 hour, after which time, it was quenched by the slow addition of

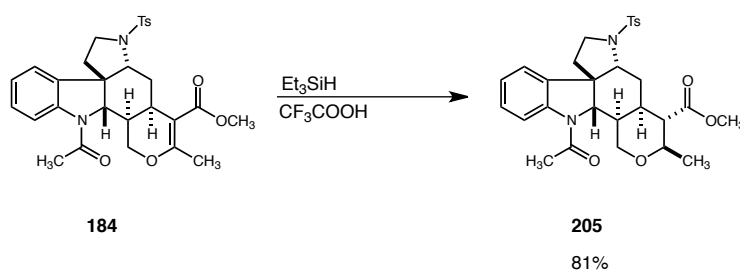
AcOH (2 mL, CAUTION! N<sub>2</sub> evolution). The reaction was concentrated in *vacuo*, EtOAc (10 mL) was added followed by sat. NaHCO<sub>3</sub> (2 mL). The resulting biphasic solution was separated and the aqueous layer was extracted with EtOAc (3 x 10 mL). The combined organic layers were washed with brine (20 mL), dried over anhydrous Na<sub>2</sub>SO<sub>4</sub>, and concentrated *in vacuo*. Purification by chromatography on silica gel (1:1 hexanes/EtOAc) afforded *N*-tosyldehydromalagashanine **184** (0.010 g, 97%); **R<sub>f</sub>** 0.40 (1:1 hexanes/EtOAc); **<sup>1</sup>H NMR** (CDCl<sub>3</sub>, 600 MHz) (CDCl<sub>3</sub>, 600 MHz) (1:0.7 mixture of rotamers) δ 8.04 (d, 0.7H, *J* = 8.0 Hz), 7.72 – 7.65 (m, 3.4H), 7.63 (d, 1H, *J* = 8.0 Hz), 7.56 (d, 0.7H, *J* = 7.5 Hz), 7.41 – 7.38 (m, 3.4H), 7.32 – 7.27 (m, 1.7H), 7.17 – 7.10 (m, 1.7H), 4.57 (d, 1H, *J* = 6.0 Hz), 4.07 – 3.98 (m, 1.7H), 3.97 (d, 0.7H, *J* = 6.5 Hz), 3.95 – 3.89 (m, 1.7H), 3.79 (s, 1.8H), 3.75 (s, 3H), 3.53 (tt, 1.7H, *J* = 11.4, 6.3 Hz), 3.37 – 3.31, (m, 1.7H), 3.11 (dd, 0.7H, *J* = 12.5, 4.4 Hz), 3.04 (dd, 1H, *J* = 12.5, 4.4 Hz), 2.92 – 2.85 (m, 0.7H), 2.83 – 2.75 (m, 1H), 2.70 (dt, 0.7H, *J* = 14.1, 4.4 Hz), 2.61 (dt, 1H, *J* = 14.1, 4.4 Hz), 2.47 (s, 4.8H), 2.38 (s, 3H), 2.26 (s, 1.8H), 2.21 (s, 3H), 2.19 (s, 1.8H), 2.14 – 2.07 (m, 1.7H), 1.90 – 1.77 (m, 1.7H), 1.64 (dd, 0.7 H, *J* = 11.8, 6.8 Hz), 1.50 – 1.37 (m, 1.7H). **<sup>13</sup>C NMR** (CDCl<sub>3</sub>, 150 MHz) δ 168.5, 168.2, 167.8, 164.7, 163.3, 144.2, 141.1, 136.2, 134.3, 132.1, 130.1, 130.0, 130.0, 128.8, 128.6, 126.3, 125.0, 124.7, 119.6, 116.7, 106.2, 105.6, 67.9, 67.3, 66.1, 64.9, 58.7, 58.5, 54.6, 53.3, 51.6, 51.4, 47.0, 46.8, 39.2, 38.9, 36.0, 35.8, 31.9, 30.9, 29.1, 29.0, 23.7, 21.8, 20.1, 19.8. **IR** (thin film, cm<sup>-1</sup>) 2948.6, 1704.7, 1660.5, 1475.6, 1393.2, 1163.0, 1092.2, 732.6, 665.6.





To a solution of dihydropyran carboxylate **200** (0.100 g, 0.64 mmol) in EtOAc (3 mL) in a vial, was added Pd(OH)<sub>2</sub>/C (20 wt%, 0.090 g, 1.28 mmol). The heterogenous mixture was then submitted to H<sub>2(g)</sub> (120 psi) and 70 °C for 24 h. The mixture was filtered through celite and the filter cake was washed with EtOAc (10 mL). The clear solution obtained was concentrated *in vacuo*. Purification by chromatography on silica gel (85:15 Hexane/EtOAc, silica gel) afforded pyran carboxylate **66** as a colorless oil (0.050 g, 50%); <sup>1</sup>H NMR (CDCl<sub>3</sub>, 400 MHz) δ 3.99 – 3.88 (m, 1H), 3.82 (qd, *J* = 6.7, 3.7 Hz, 1H), 3.69 (s, 3H), 3.51 (ddd, *J* = 11.4, 9.3, 3.2 Hz, 1H), 2.60 (dd, *J* = 8.6, 4.8 Hz, 1H), 2.08 – 1.93 (m, 2H), 1.81-1.69 (m, 1H), 1.49 – 1.38 (m, 1H), 1.24 (d, *J* = 6.7 Hz, 3H); <sup>13</sup>C NMR (CDCl<sub>3</sub>, 151 MHz) δ 72.8, 66.4, 51.6, 44.3, 24.5, 22.8, 18.1; IR (thin film, cm<sup>-1</sup>) 2953.3, 1731.6, 1698.5, 1496.3, 1350.5, 1169.0, 838.1, 695.1; HRMS (+APCI) calculated for C<sub>8</sub>H<sub>14</sub>NaO<sub>3</sub> 181.0841, found 181.1013 [M+Na]<sup>+</sup>.

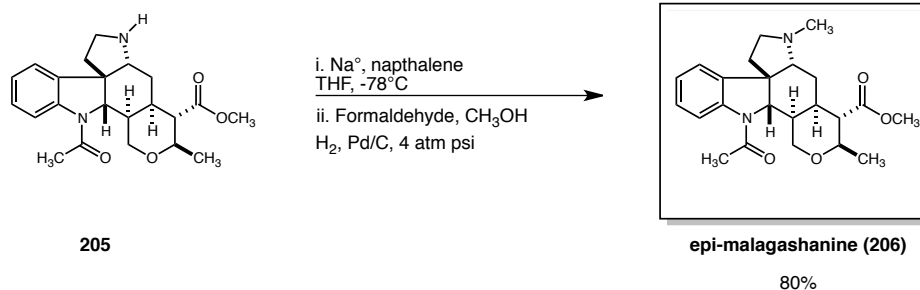
### Synthesis of *N*-tosylepimalagashanine **205**:



To a solution of unsaturated ester **184** (0.017 g, 0.032 mmol) in TFA (0.5 mL) was added freshly distilled Et<sub>3</sub>SiH (0.051 mL, 0.32 mmol) at room temperature and the mixture was stirred for 1 hour. IPAc (20 mL) was added followed by slow quench with saturated NaHCO<sub>3</sub> solution (2 mL). The resulting biphasic mixture was stirred vigorously for 15

minutes. The organic layer was separated, and the aqueous layer was extracted with IPAc (3 x 20 mL). The organic extracts were combined, washed with brine (10 mL), dried over anhydrous NaSO<sub>4</sub>, and concentrated *in vacuo*. Purification by chromatography on silica gel (1:1 hexanes/EtOAc) afforded saturated ester **205** (0.06 g, 81%); **R<sub>f</sub>** 0.30 (1:1 hexanes/EtOAc); **<sup>1</sup>H NMR** **<sup>1</sup>H NMR** (CDCl<sub>3</sub>, 600 MHz) (1:0.7 mixture of rotamers) δ 7.99 (d, 1 H, *J* = 7.6 Hz), 7.87 – 7.81 (m, 3.4H), 7.68 (d, 0.7H, *J* = 7.6 Hz), 7.62 (d, 0.7H, *J* = 9.8 Hz), 7.44 (d, 3.4H, *J* = 7.8 Hz), 7.29 – 7.25 (m, 3.4H), 7.15 – 7.09 (m, 1.7H), 4.87 (d, 2H, *J* = 9.8 Hz), 4.18 (d, 1H, *J* = 9.8 Hz), 4.02 (d, 1H, *J* = 11.8 Hz), 3.88 – 3.83 (m, 5.1H), 3.62 – 3.54 (m, 1H), 3.53 – 3.41 (m, 5.1H), 3.34 (dd, 1H, *J* = 13.0, 3.4 Hz), 3.30 – 3.23 (m, 1.7H), 2.53 – 2.49 (m, 5.1H), 2.47 – 2.33 (m, 8.5H), 2.26 (s, 3.5H), 2.01 – 1.86 (m, 1.7 H), 1.64 – 1.55 (m, 4.7H), 1.53 – 1.45 (m, 1.7H). **<sup>13</sup>C NMR** (CDCl<sub>3</sub>, 150 MHz) δ 173.0, 168.1, 144.2, 140.9, 137.1, 135.13, 132.3, 131.1, 130.1, 129.0, 128.6, 128.5, 128.3, 126.3, 125.1, 125.0, 124.9, 120.3, 118.1, 68.9, 68.2, 65.2, 64.1, 59.2, 59.0, 55.8, 52.4, 52.2, 50.5, 50.3, 46.6, 46.5, 38.3, 38.0, 37.4, 37.0, 35.6, 35.3, 32.1, 29.9, 29.6, 29.2, 28.8, 28.6, 27.2, 23.6, 23.2, 22.9, 21.8, 20.5, 20.5, 14.3, 14.3. **HRMS** (+APCI) calculated for C<sub>29</sub>H<sub>35</sub>N<sub>2</sub>O<sub>6</sub>S 539.2210, found 539.2208 [M+H]<sup>+</sup>.

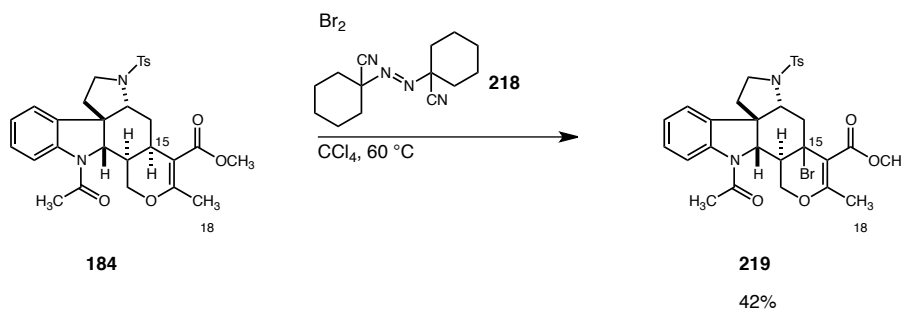
### Epimalagashanine



THF (4.4 mL) was added to a flask charged with naphthalene (0.728 g, 5.68 mmol) and sodium metal (0.106 g, 4.61 mmol). The resulting dark green mixture was stirred at r.t. for 1 h. In a separate flask, a solution of tosylamine **205** (0.019 g, 0.035 mmol) in THF (1.0 mL) was cooled to -78 °C. The sodium naphthalide solution (100  $\mu$ L, 0.056 mmol) was added slowly by syringe until the clear starting material solution turned green. The reaction was aged for an additional hour at -78 °C. The reaction was then quenched quenched by addition of a saturated solution of NaHCO<sub>3</sub> (2 mL). The resulting mixture was warmed to room temperature and EtOAc (10 mL) was added. After phase separation, the aqueous layer was re-extracted with additional EtOAc (3x 10 mL). The organic extracts were combined, washed with brine (10 mL), dried over anhydrous NaSO<sub>4</sub>, and concentrated *in vacuo*. Purification by chromatography on silica gel (1:1 hexanes/EtOAc until all excess naphthalene comes out followed by 92:8 CH<sub>2</sub>Cl<sub>2</sub>/methanol) afforded secondary amine **209** (9.0 mg, 80%). To a solution of secondary amine **209** (9.0 mg, 0.023 mmol) in CH<sub>3</sub>OH (2 mL) was added formaldehyde solution (10  $\mu$ L, 0.058 mmol) and Pd/C (10 wt%, 0.012g). The heterogenous mixture was then submitted to H<sub>2(g)</sub> (59 psi) for 4 h. The mixture was filtered through celite and the filter cake was washed with MeOH (2x 10 mL). The clear solution obtained was concentrated *in vacuo*. Purification by chromatography on silica gel (93:7 CH<sub>2</sub>Cl<sub>2</sub>/methanol) afforded amine epimalagashanine **206** as a white amorphous solid (3.5 mg, 75%); **R<sub>f</sub>** 0.35 (93:7 CH<sub>2</sub>Cl<sub>2</sub>/methanol); **<sup>1</sup>H NMR** (CDCl<sub>3</sub>, 600 MHz) (1:0.5 mixture of rotamers)  $\delta$  7.97 (d, 1.0H, *J* = 8.0 Hz), 7.77 (d, 0.5H, *J* = 7.5 Hz), 7.64 (d, 1H, *J* = 7.5 Hz), 7.20 – 7.16 (m, 1.5H), 7.09 (d, 1.4H, *J* = 8.0 Hz), 7.06 – 7.00 (m, 1.5H), 4.98 (d, 0.5H, *J* = 9.7 Hz), 4.25 (d, 1.0H, *J* = 9.7 Hz), 4.09 (d, 1.0H, *J* = 11.6 Hz), 3.99 (d, 1.5H, *J* = 12.6 Hz), 3.75 – 3.69

(m, 4.5H), 3.62 – 3.55 (m, 1.5H), 3.54 – 3.39 (m, 3H), 3.27– 3.16 (m, 1.5H), 2.64 (dd, 1.0H,  $J = 12.9, 3.0$  Hz), 2.62 – 2.53 (m, 2.5H), 2.37 – 2.29 (m, 9.5H), 2.03 – 1.95 (m, 1.5H), 1.67 – 1.40 (m, 6.0H), 1.23 - 1.18 (m, 4.5H).  $^{13}\text{C}$  NMR ( $\text{CDCl}_3$ , 150 MHz)  $\delta$  173.5, 168.8, 168.3, 140.9, 140.8, 140.1, 138.1, 127.6, 127.3, 127.2, 126.0, 124.6, 124.3, 119.9, 117.7, 76.3, 75.9, 69.1, 68.5, 66.1, 64.8, 64.5, 55.9, 55.0, 52.8, 52.7, 51.8, 51.7, 50.4, 50.2, 41.2, 41.1, 39.2, 39.0, 38.0, 37.7, 37.1, 36.8, 29.9, 27.1, 26.9, 23.8, 23.4, 20.5, 20.4. IR (thin film,  $\text{cm}^{-1}$ ) 2940.7, 2849.8, 2231.1, 2032.4, 1731.7, 1657.7, 1461.9, 1393.7, 1108.5, 761.0. HRMS (+APCI) calculated for  $\text{C}_{23}\text{H}_{31}\text{N}_2\text{O}_4$  399.2278, found 399.2273  $[\text{M}+\text{H}]^+$ .

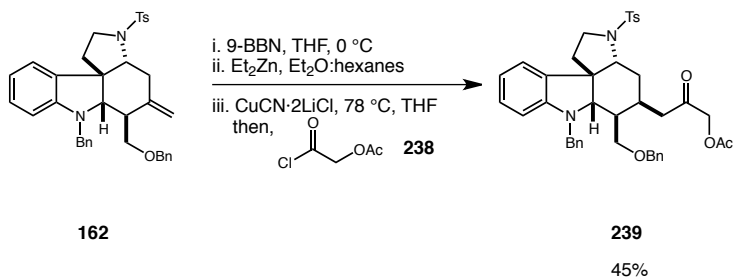
### Synthesis of bromide **219**:



To a solution of ester **184** (0.01 g, 0.019 mmol) in  $\text{CCl}_4$  (4 mL) was added NBS (0.004 g, 0.02 mmol) and 1,1'-azobis(cyclohexanecarbonitrile) (**218**) (0.002 g, 0.002 mmol). The reaction mixture was warmed to  $60^\circ\text{C}$  and aged at this temperature for 1 hour. The reaction was concentrated in *vacuo*, and the crude was purified *via* preparatory silica gel TLC plate (1:1 hexanes/EtOAc) to afford bromide **219** (0.005 g, 42%);  $R_f$  0.18 (1:1 hexanes/EtOAc);  $^1\text{H}$  NMR ( $\text{CDCl}_3$ , 400 MHz)  $\delta$  7.76 (dd,  $J = 8.1, 3.4$  Hz, 2H), 7.41 (d,  $J = 7.9$  Hz, 1H), 7.36 – 7.28 (m, 1H), 7.15 ? 7.08 (m, 1H), 3.79 – 3.63 (m, 3H), 3.41 (d,  $J = 11.6$  Hz, 1H), 2.78 (s, 3H), 2.46 (d,  $J = 14.9$  Hz, 3H), 2.26 (s, 1H), 1.80 (d,  $J = 7.6$  Hz,

2H), 1.25 (s, 10H), 0.86 (dt,  $J = 13.9, 6.7$  Hz, 4H). **HRMS** (+APCI) calculated for  $C_{29}H_{32}BrN_2O_6S$  615.1164, found 615.1152  $[M+H]^+$ .

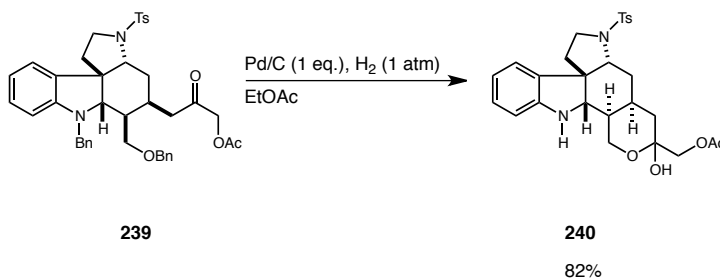
### Synthesis of Acetoxyketone **239**:



To tetracycle **162** (0.500 g, 0.84 mmol) at 0 °C was added 9-BBN (0.5 M in THF, 2.0 mL, 1.01 mmol) and the resulting solution was stirred at room temperature overnight. After removal of the volatiles *in vacuo* (0.1 mmHg, 25 °C, 1 hour),  $Et_2O$  (4.0 mL) and  $Et_2Zn$  (1 M in hexanes, 12.6 mL, 12.6 mmol) were added, and the resulting solution was stirred for 3 hours. The volatiles were removed *in vacuo* (0.1 mmHg, 25 °C, 1 hour), the grey-black residue was diluted with THF (13.0 mL), and the mixture was cooled to -78 °C. A freshly prepared solution of  $CuCN \cdot 2LiCl$  (1 M in THF, 13.0 mL, 12.6 mmol) was added over 30 minutes, and the mixture was stirred at -78 °C for 30 minutes. Acetoxyacetyl chloride (4 mL, 38.0 mmol) was added slowly over 30 minutes, and the resulting solution was warmed to -20 °C and stirred for 12 hours. The reaction was quenched with saturated aqueous  $NH_4Cl$  (100 mL) and diluted with  $EtOAc$  (50 mL). The resulting biphasic mixture was stirred vigorously for 15 minutes. The organic layer was separated, and the aqueous layer was extracted with  $EtOAc$  (3 x 50.0 mL). The organic extracts were combined, washed with saturated  $NaHCO_3$  (50 mL) and brine (50.0 mL),

dried over anhydrous  $\text{Na}_2\text{SO}_4$ , and concentrated *in vacuo*. Purification by chromatography on silica gel (4:1  $\rightarrow$  1:1 hexanes/EtOAc) afforded acetoxo ketone **239** as an amorphous white solid (0.260 g, 45%);  $R_f$  0.30 (1:1 hexanes/EtOAc);  $^1\text{H NMR}$  ( $\text{CDCl}_3$ , 600 MHz)  $\delta$  7.78 – 7.68 (m, 3H), 7.40 – 7.30 (m, 7H), 7.30 – 7.19 (m, 4H), 7.06 (t, 1H,  $J = 7.4$  Hz), 6.62 (t, 1H,  $J = 7.4$  Hz), 6.34 (d, 1H,  $J = 7.5$  Hz), 4.56 (d, 1H,  $J = 15.6$  Hz), 4.50 (d, 1H,  $J = 16.8$  Hz), 4.39 (d, 1H,  $J = 16.8$  Hz), 4.35 (s, 2H), 4.25 (d, 1H,  $J = 15.6$  Hz), 3.68 (td, 1H,  $J = 10.9, 7.0$  Hz), 3.46 – 3.37 (m, 3H), 3.29 (dd, 1H,  $J = 9.7, 5.9$  Hz), 3.15 (dd, 1H,  $J = 10.6, 7.4$  Hz), 1.93 – 1.80 (m, 2H), 1.34 (q, 1H,  $J = 10.7$  Hz);  $^{13}\text{C NMR}$  ( $\text{CDCl}_3$ , 150 MHz)  $\delta$  202.6, 170.2, 150.5, 143.9, 138.3, 137.9, 138.1, 131.1, 129.9, 128.8, 128.6, 128.0, 127.9, 127.9, 127.2, 124.3, 117.0, 105.7, 73.2, 70.9, 70.1, 59.4, 53.7, 48.0, 47.8, 42.6, 39.1, 37.4, 30.9, 27.3, 21.7, 20.7; **IR** (thin film,  $\text{cm}^{-1}$ ) 3029.8, 2925.3, 1750.3, 1731.8, 1599.2, 1483.5, 1161.5, 1091.0, 731.4 **HRMS** (+APCI) calculated for  $\text{C}_{25}\text{H}_{29}\text{N}_2\text{O}_3\text{S}$  437.1899, found 437.1895  $[\text{M}+\text{H}]^+$ ;

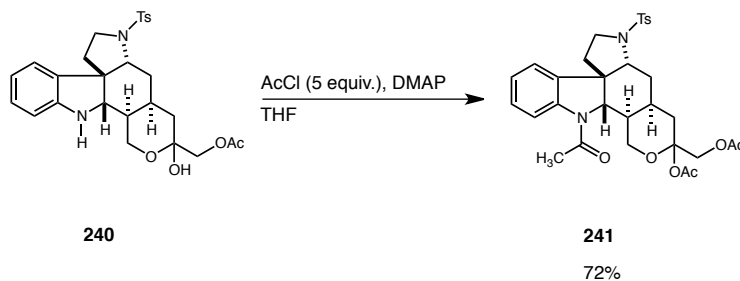
### Synthesis of hemiacetal **240**:



Palladium on carbon (5% wt, 0.307 mg, 0.144 mmol) was added to a solution of acetoxo ketone **239** (0.1 g, 0.140 mmol) in EtOAc (7.0 mL). The suspension was deoxygenated by sparging with nitrogen gas for 15 minutes. Subsequently hydrogen gas was bubbled

through the mixture for 15 minutes. The suspension was stirred for 2 hours under a hydrogen atmosphere (1 atm). The suspension was filtered through celite, and the filter cake was washed with EtOAc (3 x 70 mL). The organic layer was concentrated *in vacuo*. Purification by chromatography on silica gel (3:2 → 1:1 hexanes/EtOAc) afforded hemiacetal **240** as an amorphous white solid (0.058 g, 82%);  $R_f$  0.1 (1:1 hexanes/EtOAc);  $^1\text{H NMR}$  ( $\text{CDCl}_3$ , 600 MHz)  $\delta$  7.72 (d, 2H,  $J = 8.1$  Hz), 7.50 (dd, 1H,  $J = 7.7, 1.3$  Hz), 7.38 (d, 2H,  $J = 8.1$  Hz), 7.08 (td, 1H,  $J = 7.5, 1.0$  Hz), 7.72 (td, 1H,  $J = 7.5, 1.0$  Hz), 6.68 (d, 2H,  $J = 7.7$  Hz), 4.09 (d, 1H,  $J = 11.2$  Hz), 4.06 (dd, 1H,  $J = 12.1, 3.3$  Hz), 3.93 (d, 1H,  $J = 11.2$  Hz), 3.57 (d, 1H,  $J = 12.0$  Hz), 3.56 – 3.50 (m, 1H), 3.44 (d, 1H,  $J = 9.4$  Hz), 3.38 (at, 1H,  $J = 10.2$  Hz), 3.03 (dd, 1H,  $J = 12.9, 3.4$  Hz), 2.68 (bs, 1H), 2.49 (s, 3H), 2.35 (dt, 1H,  $J = 13.5, 3.0$  Hz), 2.15 (s, 3H), 2.02 (td, 1H,  $J = 13.2, 4.9$  Hz), 1.70 (dd, 1H,  $J = 10.8, 6.6$  Hz), 1.54 – 1.46 (m, 2H), 1.38 (t, 1H,  $J = 13.4$  Hz), 1.33 – 1.21 (m, 1H).;  $^{13}\text{C NMR}$  ( $\text{CDCl}_3$ , 150 MHz)  $\delta$  170.9, 149.0, 144.2, 132.5, 131.3, 130.0, 128.3, 128.1, 125.6, 120.0, 111.9, 95.0, 69.9, 62.6, 61.4, 60.6, 59.0, 55.9, 47.2, 38.2, 35.8, 31.7, 30.4, 28.3, 21.8, 21.0.; **IR** (thin film,  $\text{cm}^{-1}$ ) 3365.0, 2933.0, 1742.6, 1604.9, 1160.7, 1090.2, 751.4 **HRMS** (+APCI) calculated for  $\text{C}_{27}\text{H}_{33}\text{N}_2\text{O}_6\text{S}$  513.2054, found 513.2054  $[\text{M}+\text{H}]^+$ ;

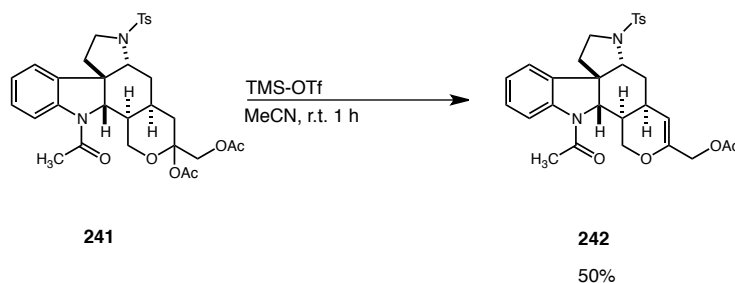
### Synthesis of bis acetoxy acetamide **241**:





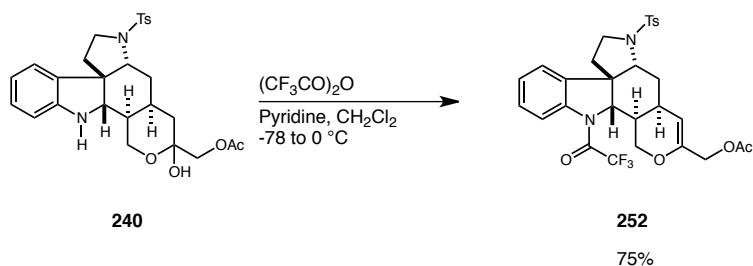
Acetyl chloride (0.021 mL, 0.29 mmol) was added dropwise to a solution of hemiacetal **240** (0.03 g, 0.059 mmol) and DMAP (0.039 g, 0.32 mmol) in THF (2.3 mL) at room temperature. The resulting mixture was stirred for 1 hour. The reaction was quenched with saturated aqueous NaHCO<sub>3</sub> (3 mL). The resulting biphasic mixture was stirred vigorously for 15 minutes. The organic layer was separated, and the aqueous layer was extracted with EtOAc (3 x 15 mL). The organic extracts were combined, washed with brine (10 mL), dried over anhydrous Na<sub>2</sub>SO<sub>4</sub>, and concentrated *in vacuo*. Purification by chromatography on silica gel (3:2 → 1:1 hexanes/EtOAc) afforded bis acetoxy acetamide **xxx** as an amorphous white solid (0.023 g, 72%); **R<sub>f</sub>** 0.32 (3:7 hexanes/EtOAc); **<sup>1</sup>H NMR** (CDCl<sub>3</sub>, 600 MHz) (1:0.7 mixture of rotamers) δ 7.98 (d, 1H, *J* = 7.8 Hz), 7.73 – 7.65 (m, 4.1H), 7.60 (d, 1H, *J* = 7.4 Hz), 7.40 (d, 3.4H, *J* = 8.0 Hz), 7.28 – 7.24 (m, 0.7H), 7.15 – 7.08 (m, 2.7H), 4.87 (d, 0.7H, *J* = 9.8 Hz), 4.16 – 4.08 (m, 3.7 H), 4.05 – 3.99 (m, 3.4H), 3.71 (d, 0.7H, *J* = 11.6), 3.61 (d, 1H, *J* = 11.6 Hz), 3.55 – 3.47 (m, 1.7 H), 3.42 – 3.32 (m, 1.7H), 3.09 (dd, 1H, *J* = 13.0, 3.6 Hz), 2.99 (dd, 1H, *J* = 13.0, 3.6 Hz), 2.73 (s, 1H), 2.63 (s, 0.7H), 2.50 (s, 5.1H), 2.40 – 2.30 (m, 3.8H), 2.23 (s, 2.1H) 2.19 – 2.11 (m, 5.1H), 1.99 (m, 1.7H), 1.64 (dd, 0.7H, *J* = 11.0, 7.6 Hz), 1.58 – 1.37 (m, 3.4H); **HRMS** (+APCI) calculated for C<sub>29</sub>H<sub>34</sub>N<sub>2</sub>NaO<sub>7</sub>S 577.1979, found 577.1980 [M-OAc+H<sub>2</sub>O+Na]<sup>+</sup>.

### Synthesis of unsaturated acetamide **242**:



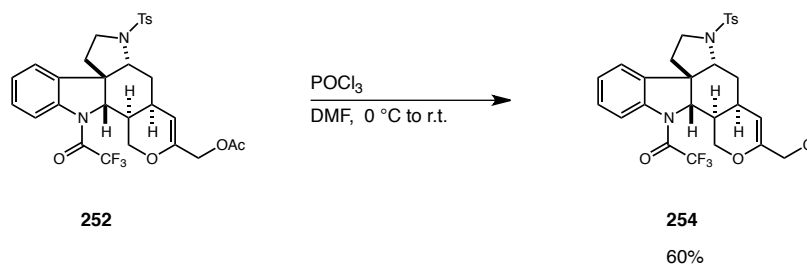
To a solution of bis-acetoxyacetamide **241** (0.018 g, 0.03 mmol) in CH<sub>3</sub>CN (0.1 mL) was added TMSOTf (0.05 mL, 0.68 mmol) and stirred for an additional 3 hours. The reaction was quenched with K<sub>2</sub>CO<sub>3</sub> and 1 mL of H<sub>2</sub>O. The volatiles were removed *in vacuo*. Purification by chromatography on silica gel (1:1 hexanes/EtOAc) afforded acetamide **242** (0.008 g, 50%); *R<sub>f</sub>* 0.80 (1:1 hexanes/EtOAc); <sup>1</sup>H NMR (CDCl<sub>3</sub>, 400 MHz) (1:0.8 mixture of rotamers) δ 8.00 (d, 1H, *J* = 7.9 Hz), 7.73 (at, 3.6, *J* = 8.1 Hz), 7.64 (d, 1H, *J* = 7.3 Hz), 7.56 (d, 0.8H, *J* = 7.4 Hz), 7.41 – 7.30 (m, 3.6H), 7.20 – 7.15 (m, 1.8H), 4.71 (d, 0.8H, *J* = 8.5 Hz), 4.68 (s, 1H), 4.62 (s, 0.8H), 4.48 – 4.35 (m, 4.6H), 4.31 (d, 0.8H, *J* = 9.5 Hz), 4.20 (d, 1H, *J* = 9.5 Hz), 4.02 (d, 1.8H, *J* = 8.6 Hz), 3.94 (d, 1H, *J* = 10.8 Hz), 3.84 (d, 0.8H, *J* = 10.8 Hz), 3.55 – 3.45 (m, 3.6H), 3.40 (t, 1.3H, *J* = 10.5 Hz), 3.07 (dd, 1H, *J* = 9.7, 3.1 Hz), 3.01 (dd, 0.8H, *J* = 9.7, 3.1 Hz), 2.85 – 2.68 (m, 1.8H), 2.55 – 2.40 (m, 7.2H), 2.37 (s, 2.8H), 2.28 (s, 3H), 2.15 – 1.80 (m, 7.6H), 1.75 – 1.60 (m, 1.8H); HRMS (+APCI) calculated for C<sub>29</sub>H<sub>32</sub>Na<sub>1</sub>N<sub>2</sub>O<sub>6</sub>S 559.1873, found 533.1875 [M+Na]<sup>+</sup>.

### Synthesis of trifluoroacetamide **252**:



A solution of hemiacetal **240** (0.058 g, 0.113 mmol) in CH<sub>2</sub>Cl<sub>2</sub> (6.0 mL) was cooled to -78 °C. Pyridine (0.05 mL, 0.68 mmol) was added, followed by dropwise addition of trifluoroacetic anhydride (0.05 mL, 0.34 mmol), and the resulting mixture was stirred

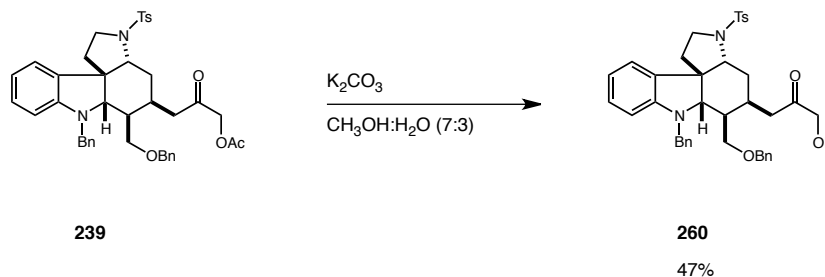
at -78 °C for 30 minutes. The reaction was then warmed to 0 °C and stirred for an additional 1 hour. The reaction was quenched with aqueous phosphate buffer (pH = 7.0, 10 mL). The resulting biphasic mixture was warmed to room temperature and stirred vigorously for 15 minutes. The organic layer was separated, and the aqueous layer was extracted with EtOAc (3 x 10 mL). The organic extracts were combined, washed with brine (20 mL), dried over anhydrous Na<sub>2</sub>SO<sub>4</sub>, and concentrated *in vacuo*. Purification by chromatography on silica gel (17:3 hexanes/EtOAc) afforded trifluoroacetamide **252** as an amorphous white solid (0.05 g, 75%); *R<sub>f</sub>* 0.80 (1:1 hexanes/EtOAc); <sup>1</sup>H NMR (CDCl<sub>3</sub>, 600 MHz) (1:0.3 mixture of rotamers) δ 7.94 (d, 1H, *J* = 7.9 Hz), 7.74 (ad, 2.9H, *J* = 7.8 Hz), 7.66 (d, 1.3H, *J* = 7.5 Hz), 7.40 (ad, 2.9H, *J* = 7.5 Hz), 7.35 (t, 1H, *J* = 7.5 Hz), 7.30 – 7.20 (m, 0.3H), 4.76 (d, 0.3H, *J* = 8.5 Hz), 4.62 (bs, 1.3H), 4.45 – 4.36 (m, 2.6H), 4.17 (d, 1H, *J* = 11.8 Hz), 3.89 (d, 1.3H, *J* = 11.8 Hz), 3.55 – 3.45 (m, 1.3H), 3.42 – 3.50 (m, 1.3H), 3.11 (dd, 1H, *J* = 12.6, 3.5 Hz), 3.02 (d, 0.3H, *J* = 12.6 Hz), 2.78 (s, 1.3H), 2.49 (bs, 3.9H), 2.09 (bs, 3.9H), 2.07 – 2.00 (m, 1H), 1.75 – 1.5 H(m, 3.9H); <sup>13</sup>C NMR (CDCl<sub>3</sub>, 150 MHz) (1:0.3 mixture of rotamers) 170.7, 155.0, 154.7, 150.8, 144.6, 140.8, 135.3, 132.4, 130.1, 128.8, 128.2, 128.1, 127.2, 126.9, 126.2, 125.7, 121.2, 117.2, 115.31, 103.3, 67.6, 66.5, 65.7, 63.9, 58.3, 55.4, 46.7, 36.2, 35.1, 34.9, 31.8, 30.2, 29.9, 21.9, 21.1; HRMS (+APCI) calculated for C<sub>29</sub>H<sub>29</sub>F<sub>3</sub>Na<sub>1</sub>N<sub>2</sub>O<sub>6</sub>S 613.1591, found 613.1596 [M+Na]<sup>+</sup>.

**Synthesis of chloride 254:**

Phosphoryl chloride (20  $\mu\text{L}$ , 0.22 mmol) was added dropwise to DMF (1.0 mL) at 0  $^{\circ}\text{C}$ , and the resulting mixture was stirred for 10 minutes. A solution of trifluoroacetamide **397** (0.022 g, 0.037 mmol) in DMF (0.2 mL) was added over 5 minutes to the Vilsmeier reagent solution, and the mixture was stirred at 0  $^{\circ}\text{C}$  for 30 minutes, warmed to room temperature and stirred for a further 30 minutes. The mixture was cooled to 0  $^{\circ}\text{C}$  and quenched with aqueous phosphate buffer (pH = 7.0, 5 mL). The resulting biphasic mixture was stirred vigorously for 15 minutes. The organic layer was separated, and the aqueous layer was extracted with EtOAc (3 x 5 mL). The organic extracts were combined, washed with water (3 x 5 mL), brine (5 mL), dried over anhydrous  $\text{Na}_2\text{SO}_4$ , and concentrated *in vacuo*. Purification by chromatography on silica gel (95:5  $\rightarrow$  7:3 hexanes/EtOAc) afforded chloride **254** (0.043 g, 60%);  $R_f$  0.6 (1:1 hexanes/EtOAc);  $^1\text{H NMR}$  (( $\text{CDCl}_3$ , 600 MHz)  $\delta$  7.94 (d,  $J = 7.9$  Hz, 1H), 7.74 (d,  $J = 8.0$  Hz, 2H), 7.67 (d,  $J = 7.6$  Hz, 1H), 7.41 (d,  $J = 7.8$  Hz, 2H), 7.36 (q,  $J = 8.1$  Hz, 1H), 7.29 – 7.25 (m, 4H), 4.71 (d,  $J = 16.2$  Hz, 2H), 4.36 (d,  $J = 8.3$  Hz, 1H), 4.21 (dd,  $J = 11.7, 2.4$  Hz, 1H), 4.12 (q,  $J = 7.2$  Hz, 1H), 3.90 – 3.87 (m, 4H), 3.52 (tt,  $J = 10.9, 6.8$  Hz, 2H), 3.46 – 3.39 (m, 2H), 3.08 (dd,  $J = 12.7, 3.4$  Hz, 1H), 3.00 (dt,  $J = 12.7, 3.6$  Hz, 0H), 2.79 (d,  $J = 6.0$  Hz, 2H), 2.54 – 2.46 (m, 6H), 2.08 (dd,  $J = 13.1, 4.9$  Hz, 1H), 1.71 (t,  $J = 7.3$  Hz, 1H),

1.61 (dd,  $J = 11.8, 6.9$  Hz, 2H). **HRMS** (+APCI) calculated for  $C_{27}H_{27}ClF_3N_2O_4S$  567.1327, found 567.1338  $[M+H]^+$ .

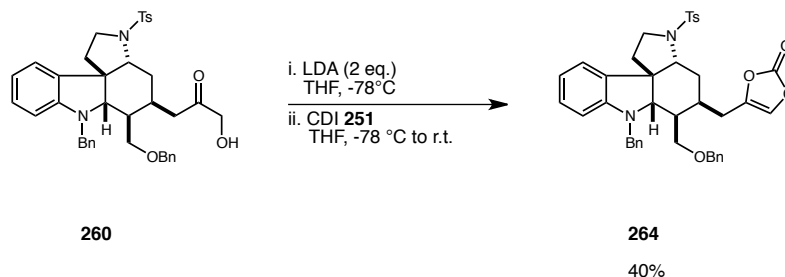
### Alpha hydroxy ketone **260**:



To solution of acetoxy ketone **239** (0.1 g, 0.158 mmol) in  $\text{CH}_3\text{OH}$  (2 mL) was added  $\text{H}_2\text{O}$  (0.4 mL) and  $\text{K}_2\text{CO}_3$  (0.17 g). The resulting mixture was stirred at room temperature for 1 hour, after which time  $\text{EtOAc}$  (5 mL) and  $\text{H}_2\text{O}$  (2 mL) were added. The organic layer was separated, and the aqueous layer was extracted with  $\text{EtOAc}$  (3 x 5 mL). The organic extracts were combined, washed with brine (5 mL), dried over anhydrous  $\text{Na}_2\text{SO}_4$ , and concentrated *in vacuo*. Purification by chromatography on silica gel (3:2  $\rightarrow$  1:1 hexanes/ $\text{EtOAc}$ ) afforded hydroxyl ketone **260** as a clear oil (0.047 g, 47%);  $R_f$  0.32 (3:7 hexanes/ $\text{EtOAc}$ );  $^1\text{H NMR}$  ( $\text{CDCl}_3$ , 600 MHz)  $\delta$  7.70 (d,  $J = 8.0$  Hz, 1H), 7.36 – 7.29 (m, 5H), 7.28 – 7.20 (m, 5H), 7.19 – 7.15 (m, 2H), 7.06 (dd,  $J = 7.8, 1.3$  Hz, 1H), 6.62 (dd,  $J = 7.8, 1.3$  Hz, 1H), 6.35 (d,  $J = 7.8$  Hz, 1H), 4.53 (d,  $J = 15.5$  Hz, 1H), 4.35 – 4.27 (m, 2H), 4.22 (d,  $J = 15.6$  Hz, 1H), 4.07 – 3.96 (m, 2H), 3.66 (td,  $J = 11.0, 7.1$  Hz, 1H), 3.43 – 3.35 (m, 2H), 3.26 (dd,  $J = 9.6, 6.0$  Hz, 1H), 3.15 – 3.08 (m, 1H), 2.99 (dd,  $J = 9.6, 4.8$  Hz, 1H), 2.53 – 2.44 (m, 1H), 2.43 (s, 3H), 2.37 – 2.28 (m, 1H), 2.22 – 2.09 (m, 2H), 2.10 – 2.01 (m, 1H), 1.88 – 1.76 (m, 2H).  $^{13}\text{C NMR}$  ( $\text{CDCl}_3$ , 150 MHz)  $\delta$  208.4, 150.4,

144.0, 138.3, 137.8, 133.0, 131.1, 129.9, 128.9, 128.7, 128.7, 128.2, 127.9, 127.8, 127.7, 127.6, 127.4, 124.4, 117.2, 105.8, 73.3, 70.9, 70.0, 68.2, 59.4, 53.8, 48.3, 47.8, 42.1, 39.7, 37.4, 31.0, 27.6, 21.8.

### Synthesis of carbonate **264**:

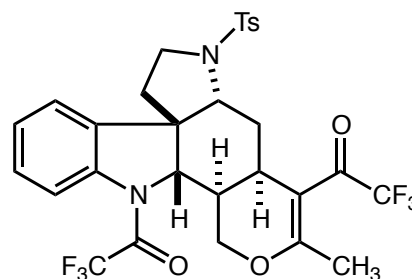
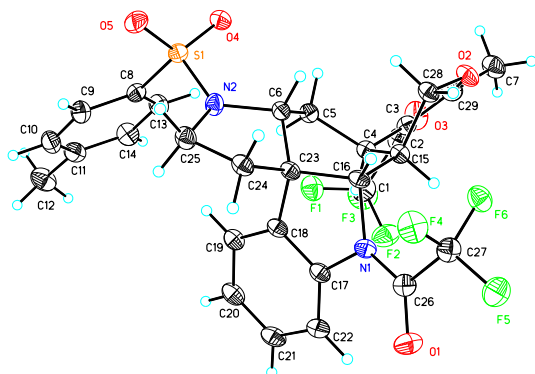


A solution of hydroxy ketone **260** (0.022 g, 0.035 mmol) in THF (1.0 mL) was added to a freshly prepared LDA solution (0.1 M in THF, 0.85 mL, 0.093 mmol) at -78 °C over 10 minutes *via* cannula. The reaction was stirred for 1 h at -78 °C. A solution of carbonyldiimidazole (**254**) (0.015 g, 0.09 mmol) in THF (1.0 mL) was added and the mixture was stirred for 1 h for -78 °C. The reaction was warmed to 0 °C and stirred for an additional 1 hour. The reaction was quenched with saturated aqueous NH<sub>4</sub>Cl (3.0 mL). H<sub>2</sub>O (3 mL) was added and the mixture was stirred for 5 minutes. The organic layer was separated, and the aqueous layer was extracted with Et<sub>2</sub>O (2 x 25 mL). The organic extracts were combined, washed with brine (12 mL), dried over anhydrous Na<sub>2</sub>SO<sub>4</sub>, and concentrated *in vacuo*. Purification by chromatography on silica gel (1:1 hexanes/EtOAc) afforded carbonate **264** as a colorless oil (0.091 g, 40%); **R<sub>f</sub>** 0.3 (7:3 hexanes/EtOAc); <sup>1</sup>H NMR (CDCl<sub>3</sub>, 600 MHz) δ 7.71 (d, 1H, *J* = 8Hz), 7.35 – 7.29 (m, 5H), 7.24 (d, 1H, *J* = 6.5 Hz), 7.20 (d, 1H, *J* = 6.5 Hz), 7.19 – 7.16 (m, 2H), 7.06 (d, 1H, *J* = 7.6 Hz), 6.33 (d, 1H, *J* = 7.6 Hz), 6.49 (s, 1H), 6.33 (d, 1H, *J* = 7.3 Hz), 4.46 (d, 2H, *J* = 15.7 Hz), 4.35 (q,

$J = 12.0$  Hz, 4H), 4.19 (d, 2H,  $J = 15.7$  Hz), 3.69 – 3.61 (m, 1H), 3.45 (s, 2H), 3.41 (dd, 1H,  $J = 11.2, 9.7$  Hz), 3.34 – 3.29 (m, 1H), 3.29 – 3.21 (m, 1H), 3.13 – 3.04 (m, 1H), 2.44 (s, 3H), 2.39 – 2.33 (m, 1H), 2.25 (dd, 1H,  $J = 15.8, 6.5$  Hz), 2.10 – 2.03 (m, 3H), 1.88 – 1.74 (m, 2H), 1.36 – 1.28 (m, 1H), 0.88 (dd, 1H,  $J = 15.8, 6.5$  Hz). **HRMS** (+APCI) calculated for  $C_{40}H_{41}N_2O_6S$  677.2680, found 677.2686  $[M+H]^+$ .

## 9.7 X-ray Structures-Part 3.

## Compound 195



195

Table 1. Crystal data and structure refinement for DM\_237.

Identification code	dm_237	
Empirical formula	C <sub>29</sub> H <sub>26</sub> F <sub>6</sub> N <sub>2</sub> O <sub>5</sub> S	
Formula weight	628.58	
Temperature	173(2) K	
Wavelength	1.54178 Å	
Crystal system	Triclinic	
Space group	P-1	
Unit cell dimensions	a = 9.3739(4) Å	∠ = 67.151(3)°.
	b = 11.8076(5) Å	∠ = 82.577(3)°.
	c = 13.6198(5) Å	∠ = 84.940(3)°.
Volume	1376.36(10) Å <sup>3</sup>	
Z	2	
Density (calculated)	1.517 Mg/m <sup>3</sup>	
Absorption coefficient	1.809 mm <sup>-1</sup>	
F(000)	648	
Crystal size	0.05 x 0.04 x 0.02 mm <sup>3</sup>	
Theta range for data collection	3.54 to 67.50°.	
Index ranges	-11 ≤ h ≤ 11, -13 ≤ k ≤ 13, -15 ≤ l ≤ 16	



Reflections collected	16646
Independent reflections	4606 [R(int) = 0.0282]
Completeness to theta = 67.50°	92.8 %
Absorption correction	Semi-empirical from equivalents
Max. and min. transmission	0.9647 and 0.9150
Refinement method	Full-matrix least-squares on F <sup>2</sup>
Data / restraints / parameters	4606 / 0 / 388
Goodness-of-fit on F <sup>2</sup>	1.024
Final R indices [I>2sigma(I)]	R1 = 0.0412, wR2 = 0.1087
R indices (all data)	R1 = 0.0515, wR2 = 0.1147
Largest diff. peak and hole	0.330 and -0.417 e.Å <sup>-3</sup>

Table 2. Atomic coordinates ( $\times 10^4$ ) and equivalent isotropic displacement parameters ( $\text{\AA}^2 \times 10^3$ ) for DM\_237.  $U(\text{eq})$  is defined as one third of the trace of the orthogonalized  $U^{ij}$  tensor.

	x	y	z	U(eq)
C(1)	7529(3)	-380(2)	9489(2)	49(1)
C(2)	6117(3)	-579(2)	9104(2)	42(1)
C(3)	5910(2)	26(2)	7970(2)	34(1)
C(4)	6771(2)	1136(2)	7257(2)	30(1)
C(5)	6079(2)	2331(2)	7389(2)	32(1)
C(6)	6294(2)	3446(2)	6346(2)	29(1)
C(7)	4065(3)	-1528(2)	8140(2)	50(1)
C(8)	6142(2)	5401(2)	8045(2)	34(1)
C(9)	6860(3)	6479(2)	7780(2)	41(1)
C(10)	7629(3)	6605(2)	8531(2)	46(1)
C(11)	7700(3)	5675(2)	9541(2)	44(1)
C(12)	8472(3)	5840(3)	10374(2)	60(1)
C(13)	6220(3)	4455(2)	9033(2)	41(1)
C(14)	6997(3)	4596(2)	9774(2)	47(1)
C(15)	6901(2)	1209(2)	6090(2)	29(1)
C(16)	7725(2)	2342(2)	5276(2)	29(1)
C(17)	9970(2)	2237(2)	5928(2)	31(1)
C(18)	9055(2)	2998(2)	6314(2)	30(1)
C(19)	9449(2)	3311(2)	7119(2)	36(1)
C(20)	10774(3)	2857(2)	7516(2)	42(1)
C(21)	11670(2)	2113(2)	7109(2)	41(1)
C(22)	11289(2)	1787(2)	6305(2)	37(1)
C(23)	7728(2)	3367(2)	5699(2)	28(1)
C(24)	7856(2)	4689(2)	4864(2)	34(1)
C(25)	7367(3)	5465(2)	5529(2)	38(1)
C(26)	10007(2)	1633(2)	4392(2)	35(1)
C(27)	9130(3)	1608(2)	3522(2)	39(1)
C(28)	5410(2)	1155(2)	5794(2)	33(1)
C(29)	4967(2)	-437(2)	7558(2)	37(1)
F(1)	7718(2)	795(1)	9321(1)	56(1)
F(2)	8689(2)	-751(2)	8981(1)	65(1)

F(3)	7558(2)	-1018(2)	10522(1)	78(1)
F(4)	8805(2)	2753(1)	2853(1)	53(1)
F(5)	9894(2)	1039(2)	2945(1)	57(1)
F(6)	7896(1)	1032(1)	3909(1)	45(1)
N(1)	9289(2)	2005(2)	5144(1)	31(1)
N(2)	6376(2)	4660(2)	6412(2)	35(1)
O(1)	11290(2)	1356(2)	4330(1)	48(1)
O(2)	4736(2)	37(1)	6513(1)	40(1)
O(3)	5316(2)	-1287(2)	9802(1)	60(1)
O(4)	4125(2)	4340(1)	7605(1)	41(1)
O(5)	4757(2)	6454(1)	6385(1)	45(1)
S(1)	5188(1)	5237(1)	7079(1)	34(1)

---

Table 3. Bond lengths [ $\text{\AA}$ ] and angles [ $^\circ$ ] for DM\_237.

---

C(1)-F(3)	1.316(3)
C(1)-F(1)	1.340(3)
C(1)-F(2)	1.345(3)
C(1)-C(2)	1.553(4)
C(2)-O(3)	1.214(3)
C(2)-C(3)	1.458(3)
C(3)-C(29)	1.359(3)
C(3)-C(4)	1.519(3)
C(4)-C(15)	1.547(3)
C(4)-C(5)	1.564(3)
C(4)-H(4)	1.0000
C(5)-C(6)	1.520(3)
C(5)-H(5A)	0.9900
C(5)-H(5B)	0.9900
C(6)-N(2)	1.480(3)
C(6)-C(23)	1.526(3)
C(6)-H(6)	1.0000
C(7)-C(29)	1.493(3)
C(7)-H(2A)	0.9800
C(7)-H(2B)	0.9800
C(7)-H(2C)	0.9800
C(8)-C(13)	1.381(3)
C(8)-C(9)	1.392(3)
C(8)-S(1)	1.761(2)
C(9)-C(10)	1.383(3)
C(9)-H(9)	0.9500
C(10)-C(11)	1.393(4)
C(10)-H(10)	0.9500
C(11)-C(14)	1.392(4)
C(11)-C(12)	1.502(3)
C(12)-H(12A)	0.9800
C(12)-H(12B)	0.9800
C(12)-H(12C)	0.9800
C(13)-C(14)	1.386(3)

C(13)-H(13)	0.9500
C(14)-H(14)	0.9500
C(15)-C(28)	1.518(3)
C(15)-C(16)	1.557(3)
C(15)-H(15)	1.0000
C(16)-N(1)	1.491(3)
C(16)-C(23)	1.530(3)
C(16)-H(16)	1.0000
C(17)-C(22)	1.382(3)
C(17)-C(18)	1.390(3)
C(17)-N(1)	1.436(3)
C(18)-C(19)	1.385(3)
C(18)-C(23)	1.526(3)
C(19)-C(20)	1.398(3)
C(19)-H(19)	0.9500
C(20)-C(21)	1.383(3)
C(20)-H(20)	0.9500
C(21)-C(22)	1.388(3)
C(21)-H(21)	0.9500
C(22)-H(22)	0.9500
C(23)-C(24)	1.537(3)
C(24)-C(25)	1.527(3)
C(24)-H(24A)	0.9900
C(24)-H(24B)	0.9900
C(25)-N(2)	1.481(3)
C(25)-H(25A)	0.9900
C(25)-H(25B)	0.9900
C(26)-O(1)	1.219(3)
C(26)-N(1)	1.346(3)
C(26)-C(27)	1.538(3)
C(27)-F(5)	1.328(3)
C(27)-F(6)	1.334(3)
C(27)-F(4)	1.339(3)
C(28)-O(2)	1.443(2)
C(28)-H(28A)	0.9900
C(28)-H(28B)	0.9900

C(29)-O(2)	1.352(3)
N(2)-S(1)	1.6163(19)
O(4)-S(1)	1.4286(16)
O(5)-S(1)	1.4359(16)
F(3)-C(1)-F(1)	106.9(2)
F(3)-C(1)-F(2)	107.4(2)
F(1)-C(1)-F(2)	106.5(2)
F(3)-C(1)-C(2)	110.9(2)
F(1)-C(1)-C(2)	113.8(2)
F(2)-C(1)-C(2)	110.9(2)
O(3)-C(2)-C(3)	126.8(2)
O(3)-C(2)-C(1)	114.3(2)
C(3)-C(2)-C(1)	118.8(2)
C(29)-C(3)-C(2)	119.1(2)
C(29)-C(3)-C(4)	120.7(2)
C(2)-C(3)-C(4)	120.3(2)
C(3)-C(4)-C(15)	108.69(17)
C(3)-C(4)-C(5)	110.62(16)
C(15)-C(4)-C(5)	113.40(17)
C(3)-C(4)-H(4)	108.0
C(15)-C(4)-H(4)	108.0
C(5)-C(4)-H(4)	108.0
C(6)-C(5)-C(4)	111.18(16)
C(6)-C(5)-H(5A)	109.4
C(4)-C(5)-H(5A)	109.4
C(6)-C(5)-H(5B)	109.4
C(4)-C(5)-H(5B)	109.4
H(5A)-C(5)-H(5B)	108.0
N(2)-C(6)-C(5)	117.89(17)
N(2)-C(6)-C(23)	100.88(16)
C(5)-C(6)-C(23)	112.44(17)
N(2)-C(6)-H(6)	108.4
C(5)-C(6)-H(6)	108.4
C(23)-C(6)-H(6)	108.4
C(29)-C(7)-H(2A)	109.5

C(29)-C(7)-H(2B)	109.5
H(2A)-C(7)-H(2B)	109.5
C(29)-C(7)-H(2C)	109.5
H(2A)-C(7)-H(2C)	109.5
H(2B)-C(7)-H(2C)	109.5
C(13)-C(8)-C(9)	120.7(2)
C(13)-C(8)-S(1)	120.41(17)
C(9)-C(8)-S(1)	118.85(18)
C(10)-C(9)-C(8)	119.1(2)
C(10)-C(9)-H(9)	120.5
C(8)-C(9)-H(9)	120.5
C(9)-C(10)-C(11)	121.4(2)
C(9)-C(10)-H(10)	119.3
C(11)-C(10)-H(10)	119.3
C(14)-C(11)-C(10)	118.2(2)
C(14)-C(11)-C(12)	120.5(2)
C(10)-C(11)-C(12)	121.2(2)
C(11)-C(12)-H(12A)	109.5
C(11)-C(12)-H(12B)	109.5
H(12A)-C(12)-H(12B)	109.5
C(11)-C(12)-H(12C)	109.5
H(12A)-C(12)-H(12C)	109.5
H(12B)-C(12)-H(12C)	109.5
C(8)-C(13)-C(14)	119.4(2)
C(8)-C(13)-H(13)	120.3
C(14)-C(13)-H(13)	120.3
C(13)-C(14)-C(11)	121.2(2)
C(13)-C(14)-H(14)	119.4
C(11)-C(14)-H(14)	119.4
C(28)-C(15)-C(4)	108.89(17)
C(28)-C(15)-C(16)	112.62(16)
C(4)-C(15)-C(16)	113.34(16)
C(28)-C(15)-H(15)	107.2
C(4)-C(15)-H(15)	107.2
C(16)-C(15)-H(15)	107.2
N(1)-C(16)-C(23)	102.38(15)

N(1)-C(16)-C(15)	110.02(16)
C(23)-C(16)-C(15)	112.19(16)
N(1)-C(16)-H(16)	110.7
C(23)-C(16)-H(16)	110.7
C(15)-C(16)-H(16)	110.7
C(22)-C(17)-C(18)	122.5(2)
C(22)-C(17)-N(1)	128.6(2)
C(18)-C(17)-N(1)	108.80(18)
C(19)-C(18)-C(17)	119.7(2)
C(19)-C(18)-C(23)	131.3(2)
C(17)-C(18)-C(23)	109.05(18)
C(18)-C(19)-C(20)	118.7(2)
C(18)-C(19)-H(19)	120.7
C(20)-C(19)-H(19)	120.7
C(21)-C(20)-C(19)	120.4(2)
C(21)-C(20)-H(20)	119.8
C(19)-C(20)-H(20)	119.8
C(20)-C(21)-C(22)	121.7(2)
C(20)-C(21)-H(21)	119.1
C(22)-C(21)-H(21)	119.1
C(17)-C(22)-C(21)	117.0(2)
C(17)-C(22)-H(22)	121.5
C(21)-C(22)-H(22)	121.5
C(18)-C(23)-C(6)	116.41(16)
C(18)-C(23)-C(16)	101.88(16)
C(6)-C(23)-C(16)	110.23(16)
C(18)-C(23)-C(24)	109.63(16)
C(6)-C(23)-C(24)	102.27(16)
C(16)-C(23)-C(24)	117.06(17)
C(25)-C(24)-C(23)	102.72(16)
C(25)-C(24)-H(24A)	111.2
C(23)-C(24)-H(24A)	111.2
C(25)-C(24)-H(24B)	111.2
C(23)-C(24)-H(24B)	111.2
H(24A)-C(24)-H(24B)	109.1
N(2)-C(25)-C(24)	103.33(16)



N(2)-C(25)-H(25A)	111.1
C(24)-C(25)-H(25A)	111.1
N(2)-C(25)-H(25B)	111.1
C(24)-C(25)-H(25B)	111.1
H(25A)-C(25)-H(25B)	109.1
O(1)-C(26)-N(1)	125.5(2)
O(1)-C(26)-C(27)	118.1(2)
N(1)-C(26)-C(27)	116.42(19)
F(5)-C(27)-F(6)	107.16(18)
F(5)-C(27)-F(4)	107.52(18)
F(6)-C(27)-F(4)	107.41(19)
F(5)-C(27)-C(26)	110.04(19)
F(6)-C(27)-C(26)	113.80(17)
F(4)-C(27)-C(26)	110.65(18)
O(2)-C(28)-C(15)	110.79(17)
O(2)-C(28)-H(28A)	109.5
C(15)-C(28)-H(28A)	109.5
O(2)-C(28)-H(28B)	109.5
C(15)-C(28)-H(28B)	109.5
H(28A)-C(28)-H(28B)	108.1
O(2)-C(29)-C(3)	123.39(19)
O(2)-C(29)-C(7)	109.2(2)
C(3)-C(29)-C(7)	127.4(2)
C(26)-N(1)-C(17)	123.81(18)
C(26)-N(1)-C(16)	128.32(18)
C(17)-N(1)-C(16)	107.71(16)
C(6)-N(2)-C(25)	111.73(16)
C(6)-N(2)-S(1)	124.70(14)
C(25)-N(2)-S(1)	120.59(14)
C(29)-O(2)-C(28)	119.80(16)
O(4)-S(1)-O(5)	119.59(10)
O(4)-S(1)-N(2)	107.07(9)
O(5)-S(1)-N(2)	108.86(10)
O(4)-S(1)-C(8)	109.20(10)
O(5)-S(1)-C(8)	106.90(10)
N(2)-S(1)-C(8)	104.19(10)

---

Symmetry transformations used to generate equivalent atoms:

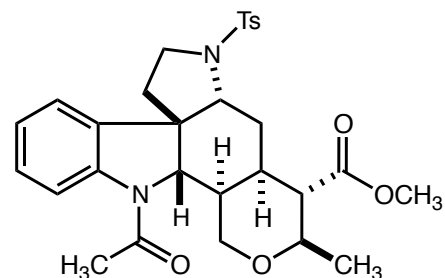
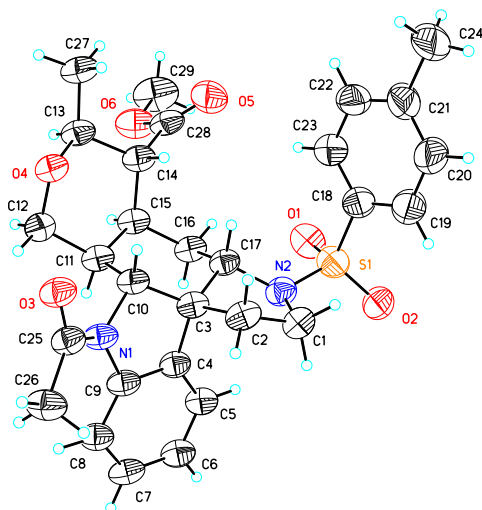
Table 4. Anisotropic displacement parameters ( $\text{\AA}^2 \times 10^3$ ) for DM\_237. The anisotropic displacement factor exponent takes the form:  $-2\pi^2 [ h^2 a^{*2} U^{11} + \dots + 2 h k a^* b^* U^{12} ]$

	U <sup>11</sup>	U <sup>22</sup>	U <sup>33</sup>	U <sup>23</sup>	U <sup>13</sup>	U <sup>12</sup>
C(1)	63(2)	47(2)	29(1)	-6(1)	-10(1)	4(1)
C(2)	52(2)	34(1)	35(1)	-9(1)	2(1)	-3(1)
C(3)	36(1)	29(1)	31(1)	-6(1)	0(1)	-1(1)
C(4)	30(1)	30(1)	26(1)	-6(1)	-5(1)	-2(1)
C(5)	32(1)	32(1)	29(1)	-9(1)	0(1)	-5(1)
C(6)	29(1)	27(1)	30(1)	-9(1)	-6(1)	-3(1)
C(7)	47(2)	40(1)	53(2)	-5(1)	-4(1)	-15(1)
C(8)	33(1)	34(1)	35(1)	-15(1)	-2(1)	2(1)
C(9)	45(1)	36(1)	41(1)	-13(1)	-3(1)	-5(1)
C(10)	46(1)	44(1)	51(2)	-21(1)	-2(1)	-11(1)
C(11)	38(1)	59(2)	43(1)	-28(1)	-1(1)	-5(1)
C(12)	55(2)	85(2)	51(2)	-36(2)	-7(1)	-13(2)
C(13)	46(1)	38(1)	39(1)	-11(1)	-7(1)	-7(1)
C(14)	53(2)	49(2)	36(1)	-11(1)	-6(1)	-6(1)
C(15)	30(1)	29(1)	26(1)	-7(1)	-5(1)	-3(1)
C(16)	25(1)	34(1)	25(1)	-7(1)	-6(1)	-3(1)
C(17)	30(1)	34(1)	26(1)	-7(1)	-3(1)	-8(1)
C(18)	28(1)	32(1)	25(1)	-4(1)	-3(1)	-7(1)
C(19)	37(1)	38(1)	30(1)	-10(1)	-6(1)	-7(1)
C(20)	42(1)	52(1)	32(1)	-12(1)	-11(1)	-12(1)
C(21)	32(1)	50(1)	34(1)	-5(1)	-13(1)	-5(1)
C(22)	30(1)	41(1)	34(1)	-8(1)	-5(1)	-3(1)
C(23)	27(1)	30(1)	25(1)	-7(1)	-5(1)	-5(1)
C(24)	33(1)	34(1)	29(1)	-5(1)	-4(1)	-7(1)
C(25)	41(1)	30(1)	38(1)	-6(1)	-3(1)	-8(1)
C(26)	37(1)	33(1)	28(1)	-6(1)	-2(1)	-2(1)
C(27)	42(1)	42(1)	31(1)	-14(1)	2(1)	-3(1)
C(28)	32(1)	33(1)	30(1)	-6(1)	-5(1)	-7(1)

C(29)	33(1)	32(1)	37(1)	-7(1)	-1(1)	-1(1)
F(1)	66(1)	57(1)	49(1)	-20(1)	-18(1)	-4(1)
F(2)	58(1)	78(1)	59(1)	-28(1)	-16(1)	18(1)
F(3)	105(2)	79(1)	32(1)	1(1)	-22(1)	-1(1)
F(4)	69(1)	50(1)	32(1)	-4(1)	-14(1)	-3(1)
F(5)	60(1)	74(1)	48(1)	-37(1)	4(1)	-3(1)
F(6)	48(1)	53(1)	39(1)	-20(1)	-4(1)	-11(1)
N(1)	28(1)	36(1)	27(1)	-10(1)	-4(1)	-2(1)
N(2)	41(1)	28(1)	37(1)	-12(1)	2(1)	-6(1)
O(1)	37(1)	64(1)	45(1)	-23(1)	-3(1)	8(1)
O(2)	37(1)	36(1)	41(1)	-5(1)	-9(1)	-12(1)
O(3)	83(1)	51(1)	37(1)	-7(1)	11(1)	-23(1)
O(4)	32(1)	44(1)	48(1)	-19(1)	0(1)	-6(1)
O(5)	47(1)	37(1)	49(1)	-11(1)	-17(1)	9(1)
S(1)	33(1)	32(1)	37(1)	-12(1)	-8(1)	1(1)

---

## Compound 205



**205**

Table 1. Crystal data and structure refinement for DM\_II\_253.

Identification code	dm_ii_253	
Empirical formula	C <sub>29</sub> H <sub>34</sub> N <sub>2</sub> O <sub>6</sub> S	
Formula weight	538.64	
Temperature	173(2) K	
Wavelength	1.54178 Å	
Crystal system	Tetragonal	
Space group	I4(1)/a	
Unit cell dimensions	a = 29.2891(19) Å	∠ = 90°.
	b = 29.2891(19) Å	∠ = 90°.
	c = 18.1917(13) Å	∠ = 90°.
Volume	15605.8(18) Å <sup>3</sup>	
Z	16	
Density (calculated)	0.917 Mg/m <sup>3</sup>	
Absorption coefficient	1.002 mm <sup>-1</sup>	
F(000)	4576	
Crystal size	0.36 x 0.23 x 0.11 mm <sup>3</sup>	
Theta range for data collection	2.86 to 66.59°.	

Index ranges	-32<=h<=31, -33<=k<=29, -21<=l<=21
Reflections collected	39388
Independent reflections	6619 [R(int) = 0.1214]
Completeness to theta = 66.59°	96.1 %
Absorption correction	Semi-empirical from equivalents
Max. and min. transmission	0.8978 and 0.7144
Refinement method	Full-matrix least-squares on F <sup>2</sup>
Data / restraints / parameters	6619 / 0 / 344
Goodness-of-fit on F <sup>2</sup>	1.092
Final R indices [I>2sigma(I)]	R1 = 0.1524, wR2 = 0.3671
R indices (all data)	R1 = 0.2510, wR2 = 0.4339
Extinction coefficient	0.00160(16)
Largest diff. peak and hole	1.195 and -0.431 e.Å <sup>-3</sup>

Table 2. Atomic coordinates ( $\times 10^4$ ) and equivalent isotropic displacement parameters ( $\text{\AA}^2 \times 10^3$ ) for DM\_II\_253.  $U(\text{eq})$  is defined as one third of the trace of the orthogonalized  $U^{ij}$  tensor.

	x	y	z	U(eq)
C(1)	5406(3)	3545(3)	626(6)	104(3)
C(2)	5161(3)	3945(3)	248(5)	96(3)
C(3)	5520(3)	4111(3)	-332(5)	82(2)
C(4)	5483(3)	3795(3)	-996(5)	84(2)
C(5)	5632(3)	3347(3)	-1129(5)	90(2)
C(6)	5514(3)	3130(3)	-1770(6)	98(3)
C(7)	5261(3)	3351(3)	-2303(6)	97(3)
C(8)	5111(3)	3803(3)	-2193(5)	94(3)
C(9)	5218(3)	4008(3)	-1519(5)	87(2)
C(10)	5440(3)	4570(3)	-687(5)	82(2)
C(11)	5887(3)	4745(3)	-1082(5)	86(2)
C(12)	5823(3)	5239(3)	-1363(5)	94(3)
C(13)	6292(3)	5560(3)	-417(5)	96(3)
C(14)	6362(3)	5086(3)	-45(5)	91(3)
C(15)	6326(3)	4695(3)	-618(5)	86(2)
C(16)	6374(3)	4210(3)	-288(5)	89(2)
C(17)	5946(3)	4102(3)	145(5)	84(2)
C(18)	6153(4)	3812(4)	1927(6)	110(3)
C(19)	5858(5)	3661(4)	2482(7)	148(5)
C(20)	5797(6)	3932(5)	3099(7)	167(6)
C(21)	5999(6)	4349(5)	3184(7)	153(5)
C(22)	6289(5)	4494(4)	2633(7)	131(4)
C(23)	6368(4)	4233(4)	1995(6)	115(3)
C(24)	5931(7)	4636(5)	3882(7)	200(7)
C(25)	4711(3)	4718(3)	-1383(5)	88(2)
C(26)	4351(3)	4532(3)	-1885(6)	110(3)
C(27)	6291(3)	5957(3)	118(6)	113(3)
C(28)	6815(4)	5073(3)	360(8)	107(3)
C(29)	7630(3)	5124(4)	167(8)	165(5)
N(1)	5104(2)	4466(2)	-1281(4)	84(2)
N(2)	5908(3)	3645(2)	497(4)	98(2)

O(1)	6710(2)	3573(3)	894(4)	126(2)
O(2)	6122(3)	3007(2)	1328(4)	137(3)
O(3)	4661(2)	5081(2)	-1056(3)	97(2)
O(4)	5847(2)	5560(2)	-761(3)	92(2)
O(5)	6869(3)	5030(3)	1000(5)	143(3)
O(6)	7168(2)	5134(2)	-132(4)	129(3)
S(1)	6254(1)	3472(1)	1147(2)	115(1)

---

Table 3. Bond lengths [ $\text{\AA}$ ] and angles [ $^\circ$ ] for DM\_II\_253.

---

C(1)-N(2)	1.519(11)
C(1)-C(2)	1.537(12)
C(1)-H(1A)	0.9900
C(1)-H(1B)	0.9900
C(2)-C(3)	1.567(11)
C(2)-H(2A)	0.9900
C(2)-H(2B)	0.9900
C(3)-C(10)	1.511(11)
C(3)-C(17)	1.520(11)
C(3)-C(4)	1.525(11)
C(4)-C(9)	1.376(11)
C(4)-C(5)	1.403(11)
C(5)-C(6)	1.374(11)
C(5)-H(5A)	0.9500
C(6)-C(7)	1.382(12)
C(6)-H(6A)	0.9500
C(7)-C(8)	1.408(11)
C(7)-H(7A)	0.9500
C(8)-C(9)	1.400(11)
C(8)-H(8A)	0.9500
C(9)-N(1)	1.448(9)
C(10)-N(1)	1.494(9)
C(10)-C(11)	1.578(11)
C(10)-H(10A)	1.0000
C(11)-C(15)	1.544(11)
C(11)-C(12)	1.546(11)
C(11)-H(11A)	1.0000
C(12)-O(4)	1.444(9)
C(12)-H(12A)	0.9900
C(12)-H(12B)	0.9900
C(13)-O(4)	1.445(9)
C(13)-C(27)	1.518(11)
C(13)-C(14)	1.557(11)
C(13)-H(13A)	1.0000



C(14)-C(28)	1.519(13)
C(14)-C(15)	1.553(11)
C(14)-H(14A)	1.0000
C(15)-C(16)	1.549(11)
C(15)-H(15A)	1.0000
C(16)-C(17)	1.514(11)
C(16)-H(16A)	0.9900
C(16)-H(16B)	0.9900
C(17)-N(2)	1.488(10)
C(17)-H(17A)	1.0000
C(18)-C(23)	1.390(14)
C(18)-C(19)	1.401(15)
C(18)-S(1)	1.759(10)
C(19)-C(20)	1.388(16)
C(19)-H(19A)	0.9500
C(20)-C(21)	1.365(17)
C(20)-H(20A)	0.9500
C(21)-C(22)	1.382(16)
C(21)-C(24)	1.536(15)
C(22)-C(23)	1.409(14)
C(22)-H(22A)	0.9500
C(23)-H(23A)	0.9500
C(24)-H(24A)	0.9800
C(24)-H(24B)	0.9800
C(24)-H(24C)	0.9800
C(25)-O(3)	1.225(9)
C(25)-N(1)	1.380(10)
C(25)-C(26)	1.498(11)
C(26)-H(26A)	0.9800
C(26)-H(26B)	0.9800
C(26)-H(26C)	0.9800
C(27)-H(27A)	0.9800
C(27)-H(27B)	0.9800
C(27)-H(27C)	0.9800
C(28)-O(5)	1.182(12)
C(28)-O(6)	1.377(13)

C(29)-O(6)	1.460(11)
C(29)-H(29A)	0.9800
C(29)-H(29B)	0.9800
C(29)-H(29C)	0.9800
N(2)-S(1)	1.636(8)
O(1)-S(1)	1.445(7)
O(2)-S(1)	1.453(7)
N(2)-C(1)-C(2)	103.7(7)
N(2)-C(1)-H(1A)	111.0
C(2)-C(1)-H(1A)	111.0
N(2)-C(1)-H(1B)	111.0
C(2)-C(1)-H(1B)	111.0
H(1A)-C(1)-H(1B)	109.0
C(1)-C(2)-C(3)	102.9(7)
C(1)-C(2)-H(2A)	111.2
C(3)-C(2)-H(2A)	111.2
C(1)-C(2)-H(2B)	111.2
C(3)-C(2)-H(2B)	111.2
H(2A)-C(2)-H(2B)	109.1
C(10)-C(3)-C(17)	112.7(6)
C(10)-C(3)-C(4)	100.9(7)
C(17)-C(3)-C(4)	120.1(7)
C(10)-C(3)-C(2)	117.4(7)
C(17)-C(3)-C(2)	99.3(7)
C(4)-C(3)-C(2)	107.4(7)
C(9)-C(4)-C(5)	118.7(8)
C(9)-C(4)-C(3)	108.3(7)
C(5)-C(4)-C(3)	132.9(8)
C(6)-C(5)-C(4)	120.1(9)
C(6)-C(5)-H(5A)	119.9
C(4)-C(5)-H(5A)	119.9
C(5)-C(6)-C(7)	120.8(9)
C(5)-C(6)-H(6A)	119.6
C(7)-C(6)-H(6A)	119.6
C(6)-C(7)-C(8)	120.5(9)

C(6)-C(7)-H(7A)	119.7
C(8)-C(7)-H(7A)	119.7
C(9)-C(8)-C(7)	117.3(9)
C(9)-C(8)-H(8A)	121.3
C(7)-C(8)-H(8A)	121.3
C(4)-C(9)-C(8)	122.4(8)
C(4)-C(9)-N(1)	110.1(7)
C(8)-C(9)-N(1)	127.4(9)
N(1)-C(10)-C(3)	103.3(6)
N(1)-C(10)-C(11)	106.5(7)
C(3)-C(10)-C(11)	110.9(6)
N(1)-C(10)-H(10A)	111.9
C(3)-C(10)-H(10A)	111.9
C(11)-C(10)-H(10A)	111.9
C(15)-C(11)-C(12)	111.8(7)
C(15)-C(11)-C(10)	114.2(7)
C(12)-C(11)-C(10)	110.8(7)
C(15)-C(11)-H(11A)	106.5
C(12)-C(11)-H(11A)	106.5
C(10)-C(11)-H(11A)	106.5
O(4)-C(12)-C(11)	110.5(7)
O(4)-C(12)-H(12A)	109.5
C(11)-C(12)-H(12A)	109.5
O(4)-C(12)-H(12B)	109.5
C(11)-C(12)-H(12B)	109.5
H(12A)-C(12)-H(12B)	108.1
O(4)-C(13)-C(27)	106.1(7)
O(4)-C(13)-C(14)	107.9(6)
C(27)-C(13)-C(14)	113.9(8)
O(4)-C(13)-H(13A)	109.6
C(27)-C(13)-H(13A)	109.6
C(14)-C(13)-H(13A)	109.6
C(28)-C(14)-C(15)	111.4(7)
C(28)-C(14)-C(13)	110.5(7)
C(15)-C(14)-C(13)	110.9(7)
C(28)-C(14)-H(14A)	108.0

C(15)-C(14)-H(14A)	108.0
C(13)-C(14)-H(14A)	108.0
C(11)-C(15)-C(16)	112.1(6)
C(11)-C(15)-C(14)	110.7(6)
C(16)-C(15)-C(14)	114.3(7)
C(11)-C(15)-H(15A)	106.4
C(16)-C(15)-H(15A)	106.4
C(14)-C(15)-H(15A)	106.4
C(17)-C(16)-C(15)	108.5(7)
C(17)-C(16)-H(16A)	110.0
C(15)-C(16)-H(16A)	110.0
C(17)-C(16)-H(16B)	110.0
C(15)-C(16)-H(16B)	110.0
H(16A)-C(16)-H(16B)	108.4
N(2)-C(17)-C(16)	118.2(7)
N(2)-C(17)-C(3)	101.5(6)
C(16)-C(17)-C(3)	112.2(7)
N(2)-C(17)-H(17A)	108.1
C(16)-C(17)-H(17A)	108.1
C(3)-C(17)-H(17A)	108.1
C(23)-C(18)-C(19)	119.8(10)
C(23)-C(18)-S(1)	119.9(9)
C(19)-C(18)-S(1)	120.3(9)
C(20)-C(19)-C(18)	118.8(13)
C(20)-C(19)-H(19A)	120.6
C(18)-C(19)-H(19A)	120.6
C(21)-C(20)-C(19)	123.2(13)
C(21)-C(20)-H(20A)	118.4
C(19)-C(20)-H(20A)	118.4
C(20)-C(21)-C(22)	117.5(12)
C(20)-C(21)-C(24)	121.8(14)
C(22)-C(21)-C(24)	120.7(15)
C(21)-C(22)-C(23)	122.1(12)
C(21)-C(22)-H(22A)	119.0
C(23)-C(22)-H(22A)	119.0
C(18)-C(23)-C(22)	118.7(11)

C(18)-C(23)-H(23A)	120.7
C(22)-C(23)-H(23A)	120.7
C(21)-C(24)-H(24A)	109.5
C(21)-C(24)-H(24B)	109.5
H(24A)-C(24)-H(24B)	109.5
C(21)-C(24)-H(24C)	109.5
H(24A)-C(24)-H(24C)	109.5
H(24B)-C(24)-H(24C)	109.5
O(3)-C(25)-N(1)	119.9(8)
O(3)-C(25)-C(26)	121.9(8)
N(1)-C(25)-C(26)	118.2(8)
C(25)-C(26)-H(26A)	109.5
C(25)-C(26)-H(26B)	109.5
H(26A)-C(26)-H(26B)	109.5
C(25)-C(26)-H(26C)	109.5
H(26A)-C(26)-H(26C)	109.5
H(26B)-C(26)-H(26C)	109.5
C(13)-C(27)-H(27A)	109.5
C(13)-C(27)-H(27B)	109.5
H(27A)-C(27)-H(27B)	109.5
C(13)-C(27)-H(27C)	109.5
H(27A)-C(27)-H(27C)	109.5
H(27B)-C(27)-H(27C)	109.5
O(5)-C(28)-O(6)	123.6(10)
O(5)-C(28)-C(14)	126.6(12)
O(6)-C(28)-C(14)	109.7(11)
O(6)-C(29)-H(29A)	109.5
O(6)-C(29)-H(29B)	109.5
H(29A)-C(29)-H(29B)	109.5
O(6)-C(29)-H(29C)	109.5
H(29A)-C(29)-H(29C)	109.5
H(29B)-C(29)-H(29C)	109.5
C(25)-N(1)-C(9)	130.5(7)
C(25)-N(1)-C(10)	122.5(7)
C(9)-N(1)-C(10)	104.6(6)
C(17)-N(2)-C(1)	108.2(6)

C(17)-N(2)-S(1)	123.0(6)
C(1)-N(2)-S(1)	115.3(6)
C(12)-O(4)-C(13)	111.9(6)
C(28)-O(6)-C(29)	116.8(10)
O(1)-S(1)-O(2)	120.7(5)
O(1)-S(1)-N(2)	106.1(4)
O(2)-S(1)-N(2)	106.9(4)
O(1)-S(1)-C(18)	107.2(5)
O(2)-S(1)-C(18)	107.7(5)
N(2)-S(1)-C(18)	107.7(4)

---

Symmetry transformations used to generate equivalent atoms:

Table 4. Anisotropic displacement parameters ( $\text{\AA}^2 \times 10^3$ ) for DM\_II\_253. The anisotropic displacement factor exponent takes the form:  $-2\pi^2 [ h^2 a^{*2}U^{11} + \dots + 2 h k a^* b^* U^{12} ]$

	U <sup>11</sup>	U <sup>22</sup>	U <sup>33</sup>	U <sup>23</sup>	U <sup>13</sup>	U <sup>12</sup>
C(1)	102(8)	91(7)	120(8)	3(5)	4(6)	-5(5)
C(2)	78(6)	82(6)	128(7)	-16(5)	11(5)	1(4)
C(3)	68(5)	78(6)	99(6)	-16(4)	8(4)	1(4)
C(4)	77(6)	75(6)	99(6)	-14(5)	2(5)	4(4)
C(5)	74(6)	85(6)	111(7)	-18(5)	1(5)	7(4)
C(6)	82(6)	87(6)	124(8)	-24(6)	8(5)	6(5)
C(7)	76(6)	82(6)	133(8)	-31(6)	11(5)	-7(4)
C(8)	82(6)	90(6)	111(7)	-22(5)	-2(5)	2(4)
C(9)	79(6)	75(6)	109(7)	-23(5)	3(5)	1(4)
C(10)	69(5)	75(5)	101(6)	-18(4)	-4(4)	2(4)
C(11)	69(5)	79(6)	110(6)	-18(5)	4(5)	0(4)
C(12)	96(7)	87(6)	99(6)	-6(5)	3(5)	-4(5)
C(13)	78(6)	83(6)	127(7)	-19(5)	-8(5)	-9(4)
C(14)	71(6)	86(6)	116(7)	-18(5)	-2(5)	0(4)
C(15)	65(5)	82(6)	110(6)	-21(5)	5(4)	1(4)
C(16)	71(6)	82(6)	116(7)	-17(5)	2(5)	1(4)
C(17)	73(6)	74(6)	103(6)	-9(4)	-2(5)	3(4)
C(18)	129(9)	89(7)	113(8)	-12(6)	5(7)	17(6)
C(19)	215(14)	110(9)	118(9)	-12(8)	32(9)	-2(8)
C(20)	264(18)	110(10)	126(11)	-6(8)	37(10)	-12(11)
C(21)	236(17)	123(11)	100(9)	-5(8)	21(10)	14(10)
C(22)	167(12)	102(9)	125(10)	-12(8)	-28(8)	9(7)
C(23)	109(8)	113(9)	124(9)	-7(7)	-4(6)	5(6)
C(24)	350(20)	133(11)	116(10)	-32(8)	21(12)	24(12)
C(25)	67(6)	79(6)	117(7)	-9(5)	-7(5)	1(4)
C(26)	77(6)	105(7)	148(9)	-33(6)	-26(6)	18(5)
C(27)	111(8)	82(6)	146(9)	-32(6)	-6(6)	-2(5)
C(28)	93(8)	81(7)	148(10)	-18(7)	-18(8)	-15(5)
C(29)	60(7)	176(12)	258(16)	-41(11)	-21(8)	10(6)
N(1)	61(4)	76(5)	116(5)	-22(4)	-6(4)	1(3)
N(2)	99(6)	82(5)	112(6)	-4(4)	-4(4)	7(4)

O(1)	98(5)	154(6)	126(6)	-13(4)	2(4)	33(4)
O(2)	207(8)	76(5)	129(6)	3(4)	-14(5)	20(4)
O(3)	89(4)	77(4)	126(5)	-19(3)	-6(3)	7(3)
O(4)	83(4)	78(4)	115(4)	-13(3)	1(3)	-2(3)
O(5)	119(6)	165(8)	144(7)	-3(6)	-37(6)	-28(5)
O(6)	76(5)	145(6)	166(7)	-35(5)	-3(4)	-11(4)
S(1)	126(3)	105(2)	112(2)	-11(2)	-6(2)	26(2)

---



Table 5. Hydrogen coordinates ( $\times 10^4$ ) and isotropic displacement parameters ( $\text{\AA}^2 \times 10^{-3}$ ) for DM\_II\_253.

	x	y	z	U(eq)
H(1A)	5335	3536	1158	125
H(1B)	5317	3250	401	125
H(2A)	5088	4190	605	115
H(2B)	4876	3843	7	115
H(5A)	5814	3194	-774	108
H(6A)	5607	2823	-1849	117
H(7A)	5187	3198	-2748	116
H(8A)	4945	3962	-2560	113
H(10A)	5319	4799	-329	98
H(11A)	5930	4549	-1527	103
H(12A)	6063	5311	-1728	113
H(12B)	5523	5267	-1610	113
H(13A)	6532	5609	-798	115
H(14A)	6113	5043	325	109
H(15A)	6588	4735	-964	103
H(16A)	6415	3983	-687	107
H(16B)	6645	4196	37	107
H(17A)	5911	4339	537	100
H(19A)	5703	3378	2436	177
H(20A)	5604	3823	3481	200
H(22A)	6440	4780	2685	158
H(23A)	6565	4343	1618	138
H(24A)	5715	4482	4209	301
H(24B)	5811	4937	3748	301
H(24C)	6225	4673	4133	301
H(26A)	4094	4745	-1908	165
H(26B)	4245	4237	-1698	165
H(26C)	4480	4491	-2379	165
H(27A)	6261	6244	-154	170
H(27B)	6578	5959	395	170

H(27C)	6034	5925	459	170
H(29A)	7851	5174	-230	247
H(29B)	7687	4826	396	247
H(29C)	7664	5365	537	247

---

Table 6. Torsion angles [°] for DM\_II\_253.

---

N(2)-C(1)-C(2)-C(3)	23.8(9)
C(1)-C(2)-C(3)-C(10)	-166.1(7)
C(1)-C(2)-C(3)-C(17)	-44.5(8)
C(1)-C(2)-C(3)-C(4)	81.2(8)
C(10)-C(3)-C(4)-C(9)	-25.0(8)
C(17)-C(3)-C(4)-C(9)	-149.4(8)
C(2)-C(3)-C(4)-C(9)	98.4(8)
C(10)-C(3)-C(4)-C(5)	160.5(9)
C(17)-C(3)-C(4)-C(5)	36.1(14)
C(2)-C(3)-C(4)-C(5)	-76.1(11)
C(9)-C(4)-C(5)-C(6)	0.1(13)
C(3)-C(4)-C(5)-C(6)	174.2(8)
C(4)-C(5)-C(6)-C(7)	2.1(13)
C(5)-C(6)-C(7)-C(8)	-1.2(14)
C(6)-C(7)-C(8)-C(9)	-1.8(13)
C(5)-C(4)-C(9)-C(8)	-3.3(13)
C(3)-C(4)-C(9)-C(8)	-178.7(8)
C(5)-C(4)-C(9)-N(1)	-179.7(7)
C(3)-C(4)-C(9)-N(1)	4.9(10)
C(7)-C(8)-C(9)-C(4)	4.1(13)
C(7)-C(8)-C(9)-N(1)	179.8(8)
C(17)-C(3)-C(10)-N(1)	163.9(6)
C(4)-C(3)-C(10)-N(1)	34.6(7)
C(2)-C(3)-C(10)-N(1)	-81.7(8)
C(17)-C(3)-C(10)-C(11)	50.1(9)
C(4)-C(3)-C(10)-C(11)	-79.2(7)
C(2)-C(3)-C(10)-C(11)	164.5(7)
N(1)-C(10)-C(11)-C(15)	-157.5(6)
C(3)-C(10)-C(11)-C(15)	-45.8(9)
N(1)-C(10)-C(11)-C(12)	75.1(8)
C(3)-C(10)-C(11)-C(12)	-173.1(7)
C(15)-C(11)-C(12)-O(4)	-53.0(9)
C(10)-C(11)-C(12)-O(4)	75.6(8)
O(4)-C(13)-C(14)-C(28)	-177.2(8)

C(27)-C(13)-C(14)-C(28)	-59.7(11)
O(4)-C(13)-C(14)-C(15)	58.7(9)
C(27)-C(13)-C(14)-C(15)	176.2(7)
C(12)-C(11)-C(15)-C(16)	175.9(7)
C(10)-C(11)-C(15)-C(16)	49.1(9)
C(12)-C(11)-C(15)-C(14)	47.1(10)
C(10)-C(11)-C(15)-C(14)	-79.7(8)
C(28)-C(14)-C(15)-C(11)	-173.8(8)
C(13)-C(14)-C(15)-C(11)	-50.3(9)
C(28)-C(14)-C(15)-C(16)	58.6(10)
C(13)-C(14)-C(15)-C(16)	-177.9(7)
C(11)-C(15)-C(16)-C(17)	-55.1(9)
C(14)-C(15)-C(16)-C(17)	71.8(9)
C(15)-C(16)-C(17)-N(2)	178.2(7)
C(15)-C(16)-C(17)-C(3)	60.6(9)
C(10)-C(3)-C(17)-N(2)	172.8(6)
C(4)-C(3)-C(17)-N(2)	-68.7(9)
C(2)-C(3)-C(17)-N(2)	47.8(7)
C(10)-C(3)-C(17)-C(16)	-60.0(9)
C(4)-C(3)-C(17)-C(16)	58.5(10)
C(2)-C(3)-C(17)-C(16)	175.0(6)
C(23)-C(18)-C(19)-C(20)	-1.7(19)
S(1)-C(18)-C(19)-C(20)	178.2(10)
C(18)-C(19)-C(20)-C(21)	2(2)
C(19)-C(20)-C(21)-C(22)	-2(2)
C(19)-C(20)-C(21)-C(24)	-178.7(14)
C(20)-C(21)-C(22)-C(23)	2(2)
C(24)-C(21)-C(22)-C(23)	178.3(12)
C(19)-C(18)-C(23)-C(22)	1.3(16)
S(1)-C(18)-C(23)-C(22)	-178.7(8)
C(21)-C(22)-C(23)-C(18)	-1.2(18)
C(15)-C(14)-C(28)-O(5)	-120.1(12)
C(13)-C(14)-C(28)-O(5)	116.1(12)
C(15)-C(14)-C(28)-O(6)	62.0(10)
C(13)-C(14)-C(28)-O(6)	-61.7(10)
O(3)-C(25)-N(1)-C(9)	170.8(9)

C(26)-C(25)-N(1)-C(9)	-7.9(14)
O(3)-C(25)-N(1)-C(10)	11.2(13)
C(26)-C(25)-N(1)-C(10)	-167.6(8)
C(4)-C(9)-N(1)-C(25)	-144.6(9)
C(8)-C(9)-N(1)-C(25)	39.2(14)
C(4)-C(9)-N(1)-C(10)	17.8(9)
C(8)-C(9)-N(1)-C(10)	-158.4(8)
C(3)-C(10)-N(1)-C(25)	131.1(8)
C(11)-C(10)-N(1)-C(25)	-111.9(8)
C(3)-C(10)-N(1)-C(9)	-33.0(8)
C(11)-C(10)-N(1)-C(9)	83.9(7)
C(16)-C(17)-N(2)-C(1)	-157.8(7)
C(3)-C(17)-N(2)-C(1)	-34.6(8)
C(16)-C(17)-N(2)-S(1)	63.7(10)
C(3)-C(17)-N(2)-S(1)	-173.1(6)
C(2)-C(1)-N(2)-C(17)	6.2(9)
C(2)-C(1)-N(2)-S(1)	148.2(6)
C(11)-C(12)-O(4)-C(13)	63.8(9)
C(27)-C(13)-O(4)-C(12)	171.4(7)
C(14)-C(13)-O(4)-C(12)	-66.2(9)
O(5)-C(28)-O(6)-C(29)	2.9(15)
C(14)-C(28)-O(6)-C(29)	-179.2(8)
C(17)-N(2)-S(1)-O(1)	-47.8(8)
C(1)-N(2)-S(1)-O(1)	176.3(6)
C(17)-N(2)-S(1)-O(2)	-177.8(7)
C(1)-N(2)-S(1)-O(2)	46.3(7)
C(17)-N(2)-S(1)-C(18)	66.7(8)
C(1)-N(2)-S(1)-C(18)	-69.2(8)
C(23)-C(18)-S(1)-O(1)	29.6(10)
C(19)-C(18)-S(1)-O(1)	-150.4(10)
C(23)-C(18)-S(1)-O(2)	160.8(8)
C(19)-C(18)-S(1)-O(2)	-19.1(11)
C(23)-C(18)-S(1)-N(2)	-84.2(9)
C(19)-C(18)-S(1)-N(2)	95.8(10)

---

Symmetry transformations used to generate equivalent atoms:



Table 5. Hydrogen coordinates ( $\times 10^4$ ) and isotropic displacement parameters ( $\text{\AA}^2 \times 10^{-3}$ ) for DM\_237.

	x	y	z	U(eq)
H(4)	7762	1004	7490	36
H(5A)	5036	2227	7616	38
H(5B)	6522	2466	7954	38
H(6)	5500	3496	5904	35
H(2A)	3145	-1267	8437	75
H(2B)	4571	-2129	8724	75
H(2C)	3886	-1903	7642	75
H(9)	6824	7120	7094	49
H(10)	8119	7340	8354	55
H(12A)	7800	6202	10797	90
H(12B)	9271	6387	10021	90
H(12C)	8848	5039	10847	90
H(13)	5745	3714	9202	50
H(14)	7051	3945	10453	57
H(15)	7465	456	6074	35
H(16)	7316	2658	4570	34
H(19)	8831	3823	7395	43
H(20)	11062	3060	8070	50
H(21)	12569	1818	7386	49
H(22)	11908	1276	6026	44
H(24A)	8860	4851	4535	40
H(24B)	7221	4849	4293	40
H(25A)	8195	5664	5807	46
H(25B)	6864	6239	5100	46
H(28A)	4808	1874	5828	39
H(28B)	5483	1192	5050	39

Table 6. Torsion angles [°] for DM\_237.

---

F(3)-C(1)-C(2)-O(3)	-1.1(3)
F(1)-C(1)-C(2)-O(3)	-121.7(2)
F(2)-C(1)-C(2)-O(3)	118.2(2)
F(3)-C(1)-C(2)-C(3)	-178.2(2)
F(1)-C(1)-C(2)-C(3)	61.2(3)
F(2)-C(1)-C(2)-C(3)	-58.9(3)
O(3)-C(2)-C(3)-C(29)	-18.6(4)
C(1)-C(2)-C(3)-C(29)	158.1(2)
O(3)-C(2)-C(3)-C(4)	163.1(2)
C(1)-C(2)-C(3)-C(4)	-20.2(3)
C(29)-C(3)-C(4)-C(15)	-24.5(3)
C(2)-C(3)-C(4)-C(15)	153.7(2)
C(29)-C(3)-C(4)-C(5)	100.6(2)
C(2)-C(3)-C(4)-C(5)	-81.2(2)
C(3)-C(4)-C(5)-C(6)	-147.38(18)
C(15)-C(4)-C(5)-C(6)	-25.0(2)
C(4)-C(5)-C(6)-N(2)	-150.96(18)
C(4)-C(5)-C(6)-C(23)	-34.2(2)
C(13)-C(8)-C(9)-C(10)	-1.6(3)
S(1)-C(8)-C(9)-C(10)	-179.04(18)
C(8)-C(9)-C(10)-C(11)	0.2(4)
C(9)-C(10)-C(11)-C(14)	1.2(4)
C(9)-C(10)-C(11)-C(12)	-176.8(2)
C(9)-C(8)-C(13)-C(14)	1.5(4)
S(1)-C(8)-C(13)-C(14)	178.90(19)
C(8)-C(13)-C(14)-C(11)	0.0(4)
C(10)-C(11)-C(14)-C(13)	-1.3(4)
C(12)-C(11)-C(14)-C(13)	176.7(2)
C(3)-C(4)-C(15)-C(28)	52.0(2)
C(5)-C(4)-C(15)-C(28)	-71.5(2)
C(3)-C(4)-C(15)-C(16)	178.15(17)
C(5)-C(4)-C(15)-C(16)	54.7(2)
C(28)-C(15)-C(16)-N(1)	-144.07(18)
C(4)-C(15)-C(16)-N(1)	91.7(2)



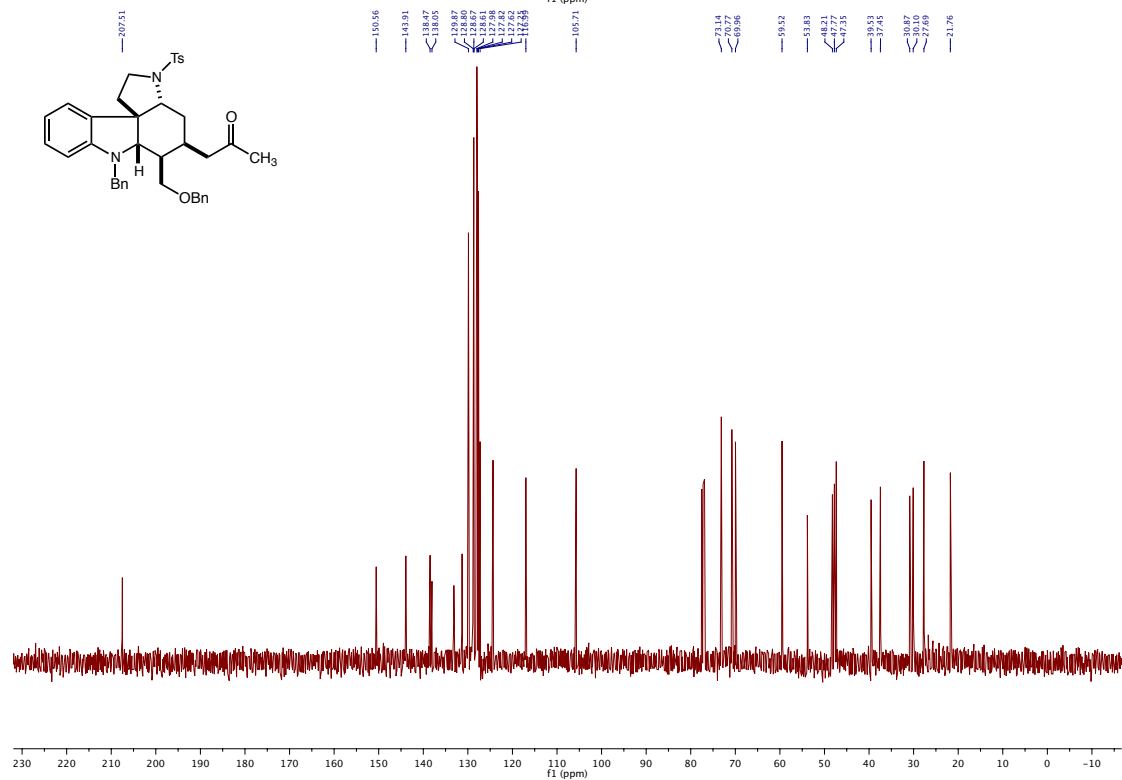
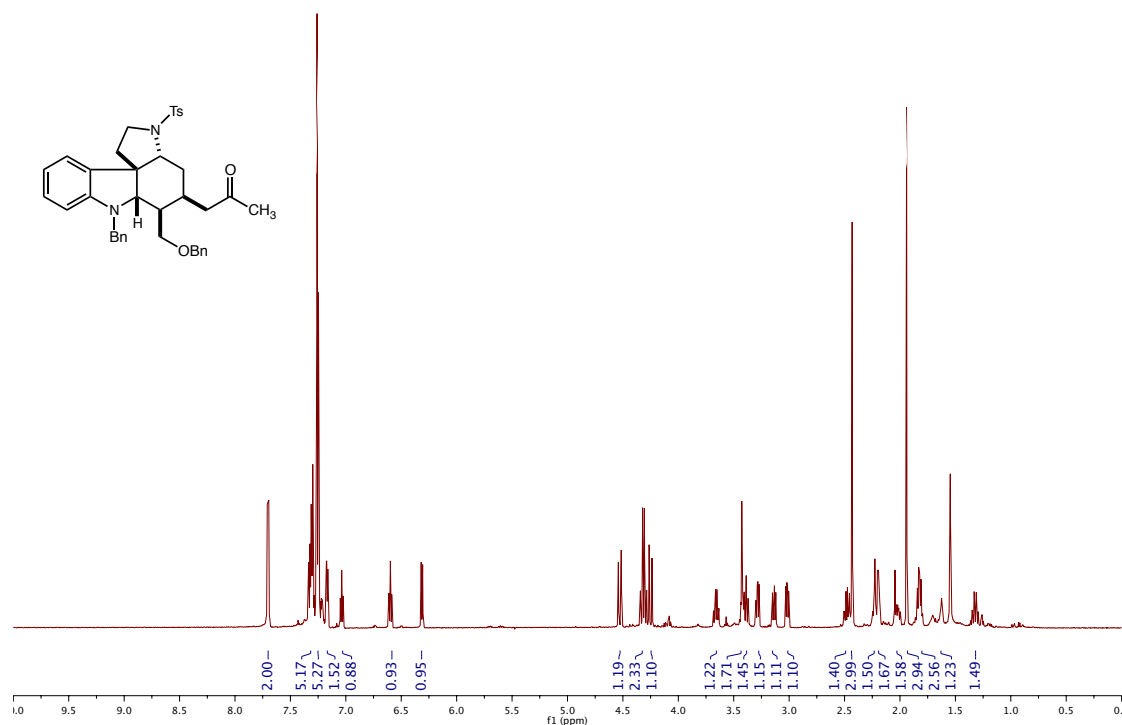
C(28)-C(15)-C(16)-C(23)	102.7(2)
C(4)-C(15)-C(16)-C(23)	-21.5(2)
C(22)-C(17)-C(18)-C(19)	-1.1(3)
N(1)-C(17)-C(18)-C(19)	177.15(18)
C(22)-C(17)-C(18)-C(23)	177.71(19)
N(1)-C(17)-C(18)-C(23)	-4.0(2)
C(17)-C(18)-C(19)-C(20)	0.6(3)
C(23)-C(18)-C(19)-C(20)	-177.9(2)
C(18)-C(19)-C(20)-C(21)	0.1(3)
C(19)-C(20)-C(21)-C(22)	-0.4(4)
C(18)-C(17)-C(22)-C(21)	0.8(3)
N(1)-C(17)-C(22)-C(21)	-177.1(2)
C(20)-C(21)-C(22)-C(17)	-0.1(3)
C(19)-C(18)-C(23)-C(6)	-39.3(3)
C(17)-C(18)-C(23)-C(6)	142.01(18)
C(19)-C(18)-C(23)-C(16)	-159.3(2)
C(17)-C(18)-C(23)-C(16)	22.1(2)
C(19)-C(18)-C(23)-C(24)	76.1(3)
C(17)-C(18)-C(23)-C(24)	-102.58(19)
N(2)-C(6)-C(23)-C(18)	79.4(2)
C(5)-C(6)-C(23)-C(18)	-47.0(2)
N(2)-C(6)-C(23)-C(16)	-165.21(16)
C(5)-C(6)-C(23)-C(16)	68.3(2)
N(2)-C(6)-C(23)-C(24)	-40.01(19)
C(5)-C(6)-C(23)-C(24)	-166.50(16)
N(1)-C(16)-C(23)-C(18)	-30.35(18)
C(15)-C(16)-C(23)-C(18)	87.56(18)
N(1)-C(16)-C(23)-C(6)	-154.55(16)
C(15)-C(16)-C(23)-C(6)	-36.6(2)
N(1)-C(16)-C(23)-C(24)	89.2(2)
C(15)-C(16)-C(23)-C(24)	-152.91(17)
C(18)-C(23)-C(24)-C(25)	-81.4(2)
C(6)-C(23)-C(24)-C(25)	42.74(19)
C(16)-C(23)-C(24)-C(25)	163.30(18)
C(23)-C(24)-C(25)-N(2)	-27.8(2)
O(1)-C(26)-C(27)-F(5)	12.5(3)

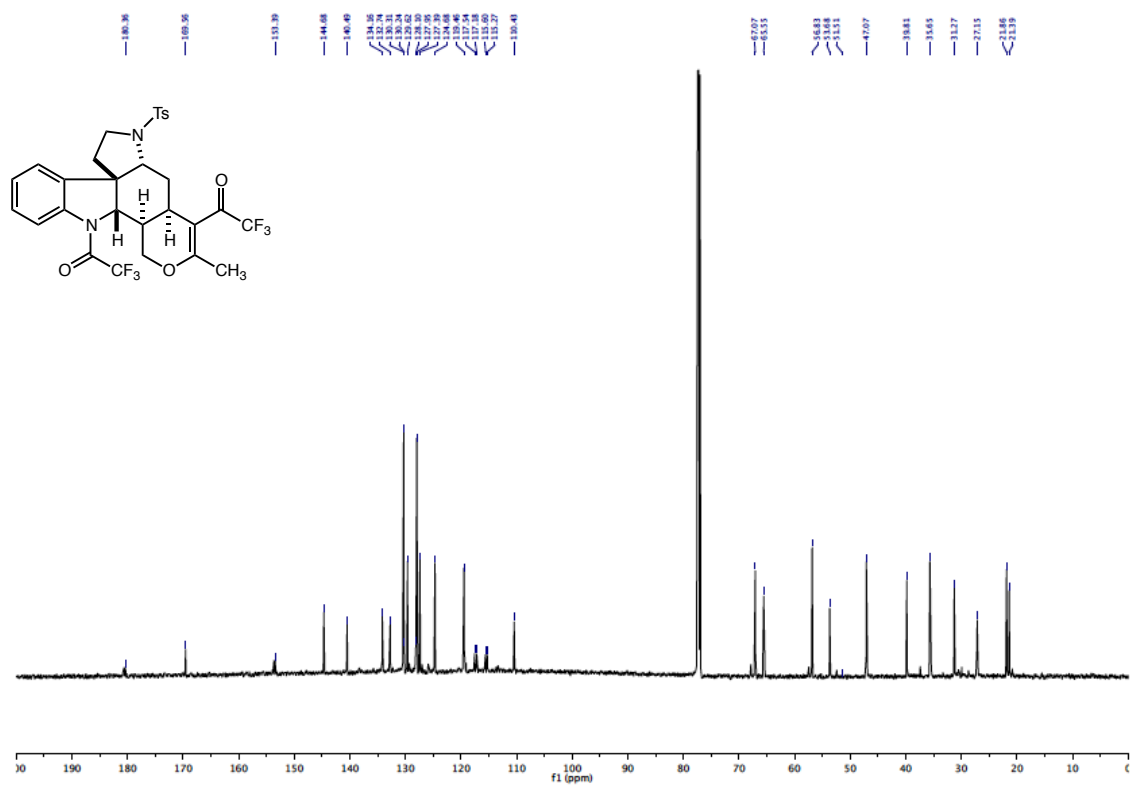
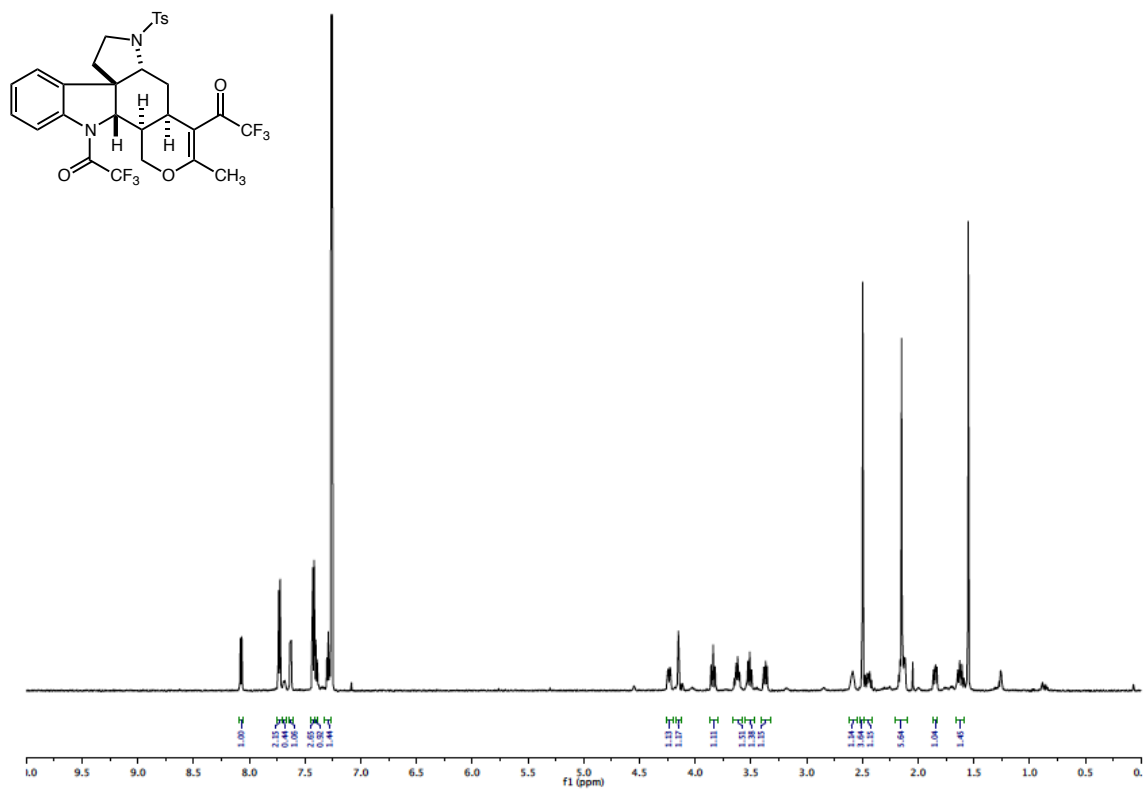
N(1)-C(26)-C(27)-F(5)	-169.70(18)
O(1)-C(26)-C(27)-F(6)	132.8(2)
N(1)-C(26)-C(27)-F(6)	-49.4(3)
O(1)-C(26)-C(27)-F(4)	-106.2(2)
N(1)-C(26)-C(27)-F(4)	71.6(2)
C(4)-C(15)-C(28)-O(2)	-58.6(2)
C(16)-C(15)-C(28)-O(2)	174.83(16)
C(2)-C(3)-C(29)-O(2)	-177.9(2)
C(4)-C(3)-C(29)-O(2)	0.4(3)
C(2)-C(3)-C(29)-C(7)	0.5(4)
C(4)-C(3)-C(29)-C(7)	178.8(2)
O(1)-C(26)-N(1)-C(17)	6.1(3)
C(27)-C(26)-N(1)-C(17)	-171.53(18)
O(1)-C(26)-N(1)-C(16)	-179.2(2)
C(27)-C(26)-N(1)-C(16)	3.2(3)
C(22)-C(17)-N(1)-C(26)	-22.9(3)
C(18)-C(17)-N(1)-C(26)	159.02(19)
C(22)-C(17)-N(1)-C(16)	161.5(2)
C(18)-C(17)-N(1)-C(16)	-16.7(2)
C(23)-C(16)-N(1)-C(26)	-145.6(2)
C(15)-C(16)-N(1)-C(26)	94.9(2)
C(23)-C(16)-N(1)-C(17)	29.8(2)
C(15)-C(16)-N(1)-C(17)	-89.66(19)
C(5)-C(6)-N(2)-C(25)	146.43(19)
C(23)-C(6)-N(2)-C(25)	23.6(2)
C(5)-C(6)-N(2)-S(1)	-53.1(3)
C(23)-C(6)-N(2)-S(1)	-175.90(15)
C(24)-C(25)-N(2)-C(6)	2.6(2)
C(24)-C(25)-N(2)-S(1)	-158.76(15)
C(3)-C(29)-O(2)-C(28)	-5.8(3)
C(7)-C(29)-O(2)-C(28)	175.59(19)
C(15)-C(28)-O(2)-C(29)	35.6(3)
C(6)-N(2)-S(1)-O(4)	2.5(2)
C(25)-N(2)-S(1)-O(4)	161.28(17)
C(6)-N(2)-S(1)-O(5)	-128.14(18)
C(25)-N(2)-S(1)-O(5)	30.7(2)

C(6)-N(2)-S(1)-C(8)	118.08(18)
C(25)-N(2)-S(1)-C(8)	-83.09(19)
C(13)-C(8)-S(1)-O(4)	24.4(2)
C(9)-C(8)-S(1)-O(4)	-158.16(17)
C(13)-C(8)-S(1)-O(5)	155.06(19)
C(9)-C(8)-S(1)-O(5)	-27.5(2)
C(13)-C(8)-S(1)-N(2)	-89.8(2)
C(9)-C(8)-S(1)-N(2)	87.72(19)

---

Symmetry transformations used to generate equivalent atoms:







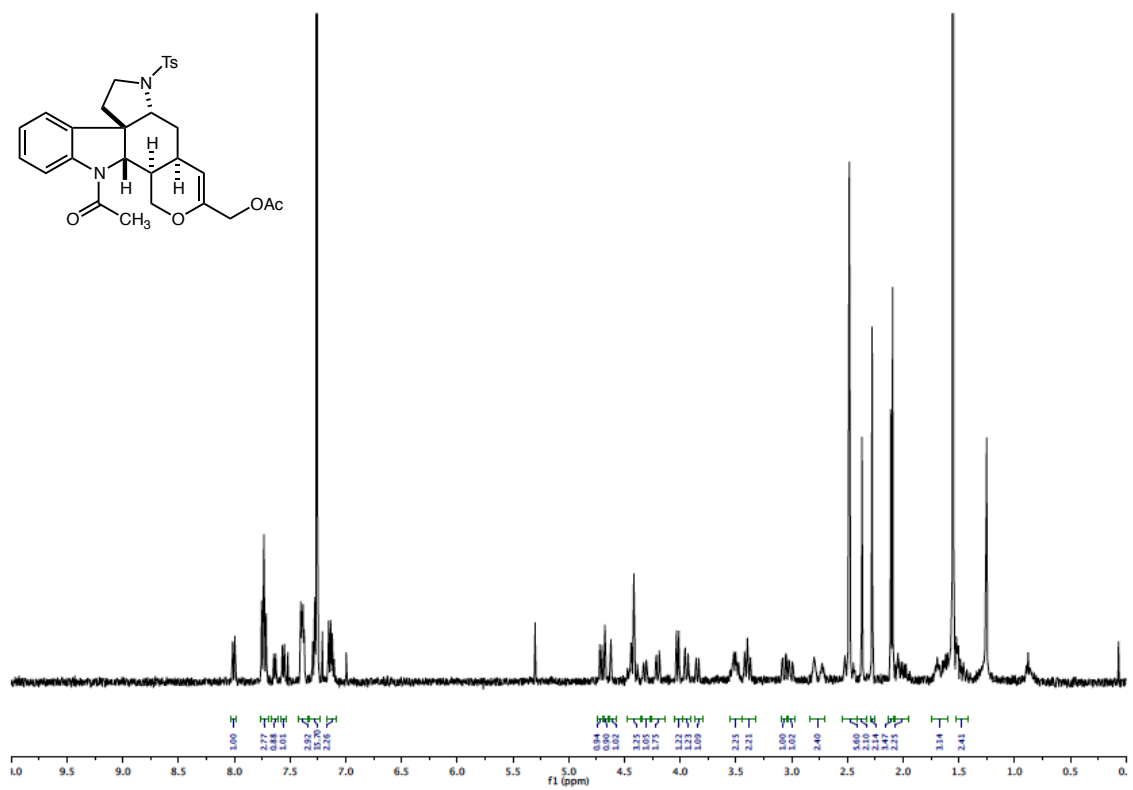
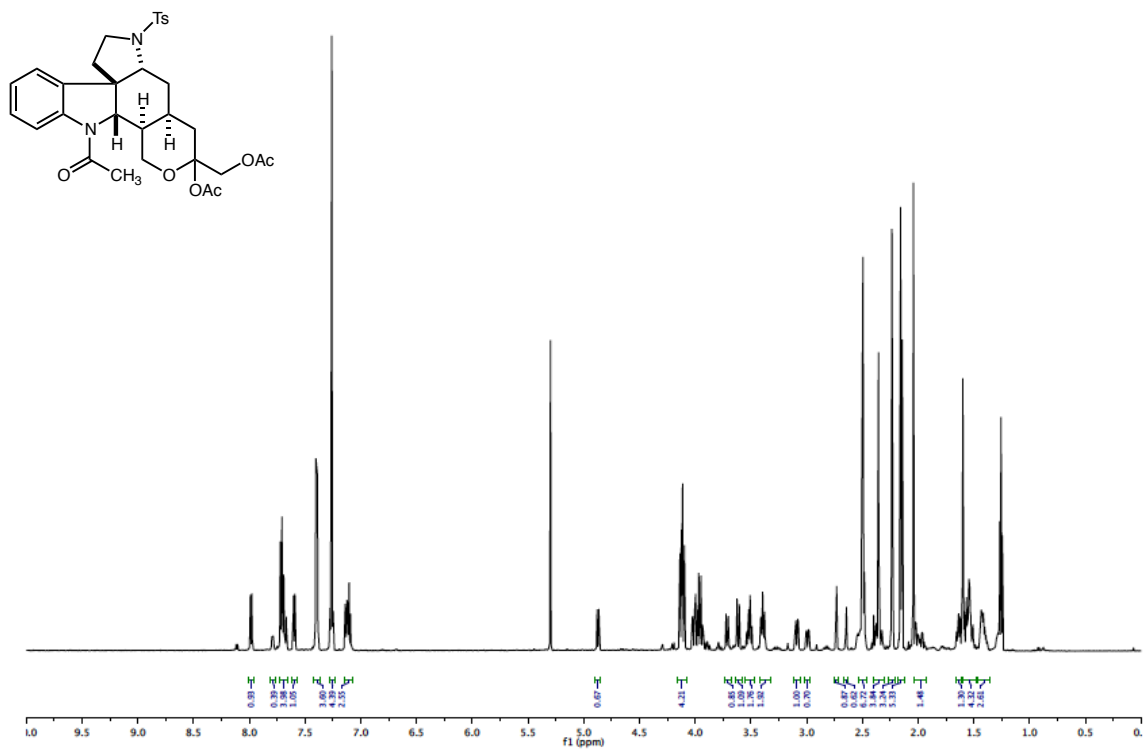




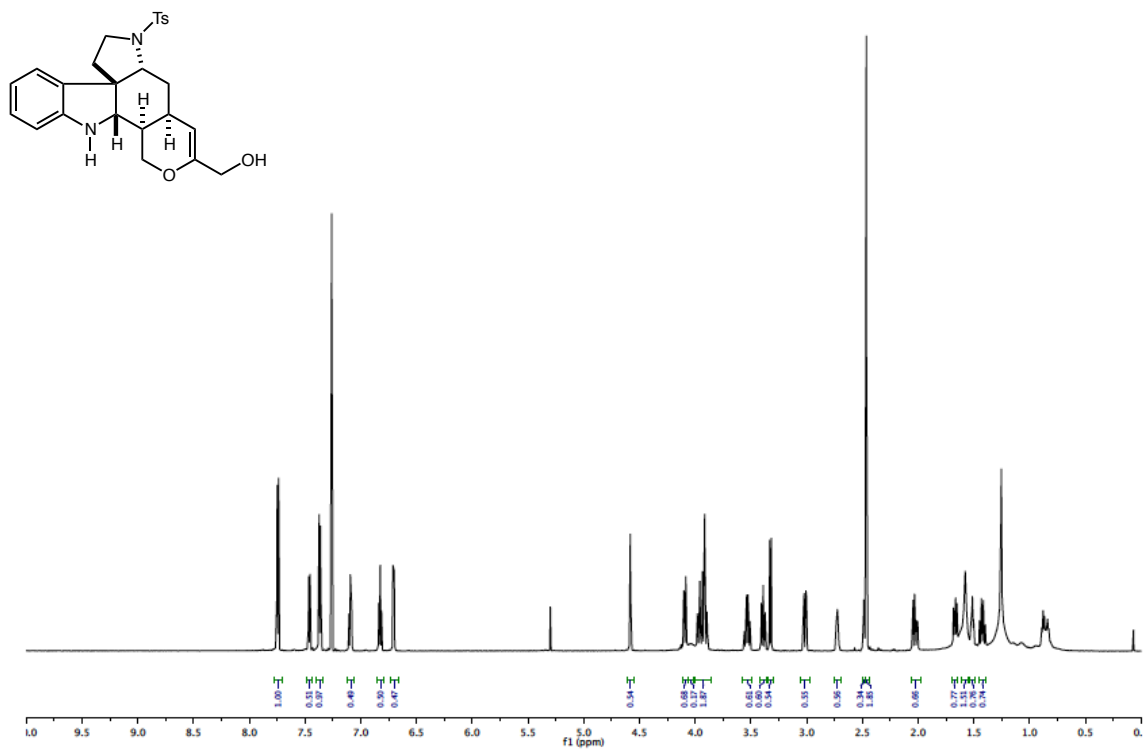




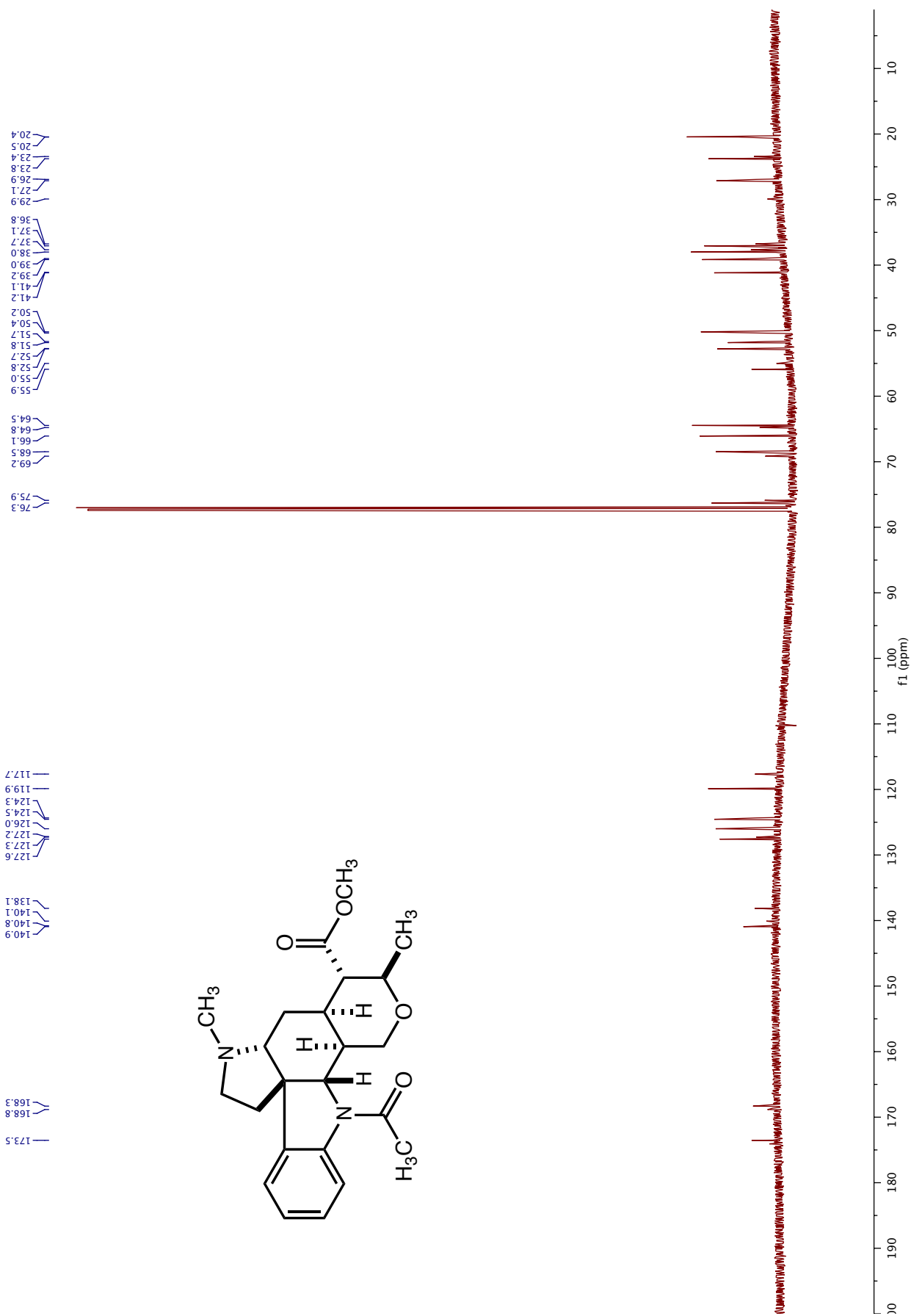
















## 10 References.

1. Bergmeier, S. C., *Tetrahedron* **2000**, *56*, 2561-2576.
2. Larrow, J.; Jacobsen, E., Asymmetric Processes Catalyzed by Chiral (Salen)Metal Complexes. In *Organometallics in Process Chemistry*, Springer Berlin Heidelberg 2004; Vol. 6, pp 123-152.
3. Jiang, S.; Zeng, Q.; Gettayacamin, M.; Tungtaeng, A.; Wannaying, S.; Lim, A.; Hansukjariya, P.; Okunji, C. O.; Zhu, S.; Fang, D., *Antimicrob. Agents Chemother.* **2005**, *49*, 1169-76.
4. Jantikar, A.; Brashier, B.; Maganji, M.; Raghupathy, A.; Mahadik, P.; Gokhale, P.; Gogtay, J.; Salvi, S., *Respir Med* **2007**, *101*, 845-9.
5. Hale, S. L.; Kloner, R. A., *J. Cardiovasc. Pharmacol. Ther.* **2006**, *11*, 249-55.
6. Jensen, K. H.; Sigman, M. S., *Org. Biomol. Chem.* **2008**, *6*, 4083-4088.
7. Li, G.; Chang, H.-T.; Sharpless, K. B., *Angew. Chem. Int. Ed. Engl.* **1996**, *35*, 451-454.
8. Li G Fau - Sharpless, K. B.; Sharpless, K. B., *Acta Chem Scand* **1996**, *50*, 649-51.
9. Donohoe, T. J.; Bataille, C. J. R.; Gattrell, W.; Kloesges, J.; Rossignol, E., *Org. Lett.* **2007**, *9*, 1725-1728.
10. Desai, L. V.; Sanford, M. S., *Angew. Chem. Int. Ed.* **2007**, *46*, 5737-5740.
11. Alexanian, E. J.; Lee, C.; Sorensen, E. J., *J. Am. Chem. Soc.* **2005**, *127*, 7690-7691.
12. . a) Paderes, M. C.; Chemler, S. R., *Org. Lett.* **2009**, *11*, 1915-1918. b) Fuller, P. H.; Kim, J.-W.; Chemler, S. R., *J. Am. Chem. Soc.* **2008**, *130*, 17638-17639.
13. Sherman, E. S.; Chemler, S. R., *Adv. Synth. Catal.* **2009**, *351*, 467-471.
14. de Haro, T.; Nevado, C., *Angew Chem Int Ed Engl* **2011**, *50*, 906-10.
15. Liu, G.; Stahl, S. S., *J. Am. Chem. Soc.* **2006**, *128*, 7179-7181.
16. . a) Wardrop, D. J.; Bowen, E. G.; Forslund, R. E.; Sussman, A. D.; Weerasekera, S. L., *J. Am. Chem. Soc.* **2009**, *132*, 1188-1189. b) Lovick, H. M.; Michael, F. E., *J. Am. Chem. Soc.* **2010**, *132*, 1249-1251.
17. Mancheno, D. E.; Thornton, A. R.; Stoll, A. H.; Kong, A.; Blakey, S. B., *Org. Lett.* **2010**, *12*, 4110-4113.
18. Wang, L.; Prabhudas, B.; Clive, D. L. J., *J. Am. Chem. Soc.* **2009**, *131*, 6003-6012.
19. Hu, X.; Nguyen, K. T.; Jiang, V. C.; Lofland, D.; Moser, H. E.; Pei, D., *J. Med. Chem.* **2004**, *47*, 4941-4949.
20. Liu, G.; Stahl, S. S., *J. Am. Chem. Soc.* **2007**, *129*, 6328-6335.
21. Zabawa, T. P.; Kasi, D.; Chemler, S. R., *J. Am. Chem. Soc.* **2005**, *127*, 11250-11251.
22. Holzgrabe, U.; Wawer, I.; Diehl, B., *NMR spectroscopy in pharmaceutical analysis*. Elsevier: Oxford, 2008; p xxi, 501 p.
23. Leggio, A.; Di Gioia, M. L.; Perri, F.; Liguori, A., *Tetrahedron* **2007**, *63*, 8164-8173.
24. Bender, C. F.; Widenhoefer, R. A., *J. Am. Chem. Soc.* **2005**, *127*, 1070-1071.

25. Raucher, S.; Jones, D. S., *Synth. Commun.* **1985**, *15*, 1025-1031.
26. Martínez-Estibalez, U.; Sotomayor, N.; Lete, E., *Tetrahedron Lett.* **2007**, *48*, 2919-2922.
27. Jacquemard, U.; Bénéteau, V.; Lefoix, M.; Routier, S.; Mérour, J.-Y.; Coudert, G., *Tetrahedron* **2004**, *60*, 10039-10047.
28. Gribkov, D. V.; Hultzsch, K. C.; Hampel, F., *J. Am. Chem. Soc.* **2006**, *128*, 3748-3759.
29. . a) Santo, R.; Miyamoto, R.; Tanaka, R.; Nishioka, T.; Sato, K.; Toyota, K.; Obata, M.; Yano, S.; Kinoshita, I.; Ichimura, A.; Takui, T., *Angew. Chem. Int. Ed.* **2006**, *45*, 7611-7614. b) Ribas, X.; Jackson, D. A.; Donnadieu, B.; Mahía, J.; Parella, T.; Xifra, R.; Hedman, B.; Hodgson, K. O.; Llobet, A.; Stack, T. D. P., *Angew. Chem. Int. Ed.* **2002**, *41*, 2991-2994. c) Furuta, H.; Maeda, H.; Osuka, A., *J. Am. Chem. Soc.* **2000**, *122*, 803-807. d) Naumann, D.; Roy, T.; Tebbe, K.-F.; Crump, W., *Angew. Chem. Int. Ed. Engl.* **1993**, *32*, 1482-1483. e) Willert-Porada, M. A.; Burton, D. J.; Baenziger, N. C., *J. Chem. Soc., Chem. Commun.* **1989**, *0*, 1633-1634.
30. . a) Casitas, A.; King, A. E.; Parella, T.; Costas, M.; Stahl, S. S.; Ribas, X., *Chemical Science* **2010**, *1*, 326-330. b) Huffman, L. M.; Stahl, S. S., *J. Am. Chem. Soc.* **2008**, *130*, 9196-9197.
31. . a) Bäckvall, J. E., *Acc. Chem. Res.* **1983**, *16*, 335-342. b) Hegedus, L. S.; Allen, G. F.; Waterman, E. L., *J. Am. Chem. Soc.* **1976**, *98*, 2674-2676. c) Åkermark, B.; E. Bäckvall, J.; Siirala-Hanseñ, K.; Sjöberg, K.; Zetterberg, K., *Tetrahedron Lett.* **1974**, *15*, 1363-1366. d) Åkermark, B.; Bäckvall, J. E.; Hegedus, L. S.; Zetterberg, K.; Siirala-Hansén, K.; Sjöberg, K., *J. Organomet. Chem.* **1974**, *72*, 127-138.
32. Thornton, A. R. Metallonitrene/alkyne cascade reactions : development of a versatile process for organic synthesis. Thesis (Ph D ), Emory University, 2010.
33. Wenkert, E.; Michelotti, E. L.; Swindell, C. S.; Tingoli, M., *J. Org. Chem.* **1984**, *49*, 4894-4899.
34. Kaga, H.; Goto, K.; Takahashi, T.; Hino, M.; Tokuhashi, T.; Orito, K., *Tetrahedron* **1996**, *52*, 8451-8470.
35. Pluotno, A.; Carmeli, S., *Tetrahedron* **2005**, *61*, 575-583.
36. Schindler, C. S.; Bertschi, L.; Carreira, E. M., *Angew. Chem. Int. Ed.* **2010**, *49*, 9229-9232.
37. Ersmark, K.; Del Valle, J. R.; Hanessian, S., *Angew. Chem. Int. Ed.* **2008**, *47*, 1202-1223.
38. Sano, T.; Beattie, K. A.; Codd, G. A.; Kaya, K., *J. Nat. Prod.* **1998**, *61*, 851-853.
39. Martin, T. J., Inhibitors against Human Mast Cell Tryptase: A Potential Approach to Attack Asthma? In *Highlights in Bioorganic Chemistry*, Wiley-VCH Verlag GmbH & Co. KGaA2005; pp 227-241.
40. Schindler, C. S.; Stephenson, C. R. J.; Carreira, E. M., *Angew. Chem. Int. Ed.* **2008**, *47*, 8852-8855.
41. Delgado, R.; Blakey, S. B., *Eur. J. Org. Chem.* **2009**, *2009*, 1506-1510.
42. Delgado, R. Development of a novel cascade cyclization reaction and its application towards the total synthesis of malagashanine : a chloroquine efflux inhibitor. Thesis (Ph D ), Emory University, 2010.
43. Espino, C. G.; Du Bois, J., *Angew. Chem. Int. Ed.* **2001**, *40*, 598-600.

44. . a) Chen, M. S.; Prabakaran, N.; Labenz, N. A.; White, M. C., *J. Am. Chem. Soc.* **2005**, *127*, 6970-6971. b) Chen, M. S.; White, M. C., *J. Am. Chem. Soc.* **2004**, *126*, 1346-1347.
45. Itoh, K.; Yogo, T.; Ishii, Y., *Chem. Lett.* **1977**, *6*, 103-106.
46. Martin, M. J., Sixt Process for producing diketene. 1940.
47. Wakabayashi, S.; Saito, N.; Sugihara, Y.; Sugimura, T.; Murata, I., *Synth. Commun.* **1995**, *25*, 2019-2027.
48. . a) Fleischer, R.; Wunderlich, H.; Braun, M., *Eur. J. Org. Chem.* **1998**, *1998*, 1063-1070. b) Clinet, J. C.; Linstumelle, G., *Synthesis* **1981**, 875-8.
49. Abarbri, M.; Parrain, J.-L.; Kitamura, M.; Noyori, R.; Duchene, A., *J. Org. Chem.* **2000**, *65*, 7475-7478.
50. Ireland, R. E.; Meissner, R. S.; Rizzacasa, M. A., *J. Am. Chem. Soc.* **1993**, *115*, 7166-7172.
51. Schmieder-van de Vondervoort, L.; Bouttemy, S.; Padrón, J. M.; Bras, J. L.; Muzart, J.; Alsters, P. L., *Synlett* **2002**, *2002*, 0243-0246.
52. Corey, E. J.; Trybulski, E. J.; Melvin, L. S.; Nicolaou, K. C.; Secrist, J. A.; Lett, R.; Sheldrake, P. W.; Falck, J. R.; Brunelle, D. J., *J. Am. Chem. Soc.* **1978**, *100*, 4618-4620.
53. . a) Jung, J.-W.; Shin, D.-Y.; Seo, S.-Y.; Kim, S.-H.; Paek, S.-M.; Jung, J.-K.; Suh, Y.-G., *Tetrahedron Lett.* **2005**, *46*, 573-575. b) Sames, D.; Liu, Y.; DeYoung, L.; Polt, R., *J. Org. Chem.* **1995**, *60*, 2153-2159. c) Suh, Y.-G.; Kim, S.-H.; Jung, J.-K.; Shin, D.-Y., *Tetrahedron Lett.* **2002**, *43*, 3165-3167.
54. . a) Carpino, L. A.; El-Faham, A.; Albericio, F., *J. Org. Chem.* **1995**, *60*, 3561-3564. b) Sole, N.; Torres, J. L.; Anton, J. M. G.; Valencia, G.; Reig, F., *Tetrahedron* **1986**, *42*, 193-198.
55. Bergmann, M.; Zervas, L., *Chem. Ber.* **1932**, *65*, 1192-1201.
56. Angle, S. R.; Arnaiz, D. O., *Tetrahedron Lett.* **1989**, *30*, 515-518.
57. Sakaitani, M.; Hori, K.; Ohfuné, Y., *Tetrahedron Lett.* **1988**, *29*, 2983-2984.
58. McManus, H. A.; Fleming, M. J.; Lautens, M., *Angew. Chem. Int. Ed.* **2007**, *46*, 433 - 436.
59. Hardinger, S. A.; Wijaya, N., *Tetrahedron Lett.* **1993**, *34*, 3821 - 3824.
60. Denmark, S. E.; Almstead, N. G., *Journal of the Mexican Chemical Society* **2009**, *53*, 174-192.
61. . a) Akiyama, T., *Chem. Rev. (Washington, DC, U. S.)* **2007**, *107*, 5744-5758. b) Doyle, A. G.; Jacobsen, E. N., *Chem. Rev. (Washington, DC, U. S.)* **2007**, *107*, 5713-5743.
62. Phipps, R. J.; Hamilton, G. L.; Toste, F. D., *Nat Chem* **2012**, *4*, 603-614.
63. Raheem, I. T.; Thiara, P. S.; Peterson, E. A.; Jacobsen, E. N., *J. Am. Chem. Soc.* **2007**, *129*, 13404-13405.
64. Xu, H.; Zuend, S. J.; Woll, M. G.; Tao, Y.; Jacobsen, E. N., *Science* **2010**, *327*, 986-990.
65. Knowles, R. R.; Lin, S.; Jacobsen, E. N., *J. Am. Chem. Soc.* **2010**, *132*, 5030-5032.
66. Arimori, S.; Consiglio, G. A.; Phillips, M. D.; James, T. D., *Tetrahedron Lett.* **2003**, *44*, 4789 - 4792.
67. Braun, M.; Kotter, W., *Angew. Chem. Int. Ed.* **2004**, *43*, 514-517.

68. Aggarwal, V. K.; Eames, J.; Villa, M.-J.; McIntyre, S.; Sansbury, F. H.; Warren, S., *Journal of the Chemical Society, Perkin Transactions 1* **2000**, 533-546.
69. House, H. O.; Fischer Jr, W. F., *J. Org. Chem.* **1968**, *33*, 949-956.
70. Ramanitrahambola, D.; Rasoanaivo, P.; Ratsimamanga, S.; Vial, H., *Molecular and biochemical parasitology* **2006**, *146*, 58-67.
71. Rasoanaivo, P.; Galeffi, C.; De Vicente, Y.; Nicoletti, M., *Rev Latinoam Quim* **1991**, *22*, 32-34.
72. Martin, M.-T.; Rasoanaivo, P.; Palazzino, G.; Galeffi, C.; Nicoletti, M.; Trigalo, F.; Frappier, F., *Phytochemistry* **1999**, *51*, 479-486.
73. Rasoanaivo, P.; Palazzino, G.; Nicoletti, M.; Galeffi, C., *Phytochemistry* **2001**, *56*, 863-867.
74. Rasoanaivo, P.; Galeffi, G.; de Vicente, Y.; Nicoletti, M., *Rev. Latinoamer. Quim.* **1991**, *22*, 32-34.
75. Caira, M. R.; Rasoanaivo, P., *Journal of chemical crystallography* **1995**, *25*, 725-729.
76. Martin, M.-T.; Rasoanaivo, P.; Palazzino, G.; Galeffi, C.; Nicoletti, M.; Trigalo, F.; Frappier, F., *Phytochemistry* **1999**, *51*, 479-486.
77. Organization, W. H. *Global report on antimalarial efficacy and drug resistance: 2000-2010*; 2010; [http://whqlibdoc.who.int/publications/2010/9789241500470\\_eng.pdf](http://whqlibdoc.who.int/publications/2010/9789241500470_eng.pdf).
78. Mangoyi, R.; Hayeshi, R.; Ngadjui, B.; Ngandeu, F.; Bezabih, M.; Abegaz, B.; Razafimahefa, S.; Rasoanaivo, P.; Mukanganyama, S., *J. Enzyme Inhib. Med. Chem.* **2010**, *25*, 854-62.
79. Rasoanaivo, P.; Ratsimamanga-Urverg, S.; Milijaona, R.; Rafatro, H.; Rakoto-Ratsimamanga, A.; Galeffi, C.; Nicoletti, M., *Planta Med.* **1994**, *60*, 13-16.
80. Henry, M.; Alibert, S.; Orlandi-Pradines, E.; Bogreau, H.; Fusai, T.; Rogier, C.; Barbe, J.; Pradines, B., *Curr. Drug Targets* **2006**, *7*, 935-948.
81. Hayeshi, R.; Masimirembwa, C.; Mukanganyama, S.; Ungell, A.-L. B., *Eur. J. Pharm. Sci.* **2006**, *29*, 70-81.
82. Trigalo, F.; Joyeau, R.; Pham, V. C.; Youté, J. J.; Rasoanaivo, P.; Frappier, F., *Tetrahedron* **2004**, *60*, 5471-5474.
83. . a) Ando, M.; Buechi, G.; Ohnuma, T., *J. Am. Chem. Soc.* **1975**, *97*, 6880-6881. b) Büchi, G.; Matsumoto, K. E.; Nishimura, H., *J. Am. Chem. Soc.* **1971**, *93*, 3299-3301. c) He, F.; Bo, Y.; Altom, J. D.; Corey, E., *J. Am. Chem. Soc.* **1999**, *121*, 6771-6772. d) Heures, N.; Wouters, J.; Markó, I. E., *Org. Lett.* **2005**, *7*, 5245-5248. e) Turet, L.; Markó, I. E.; Tinant, B.; Declercq, J.-P.; Touillaux, R., *Tetrahedron Lett.* **2002**, *43*, 6591-6595. f) Van Tamelen, E.; Dolby, L.; Lawton, R., *Tetrahedron Lett.* **1960**, *1*, 30-35.
84. . a) Hupe, E.; Calaza, M. I.; Knochel, P., *Tetrahedron Lett.* **2001**, *42*, 8829-8831. b) Hupe, E.; Calaza, M. I.; Knochel, P., *Chem. Eur. J.* **2003**, *9*, 2789-2796.
85. Yamaguchi, M.; Hirao, I., *Tetrahedron Lett.* **1983**, *24*, 391-394.
86. . a) Liu, X.; Ready, J. M., *Tetrahedron* **2008**, *64*, 6955-6960. b) Zhang, D.; Ready, J. M., *J. Am. Chem. Soc.* **2007**, *129*, 12088-12089.
87. Dobarro, A.; Velasco, D., *Tetrahedron* **1996**, *52*, 13733-13738.
88. Polt, R.; Peterson, M. A.; DeYoung, L., *J. Org. Chem.* **1992**, *57*, 5469-5480.
89. *Early studies showed that acetamide group reacted with the Vilsmeier reagent. Thus, temporary protection of the indoline nitrogen was necessary for high and reproducible yields (see ref. 15a).*

90. Ramesh, N. G.; Balasubramanian, K. K., *Tetrahedron Lett.* **1991**, *31*, 3875-3878.
91. Shimokawa, J.; Ishiwata, T.; Shirai, K.; Koshino, H.; Tanatani, A.; Nakata, T.; Hashimoto, Y.; Nagasawa, K., *Chem. Eur. J.* **2005**, *11*, 6878-6888.
92. Nishiwaki, E.; Tanaka, S.; Lee, H.; Shibuya, M., *Heterocycles* **1988**, *27*, 1945-1952.
93. . a) Bailey, D. M.; Johnson, R. E., *J. Med. Chem.* **1973**, *16*, 1300-1302. b) Barker, P.; Gendler, P.; Rapoport, H., *J. Org. Chem.* **1978**, *43*, 4849-4853.
94. Trost, B. M.; Balkovec, J. M.; Mao, M. K., *J. Am. Chem. Soc.* **1986**, *108*, 4974-4983.
95. Harbuck, J. W.; Rapoport, H., *J. Org. Chem.* **1972**, *37*, 3618-3622.
96. Delgado, A.; Clardy, J., *Tetrahedron Lett.* **1992**, *33*, 2789-2790.
97. . a) Bellur, E.; Freifeld, I.; Böttcher, D.; Bornscheuer, U. T.; Langer, P., *Tetrahedron* **2006**, *62*, 7132-7139. b) Blouin, M.; Béland, M.-C.; Bressard, P., *J. Org. Chem.* **1990**, *55*, 1466-1471. c) Juhász, L.; Szilágyi, L.; Antus, S.; Visy, J.; Zsila, F.; Simonyo, M., *Tetrahedron* **2002**, *58*, 4261-4265. d) Schatz, P. F.; Ralph, J.; Lu, F.; Guzei, I. A.; Buzel, M., *Org. Biomol. Chem.* **2006**, *4*, 2801-2806. e) Pohmakotr, M.; Issaree, A.; Sampaongoen, L.; Tuchinda, P.; Reutrakul, V., *Tetrahedron Lett.* **2003**, *44*, 7937-7940.
98. Hoveyda, A. H.; Evans, D. A.; Fu, G. C., *Chem. Rev. (Washington, DC, U. S.)* **1993**, *93*, 1307-1370.
99. . a) Bartlett, P. A.; Meadows, J. D.; Ottow, E., *J. Am. Chem. Soc.* **1984**, *106*, 5304-5311. b) Brandänge, S.; Färnbäck, M.; Leijonmarck, H.; Sundin, A., *J. Am. Chem. Soc.* **2003**, *125*, 11942-11955. c) Honda, T.; Satoh, A.; Yamada, T.; Hayakawa, T.; Kanai, K., *J. Chem. Soc. Perkin Trans. I* **1998**, 397. d) Kametani, T.; Katoh, T.; Fujio, J.; Nogiwa, I.; Tsubuki, M.; Honda, T., *J. Org. Chem.* **1988**, *53*, 1982-1991. e) Kametani, T.; Katoh, T.; Tsubuki, M.; Honda, T., *J. Am. Chem. Soc.* **1986**, *108*, 7055-7060. f) Lee, J. Y.; Kim, B. H., *Tetrahedron* **1996**, *52*, 571-588.
100. Schann, S.; Bruban, V.; Pompermayer, K.; Feldman, J.; Pfeiffer, B.; Renard, P.; Scalbert, E.; Bousquet, P.; Ehrhardt, J.-D., *J. Med. Chem.* **2001**, *44*, 1588-1593.
101. . a) Lanzilotti, A. E.; Littell, R.; Fanshawe, W. J.; McKenzie, T. C.; Lovell, F. M., *J. Org. Chem.* **1979**, *44*, 4809-4813. b) Song, Z. J.; King, A. O.; Waters, M. S.; Lang, F.; Zewge, D.; Bio, M.; Leazer, J. L.; Javadi, G.; Kassim, A.; Tschaen, D. M., *Proc. Natl. Acad. Sci. U. S. A.* **2004**, *101*, 5776-5781.
102. Fry, J. L., Triethylsilane–Trifluoroacetic Acid. In *e-EROS Encyclopedia of Reagents for Organic Synthesis*, 2001.
103. . a) Ji, S.; Gortler, L. B.; Waring, A.; Battisti, A. J.; Bank, S.; Closson, W. D.; Wriede, P. A., *J. Am. Chem. Soc.* **1967**, *89*, 5311-5312. b) McIntosh, J. M.; Matassa, L. C., *J. Org. Chem.* **1988**, *53*, 4452-4457. c) Heathcock, C. H.; Blumenkopf, T. A.; Smith, K. M., *J. Org. Chem.* **1989**, *54*, 1548-1562.
104. Okitsu, O.; Suzuki, R.; Kobayashi, S., *J. Org. Chem.* **2001**, *66*, 809-823.
105. Ehrenstein, W.; Korte, F., *Chem. Ber.* **1971**, *104*, 734-738.
106. Smith, M.; March, J.; March, J., *March's advanced organic chemistry : reactions, mechanisms, and structure*. 5th ed.; Wiley: New York, 2001; p xviii, 2083 p.
107. Andrews, I. P.; Lewis, N. J.; McKillop, A.; Wells, A. S., *Heterocycles* **1996**, *43*, 1151-1158.

108. West, S. P.; Bisai, A.; Lim, A. D.; Narayan, R. R.; Sarpong, R., *J. Am. Chem. Soc.* **2009**, *131*, 11187-11194.
109. Mortier, J.; Moyroud, J.; Bennetau, B.; Cain, P. A., *J. Org. Chem.* **1994**, *59*, 4042-4044.
110. Novák, P.; Correa, A.; Gallardo-Donaire, J.; Martin, R., *Angew. Chem.* **2011**, *123*, 12444-12447.
111. Claesson, A.; Luthman, K., *Acta Chem. Scand., Ser. B* **1982**, *B36*, 719-20.
112. Meyers, A.; Price, D. A.; Andres, C., *Synlett* **1997**, *1997*, 533-534.
113. Hanessian, S.; Szychowski, J.; Maianti, J. P., *Org. Lett.* **2008**, *11*, 429-432.
114. Mori, K.; Sasaki, M., *Tetrahedron Lett.* **1979**, *20*, 1329-1332.
115. Jerris, P. J.; Wovkulich, P. M.; Smith, A. B., *Tetrahedron Lett.* **1979**, *20*, 4517-4520.
116. Sundberg, R. J.; Carey, F. A., *Advanced Organic Chemistry, Part B: Reactions and Synthesis*. Plenum, US2001.
117. Williard, P. G.; Carpenter, G. B., *J. Am. Chem. Soc.* **1986**, *108*, 462-468.
118. Sun, C.-Q.; Cheng, P. T.; Stevenson, J.; Dejneka, T.; Brown, B.; Wang, T. C.; Robl, J. A.; Poss, M. A., *Tetrahedron Letters* **2002**, *43*, 1161-1164.